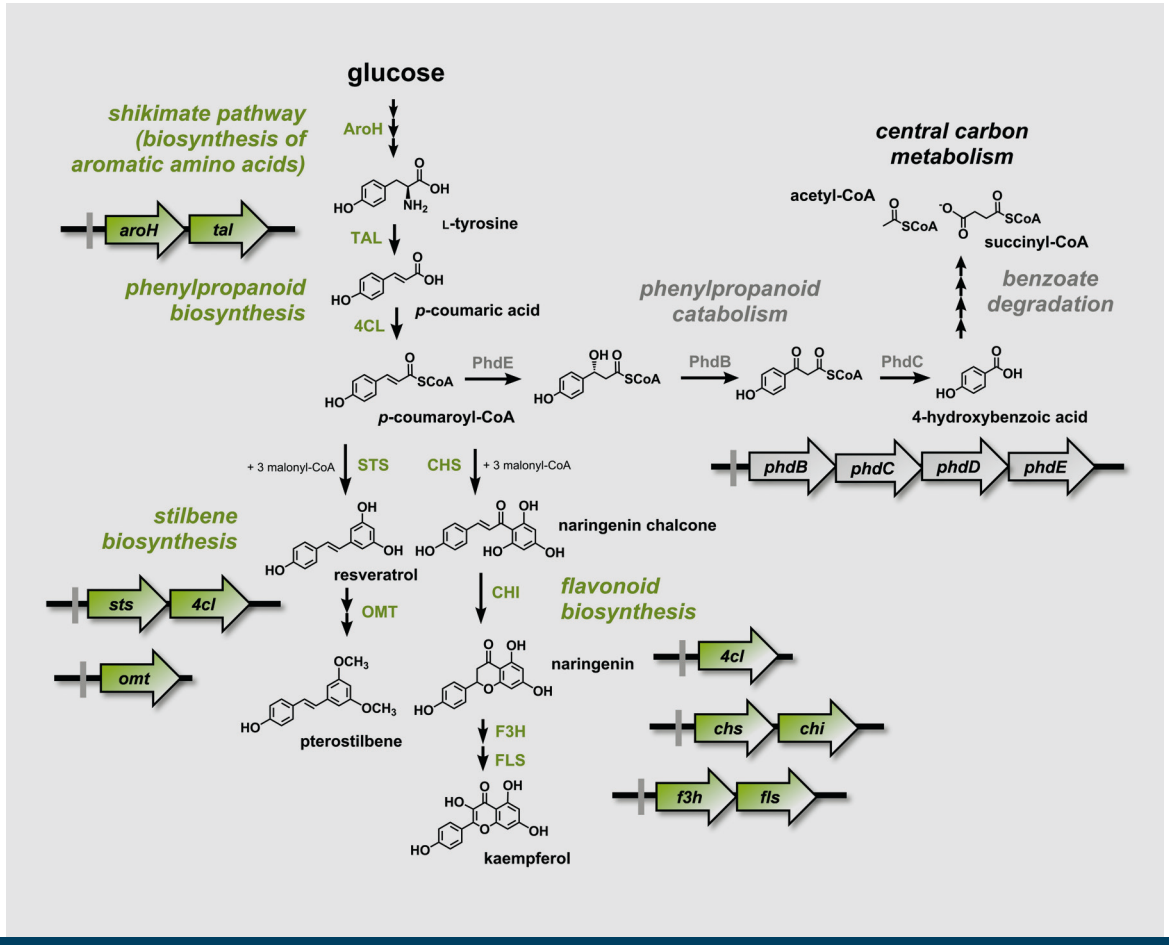

Corynebacterium glutamicum – a novel platform for the production of plant polyphenols

Nicolai Kallscheuer

Schlüsseltechnologien / Key Technologies
Band / Volume 160
ISBN 978-3-95806-291-7

Mitglied der Helmholtz-Gemeinschaft

JÜLICH
Forschungszentrum

Schriften des Forschungszentrums Jülich
Reihe Schlüsseltechnologien / Key Technologies Band / Volume 160

Forschungszentrum Jülich GmbH
Institut für Bio-und Geowissenschaften
Biotechnologie (IBG-1)

Corynebacterium glutamicum – a novel platform for the production of plant polyphenols

Nicolai Kallscheuer

Schriften des Forschungszentrums Jülich
Reihe Schlüsseltechnologien / Key Technologies Band / Volume 160

ISSN 1866-1807 ISBN 978-3-95806-291-7

Bibliografische Information der Deutschen Nationalbibliothek.
Die Deutsche Nationalbibliothek verzeichnet diese Publikation in der
Deutschen Nationalbibliografie; detaillierte Bibliografische Daten
sind im Internet über http://dnb.d-nb.de abrufbar.

Herausgeber und Vertrieb:	Forschungszentrum Jülich GmbH Zentralbibliothek, Verlag 52425 Jülich Tel.: +49 2461 61-5368 Fax: +49 2461 61-6103 zb-publikation@fz-juelich.de www.fz-juelich.de/zb
Umschlaggestaltung:	Grafische Medien, Forschungszentrum Jülich GmbH
Druck:	Grafische Medien, Forschungszentrum Jülich GmbH
Copyright:	Forschungszentrum Jülich 2018

Schriften des Forschungszentrums Jülich
Reihe Schlüsseltechnologien / Key Technologies, Band / Volume 160

D 61 (Diss., Düsseldorf, Univ., 2017)

ISSN 1866-1807
ISBN 978-3-95806-291-7

Vollständig frei verfügbar über das Publikationsportal des Forschungszentrums Jülich (JuSER)
unter www.fz-juelich.de/zb/openaccess.

„Ich drehte meinen Stuhl zum Feuer und fiel in einen Dämmerschlaf. Wieder tanzten die Atome vor meinen Augen. [...] lange Ketten, oft eng miteinander verbunden, waren alle in Bewegung, ineinander verschlungen, wanden sich wie Schlangen. Aber Achtung, was war das? Eine der Schlangen hatte ihren eigenen Schwanz gepackt und drehte sich vor meinen Augen spöttisch im Kreis. Blitzartig schreckte ich hoch.“

Friedrich August Kekulé von Stradonitz, 1829 - 1896

deutscher Chemiker und Naturwissenschaftler
(über die Entdeckung der Benzolstruktur im Traum)

Results presented in this thesis have been published in five original articles. Furthermore, a review article related to the topic of this thesis was published.

Kallscheuer, N., Vogt, M., Kappelmann, J., Krumbach, K., Noack, S., Bott, M., & Marienhagen, J. (2016). Identification of the *phd* gene cluster responsible for phenylpropanoid utilization in *Corynebacterium glutamicum*. *Applied Microbiology and Biotechnology*, 100(4): 1871-1881, permission to reuse in a thesis/dissertation: license number 4132670315887

Kallscheuer, N., Vogt, M., Stenzel, A., Gätgens, J., Bott, M., & Marienhagen, J. (2016). Construction of a *Corynebacterium glutamicum* platform strain for the production of stilbenes and (2*S*)-flavanones. *Metabolic Engineering* 38: 47-55, permission to reuse in a thesis/dissertation: license number 4132670510412

Kallscheuer, N., Gätgens, J., Lübcke, M., Pietruszka, J., Bott, M., & Polen, T. (2016). Improved production of adipate with *Escherichia coli* by reversal of β-oxidation. *Applied Microbiology and Biotechnology* 101: 2371-2382, permission to reuse in a thesis/dissertation: license number 4132680196229

Kallscheuer, N., Vogt, M., & Marienhagen, J. (2017). A novel synthetic pathway enables microbial production of polyphenols independent from the endogenous aromatic amino acid metabolism. *ACS Synthetic Biology* 6 (3): 410–415, reprinted with permission from ACS Synthetic Biology, Copyright American Chemical Society (2017), no license number required

Kallscheuer, N., Vogt, M., Bott, M., & Marienhagen, J. (2017). Functional expression of plant-derived *O*-methyltransferase, flavanone 3-hydroxylase, and flavonol synthase in *Corynebacterium glutamicum* for production of pterostilbene, kaempferol, and quercetin. *Journal of Biotechnology* 258: 190-196, permission to reuse in a thesis/dissertation: license number 4160690359006

Kallscheuer, N., Polen, T., Bott, M. & Marienhagen, J. (2017). Reversal of β-oxidation pathways for the microbial production of chemicals and polymer building blocks (review article), *Metabolic Engineering* 42: 33-42, permission to reuse in a thesis/dissertation: license number 4132680018186

Table of contents

Abstract

Plants synthesize a large diversity of more than 200,000 different secondary metabolites, which can be subdivided into terpenoids, alkaloids and polyphenols. Especially polyphenols demonstrate important pharmacological activities. Unfortunately, these compounds are produced only in small amounts rendering the extraction from plant material economically not viable. The natural synthesis of polyphenols such as stilbenes and flavonoids starts from phenylpropanoids, which in turn are obtained from aromatic amino acids. The main goal of this thesis was to exploit the yet untapped potential of *Corynebacterium glutamicum*, an industrial workhorse for amino acid production, for the synthesis of plant polyphenols by functional integration of heterologous pathways. To this end, the following results were obtained:

(1) Initial attempts to produce the stilbene resveratrol from the phenylpropanoid *p*-coumaric acid in *C. glutamicum* failed. It turned out that an unknown degradation pathway allowed *C. glutamicum* to grow with phenylpropanoids as sole carbon and energy source. The expression of a gene cluster coding for enzymes of unknown function was highly upregulated in presence of phenylpropanoids. It could be shown that the enzymes catalyze a CoA-dependent, β-oxidative side chain shortening of phenylpropanoids yielding benzoic acids, which are further degraded by well-characterized pathways in *C. glutamicum*. In addition to the identified pathway, the complex network for the degradation of aromatic compounds in *C. glutamicum* interfered with the desired production of polyphenols. To this end, a novel platform strain unable to degrade aromatic compounds (designated *C. glutamicum* DelAro^4) was constructed by deleting altogether 21 genes in four clusters in the genome.

(2) Plasmid-borne expression of genes coding for heterologous enzymes from different plant species enabled production of stilbenes (pinosylvin, resveratrol and piceatannol) as well as of (2*S*)-flavanones (naringenin and eriodictyol) depending on the supplemented phenylpropanoid in different strains derived from *C. glutamicum* DelAro^4. Stilbene and (2*S*)-flavanone titers of up to 158 mg/L and 37 mg/L could be achieved, respectively. The production of *O*-methylated stilbenes and of more complex flavonoids could be demonstrated by introduction of additional genes. The obtained product titers of the flavonols quercetin (10 mg/L) and kaempferol (23 mg/L) exceeded the highest titers produced in engineered microorganisms so far.

(3) Microbial production of resveratrol and naringenin with *C. glutamicum* could be achieved starting from glucose by deregulation of the shikimate pathway to achieve intracellular accumulation of aromatic precursor amino acids. A heterologous tyrosine ammonia lyase (TAL) connected the endogenous aromatic amino acid metabolism to the production of phenylpropanoid-derived polyphenols. The TAL activity was rate-limiting during polyphenol production from glucose. To circumvent the bottleneck at the stage of phenylpropanoid synthesis, a novel synthetic pathway for the production of the direct polyphenol precursor *p*-coumaroyl-CoA starting from the cheap 4-hydroxybenzoic acid was first designed *in silico* and then functionally introduced in *C. glutamicum*. The pathway is the non-natural reversal of a bacterial degradation pathway for phenylpropanoids and requires only acetyl-CoA and cofactors such as ATP and NADH. Initially, 5 mg/L resveratrol could be produced from 4-hydroxybenzoic acid using this novel pathway.

Zusammenfassung

Pflanzen synthetisieren mehr als 200.000 verschiedene Sekundärmetabolite, die aufgrund ihrer molekularen Struktur in die großen Gruppen der Terpenoide, Alkaloide und Polyphenole unterteilt werden können. Insbesondere Polyphenole haben pharmakologisch interessante Eigenschaften, werden aber von Pflanzen nur in so geringen Mengen produziert, dass eine Extraktion von Polyphenolen aus Pflanzenmaterial insgesamt unwirtschaftlich ist. Die Polyphenol-Synthese in Pflanzen startet von aromatischen Aminosäuren, aus denen zunächst Phenylpropanoide gebildet werden. Diese dienen dann als Vorstufen für die Synthese der Polyphenole. Durch funktionale Integration heterologer Stoffwechselwege aus Pflanzen können Polyphenole auch mit Hilfe genetisch veränderter Mikroorganismen produziert werden. *Corynebacterium glutamicum* ist ein vielversprechender Wirtsorganismus für die Polyphenol-Produktion, da er heutzutage bereits industriell zur Synthese von Aminosäuren genutzt wird. Im Rahmen dieser Arbeit wurden die folgenden Ergebnisse zur Polyphenol-Produktion mit *C. glutamicum* erzielt:

(1) Anfängliche Versuche zur Synthese des Stilbens Resveratrol aus dem Phenylpropanoid *p*-Cumarsäure scheiterten. Weitergehende Experimente zeigten, dass ein bisher unbekannter Abbauweg für Phenylpropanoide das Wachstum von *C. glutamicum* mit diesen aromatischen Substanzen als einziger Kohlenstoff- und Energiequelle ermöglichte und dadurch die Stilben-Bildung aus Phenylpropanoiden verhinderte. Untersuchungen der transkriptionellen Antwort von *C. glutamicum* auf die Anwesenheit von Phenylpropanoiden wiesen auf ein Gencluster hin, das für Enzyme bisher unbekannter Funktion codiert. Tatsächlich katalysieren diese Enzyme eine CoA-abhängige β-oxidative Verkürzung der Phenylpropanoid-Seitenkette zur Bildung von Hydroxybenzoesäuren, die über gut charakterisierte Abbauwege in *C. glutamicum* weiter verstoffwechselt werden können. Zusätzlich zum identifizierten Abbauweg erschwerte ein bereits weitestgehend bekanntes und komplexes Netzwerk aus anderen katabolen Stoffwechselwegen für aromatische Verbindungen in *C. glutamicum* die gewünschte Produktion von Polyphenolen in diesem Organismus. Durch Deletion von insgesamt 21 Genen in vier Genclustern im Genom wurde *C. glutamicum* DelAro^4 als Plattform-Stamm für die Polyphenol-Synthese konstruiert, der aromatische Verbindungen nicht mehr metabolisieren kann.

(2) Nach funktionaler Expression heterologer Gene aus verschiedenen Pflanzen produzierte *C. glutamicum* DelAro^4 abhängig vom zugegebenen Phenylpropanoid entweder die Stilbene Pinosylvin, Resveratrol und Piceatannol oder die (2*S*)-Flavanone Naringenin und Eriodictyol. Dabei wurden Stilben-Konzentrationen von bis zu 158 mg/L und (2*S*)-Flavanon-Konzentrationen von bis zu 37 mg/L erreicht. Durch Einbringen weiterer Gene gelang ebenfalls die Synthese *O*-methylierter Stilbene und komplexerer Flavonoide. Die in *C. glutamicum* erreichten Flavonoid-Titer waren sogar höher als in der Literatur für etablierte mikrobielle Polyphenol-Produktionsstämme beschrieben.

(3) Die Bildung von Resveratrol und Naringenin wurde in *C. glutamicum* auch ausgehend von Glucose ohne Zugabe von Vorläufermetaboliten erreicht. Dies wurde durch die Deregulation des Shikimat-Weges ermöglicht und führte zur Überproduktion von aromatischen Aminosäuren. Durch eine heterologe Tyrosin-Ammoniak-Lyase (TAL) konnte der endogene Aminosäuremetabolismus mit den Produktionswegen für Polyphenole verbunden werden. Es stellte sich heraus, dass die TAL-Aktivität für die Polyphenol-Produktion ausgehend von Glucose limitierend war. Um eine Phenylpropanoid-Synthese unabhängig von L-Tyrosin zu erreichen, wurde ein neuer synthetischer Weg ausgehend von der kostengünstigen 4-Hydroxybenzoesäure entwickelt und in *C. glutamicum* getestet. Der neue Weg stellt die nicht-natürliche Umkehrung eines bakteriellen Abbauweges für Phenylpropanoide dar und benötigt Acetyl-CoA und die Cofaktoren ATP und NADH. Erstmalig gelang so die Produktion von 5 mg/L Resveratrol aus 4-Hydroxybenzoesäure.

Abbreviations

Ω	Ohm
4CL	4-coumarate: CoA ligase
4-HBA	4-hydroxybenzoic acid
4-HPP	3-(4-hydroxyphenyl)propionic acid
A	Ampere
ACC	acetyl-CoA carboxylase
ADH	arogenate dehydrogenase
ADP	adenosine diphosphate
AMP	adenosine monophosphate
AT	aminotransferase
ATCC	American Type Culture Collection
ATP	adenosine triphosphate
BHI	brain heart infusion medium
bp	base pair
BTX	benzene, toluene, xylene
C4H	cinnamate 4-hydroxylase
CHI	chalcone isomerase
CHS	chalcone synthase
CM	chorismate mutase
CoA	coenzyme A
CS	chorismate synthase
DAHP	3-deoxy-D-arabino-heptulosonate-7-phosphate
DHQ	3-dehydroquinate
DHQD	3-dehydroquinate dehydratase
DHQS	3-dehydroquinate synthase
DHS	3-dehydroshikimate
DS	3-deoxy-D-arabino-heptulosonate-7-phosphate synthase
E4P	erythrose-4-phosphate
EPSP	5-enolpyruvylshikimate-3-phosphate
EPSPS	5-enolpyruvylshikimate-3-phosphate synthase
ESI	electro spray ionization
et al.	(lat.) *et alii*
F	Farad
F3H	flavanone 3-hydroxylase
FLS	flavonol synthase
GC-TOF	gas chromatography coupled to time-of-flight (mass spectrometry)
IPTG	isopropyl-β-D-thiogalactopyranoside
Kan	kanamycin
LB	lysogeny broth
LC-MS	liquid chromatography coupled to mass spectrometry
M	molar (mol/L)
MALDI-TOF	matrix-assisted laser desorption ionization time-of-flight (mass spectrometry)
NAD	nicotinamide adenine dinucleotide
Ni-NTA	nickel-nitrilotriacetic acid
nt	nucleotide
OD	optical density

OMT	resveratrol-di-*O*-methyltransferase
ORF	open reading frame
PAL	phenylalanine ammonia lyase
PCR	polymerase chain reaction
PDH	prephenate dehydrogenase
PDT	prephenate dehydratase
PEP	phosphoenolpyruvate
L-Phe	L-phenylalanine
P_i	inorganic phosphate
PP_i	pyrophosphate
rbs	ribosomal binding site
ROS	reactive oxygen species
rpm	revolutions per minute
SAM	*S*-adenosylmethionine
SCS	succinyl-CoA synthetase
SDH	shikimate dehydrogenase
SDS-PAGE	sodium dodecyl sulfate - polyacrylamide gel electrophoresis
SHK	shikimate kinase
Spec	spectinomycin
STS	stilbene synthase
TAL	tyrosine ammonia lyase
TFA	trifluoroacetic acid
L-Trp	L-tryptophan
L-Tyr	L-tyrosine
U	enzymatic activity unit (1 U = 1 µmol/min)
uHPLC	ultra-high performance liquid chromatography
w/v	weight per volume
wt	wild type

1. Scientific context and key results of this thesis

1.1 Polyphenols are secondary metabolites in plants

Plants produce a large diversity of secondary metabolites, allowing the plant to interact with its biotic and abiotic environment. The ecological significance of these metabolites includes defense against pathogens or against herbivores, attraction of pollinators or protection against UV radiation and oxidative stress. Based on different synthesis pathways and chemical structures of these compounds, secondary metabolites are subdivided into three major classes: terpenoids, alkaloids and polyphenols. The presence of individual compounds and the natural amount within the three classes of secondary metabolites strongly depends on the plant family and can even significantly differ between species of the same family. Taken together, more than 200,000 different secondary metabolites are known today (Yonekura-Sakakibara and Saito, 2009).

Hydroxylated aromatic secondary metabolites in plants typically belong to the class of polyphenols. Two major groups of plant polyphenols are stilbenes and flavonoids. Stilbenes (also called stilbenoids) are hydroxylated derivatives of the compound stilbene (1,2-diphenylethene). The tricyclic (2*S*)-flavanones contain two aromatic rings and a 2,3-dihydro-4-pyrone unit (Fig. 1). A clear classification of a compound as polyphenol is complicated as there are different definitions of the term “polyphenol”. “Poly-” can either refer to the number of phenolic hydroxy groups in a molecule (definition I) or to the presence of two or more “phenol” units (definition II). According to definition I also dihydroxylated benzoic acids such as protocatechuate (3,4-dihydroxybenzoate) belong to the class of polyphenols, while definition II requires the presence of at least two hydroxylated aromatic rings in the molecule. The situation is particularly difficult in case of the stilbene pinosylvin or the (2*S*)-flavanone pinocembrin, which both are derived from the non-hydroxylated phenylpropanoid cinnamic acid. Both are classified as polyphenols (as they belong to the class of stilbenes or flavonoids) although they contain hydroxy groups only on one of the two aromatic rings.

Polyphenols (especially flavonoids) have strong anti-oxidative properties. These effects result from direct scavenging of radicals in reactive oxygen species (ROS), while chelating of iron can contribute to reduced ROS formation (Nijveldt et al., 2001). Polyphenols are also involved in the inhibition of ROS-forming enzymes (e.g. xanthine oxidase) and are capable to recycle other antioxidants (Mierziak et al., 2014). As a result of the mentioned effects, polyphenols contribute to the protection of the photosynthesis machinery and the balancing of the redox status in plants. In addition, flavonoids serve as plant pigments or flavor

substances (Siemann and Creasy, 1992). Stilbenes are phytoalexins, which are produced as metabolic response to infections (Ahuja et al., 2012).

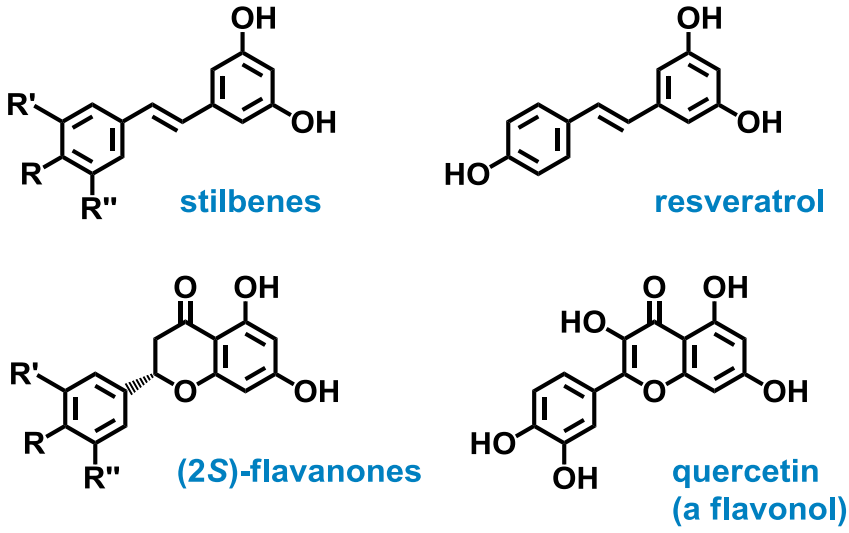

Fig. 1 Structure of stilbenes and flavonoids. Stilbenes and (2*S*)-flavanones (left) constitute the two major groups of phenylpropanoid-derived polyphenols (R = H or OH; R' = H, OH or OCH_3; R'' = H, OH or OCH_3). Resveratrol and quercetin (right) are representatives which are already commercially available.

Especially due to the potent anti-oxidative effects, many polyphenols demonstrate health-promoting activities in humans rendering these compounds highly interesting for pharmacological applications (Manach et al., 2004; Harborne and Mabry, 2013). A prominent example is the consumption of wine. Grapes contain significant amounts of the stilbene resveratrol, which acts as a potent antioxidant. It was speculated that resveratrol might be one of the factors responsible for the low incidence of cardiovascular diseases in the French population despite having a fat-rich diet (also known as “French paradox”) (Yang et al., 2014). In several studies, other polyphenols were shown to have anti-bacterial, anti-inflammatory, anti-tumor and anti-aging effects and thus play an important role in the prevention of cancer, cardiovascular and neurodegenerative diseases (Erlund, 2004; Pangeni et al., 2014).

1.2 Access to polyphenols

It is generally assumed that the daily consumption of fruits and vegetables does not lead to a polyphenol intake in amounts, which would be required for causing the desired health-promoting effects. Therefore, today some polyphenols are already commercially available as food supplements, *e.g.* the stilbene resveratrol and the flavonoid quercetin (Fig. 1). Resveratrol is typically extracted from Japanese knotweed (*Polygonum cuspidatum*) and is available as capsule with 100-500 mg resveratrol *e.g.* supplied by Natural Power Trading Ltd. (West Sussex, Great Britain) or McVital (EYVA C.V., Kerkrade, The Netherlands). Quercetin is typically extracted from onion (*Allium cepa*) or from the Japanese pagoda tree (*Sophora japonica*). Capsules containing 200-500 mg quercetin are available from LifeExtension (Fort Lauderdale, Florida, USA) or from ZeinPharma Germany GmbH (Nauheim, Germany). The recommended daily intake of one capsule with the above-mentioned amount of resveratrol or quercetin corresponds to a price ranging from 0.15 to 0.30 €. Nearly all of the commercially available polyphenol-containing food supplements contain bioactive compounds which are directly extracted from plant material.

Unfortunately, in many cases the low abundance of polyphenols in plants hinders their extraction in sufficient amounts. The natural polyphenol amount strongly varies depending on the plant species, the season and the geographical location. Especially phytoalexins such as stilbenes are not produced at constant rates but only in response to infections, which renders it even more challenging to isolate these compounds. A second challenge is the isolation of individual compounds of a complex mixture of chemically very similar polyphenols in the plant extracts. Instead of extraction from plant material, a chemical total synthesis of interesting polyphenols could serve as an attractive alternative source. However, due to the complexity of polyphenols the synthesis includes multiple reaction steps, the use of toxic chemicals and requires purification to remove undesired by-products (Quideau et al., 2011). Synthesis of more complex polyphenols even requires stereo- and regioselective reaction steps, which renders an economical synthesis in most cases unfeasible.

When considering the disadvantages and technical challenges of the natural extraction or chemical synthesis of polyphenols, it appears that the production with microorganisms is the only remaining source for valuable polyphenols. Microorganisms can reach high growth rates and biomass yields, can be easily cultivated in defined media and the production process can be easily up-scaled. As plant-derived polyphenols are not naturally produced by microorganisms, this production strategy requires genetic engineering of the host strain by functional integration of the heterologous pathways from plants. The prerequisite for strain engineering is the availability of detailed information on the required enzymatic activities and

the metabolic pathways involved in the natural polyphenol synthesis. This also includes the identification of the respective plant genes coding for enzymes showing the required activities. Polyphenols are derived from the aromatic amino acids L-phenylalanine (L-Phe) and L-tyrosine (L-Tyr), both compounds, which are already naturally synthesized by microorganisms for protein biosynthesis.

1.3 Plant metabolic pathways leading to polyphenols

The aromatic amino acid L-Phe is the major precursor for the synthesis of polyphenols in plants. L-Phe is first deaminated to the phenylpropanoid cinnamic acid in a non-oxidative manner by the activity of phenylalanine ammonia lyase (PAL) (MacDonald and D'Cunha, 2007) (Fig. 2). Cinnamic acid consists of a benzene ring attached to a propionic acid side chain containing a double bond between C2 and C3, which is formed during the deamination reaction. Cinnamic acid can be hydroxylated in *para*-position by the activity of the cytochrome P450-dependent enzyme cinnamate 4-hydroxylase (C4H) yielding the phenylpropanoid *p*-coumaric acid. PAL enzymes often have low side activities with L-Tyr to produce *p*-coumaric acid directly without the need for C4H activity. Some bacteria also produce secondary metabolites starting from phenylpropanoids. Therefore, they possess tyrosine ammonia lyases (TAL), which convert L-Tyr to *p*-coumaric acid (Jendresen et al., 2015). These enzymes can exhibit much higher activity with L-Tyr compared to L-Phe, which allows for bypassing C4H-mediated hydroxylation of L-Phe. In plants, further hydroxylation or *O*-methylation reactions of phenylpropanoids can occur, giving rise to more complex phenylpropanoids substituted in *meta*- and *para*-position (indicated by R, R' and R'' in Fig. 2) (Inoue et al., 1998; Humphreys and Chapple, 2002).

The enzyme 4-coumarate: CoA ligase (4CL) is able to catalyze the ATP-dependent CoA-ligation to phenylpropanoids (Fig. 2). The phenylpropanoid CoA-thioesters are used as substrates by two different classes of enzymes, stilbene synthase (STS) or chalcone synthase (CHS), both of which are class III polyketide synthases (Tropf et al., 1994). Both enzymes use three molecules of malonyl-CoA to convert the phenylpropanoid CoA-thioester into a tetraketide intermediate. By following different reaction mechanisms, a second aromatic ring is formed from the tetraketide giving rise to either stilbenes (catalyzed by STS) or chalcones (catalyzed by CHS) (Austin et al., 2004) (Fig. 2). Chalcones are subsequently isomerized to (2*S*)-flavanones by the activity of a chalcone isomerase (CHI). The isomerization reaction leads to the formation of an aliphatic heterocyclic ring in the (2*S*)-flavanone connecting the two aromatic rings.

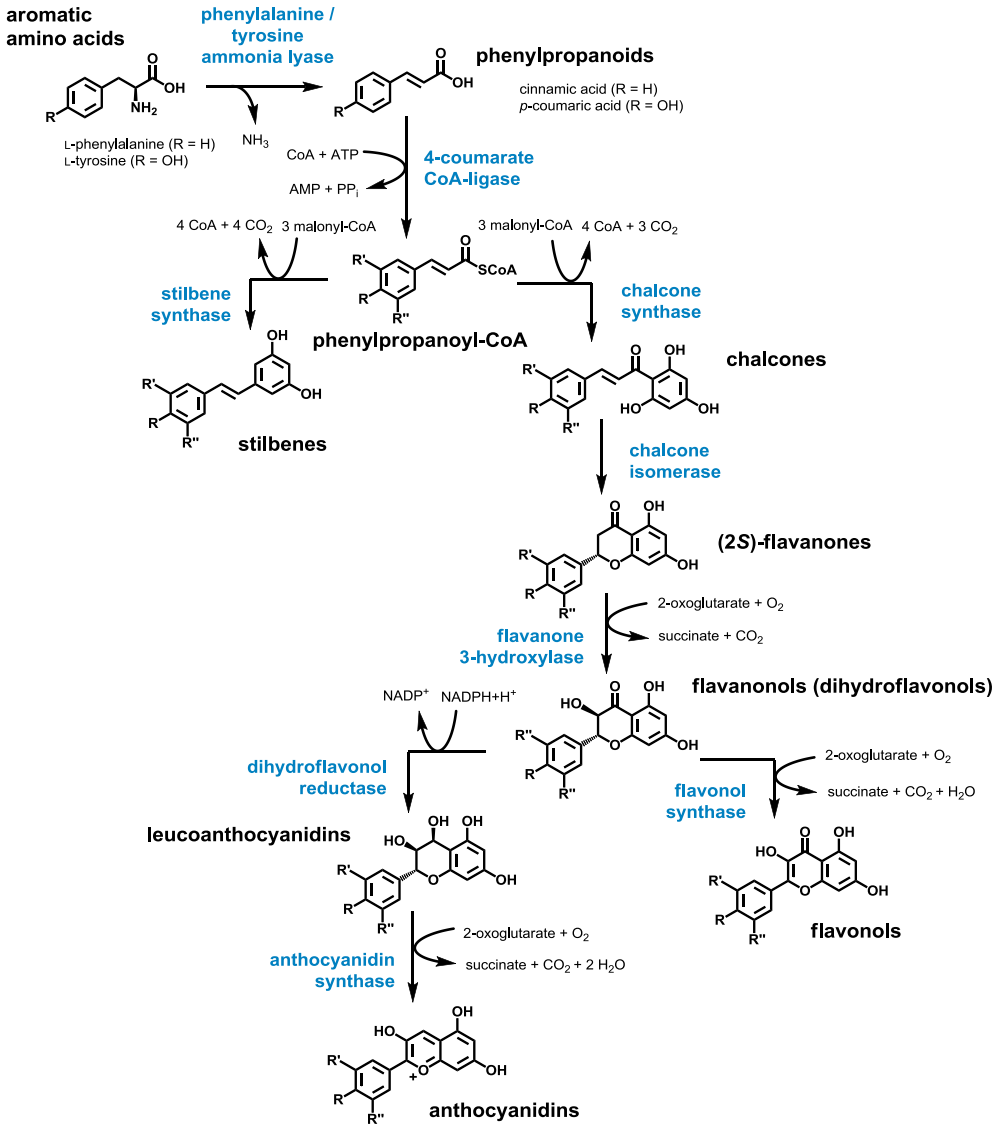

Fig. 2 Schematic overview of biosynthetic pathways leading to different polyphenols in plants. Polyphenols are phenylpropanoid-derived compounds of the secondary plant metabolism. The phenylpropanoids cinnamic acid and *p*-coumaric acid are synthesized from L-Phe and L-Tyr by non-oxidative deamination by phenylalanine ammonia lyases or tyrosine ammonia lyases. The benzene ring in phenylpropanoids can be further modified by hydroxylation and *O*-methylation in *meta*- and *para*-position (shown as R, R' and R'') by plant hydroxylases and *O*-methyltransferases. In the subsequent step, phenylpropanoids undergo CoA-ligation by 4-coumarate: CoA ligase activity. Phenylpropanoyl-CoA thioesters are converted to stilbenes by stilbene synthase or to chalcones by chalcone synthase. Both enzymes catalyze chain elongation of the starter phenylpropanoyl-CoA using three molecules of malonyl-CoA and subsequent circularization reactions. Chalcones are further isomerized to (2*S*)-flavanones. The activity of plant 2-oxoglutarate-dependent dioxygenases and NADP-dependent reductases gives rise to the shown classes of flavonoids.

The (2*S*)-flavanone backbone can be further modified by hydroxylation and reduction giving rise to flavanonols (dihydroflavonols), flavonols, and anthocyanidins (all belonging to the family of flavonoids) (Fig. 2).

Stilbenes and flavonoids contain at least two hydroxy groups, which are directly attached to aromatic rings. These hydroxy groups can be decorated with methyl-, acetyl-, other acyl-, or glycosyl-residues, which gives rise to an impressive diversity of polyphenols (Harborne and Mabry, 2013). Mostly acyltransferases and glycosyltransferases are responsible for the decoration of polyphenols in plants (Ross et al., 2001; D'Auria, 2006). Decoration contributes to increased stability or increased solubility in aqueous environments (Plaza et al., 2014). In this context, *O*-methylation of stilbenes was also found to be responsible for increased bioavailability in human cells compared to their non-methylated form (McCormack and McFadden, 2012).

1.4 Current state of polyphenol production in engineered microorganisms

Until now, microbial production of plant polyphenols focused exclusively on using *Escherichia coli* and *Saccharomyces cerevisiae* as production hosts (Marienhagen and Bott, 2013). The two-step pathway including 4-coumarate: CoA ligase and stilbene synthase was used for stilbene production starting from phenylpropanoids. In most cases, resveratrol was produced from supplemented *p*-coumaric acid (Lim et al., 2011; Shin et al., 2011). By following the same metabolic strategy, engineered *E. coli* strains also converted cinnamic acid and caffeic acid into the stilbenes pinosylvin and piceatannol, respectively (van Summeren-Wesenhagen and Marienhagen, 2015; Wang et al., 2015). The heterologous expression of genes coding for 4-coumarate: CoA ligase, chalcone synthase and chalcone isomerase enabled production of the (2*S*)-flavanones pinocembrin (from cinnamic acid) or naringenin (from *p*-coumaric acid) (Kaneko et al., 2003; Yan et al., 2005). Production strains of *E. coli* and *S. cerevisiae* additionally expressing heterologous genes coding for phenylalanine ammonia lyase and tyrosine ammonia lyase were capable to produce stilbenes and (2*S*)-flavanones from L-Phe or L-Tyr (Shin et al., 2012; Wu et al., 2013b; Zhu et al., 2014).

With the aim to overcome the need for feeding of expensive precursors, *E. coli* and *S. cerevisiae* were additionally engineered towards overproduction of aromatic amino acids. Aromatic amino acids are produced by the shikimate pathway, which is tightly controlled at the stage of gene expression and by feedback-regulation of the involved enzymes (Braus, 1991; Kikuchi et al., 1997). To achieve overproduction of L-Phe and L-Tyr, feedback-resistant enzymes were introduced and genes coding for enzymes catalyzing rate-limiting steps were

overexpressed. Application of these strategies in strains with functional polyphenol pathways led to the *de novo* synthesis of stilbenes and (2*S*)-flavanones (Wu et al., 2014; Li et al., 2015). Until today, also more complex polyphenols such as decorated stilbenes and flavonoids were successfully produced in engineered microorganisms (Kang et al., 2014; Kim et al., 2015; Cress et al., 2017).

Efforts to increase the titers of polyphenols focused on engineering of the host metabolism, especially in *E. coli* (Leonard et al., 2007; Fowler et al., 2009; Chemler et al., 2010). Thereby, rate-limiting steps during production were identified. The low intracellular availability of malonyl-CoA is the major bottleneck during production in *E. coli* (Leonard et al., 2007; Zha et al., 2009; Lim et al., 2011). Three molecules of malonyl-CoA per molecule polyphenol are required (Fig. 2). In bacteria and yeast, malonyl-CoA is exclusively consumed during fatty acid synthesis. The endogenous supply of malonyl-CoA by carboxylation of acetyl-CoA is tightly regulated and low intracellular levels of malonyl-CoA are maintained (Hasslacher et al., 1993; Davis et al., 2000). Fatty acid synthesis-inhibiting antibiotics such as cerulenin increased the production of polyphenols in engineered microorganisms because malonyl-CoA consumption for fatty acid synthesis is reduced and thus becomes available for polyphenol synthesis (Santos et al., 2011; van Summeren-Wesenhagen and Marienhagen, 2015). Unfortunately, the presence of cerulenin also abolishes the growth of the host organism as a result of the rapid depletion of fatty acids. In addition, cerulenin is very expensive and thus cost-efficient upscaling of the production process with cerulenin supplementation is not feasible. As an alternative strategy to increase the intracellular malonyl-CoA availability, genes coding for acetyl-CoA carboxylase (ACC) were overexpressed. ACC catalyzes the ATP-dependent carboxylation of acetyl-CoA to malonyl-CoA. In most cases, the genes coding for the heterodimeric ACC from *Corynebacterium glutamicum* were introduced into polyphenol-producing strains (Miyahisa et al., 2005; Katsuyama et al., 2007; Zha et al., 2009; van Summeren-Wesenhagen and Marienhagen, 2015). A malonate: CoA ligase involved in the malonate utilization pathway of *Rhizobium trifolii* was introduced into *E. coli* to increase the intracellular malonyl-CoA availability (Leonard et al., 2008; Wu et al., 2013a). Although this strategy was suitable for increased polyphenol production, it requires the supplementation of malonate as precursor.

The activity of the heterologous TAL converting L-Tyr to *p*-coumaric acid was recognized as another bottleneck during polyphenol production (Lin and Yan, 2012; Eudes et al., 2013). Several highly active TAL enzymes with a substrate specificity for L-Tyr were identified, but application of these enzymes did not boost microbial polyphenol production (Jendresen et al., 2015). Possible reasons for the limitation of product formation at this point in the heterologous biosynthetic pathways have not been identified yet.

1.5. *Corynebacterium glutamicum* as novel host strain for polyphenol production?

1.5.1 *C. glutamicum* and its industrial relevance

C. glutamicum is a Gram-positive, non-motile, non-pathogenic, biotin-auxotrophic soil actinobacterium, which was isolated in Japan during a screening campaign for identifying glutamate-producing bacteria in 1956 (Kinoshita et al., 1957). *C. glutamicum* grows in defined media with relatively high growth rates and reaches high cell densities, rendering this organism an industrial workhorse in white biotechnology (Eggeling and Bott, 2005). A large set of tools for genetic engineering of *C. glutamicum* including plasmids and strong promoters is available (Pátek and Nešvera, 2013). This enabled the construction of tailor-made strains for the industrial production of compounds with commercial relevance. Products obtained with *C. glutamicum* have GRAS ("generally recognized as safe") status. Optimized strains are currently used for the production of up to 3.0 million tons of the flavor enhancer L-glutamate and 2.2 million tons of the feed additive L-lysine per year (Becker et al., 2011; Wendisch et al., 2014). Beyond, engineered strains mainly for the production of organic acids (ketoisovalerate, shikimate), polymer precursors (succinate, lactate, cadaverine, putrescine, itaconate) and biofuels (ethanol, isobutanol, 1,2-propanediol, 3-methyl-1-butanol, 2-methyl-1-butanol) are available (Inui et al., 2005; Krause et al., 2010; Becker and Wittmann, 2012; Yamamoto et al., 2013; Heider and Wendisch, 2015; Otten et al., 2015; Siebert and Wendisch, 2015; Tsuge et al., 2015; Kogure et al., 2016; Vogt et al., 2016).

Due to its capability to produce a wide range of different industrially relevant compounds, *C. glutamicum* is also a very promising host for the production of plant polyphenols. The cost-efficient production of polyphenols in microorganism does not only require a functional introduction of the respective heterologous pathways from plants, but also engineering of the carbon metabolism of the host strain towards sufficient supply of relevant precursor metabolites. In case of polyphenols the shikimate pathway is important as it provides the aromatic amino acids L-Phe and L-Tyr, which represent the precursors of polyphenols.

Already in the 1970s, *C. glutamicum* was used for the production of aromatic amino acids, in particular L-tryptophan (L-Trp) (Hagino and Nakayama, 1975). Aromatic amino acid-producing strains were obtained from iterative cycles of mutagenesis and screening because detailed information on the regulation of the shikimate pathway in *C. glutamicum* was not available (Ikeda, 2006). Development of genetic tools such as expression plasmids allowed for rational metabolic engineering of improved production strains for aromatic amino acids (Ikeda and Katsumata, 1992; Ikeda et al., 1993; Eggeling and Bott, 2005). In the course of improving already existing production strains the shikimate pathway in *C. glutamicum* was

investigated in much detail (Ikeda and Katsumata, 1992; Katsumata and Ikeda, 1993). In a more recent study, production of L-Phe was achieved starting from the *C. glutamicum* wild-type strain by introduction of heterologous genes from *E. coli* (Zhang et al., 2013).

1.5.2 Reactions and regulation of the shikimate pathway in *C. glutamicum*

The first committed step of the shikimate pathway for biosynthesis of all three aromatic amino acids is the condensation of phosphoenolpyruvate (PEP) and the pentose phosphate pathway metabolite erythrose-4-phosphate (E4P) yielding 3-deoxy-D-arabinoheptulosonate-7-phosphate (DAHP). This reaction is catalyzed by DAHP synthase (DS) (Fig. 3). DAHP is circularized by the enzyme 3-dehydroquinate synthase (DHQS) giving rise to 3-dehydroquinate (DHQ), a highly substituted cyclohexanone derivative. 3-Dehydroquinate dehydratase (DHQD) catalyzes the elimination of water from DHQ yielding 3-dehydroshikimate (DHS), thereby introducing the first double bond into the ring. Four enzymatic reactions convert DHS to chorismate (Fig. 3). The chorismate-forming reaction catalyzed by chorismate synthase (CS) includes dephosphorylation, thereby introducing a second double bond into the ring.

Chorismate is the first branching point for the synthesis of either L-Phe/L-Tyr or L-Trp. The biosynthesis of L-Trp from chorismate requires six reaction steps, which are not described in more detail here. For the synthesis of L-Phe and L-Tyr the enzyme chorismate mutase (CM) converts chorismate to prephenate (Fig. 3). Prephenate undergoes decarboxylation and dehydration yielding phenylpyruvate or is oxidatively decarboxylated to 4-hydroxyphenyl-pyruvate. The reactions are catalyzed by prephenate dehydratase (PDT) and prephenate dehydrogenase (PDH), respectively. The ultimate step comprises the transamination of phenylpyruvate to L-Phe and of 4-hydroxyphenylpyruvate to L-Tyr and is catalyzed by an aminotransferase (AT). For the biosynthesis of L-Tyr in *C. glutamicum* prephenate is first transaminated to arogenate (pretyrosine), which is then oxidatively decarboxylated to L-Tyr in a second step (Fazel and Jensen, 1979). The last steps leading to L-Tyr in *C. glutamicum* are rather unusual (although not restricted to coryneform bacteria), therefore both routes are shown in Fig. 3.

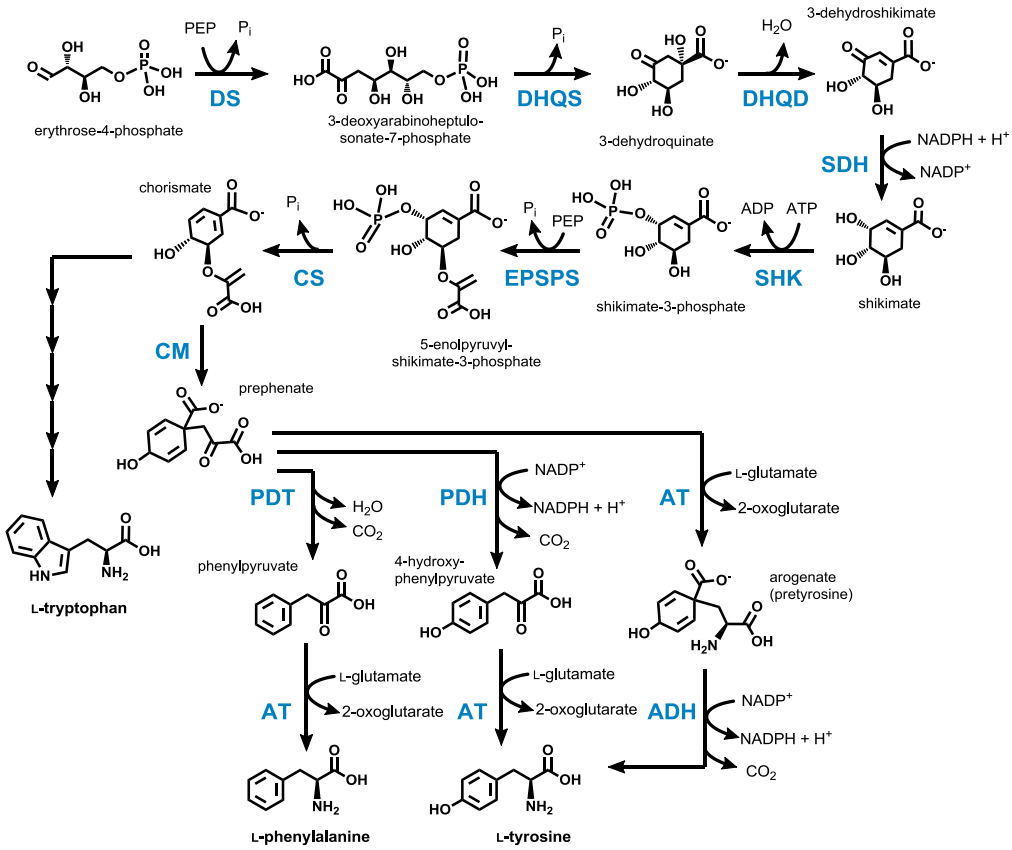

Fig. 3 Biosynthesis of aromatic amino acids by the shikimate pathway. The three aromatic amino acids L-Phe, L-Tyr, and L-Trp are synthesized by the shikimate pathway, which requires erythrose-4-phosphate and two molecules of phosphoenolpyruvate (PEP) as substrates. Abbreviations: DS: 3-deoxy-D-arabinoheptulosonate-7-phosphate synthase, DHQS: dehydroquinate synthase, DHQD: dehydroquinate dehydratase, SDH: shikimate dehydrogenase, SHK: shikimate kinase, EPSPS: 5-enolpyruvylshikimate-3-phosphate synthase, CS: chorismate synthase, CM: chorismate mutase, PDT: prephenate dehydratase, PDH: prephenate dehydrogenase, AT: aminotransferase, ADH: arogenate dehydrogenase. In *C. glutamicum*, L-Tyr is synthesized *via* arogenate whereas it is typically produced from 4-hydroxyphenylpyruvate in most other organisms (including *E. coli*).

In *C. glutamicum*, the shikimate pathway is regulated at the stage of transcription and mainly by feedback-regulation of the involved enzymes (Ikeda, 2006). The regulation of gene expression mainly affects the L-Trp branch (reaction steps from chorismate to L-Trp). The regulator LtbR was shown to inhibit the expression of the operon *trpEGDCFBA* in presence of L-Trp (Brune et al., 2007). The genes coding for the other enzymes of the shikimate pathway are either expressed constitutively or the regulation is not known. The regulation of

the genes *qsuC* and *qsuD* coding for dehydroquinate dehydratase and shikimate dehydrogenase is a special case. The operon *qsuCD* is expressed constitutively, but the expression of the operon *qsuABCD* also comprising *qsuA* and *qsuB* is activated by the regulator QsuR (Kubota et al., 2014). The reactions catalyzed by QsuC and QsuD are also part of a catabolic pathway for shikimate and quinate, which is described in more detail at the end of this chapter.

The major points of feedback-regulation at the enzyme activity level include the initial committed step catalyzed by DAHP synthase and the reaction catalyzed by chorismate mutase at the first branching point of the pathway. *C. glutamicum* has two DAHP synthase isoenzymes catalyzing the synthesis of DAHP, designated AroF and AroG. Interestingly, deletion of *aroG* abolished growth in mineral medium, while deletion of *aroF* did not lead to any observable phenotype (Liu et al., 2008). It was concluded that AroG rather than AroF is involved in the synthesis of aromatic amino acids in *C. glutamicum*. AroF is feedback-regulated by L-Tyr and to a much lesser extent by L-Phe and L-Trp. AroG is inhibited by L-Trp, but not by L-Tyr and L-Phe (Liu et al., 2008). AroG was found to physically interact with the chorismate mutase (CM) in *C. glutamicum*. The interaction stimulates the DAHP synthase activity of AroG. In the protein complex AroG-CM, AroG is allosterically regulated by chorismate and prephenate, which represent substrate and product of the reaction catalyzed by the chorimate mutase (Li et al., 2009; Li et al., 2013). The chorismate mutase activity is not inhibited by the presence of any of the three aromatic amino acids (Li et al., 2009).

Additionally, *C. glutamicum* contains a catabolic pathway for quinate and shikimate allowing growth using these compounds as sole carbon and energy source (Teramoto et al., 2009). It was found that the anabolic shikimate pathway for the synthesis of aromatic amino acids and the catabolic pathway for quinate and shikimate overlap at the stage of 3-dehydroshikimate. Intracellular chorismate was identified as an inducer for the expression of genes coding for enzymes of the catabolic pathway (Kubota et al., 2014). An increased concentration of metabolites of the (anabolic) shikimate pathway activates the catabolic pathway, which leads to the synthesis of the hydroxybenzoic acid protocatechuate from 3-dehydroshikimate. This reaction is catalyzed by the 3-dehydroshikimate dehydratase QsuB. Protocatechuate is further degraded to succinyl-CoA and acetyl-CoA by the β-ketoadipate pathway in *C. glutamicum* (Shen and Liu, 2005) (Fig. 4). This not only allows the use of quinate and shikimate as an additional carbon source, but also avoids loss of carbon and energy by an undesired overproduction of aromatic amino acids. Taken together, the shikimate pathway in *C. glutamicum* is controlled at three levels: gene expression, enzymatic activity (allosteric control) and metabolic flux.

1.5.3 Exploitation of *C. glutamicum* for the production of aromatic compounds

Surprisingly, apart from aromatic amino acids, there are only a few examples for the production of additional aromatic compounds in *C. glutamicum* and all relevant studies were published in the last two years (Lee and Wendisch, 2016). Metabolic engineering towards aromatic compound production in *C. glutamicum* focused on the deregulation of the shikimate pathway together with increased flux into the pentose phosphate pathway for supply of the precursor E4P. The combination of both strategies enabled the overproduction of shikimate in *C. glutamicum* (Kogure et al., 2016). Although shikimate itself is not an aromatic compound, the constructed strains represent a suitable basis for the production of aromatic compounds, which can be derived from the shikimate pathway. One recent example is the production of *p*-aminobenzoate in engineered *C. glutamicum* strains overproducing the precursor chorismate (Kubota et al., 2016). In another recent study, production of the hydroxylated benzoic acids protocatechuate and 4-hydroxybenzoate was demonstrated in *C. glutamicum* (Okai et al., 2016). *C. glutamicum* is recognized as a suitable host because it shows a pronounced resistance to aromatic compounds (Liu et al., 2013). However, a complex network for the degradation of aromatic compounds in this organism averted the attention of using *C. glutamicum* for the production of aromatic compounds. This might explain why only few such compounds were produced with this organism until today. Interestingly, any degradation of aromatic amino acids was not observed in this organism.

1.5.4 Degradation of aromatic compounds in *C. glutamicum*

Aromatic compounds are very abundant in environments such as water or soil. Several microorganisms (including *C. glutamicum*) are capable of degrading aromatic compounds, not only for detoxification purposes, but also to simply use them as carbon and energy sources (Fuchs et al., 2011). The underlying degradation pathways for aromatic compounds are often subdivided into peripheral and central pathways (Shen et al., 2012). In general, the central pathways are responsible for cleavage of the aromatic ring(s) and conversion of the resulting linearized molecules into metabolites of the central carbon metabolism. In most cases hydroxylated benzoic acids serve as direct substrates for the central degradation pathways. The more diverse peripheral pathways are essential for the conversion of more complex and substituted aromatics into compounds, which can be further degraded by the central catabolic pathways.

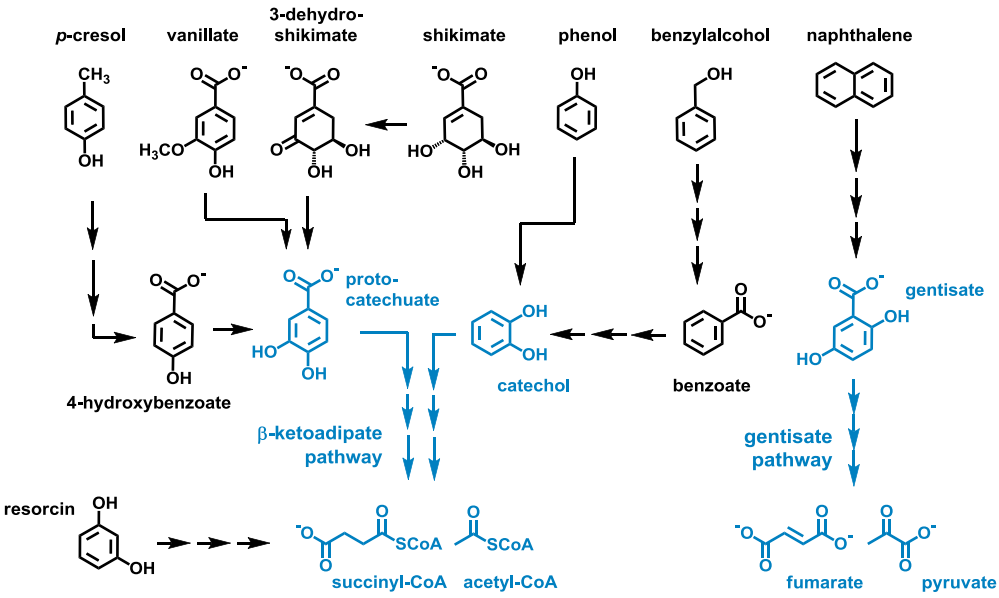

Fig. 4 Degradation of aromatic compounds in *C. glutamicum*. *C. glutamicum* is capable to use the depicted aromatic compounds as sole carbon and energy source. Peripheral degradation pathways (shown in black) convert the aromatic substrates to protocatechuate, catechol or gentisate, which are then further converted to metabolites of the central carbon metabolism using central degradation pathways (β-ketoadipate pathway or gentisate pathway, shown in blue). Protocatechuate can also be synthesized from the shikimate pathway intermediate 3-dehydroshikimate. Three arrows indicate multiple reactions steps required for degradation.

A central degradation pathway for the catabolism of aromatic compounds in *C. glutamicum* is the β-ketoadipate pathway (Harwood and Parales, 1996). The two branches of this pathway are required to degrade either catechol (1,2-dihydroxybenzene) or protocatechuate (3,4-dihydroxybenzoate) (Fig. 4). Both substrates contain two hydroxy groups in *ortho*-position, which are essential for the required (intradiol) ring fission reaction. Catechol 1,2-dioxygenase and protocatechuate-3,4-dioxygenase use dioxygen to catalyze the cleavage of catechol and protocatechuate yielding the linearized molecules *cis*,*cis*-muconate and 3-carboxy-*cis*,*cis*-muconate, respectively (Knoot et al., 2015). Further reactions in the β-ketoadipate pathway convert both intermediates into β-ketoadipyl-CoA, which is finally cleaved yielding succinyl-CoA and acetyl-CoA (Shen and Liu, 2005). The gentisate pathway is the second central degradation pathway in *C. glutamicum*, responsible for the degradation of gentisate (2,5-dihydroxybenzoate) yielding fumarate and pyruvate (Shen et al., 2005) (Fig. 4).

In *C. glutamicum*, several peripheral pathways have been identified. These pathway enable the degradation of one ring-aromatics (*e.g.* phenol, vanillate, 4-hydroxybenzoate, resorcinol,

benzyl alcohol and *p*-cresol), but also of more complex aromatics such as naphthalene and of the shikimate pathway intermediates shikimate and 3-dehydroquinate (Merkens et al., 2005; Shen et al., 2012; Kubota et al., 2014; Du et al., 2016) (Fig. 4). Taken together, *C. glutamicum* is capable to degrade a large variety of aromatic compounds (except for aromatic amino acids).

1.6 From degradation to production - Engineered reversal of β-oxidative pathways

β-Oxidation is the common biochemical strategy for the shortening of ubiquitous fatty acid carbon chains (Schulz, 1991). Interestingly, this metabolic principle is not restricted to the degradation of fatty acids but is also the basis for several microbial catabolic pathways for aromatic compounds (Biegert et al., 1996; Harrison and Harwood, 2005; Trautwein et al., 2012). β-Oxidative pathways comprise a conserved cascade of five enzyme-catalyzed reaction steps (Fig. 5). In the first reaction the carboxylic acid is converted to the respective CoA-thioester by ATP-dependent CoA-ligases (also referred to as acyl-CoA synthetases) (gray route in Fig. 5). The CoA-activated carboxylic acid (acyl-CoA) is oxidized, thereby a *trans*-2,3-double bond is introduced. This reaction is catalyzed by FAD-dependent acyl-CoA dehydrogenases. The double bond in the resulting *trans*-2,3-enoyl-CoA can be used by enoyl-CoA hydratases to introduce a water molecule yielding 3-hydroxyacyl-CoA. The hydroxy group is subsequently oxidized to a keto group by 3-hydroxyacyl-CoA dehydrogenases, forming 3-oxoacyl-CoA from 3-hydroxyacyl-CoA. 3-oxoacyl-CoA thiolases (also known as β-ketothiolases) use CoA for the thiolytic cleavage of 3-oxoacyl-CoA into acetyl-CoA and a shortened acyl-CoA molecule with n-2 carbon atoms (Fig. 5).

All reactions involved in a β-oxidation are reversible with regard to the underlying enzymatic reaction mechanisms (Clomburg et al., 2012). In addition, an *in silico* analysis of reaction thermodynamics supports the notion that β-oxidation can be functionally operated in the anabolic direction (Dellomonaco et al., 2011). This enables the exploitation of such pathways in the non-natural anabolic direction for the purpose of chain elongation (black route in Fig. 5). Until today, numerous different compounds have been synthesized in engineered microorganisms using reversal of β-oxidative pathways. The current state and the perspective of the utilization of such pathways for production purposes is summarized in a review article, which is part of this thesis (cf. chapter 2.5).

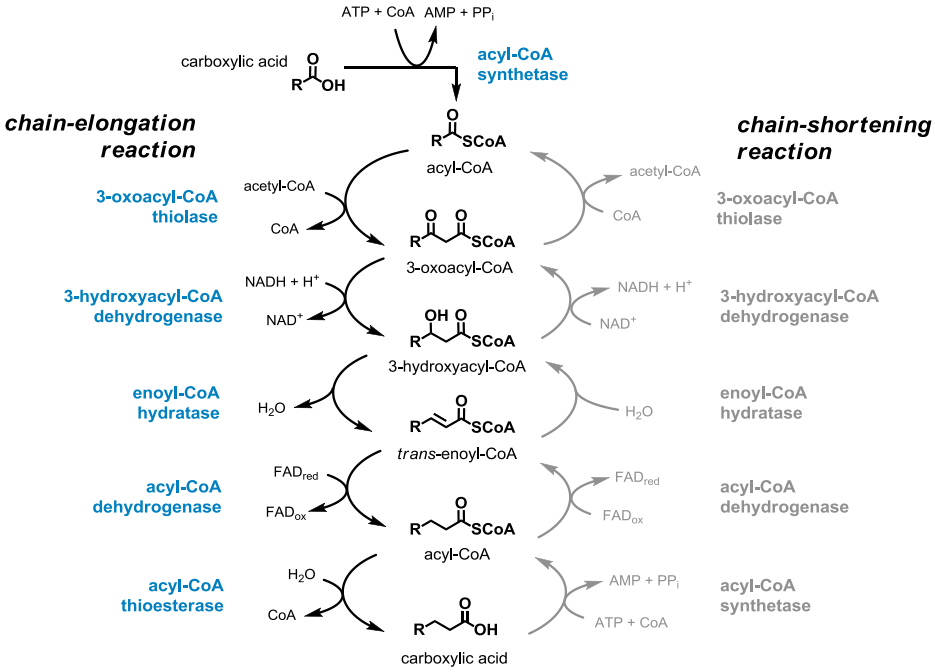

Fig. 5 Reversal of β-oxidative pathways for carbon chain elongation. The reversibility of the enzymatically catalyzed reaction steps during β-oxidation enables operation of this pathway in both directions. In the classical catabolic direction (shown in gray) a keto group is introduced at C3 of the CoA-activated carboxylic acid (acyl-CoA) yielding 3-oxoacyl-CoA, which can be used for the thiolytic cleavage yielding acetyl-CoA and a shortened acyl-CoA. The 3-oxoacyl-CoA thiolase catalyzing the cleavage reaction can also mediate the C-C ligation of acetyl-CoA and acyl-CoA for the synthesis of a 3-oxoacyl-CoA with an elongated carbon chain. The identical enzymes involved in the "catabolic" β-oxidation then catalyze the elimination of the carbonyl oxygen at C3 of 3-oxoacyl-CoA by two reduction steps and one dehydration step (shown in blue). The carboxylic acid can be released from CoA *e.g.* by acyl-CoA thioesterases.

1.7 Aims of the thesis

The major goal of this thesis is the exploitation of the yet untapped potential of *C. glutamicum* for the production of plant polyphenols. This does not only include the functional introduction of the required heterologous pathways from plants, but also the engineering of the host metabolic network towards sufficient supply of the relevant precursors. In case of the desired polyphenols, L-Tyr and malonyl-CoA are the essential building blocks, which need to be supplied by the host strain. Further engineering of *C. glutamicum* strains producing stilbene and (2*S*)-flavanone backbone molecules provides access to more complex and decorated polyphenols showing improved stability or bioavailability. This requires the expression of

additional genes coding for plant dioxygenases, reductases, and acyl- or glycosyl-transferases.

The natural pathways converting phenylpropanoids to polyphenols can be combined with novel synthetic pathways leading to phenylpropanoids, *e.g.* using reversal of β-oxidation. *p*-Coumaroyl-CoA, the direct precursor for the stilbene resveratrol, is an intermediate of a β-oxidative catabolic pathway for phenylpropanoids identified in *Aromatoleum aromaticum* EbN1 (Trautwein et al., 2012). This pathway yields 4-hydroxybenzoyl-CoA and acetyl-CoA from degradation of *p*-coumaric acid. When operating this pathway in reverse, *p*-coumaroyl-CoA can be accessed from the cheap bulk chemical 4-hydroxybenzoic acid (4-HBA). By using this novel pathway in *C. glutamicum* the need for the energy-consuming synthesis of aromatic amino acids can be circumvented.

In an unrelated project, reversal of a β-oxidation pathway should be exploited to demonstrate the synthesis of chemical building blocks in engineered *E. coli* strains (cf. chapter 2.6). To this end, enzymes of the natural phenylacetate degradation pathway of *E. coli* can be applied for the production of the nylon precursor adipic acid. The desired adipic acid production pathway starts from succinyl-CoA and acetyl-CoA, but only allows the synthesis up to the stage of the enoyl-CoA intermediate (2,3-dehydroadipyl-CoA). Candidate enzymes capable to efficiently catalyze the remaining reduction step and product release from the CoA-thioester need to be identified. Genes coding for the enzymes with the highest enzymatic activity should then be functionally introduced in *E. coli* to enable adipic acid production from renewable carbon sources.

1.8 Key results on engineering *C. glutamicum* towards polyphenol production

1.8.1 Discovery of a new phenylpropanoid degradation pathway in *C. glutamicum*

(Kallscheuer et al. 2016, Applied Microbiology and Biotechnology, cf. chapter 2.1)

The stilbene resveratrol was chosen as first target for polyphenol synthesis by *C. glutamicum* to demonstrate its capability to produce plant-derived polyphenols from supplemented phenylpropanoids. The required two-step pathway leading to resveratrol included heterologous 4-coumarate: CoA ligase (4CL) and stilbene synthase (STS). A 4CL from parsley (*Petroselinum crispum*) and an STS from peanut (*Arachis hypogaea*) were already functionally introduced in microbial hosts such as *E. coli* and *S. cerevisiae*, therefore it was decided to test these enzymes also in *C. glutamicum*. Genes coding for STS and 4CL from the mentioned organisms were codon-optimized for *C. glutamicum* and subsequently cloned

as bicistronic operon into the expression plasmid pMKEx2. Using this plasmid allows the IPTG-inducible gene expression starting from the strong T7 promoter. A suitable host strain (*C. glutamicum* MB001(DE3)) harboring the required T7 RNA polymerase was already available (Kortmann et al., 2015). The constructed strain *C. glutamicum* MB001(DE3) pMKEx2_sts_{Ah}_$4cl_{Pc}$ was cultivated in defined CGXII medium with 4 % glucose and 5 mM of the phenylpropanoid *p*-coumaric acid. Unfortunately, no resveratrol production could be observed when the heterologous gene expression was induced with different concentrations of IPTG (0, 0.02, 0.1 or 1 mM). Astonishingly, the supplemented precursor *p*-coumaric acid was completely depleted at the end of the cultivation. The same was also found for a negative control strain harboring pMKEx2. In CGXII medium without *C. glutamicum* cells, there was no decrease of the initial *p*-coumaric acid concentration, so that any instability of the phenylpropanoid in the cultivation medium could be excluded.

Instead, it turned out that *C. glutamicum* is able to degrade phenylpropanoids such as *p*-coumaric acid, allowing their utilization as sole carbon and energy source for growth. For further analysis *C. glutamicum* wild-type cells were cultivated in CGXII medium with different naturally occurring phenylpropanoids as sole carbon and energy source. The tested substrates cinnamic acid, *p*-coumaric acid, caffeic acid and ferulic acid differ in the hydroxylation pattern of the aromatic ring (Fig. 6). A fifth substrate (3-(4-hydroxyphenyl)-propionic acid) has the same hydroxylation pattern as *p*-coumaric acid but lacks the double bond in the aliphatic side chain. *C. glutamicum* degraded all tested phenylpropanoids except for cinnamic acid, thereby reaching growth rates of 0.15 - 0.23 h^{-1} depending on the tested phenylpropanoid. The degradation of phenylpropanoids was not reported in *C. glutamicum* before and no information of potentially involved pathway(s), enzymes or genes was available.

Typically, genes coding for enzymes involved in catabolic pathways for aromatic compounds are not expressed constitutively, but their expression is induced when the corresponding substrates are available. This could also be true for the genes involved in the phenylpropanoid catabolic pathway. Therefore, the transcriptomic response of *C. glutamicum* to the supplementation of phenylpropanoids was analyzed using DNA microarrays. Genes showing an increased expression level in the presence of phenylpropanoids could code for enzymes, which are active in phenylpropanoid degradation. In presence of four tested phenylpropanoids (*p*-coumaric acid, caffeic acid, ferulic acid and 3-(4-hydroxyphenyl)-propionic acid) a gene cluster of six genes (cg0340-cg0347) was significantly up-regulated (relative mRNA level > 3.0) (Fig. 6). When cells were pulsed with cinnamic acid, no significant regulation of these genes was observed. The genes were annotated as metabolite transporter protein (cg0340), fatty acid: CoA ligase (cg0341), MarR-type transcriptional

regulator (cg0343), 3-oxoacyl-CoA dehydrogenase (cg0344), metal-dependent hydrolase (cg0345), acyl-CoA dehydrogenase (cg0346) and enoyl-CoA hydratase (cg0347). The annotation of these genes suggested that they code for a set of enzymes involved in the degradation of fatty acids *via* β-oxidation (Kalinowski et al., 2003). This finding was unexpected as *C. glutamicum* is unable to degrade fatty acids by a β-oxidation pathway (Takeno et al., 2013). Instead, the encoded enzymes might catalyze a CoA-dependent, β-oxidative chain-shortening of the propionic acid side chain of the phenylpropanoids giving rise to benzoic acids, which are then degraded by known pathways in *C. glutamicum.*

To further analyze the relevance of the identified gene cluster for phenylpropanoid degradation, the identified genes were individually deleted in the *C. glutamicum* wild-type strain. The absence of the genes cg0341, cg0344, cg0345 and cg0347 abolished growth of *C. glutamicum* on all tested phenylpropanoids. Deletion of the gene cg0346 only abolished growth on 3-(4-hydroxyphenyl)propionic acid. This finding is in line with the assumed degradation pathway as 3-(4-hydroxyphenyl)propionic acid was the only one of the tested compounds lacking a double bond in the side chain. Deletion of the gene cg0340 coding for the putative metabolite transporter led to a slight reduction of the growth rate with phenylpropanoids as sole carbon and energy source, but the gene was not essential for growth with these compounds.

The constructed deletion mutants were also cultivated in CGXII medium with 4% glucose and 5 mM 3-(4-hydroxyphenyl)propionic acid to check for any accumulation of pathway intermediates of the assumed degradation pathway. Ultimately, the free acids of the CoA-bound pathway intermediates could be identified using LC-MS/MS analysis, which confirmed that the identified enzymes catalyze a CoA-dependent, β-oxidative side-chain shortening of phenylpropanoids yielding benzoic acids (Fig. 6). The last step in the iterative β-oxidation during the catabolism of fatty acid is typically catalyzed by a 3-oxoacyl-CoA thiolase, which yields acetyl-CoA and a chain-shortened acyl-CoA. None of the identified genes codes for a 3-oxoacyl-CoA thiolase. Instead, a putative hydrolase was encoded by cg0345. This enzyme catalyzes the hydrolysis at the keto group at C3 yielding acetyl-CoA and a free acid rather than a CoA-thioester. In case of 3-(4-hydroxyphenyl)propionic acid degradation 4-hydroxybenzoate is formed, which is further converted to protocatechuate. Protocatechuate is degraded by the β-ketoadipate pathway in *C. glutamicum* (Fig. 4). By using the same pathway caffeic acid and ferulic acid are degraded to protocatechuate and vanillate, respectively. The identified pathway was designated Phd pathway (phenylpropanoid degradation) and the genes were named *phdT* (cg0340), *phdA* (cg0341), *phdR* (cg0343), *phdB* (cg0344), *phdC* (cg0345), *phdD* (cg0346) and *phdE* (cg0347) (Fig. 6).

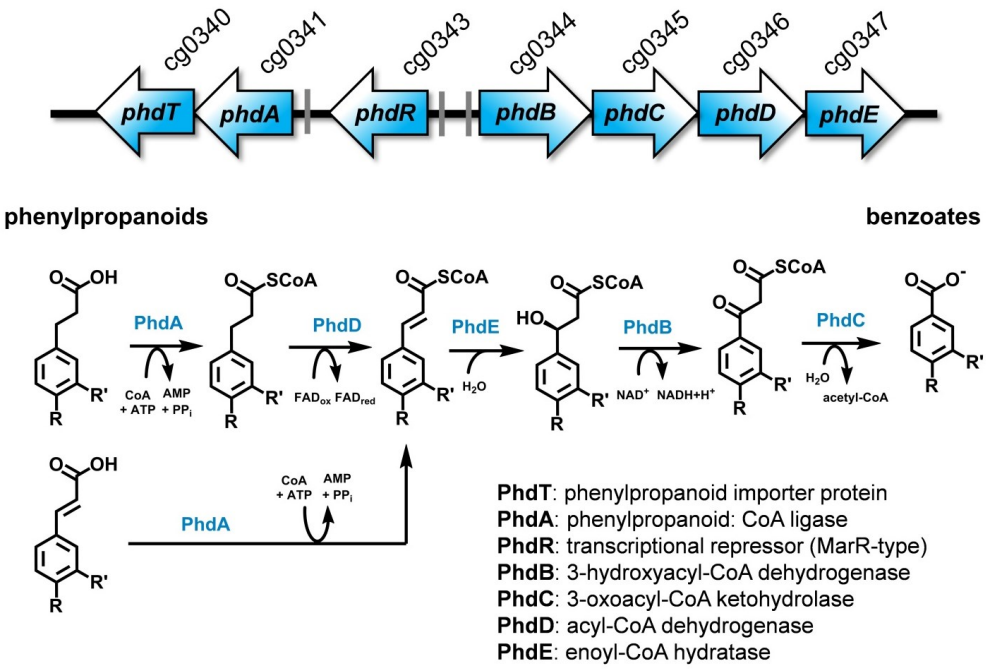

Fig. 6 The phenylpropanoid degradation pathway in *C. glutamicum*. The *phd* cluster of seven genes (cg0340-cg0347) codes for enzymes catalyzing the CoA-dependent, β-oxidative side chain shortening of phenylpropanoids yielding benzoates. The tested phenylpropanoids included cinnamic acid (R = H, R' = H), *p*-coumaric acid (R = OH, R' = H), caffeic acid (R = OH, R' = OH), ferulic acid (R = OH, R' = OCH_3) (all harboring a double in the side chain) and 3-(4-hydroxyphenyl)propionic acid (R = OH, R = H) (lacking an aliphatic double bond). The predicted promoters of the operons *phdAT* and *phdBCDE* as well as of *phdR* are indicated in gray.

The gene *phdR* codes for a putative transcriptional regulator of the MarR-family. It was assumed that this regulator controls the expression of the *phd* gene cluster. To further investigate the role of the regulator, the transcriptome of the respective *phdR* deletion strain was analyzed using DNA-microarrays. In comparison to the wild-type strain, the genes of the cluster were up-regulated 120- to 400-fold. This led to the conclusion that PhdR acts as repressor, which blocks expression of the postulated operons *phdBCDE* and *phdAT* in absence of phenylpropanoids by binding to the corresponding promoters. It is likely that there is a low basal expression of the genes coding for the transporter PhdT and the phenylpropanoid: CoA ligase PhdA as the phenylpropanoid CoA-thioesters (and not the phenylpropanoids themselves) were identified as effectors of the repressor protein.

In the experiments described above, *C. glutamicum* failed to grow on cinnamic acid as sole carbon and energy source. Two scenarios could explain this finding: either cinnamic acid does not induce expression of the genes involved in catabolism due to poor interaction with the repressor protein or the enzymes of the catabolic pathway do not show sufficient activity with cinnamic acid and the pathways intermediates derived thereof. Ultimately, the first scenario turned out to be true as the strain *C. glutamicum* Δ*phdR* with constitutive expression of the *phd* genes was capable to grow with cinnamic acid as sole carbon and energy source. The growth rate of 0.19 h^{-1} was comparable to that observed with the other phenylpropanoids. Based on these results, it seems reasonable to conclude at this stage that the ligand spectrum of PhdR is limited to phenylpropanoids bearing a hydroxylation in *para*-position.

1.8.2 Construction of a *C. glutamicum* platform strain for polyphenol production

(Kallscheuer et al. 2016, Metabolic Engineering, cf. chapter 2.2)

Based on the observation that *C. glutamicum* rapidly consumes phenylpropanoids, it was assumed that other enzymes of the complex network of catabolic pathways for aromatic compounds might also interfere with the production of polyphenols in this organism. This could *e.g.* refer to hydroxylases or aromatic ring dioxygenases, which potentially show side activity with phenylpropanoids or polyphenols as substrates. To avoid any degradation or conversion of aromatic compounds, a novel platform strain was constructed based on *C. glutamicum* MB001(DE3). In the novel strain (designated *C. glutamicum* DelAro^4) in total 21 genes of the catabolic network for aromatic compounds (organized in four gene clusters) were deleted. The genes comprised the identified operon *phdBCDE* of the phenylpropanoid catabolic pathway. The remaining genes *phdT* and *phdA* of the gene cluster coding for the phenylpropanoid importer PhdT and the phenylpropanoid: CoA ligase PhdA (an endogenous 4-coumarate: CoA ligase) were not deleted as both proteins can support polyphenol production in *C. glutamicum*.

Deletion of additional genes coding for enzymes of the β-ketoadipate pathway (cg2625-cg2640) and of *pobA* (cg1226, 4-hydroxybenzoate 3-hydroxylase) abolished growth of *C. glutamicum* with all compounds, which are degraded by this central degradation pathway (cf. Fig. 4). Production of polyphenols in *C. glutamicum* from glucose or other sugars requires the deregulation of the shikimate pathway for enabling overproduction of the precursor L-Tyr. As already described, *C. glutamicum* harbors a degradation pathway for quinate and shikimate, which also serves as an overflow metabolism for the shikimate pathway (chapter 1.5.2). To avoid that an increased flux into the shikimate pathway is redirected back into the central

carbon metabolism the gene *qsuB* (cg0502) was deleted additionally. QsuB catalyzes the irreversible dehydration of 3-dehydroshikimate yielding protocatechuate (cf. Fig. 4). *C. glutamicum* DelAro^4 did not show any negative effects on growth and biomass formation when cultivated under standard conditions (30°C, 130 rpm) in CGXII medium with glucose and was used as basis for further strain engineering.

1.8.3 Production of stilbenes and (2*S*)-flavanones with *C. glutamicum* DelAro^4

(Kallscheuer et al. 2016, Metabolic Engineering, cf. chapter 2.2)

Plasmid-borne expression of heterologous *sts* and *4cl* genes using the previously constructed plasmid pMKEx2_sts_{Ah}_$4cl_{Pc}$ in *C. glutamicum* DelAro^4 led to the first demonstration of polyphenol production from phenylpropanoids with this organism. When cultivated in CGXII medium with 4 % glucose, 5 mM *p*-coumaric acid and 1 mM IPTG 12 mg/L (0.05 mM) resveratrol were found to be produced. As the *C. glutamicum* DelAro^4 strain is no longer capable to degrade *p*-coumaric acid, more than 90 % of the initial *p*-coumaric acid was still present at the end of the cultivation and thus not converted to resveratrol.

For polyphenol production in *E. coli* and *S. cerevisiae* it was reported that the low level of malonyl-CoA (the co-substrate of the polyphenol synthesis pathway) was rate-limiting (Lim et al., 2011; Shin et al., 2012) (Fig. 2). In both organisms as well as in *C. glutamicum* malonyl-CoA is exclusively used for synthesis of fatty acids. Therefore, it is not surprising that the malonyl-CoA level is strictly regulated based on the activity of the fatty acid synthesis machinery. For improved microbial polyphenol production typically the fatty acid synthesis inhibitor cerulenin is added. This antibiotic binds covalently to the fatty acid synthase complex and inhibits the elongation reaction of the fatty acid chain (Price et al., 2001). The inhibition of fatty acid synthesis results in a growth arrest because fatty acids are essential building blocks of cell membranes and cell wall components in *C. glutamicum* (Radmacher et al., 2005). Thus, the cerulenin concentration and especially the time point of cerulenin addition to the cultivation medium are crucial for an increased production of polyphenols. In *C. glutamicum*, the highest resveratrol titers were achieved when 25 µM cerulenin was added in the late exponential growth phase at an OD_{600} of 18-25. The production culture was inoculated to an OD_{600} of 5-7 to reach the required biomass concentration after 8-10 hours. With this optimized cultivation protocol the resveratrol production could be increased more than 13-fold to 158 mg/L (0.69 mM) by addition of 25 µM cerulenin. When 5 mM of the phenylpropanoids cinnamic acid or caffeic acid were supplemented to *C. glutamicum* DelAro^4 pMKEx2_sts_{Ah}_$4cl_{Pc}$ the strain produced 121 mg/L (0.57 mM) pinosylvin and 56 mg/L (0.23

mM) piceatannol, respectively in presence of cerulenin. The stilbene isorhapontigenin derived from ferulic acid could not be produced in *C. glutamicum*. This finding is in line with published results. Due to steric hindrance, the tested STS_{Ah} is unable to synthesize the stilbene from the tetraketide intermediate obtained from feruloyl-CoA as substrate (Watts et al., 2006).

In analogy to the previously constructed plasmid for stilbene production pMKEx2_chs_{Ph}_chi_{Ph} was constructed to also enable the production of (*2S*)-flavanones with *C. glutamicum*. The novel plasmid harbors codon-optimized genes coding for chalcone synthase (CHS_{Ph}) and chalcone isomerase (CHI_{Ph}) from *Petunia x hybrida*. As the complete pathway from phenylpropanoids to (2*S*)-flavanones also includes 4-coumarate: CoA ligase activity the already tested $4cl_{Pc}$ gene was placed under control of the T7 promoter and was then integrated into the Δ*phdBCDE* locus in the genome of *C. glutamicum* DelAro^4 yielding *C. glutamicum* DelAro^4-$4cl_{Pc}$. In case of plasmid-based expression of chs_{Ph} and chi_{Ph} in the $4cl_{Pc}$-harboring strain, under optimized conditions employing cerulenin 35 mg/L (0.13 mM) naringenin and 37 mg/L (0.13 mM) eriodictyol could be produced from 5 mM *p*-coumaric acid and 5 mM caffeic acid, respectively.

1.8.4 Exploitation of *C. glutamicum* for the production of more complex polyphenols

(Kallscheuer et al. 2017, Journal of Biotechnology, cf. chapter 2.3)

The already commercially available stilbene resveratrol can by further modified by decoration, *e.g.* by acylation or glycosylation. The di-*O*-methylated resveratrol derivative pterostilbene was shown to have a significantly higher bioavailability compared to resveratrol (McCormack and McFadden, 2012). The *O*-methylation leads to an increased hydrophobicity allowing a better passage through biological membranes.

The production of pterostilbene in *C. glutamicum* requires one additional plant enzyme, a resveratrol di-*O*-methyltransferase (OMT) (Fig. 7). This enzyme uses *S*-adenosylmethionine (SAM) as methyl donor, a compound, which is also naturally produced by microorganisms. The heterologous expression of a codon-optimized gene coding for OMT from grape (*Vitis vinifera*) in *C. glutamicum* DelAro^4 pMKEx2_sts_{Ah}_$4cl_{Pc}$ pEKEx3_omt_{Vv} failed, most likely due to improper folding of the OMT polypeptide chain. In pEKEx3 the heterologous gene omt_{Vv} is expressed from the IPTG-inducible *tac* promoter. None of five tested IPTG concentrations (0, 0.01, 0.02, 0.1 or 1 mM) led to pterostilbene production, which further supported the assumption that OMT is insoluble. In order to increase the solubility of the heterologous protein in *C. glutamicum* a translational fusion of OMT to the C-terminus of the highly soluble

maltose-binding protein (MalE) of *E. coli* was tested (Duplay et al., 1984). The strategy was successful as the strain *C. glutamicum* DelAro^4 pMKEx2_*sts*$_{Ah}$_*4cl*$_{Pc}$ pEKEx3_*malE*$_{Ec}$-*omt*$_{Vv}$ produced 42 mg/L (0.16 mM) pterostilbene from 5 mM *p*-coumaric acid.

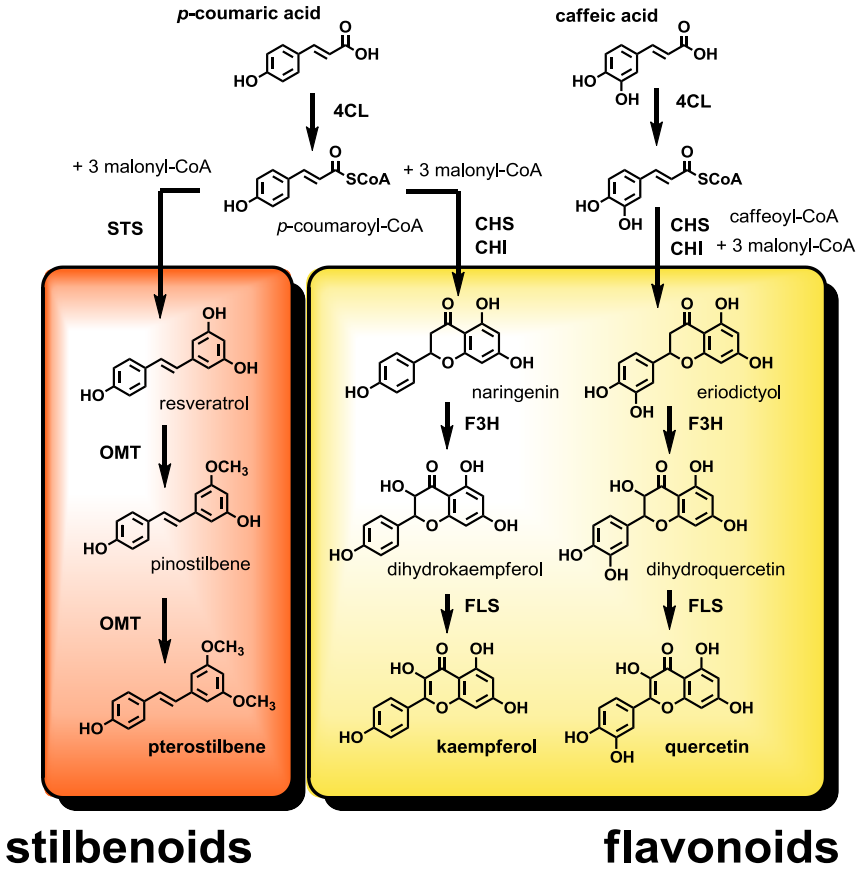

Fig. 7 Heterologous pathways for synthesis of methylated stilbenes and of flavonols. Biosynthetic pathways for the microbial production of pterostilbene and for the flavonols kaempferol and quercetin starting from phenylpropanoids are depicted. A plant-derived resveratrol-di-*O*-methyltransferase (OMT) catalyzes the double *O*-methylation of the stilbene resveratrol. The (2S)-flavanones naringenin and eriodictyol are converted to the respective flavonols kaempferol and quercetin by flavanone 3-hydroxylase (F3H) and flavonol synthase (FLS).

In parallel, (2*S*)-flavanone-producing strains were engineered towards the production of flavonols (including the commercially available quercetin). Flavonols are very potent antioxidants and quercetin is one of the most frequently studied flavonoids with regard to bioactivity (Boots et al., 2008). The production of flavonols from (2*S*)-flavanones requires the activity of two different 2-oxoglutarate-dependent dioxygenases (Fig. 7). The first step is the hydroxylation at C3, which is catalyzed by flavanone 3-hydroxlase (F3H). The reaction yields flavanonols (dihydroflavonols), which are oxidized to flavonols by flavonol synthase (FLS). The F3H from *Petunia x hybrida* and the FLS from the eastern cottonwood (*Populus deltoides*) were chosen to be tested in *C. glutamicum* as both enzymes were already characterized *in vitro* (Britsch and Grisebach, 1986; Kim et al., 2010). Codon-optimized genes coding for $F3H_{Ph}$ and FLS_{Pd} were cloned into pEKEx3 yielding pEKEx3_$f3h_{Ph}$_fls_{Pd}. This plasmid was then introduced into the (2*S*)-flavanone-producing strain *C. glutamicum* DelAro^4-$4cl_{Pc}$ pMKEx2_chs_{Ph}_chi_{Ph}. When the resulting strain was cultivated in the presence of the phenylpropanoids *p*-coumaric acid and caffeic acid, the expected flavanonols and flavonols could be identified. From 5 mM *p*-coumaric acid 20 mg/L (0.07 mM) dihydrokaempferol and 23 mg/L (0.08 mM) kaempferol were produced, while supplementation with 5 mM caffeic acid yielded 7 mg/L (0.02 mM) dihydroquercetin and 10 mg/L (0.03 mM) quercetin. The detected flavonol titers represent the highest titers achieved in an engineered microorganism to date. The results show that *C. glutamicum* can be also exploited for the production of more complex flavonoids.

1.8.5 Strain engineering towards polyphenol production from glucose

(Kallscheuer et al. 2016, Metabolic Engineering, cf. chapter 2.2)

In the studies described above, the production of stilbenes and (2*S*)-flavanones in *C. glutamicum* was based on the supplementation of phenylpropanoids as precursors. Further strain engineering focused on the production of polyphenols from cheap glucose to make the microbial production of these compounds more economical (Fig. 8A). The phenylpropanoid *p*-coumaric acid can be obtained from the aromatic amino acid L-Tyr by non-oxidative deamination. This reaction is catalyzed by a heterologous tyrosine ammonia lyase (TAL). A highly active bacterial TAL from *Flavobacterium johnsoniae* (TAL_{Fj}) with low side activity towards L-Phe was tested in *C. glutamicum*. Expression of the tal_{Fj} gene in combination with the heterologous genes for stilbene and (2*S*)-flavanone production might require the supplementation of L-Tyr as *C. glutamicum* DelAro^4 does not provide this aromatic amino acid in excess. In consequence, the polyphenol production can only be achieved with simultaneous deregulation of the feedback-control of the shikimate pathway especially at the

initial committed step catalyzed by the DAHP synthase. Due to the complex regulation of DAHP synthase and chorismate mutase activity in *C. glutamicum* (see chapter 1.5.2) the overexpression of native genes of *C. glutamicum* was not expected to be a promising strategy. In *E. coli* three different DAHP synthase isoenzymes are present and each of these is inhibited by only one of the aromatic amino acids (Wallace and Pittard, 1967). In *C. glutamicum*, the L-Trp branch was found to be strictly regulated on the transcriptional level. It is likely that an increased flux into the shikimate pathway does not lead to a significant overproduction of L-Trp. Therefore, it was decided to introduce the L-Trp-sensitive DAHP synthase AroH from *E. coli* into *C. glutamicum*, which retains full activity in absence of increased L-Trp level. The native gene *aroH* from *E. coli* MG1655 and a codon-optimized tal_{Fj} gene were cloned as bicistronic operon into pEKEx3, which can be maintained in the cell in combination with pMKEx2. The plasmid pEKEx3_$aroH_{Ec}$_tal_{Fj} allows the IPTG-inducible expression of the heterologous genes starting from the *tac* promoter and was introduced into the constructed stilbene- and (2*S*)-flavanone-producing *C. glutamicum* strains (the stilbene-producing strain is shown in Fig. 8B).

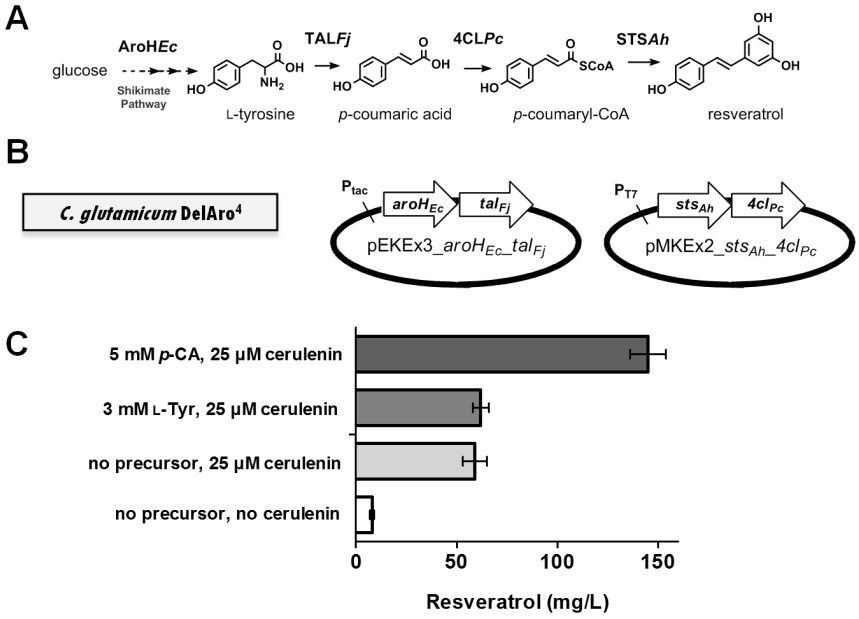

Fig. 8 Production of resveratrol in *C. glutamicum*. (A) The production of resveratrol from glucose requires overproduction of L-Tyr and its non-oxidative deamination yielding the phenylpropanoid *p*-coumaric acid (*p*-CA), which is then further converted to resveratrol by 4-coumarate: CoA ligase (4CL) and stilbene synthase (STS). (B) Constructed plasmids required for production of resveratrol in *C. glutamicum* DelAro^4. (C) Obtained resveratrol titer in presence or absence of different precursor metabolites and cerulenin.

To investigate the effect on additional expression of *aroH*$_{Ec}$ and *tal*$_{Fj}$ the strain *C. glutamicum* DelAro^4 pMKEx2_*sts*$_{Ah}$_*4cl*$_{Pc}$ pEKEx3_*aroH*$_{Ec}$_*tal*$_{Fj}$ was cultivated in the presence and absence of different precursor metabolites. In the presence of 5 mM *p*-coumaric acid 142 mg/L (0.62 mM) resveratrol were produced, which is similar to the titer achieved with the initial strain *C. glutamicum* DelAro^4 pMKEx2_*sts*$_{Ah}$_*4cl*$_{Pc}$ (Fig. 8C). When 3 mM L-Tyr was supplemented the resulting resveratrol titer was 60 mg/L (0.26 mM) (Fig. 8C). This showed that the heterologous *tal*$_{Fj}$ gene is functionally expressed under the previously optimized induction conditions (1 mM IPTG). In absence of both precursors, the strain accumulated the same amount of resveratrol (59 mg/L, 0.26 mM) as with L-Tyr supplementation (Fig. 8C). Increasing the supplemented amount of L-Tyr did not allow an improved resveratrol production, which led to the conclusion that the tyrosine ammonia lyase activity is likely to be a rate-limiting step during production. In the (2*S*)-producing strain *C. glutamicum* DelAro^4-*4cl*$_{Pc}$ pMKEx2_*chs*$_{Ph}$_*chi*$_{Ph}$ harboring pEKEx3_*aroH*$_{Ec}$_*tal*$_{Fj}$ 32 mg/L (0.12 mM) naringenin were found to be produced in absence of precursors, which is very similar to the titer of 35 mg/L (0.13 mM) produced with supplementation of *p*-coumaric acid (all cultivations were done in presence of 25 µM cerulenin).

1.8.6 Design of a novel synthetic pathway for phenylpropanoid biosynthesis

(Kallscheuer et al., 2017, ACS Synthetic Biology, cf. chapter 2.4)

The tyrosine ammonia lyase activity was identified as potential bottleneck during polyphenol production from glucose with *C. glutamicum*. The tested TAL$_{Fj}$ was shown to be a highly active tyrosine ammonia lyase in bacteria and yeast (Jendresen et al., 2015). The encoding gene *tal*$_{Fj}$ was placed under control of the strong *tac* promoter with maximal induction strength of expression. In that regard, there is not much room to further increase the TAL activity in the tested *C. glutamicum* strains. Unfortunately, the non-oxidative deamination of aromatic amino acids is the only known natural metabolic strategy to get an access to phenylpropanoids.

However, driven by the goal to circumvent this bottleneck and inspired by nature, a synthetic pathway was designed and constructed in this project. This novel pathway allows for a TAL-independent phenylpropanoid biosynthesis in *C. glutamicum*. In 2011, the β-oxidation pathway for iterative CoA-dependent chain-shortening of fatty acids was reported to be fully reversible with regard to the reaction mechanism of the involved enzymes (Dellomonaco et al., 2011) (Fig. 5). In consequence, a non-natural reversal of these reactions can also be exploited for production purposes. Interestingly, the phenylpropanoid CoA-thioesters (which are the direct precursors for polyphenol production) are enoyl-CoA intermediates of β-

oxidative degradation pathways for phenylpropanoids. Enzymes involved in the β-oxidative chain-shortening of phenylpropanoids should therefore also enable phenylpropanoid production if the pathways can be functionally operated in reverse.

A suitable β-oxidation pathway was identified in *Aromatoleum aromaticum* EbN1. This pathway is required for degradation of *p*-coumaric acid yielding 4-hydroxybenzoyl-CoA and acetyl-CoA (Trautwein et al., 2012). Assuming that also all reactions of this pathway are reversible, *p*-coumaroyl-CoA should be accessible in three enzymatic steps starting from 4-hydroxybenzoyl-CoA and acetyl-CoA (Fig. 9). 4-Hydroxybenzoate (4-HBA) is a cheap bulk chemical, which only needs to be converted to the corresponding CoA-thioester. *A. aromaticum* EbN1 also harbors an enzyme (designated HbcL1) with the desired 4-hydroxybenzoate: CoA ligase activity (Wöhlbrand et al., 2007). Although 4-HBA is a typical petroleum-based chemical, it was already produced in an engineered *C. glutamicum* strain overproducing the 4-HBA precursor and shikimate pathway intermediate chorismate (Okai et al., 2016).

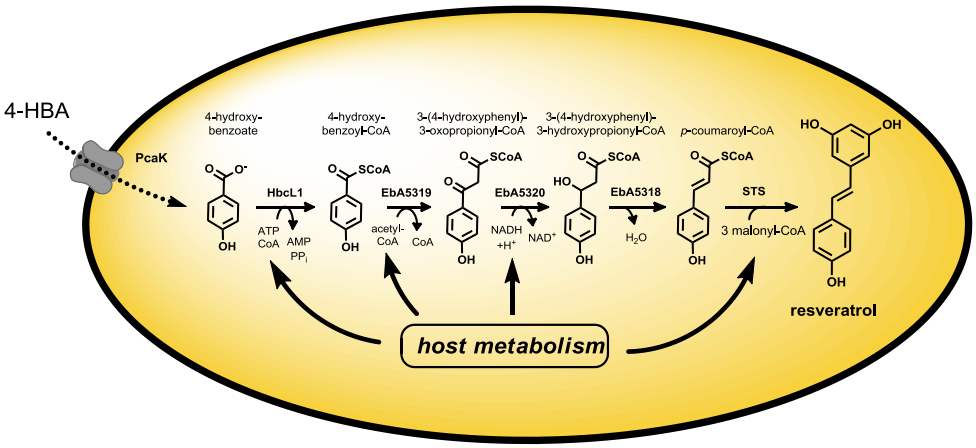

Fig. 9 The synthetic pathway for resveratrol production from 4-hydroxybenzoate. The designed synthetic pathway represents an engineered reversal of β-oxidation reactions originally involved in phenylpropanoid degradation in *A. aromaticum* EbN1. The pathway enables the conversion of 4-hydroxybenzoate (4-HBA) to the direct resveratrol precursor *p*-coumaroyl-CoA. 4-HBA is actively taken up by the native transporter PcaK (Cg1225) in the engineered *C. glutamicum* strain harboring this pathway. HbcL1: 4-hydroxybenzoate: CoA ligase, EbA5319: 3-(4-hydroxyphenyl)-3-oxopropionyl-CoA thiolase, EbA5320: 3-(4-hydroxyphenyl)-3-hydroxypropionyl-CoA dehydrogenase, EbA5318: *p*-coumaroyl-CoA hydratase.

To test the novel pathway in *C. glutamicum,* genes coding for HbcL1 and the three required enzymes EbA5319 (3-(4-hydroxyphenyl)-3-oxopropionyl-CoA thiolase), EbA5320 (3-(4-hydroxyphenyl)-3-hydroxypropionyl-CoA dehydrogenase), and EbA5318 (*p*-coumaroyl-CoA hydratase) from *A. aromaticum* EbN1 were assembled as a synthetic operon. This tetracistronic operon under control of the strong constitutive *tuf* promoter (P_{tuf}-*hbcl1*-ebA5319-ebA5320-ebA5318) was subsequently cloned into pEKEx3 yielding pEKEx3_RevBeta. The constructed strain *C. glutamicum* DelAro^4 pMKEx2_sts_{Ah}_$4cl_{Pc}$ pEKEx3_RevBeta was tested for its capability to produce resveratrol from 4-HBA by the synthetic pathway.

The host strain *C. glutamicum* DelAro^4 is unable to catabolize 4-HBA as the gene *pobA* (cg1226) coding for 4-hydroxybenzoate 3-hydroxylase was already deleted during construction of this strain. The adjacent gene *pcaK* (cg1225) coding for a 4-hydroxybenzoate transporter is still present. PcaK is involved in the active import of 4-HBA into *C. glutamicum* cells (Chaudhry et al., 2007). *C. glutamicum* DelAro^4 pMKEx2_sts_{Ah}_$4cl_{Pc}$ pEKEx3_RevBeta was cultivated in CGXII medium with 4 % glucose, 5 mM 4-HBA, 1 mM IPTG and 25 µM cerulenin. Without further optimization 5 mg/L (0.02 mM) resveratrol could be produced from 4-HBA, which is the first report on polyphenol production from supplemented benzoic acids. The results also demonstrate that phenylpropanoid synthesis can be achieved independently from aromatic amino acids and ammonia lyase activity.

1.9 Conclusions and Outlook

The results obtained in this thesis show that *C. glutamicum* is an attractive host for the production of plant polyphenols. The recombinant strains constructed in this thesis not only produced the stilbene and (2*S*)-flavanone backbone molecules, but also more complex flavonoids and decorated stilbene were obtained after functional introduction of plant enzymes. In *C. glutamicum*, the identification and abolishment of degradation pathways for phenylpropanoids and other aromatic compounds was crucial for the development of plant polyphenol-producing strains. On the other hand, knowledge of genes and enzymes involved in these catabolic pathways (such as the identified phenylpropanoid: CoA ligase PhdA in *C. glutamicum* and the enzymes of the β-oxidative degradation pathway in *A. aromaticum*) can be also exploited to support product formation. The tested synthetic pathway for resveratrol production from 4-hydroxybenzoate is one example how novel metabolic routes can possibly contribute to circumvent rate-limiting reaction steps in the polyphenol production pathways.

Although stilbene and (2*S*)-flavanone production from glucose was achieved in *C. glutamicum*, the obtained titers are much lower in comparison to other aromatic compounds obtained with this organism (*e.g.* aromatic amino acids). The low intracellular level of malonyl-CoA and the limiting tyrosine ammonia lyase activity were identified as the decisive bottlenecks during polyphenol production not only in *C. glutamicum*, but also in other engineered polyphenol-producing microorganisms. In order to render the production with *C. glutamicum* more economical, huge effort has to be put into engineering of the central carbon metabolism towards increased production of phenylpropanoids and malonyl-CoA. For an optimal connection of the host metabolism to the heterologous polyphenol production pathways, fine tuning of the expression levels of the required genes is beneficial as it can avoid the accumulation of pathway intermediates and formation of by-products. In parallel, screening of enzymes from different plant species showing higher activity in *C. glutamicum* can also be decisive to increase the polyphenol titers.

Due to their antibiotic properties polyphenols are toxic compounds. This challenge can be addressed by strain engineering towards efficient export of polyphenols (*e.g.* by introducing metabolite transporters) or by testing different product-removal strategies during process design and process up-scaling.

Taken together, *C. glutamicum* is an attractive host for the production of plant polyphenols. In order to render the polyphenol production more economical, further engineering of the host metabolism is required to increase the product titers. The functional introduction of other plant enyzmes in the constructed platform strain *C. glutamicum* DelAro^4 can also enable the production of additional phenylpropanoid-derived compounds with this organism.

2. Peer-reviewed publications

2.1 Phenylpropanoid degradation in *C. glutamicum*

Appl Microbiol Biotechnol (2016) 100:1871–1881
DOI 10.1007/s00253-015-7165-1

APPLIED MICROBIAL AND CELL PHYSIOLOGY

Identification of the *phd* gene cluster responsible for phenylpropanoid utilization in *Corynebacterium glutamicum*

Nicolai Kallscheuer[1] · Michael Vogt[1] · Jannick Kappelmann[1] · Karin Krumbach[1] · Stephan Noack[1] · Michael Bott[1] · Jan Marienhagen[1]

Received: 16 October 2015 / Accepted: 7 November 2015 / Published online: 26 November 2015

Abstract Phenylpropanoids as abundant, lignin-derived compounds represent sustainable feedstocks for biotechnological production processes. We found that the biotechnologically important soil bacterium *Corynebacterium glutamicum* is able to grow on phenylpropanoids such as *p*-coumaric acid, ferulic acid, caffeic acid, and 3-(4-hydroxyphenyl)propionic acid as sole carbon and energy sources. Global gene expression analyses identified a gene cluster (cg0340-cg0341 and cg0344-cg0347), which showed increased transcription levels in response to phenylpropanoids. The gene cg0340 (designated *phdT*) encodes for a putative transporter protein, whereas cg0341 and cg0344-cg0347 (*phdA-E*) encode enzymes involved in the β-oxidation of phenylpropanoids. The *phd* gene cluster is transcriptionally controlled by a MarR-type repressor encoded by cg0343 (*phdR*). Cultivation experiments conducted with *C. glutamicum* strains carrying single-gene deletions showed that loss of *phdA*, *phdB*, *phdC*, or *phdE* abolished growth of *C. glutamicum* with all phenylpropanoid substrates tested. The deletion of *phdD* (encoding for putative acyl-CoA dehydrogenase) additionally abolished growth with the α,β-saturated phenylpropanoid 3-(4-hydroxyphenyl)propionic acid. However, the observed growth defect of all constructed single-gene deletion strains could be abolished through plasmid-borne expression of the respective genes. These results and the intracellular accumulation of pathway intermediates determined via LC-ESI-MS/MS in single-gene deletion mutants showed that the *phd* gene cluster encodes for a CoA-dependent, β-oxidative deacetylation pathway, which is essential for the utilization of phenylpropanoids in *C. glutamicum*.

Keywords Phenylpropanoids · Aromatics · Lignin · *Corynebacterium glutamicum* · Degradation pathways · β-oxidation

Nicolai Kallscheuer and Michael Vogt contributed equally to this work.

Electronic supplementary material The online version of this article (doi:10.1007/s00253-015-7165-1) contains supplementary material, which is available to authorized users.

✉ Jan Marienhagen
j.marienhagen@fz-juelich.de

[1] Institute of Bio- and Geosciences, IBG-1: Biotechnology, Forschungszentrum Jülich, 52425 Jülich, Germany

Introduction

Microorganisms follow various biodegradative metabolic strategies for the utilization of aromatic compounds and thus play a crucial role in biogeochemical cycles (Diaz 2004). One class of abundant aromatic compounds is the group of lignin-derived phenylpropanoids, which are synthesized from the amino acids L-phenylalanine and L-tyrosine in plants. These compounds are structurally characterized by a single aromatic phenyl group and a three-carbon propene tail (Marienhagen and Bott 2013). Typically, phenylpropanoid degradation is initiated by shortening of the aliphatic side chain through cleavage of a C_2 unit (Campillo et al. 2014). This step is necessary to convert phenylpropanoids into benzoic acid derivatives, e.g., protocatechuate, before channeling these compounds into the microbial carbon metabolism, e.g., via the β-ketoadipate pathway or the gentisate pathway. Two mechanisms for this C_2 shortening reaction are described for bacteria in literature, a retro-aldol pathway and a β-oxidative pathway (Fig. 1). In both pathways, an α,β-double bond is introduced by an acyl-CoA dehydrogenase activity after conversion of the phenylpropanoid to the corresponding thioester. As example for a retro-aldol mechanism, a coupled

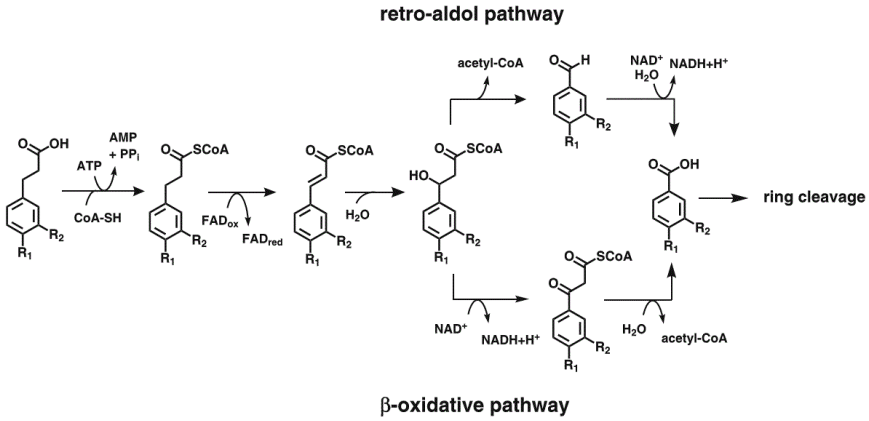

Fig. 1 Schematic representation of two chain-shortening mechanisms during phenylpropanoid degradation. The degradation of phenylpropanoids starts with the cleavage of a C_2 unit from the aliphatic side chain for conversion into benzoic acid derivatives. This can be achieved via a retro-aldol pathway or a β-oxidative pathway. As both mechanisms are CoA-dependent and yield acetyl-CoA as product, they depend on the same initial step, namely, a CoA ligation reaction leading to the corresponding phenylpropanoid CoA thioesters. If not already present, a α,β-double bond is subsequently introduced by acyl-CoA dehydrogenase activity. Hydration of the aliphatic double bond of the thioesters yields 3-hydroxyacyl-CoA intermediates which are common intermediates of both mechanisms. In the retro-aldol pathway (*upper branch*), the 3-hydroxyacyl-CoA intermediate is cleaved into a benzaldehyde derivative and acetyl-CoA. The benzaldehyde derivative is prepared for ring cleavage by oxidation of the aldehyde group to a carboxyl group. In the β-oxidative pathway (*lower branch*), the hydroxy group of the 3-hydroxyacyl-CoA intermediate is oxidized to a keto group. Subsequently, a thiolytic cleavage leads to the formation of a benzoyl-CoA derivative and acetyl-CoA or, alternatively, a hydrolytic cleavage yields a benzoate derivative and acetyl-CoA (only the hydrolytic cleavage is depicted here)

4-hydroxycinnamoyl-CoA hydratase/lyase identified in *Pseudomonas fluorescens* catalyzes the hydration of the aliphatic double bond of 4-hydroxycinnamoyl-CoA and the subsequent cleavage of the resulting 3-hydroxyacyl-CoA intermediate into a benzaldehyde derivate and acetyl-CoA (Mitra et al. 1999). An exemplary β-oxidative pathway for the catabolism of phenylpropanoids has been identified in the betaproteobacterium *Azoarcus sp*. EbN1 (inofficial but more common designation of this species "*Aromatoleum aromaticum*" EbN1) (Trautwein et al. 2012). After acyl-CoA oxidation, hydration of the double bond, oxidation of the hydroxy group, and thiolytic cleavage lead to the formation of benzoyl-CoA and acetyl-CoA.

The Gram-positive soil bacterium *Corynebacterium glutamicum* is an important platform organism for the microbial production of a variety of commercially interesting compounds (Wendisch 2014). As main products, several million tons of amino acids are produced annually with this microorganism, in particular the flavor enhancer L-glutamate and the feed additive L-lysine (Eggeling and Bott 2005). Almost all of these biotechnological processes employing *C. glutamicum* are based on glucose- or sugar-based feedstocks from starch, sugar cane, and sugar beet (Buschke et al. 2013). However, a broad range of aromatic compounds can also be utilized by *C. glutamicum* as carbon and energy sources. These compounds include benzoate (Shen et al. 2004), gentisate (Shen et al. 2005b), protocatechuate (Unthan et al. 2014), *p*-cresol, vanillate, 4-hydroxybenzoate (Shen and Liu 2005), or vanillin (Merkens et al. 2005). These substrates are first prepared for ring cleavage by diverse ring modification reactions employing "peripheral pathways" that finally yield protocatechuate, catechol, or gentisate as central metabolites of aromatic compound degradation. After ring fission and chain shortening of the linearized intermediates, these metabolites are channeled into the central carbon and energy metabolism (Shen et al. 2005a).

A degradation pathway for phenylpropanoids has not been experimentally identified in *C. glutamicum* yet. In this study, we investigated growth of *C. glutamicum* with five of the most abundant plant-derived phenylpropanoid compounds as sole carbon and energy sources. Subsequently, we applied transcriptomics for the identification of relevant genes involved in phenylpropanoid degradation, their organization, and regulation. Analysis of single-gene deletion mutants, complementation studies, and determination of accumulating pathway intermediates confirmed the relevance of the Phd pathway for phenylpropanoid utilization in *C. glutamicum*. These results show the potential of plant-derived phenylpropanoids to serve as carbon and energy sources for biotechnological applications with *C. glutamicum*.

Material and methods

Bacterial strains, plasmids, media, and growth conditions

All bacterial strains and plasmids used in this study as well as their relevant characteristics are listed in Table 1. *C. glutamicum* wild-type strain American Type Culture Collection (ATCC) 13032 (Abe et al. 1967) and corresponding deletion mutants were routinely cultivated aerobically at 30 °C in brain heart infusion (BHI) medium (Difco Laboratories, Detroit, USA) or defined CGXII medium (Keilhauer et al. 1993) with glucose or phenylpropanoids as sole carbon and energy sources. *Escherichia coli* DH5α was used for plasmid constructions and cultivated in Luria-Bertani medium (Bertani 1951) at 37 °C. Where appropriate, kanamycin (50 μg/ml for *E. coli* DH5α and 25 μg/ml for *C. glutamicum*) was added to the medium. Bacterial growth was followed by measuring the optical density at 600 nm (optical density $(OD)_{600}$).

For growth experiments using phenylpropanoid compounds as sole carbon and energy sources, substrates were fed during the cultivation experiments in order to keep the actual substrate concentration below the inhibition level of 10 mM in the culture medium. Precultures of *C. glutamicum* wild-type and deletion mutants derived thereof were grown for 6–8 h in test tubes with 5-ml BHI medium on a rotary shaker at 170 rpm and subsequently inoculated into 50-ml defined CGXII medium with 5 mM of the respective phenylpropanoid in 500-ml baffled Erlenmeyer flasks. The cell suspensions were cultivated overnight on a rotary shaker at 120 rpm. For starting the main culture, OD_{600} was adjusted to 1.5 and 5 mM of the respective phenylpropanoid was added to the cell suspension. Growth was then monitored by measuring OD_{600}. Additional substrate was fed during the course of cultivation (every 2 h) until cumulatively, 45 mM substrate was added to the cell suspension.

Table 1 Strains and plasmids used in this study

Strain or plasmid	Relevant characteristics	Source or reference
C. glutamicum strains		
Wild type	wild-type ATCC 13032, biotin auxotrophic	(Abe et al. 1967)
Δcg0340	ATCC 13032 derivative with in-frame deletion of cg0340 (*phdT*)	This study
Δcg0341	ATCC 13032 derivative with in-frame deletion of cg0341 (*phdA*)	This study
Δcg0343	ATCC 13032 derivative with in-frame deletion of cg0343 (*phdR*)	This study
Δcg0344	ATCC 13032 derivative with in-frame deletion of cg0344 (*phdB*)	This study
Δcg0345	ATCC 13032 derivative with in-frame deletion of cg0345 (*phdC*)	This study
Δcg0346	ATCC 13032 derivative with in-frame deletion of cg0346 (*phdD*)	This study
Δcg0347	ATCC 13032 derivative with in-frame deletion of cg0347 (*phdE*)	This study
E. coli strains		
DH5α	F$^-$ Φ80*lacZ*ΔM15 Δ(*lacZYA-argF*)U169 *recA*1 *endA*1 *hsdR*17 (r_K^-, m_K^+) *phoA supE*44 λ– *thi*-1 *gyrA*96 *relA*1	Invitrogen (Karlsruhe, Germany)
Plasmids		
pK19*mobsacB*	Kan^r; vector for allelic exchange in *C. glutamicum* (pK18 $oriV_{E.coli}$ *sacB lacZα*)	(Schafer et al. 1994)
pK19*mobsacB*-Δcg0340	Kan^r, pK19*mobsacB* derivative for in-frame deletion of gene cg0340 (*phdT*)	This study
pK19*mobsacB*-Δcg0341	Kan^r, pK19*mobsacB* derivative for in-frame deletion of gene cg0341(*phdA*)	This study
pK19*mobsacB*-Δcg0343	Kan^r, pK19*mobsacB* derivative for in-frame deletion of gene cg0343(*phdR*)	This study
pK19*mobsacB*-Δcg0344	Kan^r, pK19*mobsacB* derivative for in-frame deletion of gene cg0344 (*phdB*)	This study
pK19*mobsacB*-Δcg0345	Kan^r, pK19*mobsacB* derivative for in-frame deletion of gene cg0345 (*phdC*)	This study
pK19*mobsacB*-Δcg0346	Kan^r, pK19*mobsacB* derivative for in-frame deletion of gene cg0346 (*phdD*)	This study
pK19*mobsacB*-Δcg0347	Kan^r, pK19*mobsacB* derivative for in-frame deletion of gene cg0347 (*phdE*)	This study
pEKEx2	Kan^r, *C. glutamicum*/*E. coli* shuttle vector for inducible gene expressions (P_{tac}, $lacI^q$, pBL1 $oriV_{C.glutamicum}$, and pUC18 $oriV_{E.coli}$)	(Eikmanns et al. 1991)
pEKEx2-cg0340	Kan^r; pEKEx2 derivative for expression of gene cg0340	This work
pEKEx2-cg0341	Kan^r; pEKEx2 derivative for expression of gene cg0341	This work
pEKEx2-cg0344	Kan^r; pEKEx2 derivative for expression of gene cg0344	This work
pEKEx2-cg0345	Kan^r; pEKEx2 derivative for expression of gene cg0345	This work
pEKEx2-cg0346	Kan^r; pEKEx2 derivative for expression of gene cg0346	This work
pEKEx2-cg0347	Kan^r; pEKEx2 derivative for expression of gene cg0347	This work

Kan^r kanamycin resistance

For detection of intracellular metabolites, *C. glutamicum* wild-type strains with in-frame deletions of cg0344, cg0345, cg0346, or cg0347 were cultivated in defined CGXII medium with altogether 30 mM 3-(4-hydroxyphenyl)-3-propanoid acid (4-HPP) by feeding of 3 × 10 mM 4-HPP after 0, 2.5, and 4 h of cultivation. In order to enable biomass formation of the deletion strains, 4 % glucose was added as carbon and energy sources. *C. glutamicum* wild-type strain was grown with 4-HPP as sole carbon and energy sources. The strains were cultivated in 1-l shaking flasks with a culture volume of 100 ml placed in a Multitron incubator (Infors AG, Bottmingen, Switzerland) at 30 °C and 250 rpm.

Plasmid and strain construction

Standard protocols of molecular cloning such as PCR, DNA restriction, and ligation (Sambrook and Russell 2001) were carried out for recombinant DNA work. Techniques specific for *C. glutamicum*, e.g., electroporation for transformation of strains, were done as described previously (Eggeling and Bott 2005). All enzymes were obtained from ThermoScientific (Schwerte, Germany).

In-frame deletion of genes in *C. glutamicum* ATCC 13032 was done using constructed derivatives of vector pK19*mobsacB* (Schäfer et al. 1994) (Table 1) and a two-step homologous recombination method described previously (Niebisch and Bott 2001). DNA oligonucleotides used for plasmid construction (Table S1) were synthesized by Eurofins MWG Operon (Ebersfeld, Germany). The resulting amplicons were fused and then cloned via introduced restriction sites (Table S1) into vector pK19*mobsacB* (Schäfer et al. 1994), which had been digested with the respective restriction endonucleases. Gene expressions for complementation experiments were conducted using vector pEKEx2 (Eikmanns et al. 1991) (Table 1). All genes were amplified using appropriate DNA oligonucleotides (Eurofins MWG Operon, Ebersfeld, Germany) (Table S1) and cloned via introduced restriction sites into equally digested pEKEx2 plasmids. The sequences of all constructed plasmids were finally verified by DNA sequencing performed at Eurofins MWG Operon (Ebersfeld, Germany).

DNA microarray analysis

DNA microarrays were performed for the analysis of global gene expression of *C. glutamicum* wild-type cells in comparison to the same cells pulsed with phenylpropanoid substrates. Furthermore, global gene expression of *C. glutamicum* wild-type cells was compared with that of a *C. glutamicum* Δcg0343 deletion mutant both grown in defined CGXII medium with 4 % glucose.

For the generation of cell pellets used for DNA microarray analyses, strains were grown for 6–8 h in test tubes with 5-ml BHI medium on a rotary shaker at 170 rpm (first preculture) and subsequently inoculated into 50-ml defined CGXII medium with 4 % (*w*/*v*) glucose in 500-ml baffled Erlenmeyer flasks (second preculture). Cells were cultivated overnight on a rotary shaker at 120 rpm and then used for the inoculation of the main culture to an OD_{600} of 1.0. For substrate pulse experiments, a main culture of *C. glutamicum* wild-type cells was cultivated on a rotary shaker at 120 rpm to an OD_{600} of 4 and 5 mM of the respective phenylpropanoid was added at this stage. As a reference, *C. glutamicum* wild-type cells without phenylpropanoid pulse were cultivated in parallel. The cultivation was continued for 30 min (reaching OD_{600} of approximately 5) and harvested on ice by centrifugation (15 min, 4000×*g*, 4 °C). For comparison of wild-type and *C. glutamicum* Δcg0343 deletion mutants, cells were cultivated in main cultures of defined CGXII minimal medium with 4 % (*w*/*v*) glucose on a rotary shaker at 120 rpm to an OD_{600} of approximately 5 and then harvested as described above.

RNA samples were prepared using the RNeasy Mini Kit from Qiagen (Hilden, Germany) according to the manufacturer's instructions. The conduction of the DNA microarray experiments for genome-wide gene expression analysis was done as described previously (Vogt et al. 2014), using custom-made DNA microarrays (Agilent Technologies, Waldbronn, Germany) and genome annotation by Kalinowski and colleagues (Kalinowski et al. 2003) listing 3057 protein-coding genes and 80 structural RNA genes (tRNAs and rRNAs) (accession number NC_006958). The array data are publicly available in GEO by series entry GSE69449.

Sequence data analysis

The genomic nucleotide sequence of *C. glutamicum* ATCC 13032 was obtained from GenBank (accession number NC_006958) (Kalinowski et al. 2003). Nucleotide and protein sequence similarity searches were performed using BLAST programs at the BLAST server of NCBI (http://blast.ncbi.nlm.nih.gov/Blast.cgi) (Johnson et al. 2008). Pairwise protein sequence alignments were obtained using the Clustal Omega program available at the UniProt database (http://www.uniprot.org/align/) (Sievers et al. 2011).

Metabolite extraction and liquid chromatography-electrospray ionization-tandem mass spectrometry analysis

At an optical density of approximately OD_{600} = 6, cells were harvested for intracellular metabolite measurements by quenching 10-ml culture broth in 30 ml 60 % (*v*/*v*) methanol

at −50 °C. The cells were separated by centrifugation (4500 rpm, 10 min, −20 °C) in an Allegra 64R Centrifuge (Beckman Coulter, Krefeld, Germany). After decanting the supernatant, the pellet was immediately frozen at −80 °C in aluminum racks. For extraction of intracellular metabolites, the pellets were resolved in 50 % methanol in TE buffer (pH = 8) and chloroform (both at −20 °C). The volume of each solution was 50 times the intracellular volume in the pellet as measured by MultiSizer 3 (Beckman Coulter) equipped with a 30-μm capillary. Following subsequent incubation for 2 h at −20 °C in a Labquake shaker (Reax 2, Heidolph, Schwabach, Germany), the samples were again centrifuged as described above. The methanolic upper phase was filtrated through a 0.2-μm sterile filter (cellulose acetate, Dia-Nielsen, Düren, Germany) and stored at −80 °C until liquid chromatography-electrospray ionization-tandem mass spectrometry (LC-ESI-MS/MS) analysis.

Intracellular metabolites were measured by HPLC (Agilent 1200, Agilent Technologies, Waldbronn, Germany) coupled to a mass spectrometer (API 4000, ABSciex, Framingham, USA) equipped with a TurboIonSpray source in negative ionization mode. For analyte separation, a gradient elution on a C_{18} column (Synergy Hydro, 150 × 2 mm, 4 μm) from Phenomenex (Aschaffenburg, Germany) was performed with eluent A (10 mM tributylamine aqueous solution, pH adjusted to 4.95 with 15 mM acetic acid) and eluent B (methanol) at a temperature of 40 °C and at a flow of 0.45 ml min^{-1}. The gradient was as follows: 0 min 100 % A, 2 min 100 % A, 5 min 80 % A, 8 min 80 % A, 20 min 65 % A, 24 min 0 % A, 25 min 0 % A, 25 min 100 % A, and 28 min 100 % A. The injection volume was 10 μl. Samples were stored at 4 °C in the autosampler till injection. During elution, the mass transitions were monitored in non-scheduled mode. These transitions allow unique metabolite identification since various tandem MS fragmentation products specific to the metabolite in question are monitored in multiple reaction monitoring (MRM). The MS parameters for each mass transition were derived from an optimization of mass transitions using cinnamic acid as analytic standard. Furthermore, mass transitions were included, which correspond to product ions identified from a prior product ion scan using the extract samples generated as described above to enable unambiguous identification. All data were acquired by Analyst (version 1.6.2, ABSciex).

Results

C. glutamicum grows on phenylpropanoids as sole carbon and energy sources

Initially, it was investigated whether *C. glutamicum* ATCC 13032 can utilize five of the most abundant phenylpropanoids as sole carbon and energy sources. Cinnamic acid, 3-4-HPP, *p*-coumaric acid, caffeic acid, and ferulic acid differ in their hydroxylation and methoxylation patterns as well as in the saturation of the aliphatic side chain (Fig. 2). Indeed, it turned out that *C. glutamicum* is able to utilize all phenylpropanoids except cinnamic acid as sole carbon and energy sources. The determined growth rates of *C. glutamicum* ranged from 0.15 to 0.23 h^{-1} in the presence of 5 mM of the respective phenylpropanoid (Table 2). Interestingly, the organism failed to grow on cinnamic acid, which lacks a hydroxyl group on the aromatic ring (Fig. 3).

DNA microarray experiments identify a putative phenylpropanoid degradation pathway

Subsequently, DNA microarray experiments with phenylpropanoid pulses were performed to identify relevant genes or gene clusters, which might be activated in the presence of phenylpropanoids. We determined the relative messenger RNA (mRNA) levels of *C. glutamicum* wild-type cells confronted (pulsed) with phenylpropanoids compared to unpulsed cells. A pulsing time of 30 min was sufficient to detect significant differences in the gene expression patterns in response to 5 mM of all five phenylpropanoids individually. We identified six adjacent genes (cg0340-cg0341 and cg0344-cg0347; Fig. 4a), which showed enhanced transcript levels (mRNA ratio threshold ≥ 3.0) in the presence of the four ring-hydroxylated phenylpropanoids. The strongest expression of the six genes was obtained in the presence of caffeic acid, where the ratio of mRNA levels ranged from 80 to 100 (Table 3). Interestingly, *C. glutamicum* wild-type cells did not show highly altered transcript levels of the identified gene cluster (mRNA ratio < 3.0) when pulsed with cinnamic acid, which corresponds to the observation that *C. glutamicum* was not able to grow on this phenylpropanoid lacking any ring hydroxylation.

The automated annotation of the identified genes suggested that these genes code for a complete set of β-oxidation enzymes (Kalinowski et al. 2003). On the protein level, the upregulated genes in *C. glutamicum* show a strong homology to

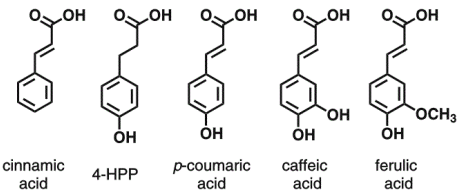

Fig. 2 Phenylpropanoids tested as sole carbon and energy sources for *C. glutamicum*. Phenylpropanoids vary in their hydroxylation and methoxylation patterns of the aromatic ring and in the saturation of the aliphatic side chain in α,β-position. Abbreviation: *4-HPP* = 3-(4-hydroxyphenyl) propionic acid. For the other phenylpropanoids, the respective trivial names are given

Table 2 Growth rates of the *C. glutamicum* wild type with different phenylpropanoids as sole carbon and energy sources

Phenylpropanoid	Growth rate μ (h^{-1})	
	Wild type	Δcg0340 (*phdT*)
Cinnamic acid	No growth	No growth
p-Coumaric acid	0.19 ± 0.01	0.17 ± 0.01
4-HPP	0.23 ± 0.04	0.16 ± 0.01
Caffeic acid	0.17 ± 0.01	0.10 ± 0.01
Ferulic acid	0.15 ± 0.01	0.10 ± 0.01

The data represent mean values and standard deviations obtained from three independent cultivations

enzymes of the soil bacterium *Rhodococcus jostii* RHA1. These enzymes were found to be involved in a β-oxidative degradation pathway for *p*-coumaric acid in this organism (Otani et al. 2014) (Table S2). This observation hints to the relevance of the identified gene cluster for the observed phenylpropanoid degradation in *C. glutamicum*. Additionally, the gene cg0343 encoding a putative MarR family transcriptional regulator is located within this cluster and is possibly involved in the control of its expression. Transcription of cg0343 itself is not regulated in response to the presence of any of the phenylpropanoids tested as no modulation of its transcription could be detected (data not shown).

In order to exclude that the expression of the cluster is unspecifically activated, we also tested if 4-hydroxybenzoic acid (4-HBA), the product of *p*-coumaric acid degradation via the assumed β-oxidative degradation, elicits the same change in the gene expression of this cluster during transcriptome analysis. Genes of the identified cluster were found to be not regulated in the presence of 4-HBA under identical experimental conditions (data not shown).

With the aim to answer the question whether the gene cluster is transcriptionally controlled by the putative MarR family regulator, a corresponding cg0343 deletion mutant was constructed and transcript levels of the resulting strain *C. glutamicum* Δcg0343 and the *C. glutamicum* wild-type strain were compared (Table 3). Indeed, transcript levels of cg0340-41 and cg0344-47 were strongly enhanced 120–200-fold in the cg0343 deletion strain (Table 3). This indicates that Cg0343 acts as a repressor, which unblocks its target promoter(s) upon interaction with an effector molecule, as it is typical for MarR-type regulators (Wilkinson and Grove 2006).

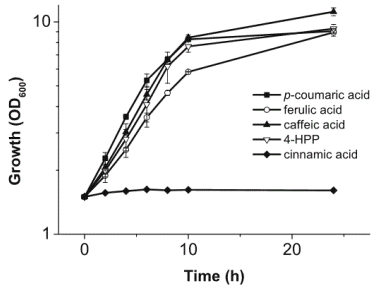

Fig. 3 Growth of *C. glutamicum* with phenylpropanoids as sole carbon and energy sources. Cultivations were performed in CGXII-defined medium with *p*-coumaric acid (*black square*), ferulic acid (*white square*), caffeic acid (*black triangle*), 4-HPP (*inverted white triangle*), and cinnamic acid (*black diamond*) as sole carbon and energy sources. Starting with an initial substrate concentration of 5 mM, phenylpropanoids were fed each 2 h during the course of the cultivation to avoid inhibiting substrate levels of >10 mM (5 mM after 2 h, 7.5 mM after 4 and 6 h, and 10 mM after 8 and 10 h). The data represent mean values and standard deviations obtained from three independent cultivations

Genomic deletions confirm the importance of the identified gene cluster for the phenylpropanoid catabolism

In addition to the cg0343 deletion mutant, we also constructed individual *C. glutamicum* deletion strains for the genes cg0340, cg0341, cg0344, cg0345, cg0346, and cg0347. Cultivation experiments were performed in defined CGXII medium with the ring-hydroxylated phenylpropanoids *p*-coumaric acid, 4-HPP, caffeic acid, or ferulic acid as sole carbon and energy sources. Interestingly, deletion of the following genes, putatively coding for β-oxidation enzymes, abolished growth on any of the following four phenylpropanoids tested: cg0341 (acyl:CoA ligase), cg0344 (3-hydroxyacyl-CoA dehydrogenase), cg0345 (hydrolase), and cg0347 (enoyl-CoA hydratase). Interestingly, deletion of cg0346 (acyl-CoA dehydrogenase) only abolished growth on 4-HPP, whereas the observed growth behavior in the presence of the other three phenylpropanoids was identical to that of the wild type (data not shown). This finding was not unexpected, as 4-HPP was the only of the tested compounds lacking a double bond in α,β-position of the aliphatic side chain. Given the annotation as acyl-CoA dehydrogenase, the corresponding enzyme Cg0346 is expected to introduce a double bond into the aliphatic side chain. In complementation experiments, plasmid-borne expressions of cg0341, cg0344, cg0345, cg0346, and cg0347 in the respective deletion strains fully restored growth when feeding 4-HPP as sole carbon and energy sources (Table S3). Deletion of the putative transporter gene cg0340 led to a reduction of the growth rate in the cultivation experiments with ring-hydroxylated phenylpropanoids. Growth rates were reduced by approximately 10 % for *p*-coumaric acid and for up to 40 % for caffeic acid (Table 2), but cg0340 was not essential for growth under the conditions tested. However, plasmid-borne expression of cg0340 in the *C. glutamicum* Δcg0340 deletion strain abolished this growth phenotype and allowed for growth rates similar to the *C. glutamicum* wild type with the same substrates (Table S3).

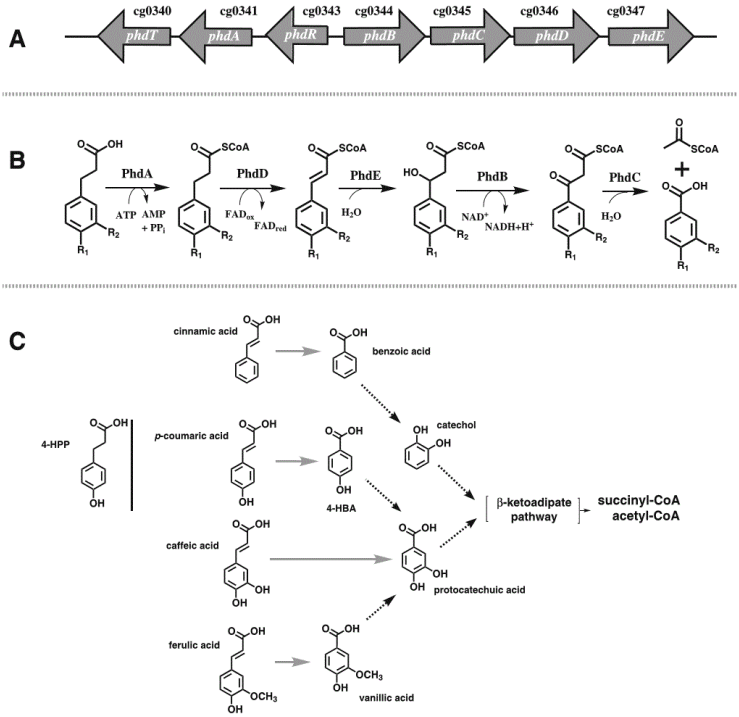

Fig. 4 Proposed phenylpropanoid degradation (Phd) pathway in *C. glutamicum*. Schematic overview of **a** the genetic organization of the identified *phd* gene cluster and **b** proposed CoA-dependent, β-oxidative deacetylation pathway for degradation of phenylpropanoids in *C. glutamicum*. Presumably, involved co-factors are also indicated. *PhdA* = acyl:CoA ligase, encoded by cg0341 (*phdA*); *PhdD* = acyl-CoA dehydrogenase, encoded by cg0346 (*phdD*); *PhdE* = enoyl-CoA hydratase, encoded by cg0347 (*phdE*); *PhdB* = 3-hydroxyacyl-CoA dehydrogenase, encoded by cg0344 (*phdB*); *PhdC* = 3-oxoacyl-CoA ketohydrolase (acetyl-CoA forming), encoded by cg0345 (*phdC*); *phdT* = transporter gene (cg0341); and *phdR* = MarR-type transcriptional repressor gene (cg0343). **c** Degradation pathways of the five tested phenylpropanoids to yield succinyl-CoA and acetyl-CoA of *C. glutamicum*. *Gray arrows* represent the β-oxidative deacetylation pathway of *C. glutamicum* as shown in **a**. Abbreviations: *4-HPP*, 3-(4-hydroxyphenyl)propionic acid; *4-HBA*, 4-hydroxybenzoic acid

Table 3 DNA microarray results for putative phenylpropanoid degradation cluster. Ratio of medians of relative mRNA levels obtained from phenylpropanoid pulse experiments for the identified phenylpropanoid catabolic gene cluster (*C. glutamicum* wild-type cells with phenylpropanoid pulse vs. unpulsed cells)

	Cinnamic acid	*p*-Coumaric acid	4-HPP	Caffeic acid	Ferulic acid	4-HBA	*C. glutamicum* Δcg0343
cg0340	2.4	3.4	70	77	4.2	0.8	211
cg0341	2.4	3.9	42	98	8.1	0.6	400
cg0344	2.3	4.4	82	80	9.2	0.8	140
cg0345	2.5	2.9	85	73	12.9	0.7	123
cg0346	2.2	3.9	102	80	9.3	0.8	167
cg0347	2.3	3.3	77	82	4.7	0.9	141

Results are mean values from at least two biological replicates (p value <0.05). Cells pulsed with the phenylpropanoid cinnamic acid as well as cells pulsed with 4-hydroxybenzoate (control for unspecific activation of the degradation pathway) showed no upregulation (mRNA ratio < 3) under the conditions tested. Additionally, mRNA ratios for comparison of *C. glutamicum* Δcg0343 versus *C. glutamicum* wild type are shown.

4-HBA 4-hydroxybenzoic acid, *4-HPP* 3-(4-hydroxyphenyl) propionic acid

Taken together, these results show that the identified gene cluster is essential for the stepwise degradation of phenylpropanoids in *C. glutamicum*, enabling growth solely on ring-hydroxylated phenylpropanoids. We therefore grouped the genes under the common designation *phd* (phenylpropanoid degradation): *phdT* (cg0340), *phdA* (cg0341), *phdR* (cg0343), *phdB* (cg0344), *phdC* (cg0345), *phdD* (cg0346), and *phdE* (cg0347) (Fig. 4a). According to the sequence analyses, the genes most likely encode for enzymes of a β-oxidative chain shortening mechanism (Fig. 4b).

Growth experiments revealed that the *C. glutamicum* wild type cannot grow on cinnamic acid, which is the only phenylpropanoid tested without any hydroxylation of the aromatic ring. We reasoned that either at least one of the enzymes of the degradation pathway has no activity with cinnamic acid (or any of the intermediates) or the interaction of cinnamic acid (or a possible intermediate of the Phd degradation pathway) with the regulator Cg0343 (PhdR) controlling the *phd* cluster is not sufficient to allow for de-repression of this catabolic gene cluster. Therefore, growth of the deletion mutant *C. glutamicum* Δcg0343, lacking the PhdR repressor, on cinnamic acid as sole carbon and energy sources was tested. Very interestingly, *C. glutamicum* Δcg0343 showed a growth rate of 0.19 h^{-1} on cinnamic acid, which is comparable to the growth rate obtained with the ring-hydroxylated phenylpropanoids tested. This implies that the enzymes of the Phd pathway also accept cinnamic acid and its degradation intermediates as substrates. Furthermore, this also shows that the MarR-type regulator PhdR only accepts ring-hydroxylated phenylpropanoids or a corresponding degradation intermediate.

Identification of the free acids of Phd pathway intermediates

With the aim of further strengthening the hypothesis that *C. glutamicum* performs β-oxidative deacetylation during phenylpropanoid degradation, we investigated the accumulation of individual Phd pathway intermediates in the constructed single-gene deletion mutants employing LC-ESI MS/MS analytics. This was necessary as the CoA-activated pathway intermediates were not commercially available for in vitro enzyme assays. The intermediates of the proposed β-oxidative pathway are CoA thioesters and as such notoriously difficult to detect in biological samples as a result of various spontaneous degradation reactions (Siegel et al. 2014). Indeed, a preliminary product ion scan of crude cell extract samples performed via LC-ESI MS/MS did not yield any detectable product ions corresponding to the mass of CoA esters of pathway intermediates (data not shown). Therefore, we focused on the detection of the free acids of pathway intermediates as a result of spontaneous hydrolysis of the CoA thioesters. With this approach, it was possible to detect 3-(4-hydroxyphenyl)-propanoic acid, *p*-coumaric acid, and 3-(4-hydroxyphenyl)-3-oxopropionic acid in the crude cell extracts of the *C. glutamicum* wild type cultivated with 4-HPP as sole carbon source (Table 4). The same intermediates were also found in the *C. glutamicum* Δcg0345 (*phdC*) mutant unable to perform the final cleavage reaction in the proposed pathway when the respective strain was cultivated with glucose and 4-HPP as carbon sources (Table 4). A strain lacking cg0346 (*phdD*) encoding a putative acyl-CoA dehydrogenase imported 4-HPP, but no *p*-coumaric acid was detectable (Table 4) on any mass trace corresponding to common tandem MS fragments of this metabolite (Table S4). In extracts of *C. glutamicum* strains lacking either cg0347 (*phdE*, coding for the putative enoyl-CoA hydratase) or cg0344 (*phdB*, coding for the putative 3-hydroxyacyl-CoA dehydrogenase), we found *p*-coumaric acid but no peak corresponding to 3-(4-hydroxyphenyl)-3-oxopropionic acid (Table 4). Unfortunately, no peak for 3-(4-hydroxyphenyl)-3-hydroxypropanoic acid could be detected in any of the analyzed samples. Typically, such metabolites with aliphatic hydroxy groups readily eliminate water upon electrospray ionization and therefore may fail to generate a quasi-molecular ion $[M\text{-}H]^-$ (Levsen et al. 2007). This may explain the absence of a peak on any mass trace of the intact hydroxylated intermediate. Nonetheless, all observations are in accordance with the model of phenylpropanoid degradation via β-oxidative deacetylation, suggesting that *C. glutamicum* follows this route during phenylpropanoid utilization.

Discussion

In this study, we identified and characterized the *phd* (phenylpropanoid degradation) gene cluster, which is responsible for the utilization of phenylpropanoids via a CoA-dependent, β-oxidative deacetylation route in *C. glutamicum*. The genes code for an integral membrane transport protein of the major facilitator superfamily (designated PhdT), a fatty acid:CoA ligase (PhdA), as well as for an acyl-CoA dehydrogenase (PhdD), an enoyl-CoA hydratase (PhdE), and a 3-hydroxyacyl-CoA dehydrogenase (PhdB). Interestingly, no thiolase that might catalyze the final cleavage reaction of the 3-oxoacyl-CoA intermediate is encoded as it has, for instance, been described for *Azoarcus* sp. EbN1 (Trautwein et al. 2012). Instead, PhdC, which is annotated as metal-dependent hydrolase of the TIM-barrel fold and contains a typical protein domain of the Amidohydrolase family (Amidohydro_2, Pfam PF04909), is involved in this pathway. We here propose that PhdC catalyzes a simple hydrolysis at the keto group at the C3 of the 3-oxoacyl-CoA intermediate, which circumvents the formation of a benzoyl-CoA derivative as it is typically the case for 3-oxoacyl-CoA thiolase catalyzed reactions (e.g., β-oxidation in fatty acid degradation). Instead, the proposed hydrolysis activity immediately leads to the formation of a benzoic acid derivative by cleaving off acetyl-CoA. Since

Table 4 LC-ESI-MS/MS results for selected free acids of the proposed ß-oxidation pathway

Metabolite		wild type	Δ*phdB*	Δ*phdC*	Δ*phdD*	Δ*phdE*
3-(4-hydroxy-phenyl)-propanoic acid	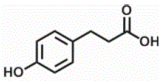	3.29*10^7	3.42*10^7	3.37*10^7	4.91*10^7	5.01*10^7
p-coumaric acid	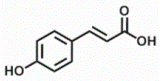	3.82*10^5	2.37*10^6	4.24*10^5	--	1.32*10^6
3-(4-hydroxy-phenyl)-3-hydroxy-propanoic acid	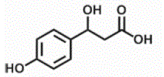	--	--	--	--	--
3-(4-hydroxy-phenyl)-3-oxopro-panoic acid	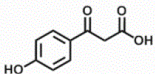	1.97*10^5	--	9.68*10^5	--	--

Peak areas on the mass transitions corresponding to a neutral loss of carbon dioxide of the indicated compound in crude cell extracts of *C. glutamicum*. On all other mass traces corresponding to the indicated metabolite, a peak was detected alike and no peaks were detected on mass traces not belonging to the respective metabolite. For the sake of brevity, peak integrations of just one mass trace per metabolite are shown. Dashed lines indicate that no peak could be detected on any mass trace belonging to the compound of interest

the Amidohydro_2 domain of PhdC is related to the large metal-dependent hydrolase superfamily, the name is misleading as the domain is also believed to be part of lactone-hydrolyzing enzymes and decarboxylases (Liu and Huo 2014; Liu and Zhang 2006).

Degradation of *p*-coumaric acid in the rhizosphere-inhabiting *Agrobacterium fabrum* also terminates with a hydrolytic step, yielding vanillic acid from ferulic acid degradation (Campillo et al. 2014). The responsible enzyme Atu1421 of *A. fabrum* harbors the same Amidohydro_2 domain as it has been also predicted for PhdC in *C. glutamicum*. Both enzymes, PhdC and Atu1421, do not show pronounced homology to known 3-oxoacyl-CoA thiolases (data not shown).

The identification of the free acids of pathway intermediates indeed confirmed the function of the individual proteins encoded by the identified *phd* gene cluster. Especially, the presence of 3-(4-hydroxyphenyl)-3-oxopropionic acid as intermediate further supports the notion that phenylpropanoid degradation in *C. glutamicum* proceeds via β-oxidation and deacetylation instead of a retro-aldol cleavage reaction. A β-oxidative degradation pathway for phenylpropanoids, very similar to the Phd pathway in *C. glutamicum*, was also described for the actinobacterium *R. jostii* RHA1 (Otani et al. 2014). The corresponding proteins in this organism show strong sequence homologies to the enzymes of the Phd pathway in *C. glutamicum* (Table S2). Interestingly, the hydrolase, catalyzing the final deacetylation (acetyl-CoA forming) reaction, also contains the same Amidohydro_2 domain as PhdC of *C. glutamicum* and Atu1421 of *A. fabrum*.

The genes *phdA*, *phdB*, *phdC*, and *phdE* are essential for growth with all tested phenylpropanoids. Additionally, *phdD* appears to be essential for growth on phenylpropanoids with an α,β-saturated side chain as we have observed it in case of 4-HPP. In contrast, deletion of *phdT* led to a reduced growth rate when *C. glutamicum* was cultivated on phenylpropanoids as sole carbon and energy sources. According to homology analyses, *phdT* codes for a putative transporter protein, presumably involved in the uptake of phenylpropanoids. The carboxylic acid group of phenylpropanoids has a pK_a value ranging from 4.3 to 4.6 (Beltran et al. 2003). As a consequence, phenylpropanoids are in the dissociated (deprotonated) form at neutral pH, which could hinder

passage across the membrane. Nonetheless, since growth of a *phdT*-deficient *C. glutamicum* strain could be observed, phenylpropanoids most likely enter the cell via other to date unknown transporters or via passive diffusion when present in high concentrations as it was the case in the performed cultivation experiments. In its natural soil environment, *C. glutamicum* is confronted with rather low substrate concentrations and transport mediated through PhdT would increase substrate uptake (Shen et al. 2005a).

Furthermore, we could show that the *C. glutamicum* ATCC 13032 wild type is unable to grow with cinnamic acid as sole carbon and energy sources. However, in the background of a *C. glutamicum* Δcg0343 mutant, lacking the transcriptional repressor PhdR, growth with cinnamic acid was possible, even allowing for a growth rate comparable to that of the other phenylpropanoids tested. Therefore, we deduce that PhdR specifically interacts with ring-hydroxylated phenylpropanoids, whereas there is no or only weak interaction with cinnamic acid devoid of any aromatic hydroxy group. As a result, there is not sufficient expression of the *phd* genes to enable growth of *C. glutamicum* with this phenylpropanoid. Degradation of other aromatic compounds in *C. glutamicum* is also mainly controlled by transcriptional regulatory proteins that sense the presence of the respective compound (Brinkrolf et al. 2006). For example, the PadR family regulator VanR controls the vanillate pathway by repressing *vanABK* gene expression (Brune et al. 2005; Shen et al. 2012). Our results indicate that PhdR, annotated as gene for a MarR-type transcriptional regulator, codes for a repressor controlling expression of the *phd* gene cluster and that PhdR-mediated repression is relieved by binding phenylpropanoids or a degradation intermediate. Regulators CouR and HcaR of the *p*-coumaric acid catabolic pathway in *Rhodopseudomonas palustris* and *Acinetobacter* sp. ADP1 (now referred to as *Acinetobacter baylyi* ADP1), respectively, have been shown to only bind to phenylpropanoid CoA thioesters and not phenylpropanoids itself as effector (Hirakawa et al. 2012; Parke and Ornston 2003). A phenylpropanoid degradation pathway in *R. jostii* RHA1 similar to the one investigated here is also regulated by a phenylpropanoid-responsive transcriptional repressor characterized recently (Otani et al. 2015). Prior to this study, a putative retro-aldol pathway was assumed to be responsible for the phenylpropanoid catabolism in *C. glutamicum* (Shen et al. 2012). In this study, three putative genes coding for an acyl-CoA synthetase (cg0480), an enoyl-CoA hydratase/lyase (cg0548), and a vanillin dehydrogenase (cg2953) were proposed to play a role in phenylpropanoid degradation based on bioinformatic analyses of the *C. glutamicum* proteom and comparison to already known phenylpropanoid catabolic enzymes (Shen et al. 2012). However, during transcriptome analyses, the three abovementioned genes did not show significantly altered transcript levels upon the presence of any of the five phenylpropanoids tested. This observation and the finding that loss of *phdA*, *phdB*, *phdC*, *phdE*, or *phdE* results in the inability to utilize phenylpropanoids under the tested conditions support our assumption that neither Cg0480 (FadD5), Cg0548 (MenB), nor Cg2953 (XylC) are involved in phenylpropanoid degradation in *C. glutamicum*.

Taken together, knowledge of the metabolic ability of *C. glutamicum* for utilizing phenylpropanoids as sole carbon and energy sources offers the possibility to use these abundant lignin-derived aromatic compounds as cheap feedstocks in biotechnological fermentation processes. Likewise, identification of this pathway is also the foundation for engineering the amino acid producer *C. glutamicum* towards the microbial synthesis of amino acid-derived phenylpropanoid-based products such as stilbenes or flavonoids. These compounds represent high-value products for food industries and pharmaceutical applications (van Summeren-Wesenhagen and Marienhagen 2013).

Acknowledgments We would like to thank Petra Geilenkirchen (Forschungszentrum Jülich) for the LC-ESI-MS/MS measurements.

Compliance with ethical standards

Ethical approval This article does not contain any studies with human participants or animals performed by any of the authors.

Conflict of interest The authors declare that they have no conflict of interest.

Funding This study was funded by the European Union Framework Program 7 "BacHBerry" (www.bachberry.eu), Project No. FP7-613,793.

References

Abe S, Takayama KI, Kinoshita S (1967) Taxonomical studies on glutamic acid-producing bacteria. J Gen Appl Microbiol 13(3): 279–301

Beltran J, Sanli N, Fonrodona G, Barron D, Özkan G, Barbosa J (2003) Spectrophotometric, potentiometric and chromatographic pK_a values of polyphenolic acids in water and acetonitrile–water media. Anal Chim Acta 484(2):253–264

Bertani G (1951) Studies on lysogenesis. I The Mode of Phage Liberation by Lysogenic *Escherichia coli*. J Bacteriol 62(3):293–300

Brinkrolf K, Brune I, Tauch A (2006) Transcriptional regulation of catabolic pathways for aromatic compounds in *Corynebacterium glutamicum*. Genet Mol Res 5(4):773–789

Brune I, Brinkrolf K, Kalinowski J, Puhler A, Tauch A (2005) The individual and common repertoire of DNA-binding transcriptional regulators of *Corynebacterium glutamicum*, *Corynebacterium efficiens*, *Corynebacterium diphtheriae* and *Corynebacterium jeikeium* deduced from the complete genome sequences. BMC Genomics 6:86

Buschke N, Schäfer R, Becker J, Wittmann C (2013) Metabolic engineering of industrial platform microorganisms for biorefinery applications—optimization of substrate spectrum and process robustness by rational and evolutive strategies. Bioresour Technol 135:544–554

Campillo T, Renoud S, Kerzaon I, Vial L, Baude J, Gaillard V, Bellvert F, Chamignon C, Comte G, Nesme X, Lavire C, Hommais F (2014) Analysis of hydroxycinnamic acid degradation in *Agrobacterium fabrum* reveals a coenzyme a-dependent, beta-oxidative deacetylation pathway. Appl Environ Microbiol 80(11):3341–3349

Diaz E (2004) Bacterial degradation of aromatic pollutants: a paradigm of metabolic versatility. Int Microbiol 7(3):173–180

Eggeling L, Bott M (2005) Handbook of *Corynebacterium glutamicum*. Taylor & Francis, Boca Raton FL

Eikmanns BJ, Kleinertz E, Liebl W, Sahm H (1991) A family of *Corynebacterium glutamicum/Escherichia coli* shuttle vectors for cloning, controlled gene expression, and promoter probing. Gene 102(1):93–98

Hirakawa H, Schaefer AL, Greenberg EP, Harwood CS (2012) Anaerobic *p*-coumarate degradation by *Rhodopseudomonas palustris* and identification of CouR, a MarR repressor protein that binds *p*-coumaroyl coenzyme a. J Bacteriol 194(8):1960–1967

Johnson M, Zaretskaya I, Raytselis Y, Merezhuk Y, McGinnis S, Madden TL (2008) NCBI BLAST: a better web interface. Nucleic Acids Res 36:W5–W9

Kalinowski J, Bathe B, Bartels D, Bischoff N, Bott M, Burkovski A, Dusch N, Eggeling L, Eikmanns BJ, Gaigalat L, Goesmann A, Hartmann M, Huthmacher K, Krämer R, Linke B, McHardy AC, Meyer F, Mockel B, Pfefferle W, Pühler A, Rey DA, Ruckert C, Rupp O, Sahm H, Wendisch VF, Wiegrabe I, Tauch A (2003) The complete *Corynebacterium glutamicum* ATCC 13032 genome sequence and its impact on the production of L-aspartate-derived amino acids and vitamins. J Biotechnol 104(1–3):5–25

Keilhauer C, Eggeling L, Sahm H (1993) Isoleucine synthesis in *Corynebacterium glutamicum*: molecular analysis of the *ilvB-ilvN-ilvC* operon. J Bacteriol 175(17):5595–5603

Levsen K, Schiebel HM, Terlouw JK, Jobst KJ, Elend M, Preiß A, Thiele H, Ingendoh A (2007) Even-electron ions: a systematic study of the neutral species lost in the dissociation of quasi-molecular ions. J Mass Spectrom 42(8):1024–1044

Liu A, and Huo L (2014) Amidohydrolase superfamily. In: eLS. John Wiley & Sons Ltd, Chichester

Liu A, Zhang H (2006) Transition metal-catalyzed nonoxidative decarboxylation reactions. Biochemistry 45(35):10407–10411

Marienhagen J, Bott M (2013) Metabolic engineering of microorganisms for the synthesis of plant natural products. J Biotechnol 163(2):166–178

Merkens H, Beckers G, Wirtz A, Burkovski A (2005) Vanillate metabolism in *Corynebacterium glutamicum*. Curr Microbiol 51(1):59–65

Mitra A, Kitamura Y, Gasson MJ, Narbad A, Parr AJ, Payne J, Rhodes MJ, Sewter C, Walton NJ (1999) 4-hydroxycinnamoyl-CoA hydratase/lyase (HCHL)—an enzyme of phenylpropanoid chain cleavage from *pseudomonas*. Arch Biochem Biophys 365(1):10–16

Niebisch A, Bott M (2001) Molecular analysis of the cytochrome bc1-aa3 branch of the *Corynebacterium glutamicum* respiratory chain containing an unusual diheme cytochrome c1. Arch Microbiol 175(4):282–294

Otani H, Lee YE, Casabon I, Eltis LD (2014) Characterization of *p*-hydroxycinnamate catabolism in a soil *Actinobacterium*. J Bacteriol 196(24):4293–4303

Otani H, Stogios PJ, Xu X, Nocek B, Li S-N, Savchenko A, Eltis LD (2015) The activity of CouR, a MarR family transcriptional regulator, is modulated through a novel molecular mechanism. Nucleic Acids Res. doi:10.1093/nar/gkv955gkv955

Parke D, Ornston LN (2003) Hydroxycinnamate (hca) catabolic genes from *Acinetobacter* sp. strain ADP1 are repressed by HcaR and are induced by hydroxycinnamoyl-coenzyme A thioesters. Appl Environ Microbiol 69(9):5398–5409

Sambrook J, Russell DW (2001) Molecular cloning: a laboratory manual, 3rd edn. Cold Spring Harbor Laboratory Press, Cold Spring Harbor, N.Y.

Schäfer A, Tauch A, Jäger W, Kalinowski J, Thierbach G, Puhler A (1994) Small mobilizable multi-purpose cloning vectors derived from the *Escherichia coli* plasmids pK18 and pK19: selection of defined deletions in the chromosome of *Corynebacterium glutamicum*. Gene 145(1):69–73

Shen XH, Liu SJ (2005) Key enzymes of the protocatechuate branch of the beta-ketoadipate pathway for aromatic degradation in *Corynebacterium glutamicum*. Sci China Ser C 48(3):241–249

Shen XH, Liu ZP, Liu SJ (2004) Functional identification of the gene locus (ncgl2319) and characterization of catechol 1,2-dioxygenase in *Corynebacterium glutamicum*. Biotechnol Lett 26(7):575–580

Shen XH, Huang Y, Liu SJ (2005a) Genomic analysis and identification of catabolic pathways for aromatic compounds in *Corynebacterium glutamicum*. Microbes Environ 20(3):160–167

Shen XH, Jiang CY, Huang Y, Liu ZP, Liu SJ (2005b) Functional identification of novel genes involved in the glutathione-independent gentisate pathway in *Corynebacterium glutamicum*. Appl Environ Microbiol 71(7):3442–3452

Shen XH, Zhou NY, Liu SJ (2012) Degradation and assimilation of aromatic compounds by *Corynebacterium glutamicum*: another potential for applications for this bacterium? Appl Microbiol Biot 95(1): 77–89

Siegel D, Permentier H, Reijngoud DJ, Bischoff R (2014) Chemical and technical challenges in the analysis of central carbon metabolites by liquid-chromatography mass spectrometry. J Chromatogr B Anal Technol Biomed Life Sci 966:21–33

Sievers F, Wilm A, Dineen D, Gibson TJ, Karplus K, Li W, Lopez R, McWilliam H, Remmert M, Soding J, Thompson JD, Higgins DG (2011) Fast, scalable generation of high-quality protein multiple sequence alignments using clustal omega. Mol Syst Biol 7:539

Trautwein K, Wilkes H, Rabus R (2012) Proteogenomic evidence for beta-oxidation of plant-derived 3-phenylpropanoids in "*Aromatoleum aromaticum*" EbN1. Proteomics 12(9):1402–1413

Unthan S, Grünberger A, van Ooyen J, Gätgens J, Heinrich J, Paczia N, Wiechert W, Kohlheyer D, Noack S (2014) Beyond growth rate 0.6: what drives *Corynebacterium glutamicum* to higher growth rates in defined medium. Biotechnol Bioeng 111(2):359–371

van Summeren-Wesenhagen PV, Marienhagen J (2013) Putting bugs to the blush: metabolic engineering for phenylpropanoid-derived products in microorganisms. Bioengineered 4(6):355–362

Vogt M, Haas S, Klaffl S, Polen T, Eggeling L, van Ooyen J, Bott M (2014) Pushing product formation to its limit: metabolic engineering of *Corynebacterium glutamicum* for L-leucine overproduction. Metab Eng 22:40–52

Wendisch VF (2014) Microbial production of amino acids and derived chemicals: synthetic biology approaches to strain development. Curr Opin Biotechnol 30:51–58

Wilkinson SP, Grove A (2006) Ligand-responsive transcriptional regulation by members of the MarR family of winged helix proteins. Curr Issues Mol Biol 8(1):51–62

2.2 Stilbene and (2*S*)-flavanone production in *C. glutamicum*

Metabolic Engineering 38 (2016) 47–55

Contents lists available at ScienceDirect

Metabolic Engineering

journal homepage: www.elsevier.com/locate/ymben

Original Research Article

Construction of a *Corynebacterium glutamicum* platform strain for the production of stilbenes and (2*S*)-flavanones

Nicolai Kallscheuer, Michael Vogt, Anton Stenzel, Jochem Gätgens, Michael Bott, Jan Marienhagen*

Institute of Bio- and Geosciences, IBG-1: Biotechnology, Forschungszentrum Jülich, D-52425 Jülich, Germany

ARTICLE INFO

Article history:
Received 10 March 2016
Received in revised form
31 May 2016
Accepted 8 June 2016
Available online 8 June 2016

Keywords:
Plant natural product
Stilbene
Flavanone
Resveratrol
Corynebacterium glutamicum
Metabolic engineering

ABSTRACT

Corynebacterium glutamicum is an important organism in industrial biotechnology for the microbial production of bulk chemicals, in particular amino acids. However, until now activity of a complex catabolic network for the degradation of aromatic compounds averted application of *C. glutamicum* as production host for aromatic compounds of pharmaceutical or biotechnological interest. In the course of the construction of a suitable *C. glutamicum* platform strain for plant polyphenol production, four gene clusters comprising 21 genes involved in the catabolism of aromatic compounds were deleted. Expression of plant-derived and codon-optimized genes coding for a chalcone synthase (CHS) and a chalcone isomerase (CHI) in this strain background enabled formation of 35 mg/L naringenin and 37 mg/L eriodictyol from the supplemented phenylpropanoids *p*-coumaric acid and caffeic acid, respectively. Furthermore, expression of genes coding for a 4-coumarate: CoA-ligase (4CL) and a stilbene synthase (STS) led to the production of the stilbenes pinosylvin, resveratrol and piceatannol starting from supplemented phenylpropanoids cinnamic acid, *p*-coumaric acid and caffeic acid, respectively. Stilbene concentrations of up to 158 mg/L could be achieved. Additional engineering of the amino acid metabolism for an optimal connection to the synthetic plant polyphenol pathways enabled resveratrol production directly from glucose. The construction of these *C. glutamicum* platform strains for the synthesis of plant polyphenols opens the door towards the microbial production of high-value aromatic compounds from cheap carbon sources with this microorganism.

1. Introduction

Corynebacterium glutamicum is an important workhorse in industrial biotechnology and highly productive strains for the production of several million tons of amino acids annually, especially L-glutamate and L-lysine have been developed (Becker et al., 2011; Koffas et al., 2003). In addition, *C. glutamicum* strains for the synthesis of a great variety of other commercially interesting compounds such as diamines, α-keto acids and alcohols have been engineered (Heider and Wendisch, 2015).

Interestingly, there was little effort for engineering *C. glutamicum* towards the synthesis of aromatic compounds other than aromatic amino acids (Ikeda, 2003). A possible reason for this could be the complex network of catabolic pathways for aromatic compounds (interestingly not for aromatic amino acids) present in this soil bacterium (Shen et al., 2012). In most cases, aromatic carbon substrates are prepared for enzymatic ring cleavage by peripheral degradation pathways leading to benzoic acid derivatives, which are subsequently converted into tricarboxylic acid cycle intermediates using the β-ketoadipate pathway or the gentisate pathway (Shen et al., 2005; Shen and Liu, 2005). In fact, *C. glutamicum* is able to utilize a broad range of aromatic compounds, such as benzoate, 4-hydroxybenzoate, *p*-cresol, resorcinol and vanillate as sole source of carbon and energy (Shen et al., 2012).

Very recently, we also found that *C. glutamicum* is able to grow on phenylpropanoids such as *p*-coumaric acid, ferulic acid, caffeic acid, and 3-(4-hydroxyphenyl)propionic acid and identified the Phd-pathway responsible for phenylpropanoid degradation in this organism (Kallscheuer et al., 2016). Phenylpropanoids, structurally characterized by a benzene residue attached to a propene tail, are derived from the aromatic amino acids L-phenylalanine or L-tyrosine through non-oxidative deamination. However, the same phenylpropanoids serve as building blocks for pharmacologically interesting plant polyphenols such as the stilbene resveratrol and the (2*S*)-flavanone naringenin (Marienhagen and Bott, 2013). Resveratrol is believed to have anti-tumor, anti-bacterial, anti-inflammatory and anti-aging effects and is discussed with respect to prevention of cardiovascular diseases (Pangeni et al., 2014). Similar

* Corresponding author.
E-mail address: j.marienhagen@fz-juelich.de (J. Marienhagen).

http://dx.doi.org/10.1016/j.ymben.2016.06.003
1096-7176/

effects including anti-mutagenic, anti-oxidant, anti-proliferative and anti-atherogenic activities were also reported for naringenin and naringenin-derived flavonoids (Erlund, 2004; Harborne, 2013). In recent years, efforts were made to engineer microorganisms such as *Saccharomyces cerevisiae* or *Escherichia coli* for the microbial synthesis of several stilbenes and flavanones, for the most part relying on precursor feeding (Marienhagen and Bott, 2013; Pandey et al. 2016).

We here describe the construction of a *C. glutamicum* platform strain for the production of plant-derived polyphenols, which is devoid of peripheral and central degradation pathways for aromatic compounds (Fig. S1). The suitability of this strain for the production of aromatic compounds was demonstrated by integrating heterologous pathways for the synthesis of the stilbenes resveratrol, pinosylvin and piceatannol and the (2*S*)-flavanones naringenin and eriodictyol from supplemented precursor molecules. Furthermore, the amino acid metabolism of *C. glutamicum* was engineered to allow for polyphenol production directly from glucose.

2. Materials and methods

2.1. Bacterial strains, plasmids, media and growth conditions

All bacterial strains and plasmids used in this study as well as their relevant characteristics are listed in Table 1. The constructed strains *C. glutamicum* DelAro^3 and *C. glutamicum* DelAro^4 are derived from *C. glutamicum* MB001(DE3), a prophage-free variant of *C. glutamicum* ATCC13032, which additionally harbors chromosomally encoded *gene 1* coding for T7 RNA polymerase allowing for (heterologous) gene expression under the control of the inducible T7 promoter (Baumgart et al., 2013; Kortmann et al., 2015). *C. glutamicum* and corresponding derivatives of this strain were routinely cultivated aerobically at 30 °C in brain heart infusion (BHI) medium (Difco Laboratories, Detroit, USA) or defined CGXII medium with glucose as sole carbon and energy source (Keilhauer et al., 1993). *E. coli* DH5α was used for plasmid constructions and was cultivated in LB medium (Bertani, 1951) at 37 °C. Where appropriate, kanamycin (50 μg/mL for *E. coli* or 25 μg/mL for *C. glutamicum*) or spectinomycin (100 μg/mL for *E. coli* and *C. glutamicum*) was added to the medium. Bacterial growth was followed by measuring the optical density at 600 nm (OD_{600}).

C. glutamicum was grown for 6–8 h in test tubes with 5 mL BHI medium on a rotary shaker at 170 rpm (first preculture) and subsequently inoculated into 50 mL CGXII medium in 500 mL baffled Erlenmeyer flasks (second preculture). The cell suspensions were cultivated overnight on a rotary shaker at 120 rpm. The main culture was inoculated to an OD_{600} of 5.0 in CGXII medium with 4% glucose. If indicated, 5 mM of phenylpropanoid (either cinnamic acid, *p*-coumaric acid, caffeic acid or ferulic acid) solved in DMSO was added. Heterologous gene expression was induced one hour after inoculation using 1 mM IPTG. If indicated, cerulenin (5–150 μM) was added to the culture medium after seven hours of cultivation (OD_{600} of 18–20). 1 mL of the culture broth was collected at defined time points and stored at −20 °C until extraction.

2.2. Plasmid and strain construction

Standard protocols of molecular cloning, such as PCR, DNA restriction, and ligation (Sambrook and Russell, 2001) were carried out for recombinant DNA work. Techniques specific for *C. glutamicum*, *e.g.* electroporation for transformation of strains, were done as described previously (Eggeling and Bott, 2005). All enzymes were obtained from ThermoScientific (Schwerte, Germany). Codon-optimized synthetic genes for *C. glutamicum* ATCC13032 were obtained from LifeTechnologies (Darmstadt, Germany). Genes were amplified by PCR using primers containing unique

Table 1
Strains and plasmids used in this study.

Strain or plasmid	Relevant characteristics	Source or reference
***C. glutamicum* strains**		
MB001(DE3)	prophage-free derivative of wild type ATCC 13032 with chromosomally encoded T7 *gene 1* (cg1122-P*lacI*-*lacI*-PlacUV5–*lacZα*-T7 *gene1*-cg1121)	Kortmann et al. (2015)
DelAro^3	MB001(DE3) derivative with in-frame deletions of cg0344-47, cg2625-40 and cg1226	This study
DelAro$^{3\text{-}4cl_{Pc}}$	DelAro^3 derivative with chromosomally encoded $4cl_{Pc}$ gene under control of the T7 promoter (Δcg0344-47:P_{T7}-$4cl_{Pc}$)	This study
DelAro^4	DelAro^3 derivative with in-frame deletion of cg0502	This study
DelAro^4-$4cl_{Pc}$	DelAro^4 derivative with chromosomally encoded $4cl_{Pc}$ gene under control of the T7 promoter (Δcg0344-47:P_{T7}-$4cl_{Pc}$)	This study
***E. coli* strains**		
DH5α	F– Φ80*lacZ*ΔM15 Δ(*lacZYA-argF*)U169 *recA1 endA1 hsdR17* (rK–, mK+) *phoA supE44* λ– *thi-1 gyrA96 relA1*	Invitrogen (Karlsruhe, Germany)
Plasmids		
pK19mobsacB	*kan*^{r}; vector for allelic exchange in *C. glutamicum* (pK18 oriV_{Ec} *sacB lacZα*)	Schäfer et al. (1994)
pK19mobsacB_cg0344-47-del	vector for in-frame deletion of cg0344-47	This study
pK19mobsacB_cg2625-40-del	vector for in-frame deletion of cg2625-40	This study
pK19mobsacB_cg1226-del	vector for in-frame deletion of cg1226	This study
pK19mobsacB_cg0502-del	vector for in-frame deletion of cg0502	This study
pMKEx2	*kan*^{r}; *E. coli*/*C. glut.* shuttle vector (*lacI*, P_{T7}, lacO1, pHM1519 ori$_{Cg}$; pACYC177 ori$_{Ec}$)	Kortmann et al. (2015)
pMKEx2_sts_{Ah}_$4cl_{Pc}$	*kan*^{r}; pMKEx2 derivative containing stilbene syntase gene and 4-coumarate CoA ligase	this study
pMKEx2_chs_{Ph}_chi_{Ph}	*kan*^{r}; pMKEx2 derivative containing chalcone syntase gene and chalcone isomerase gene	this study
pEKEx3	*spec*^{r}; *E. coli*/*C. glut.* shuttle vector (*lacI*, P_{tac}, lacO1, pBL1ori$_{Cg}$; pUCori$_{Ec}$)	Gande et al. (2007)
pEKEx3_$aroH_{Ec}$_tal_{Fj}	*spec*^{r}; pEKEx3 derivative containing $aroH_{Ec}$ from *E. coli* and tyrosine ammonia lyase gene	this study

kan^r: kanamycin resistance, *spec*^{r}: spectinomycin resistance.

Table 2
Oligonucleotides used in this study.

Primer name	Sequence (5′–3′)	Relevant site
Deletion of cg0344-47		
cg0344-7-up-s	CTCTCTAGAGCGGTGGCGATGATGATCTTCGAG	*Xba*I
cg0344-7-up-as	AAGCATATGAGCCAAGTACTATCAACGCGTCAGGGCGACTTTTCCATTGAGAGACATTTC	–
cg0344-7-down-s	CTGACGCGTTGATAGTACTTGGCTCATATGCTTTTCCTCACCCGCTTCTACGCTTAAAAG	–
cg0344-7-down-as	GACGAATTCGTGTGGCCACCACCTCAATCTGTG	*Eco*RI
del-cg0344-7-s	AGAGATTCACCCTCGGCGATGAG	–
del-cg0344-7-as	GACCCGCAATGGTGTCGCCAG	–
Deletion of cg1226		
up-cg1226-s	CACAAGCTTCCACACGATGAAAATCAATCCGCAG	*Hind*III
up-cg1226-as	TGCGGTACCCTCGCATATGATATCTCGAGAGCTAATTGCCACTGGTACGTGGTTCATG	–
down-cg1226-s	AGCTCTCGAGATATCATATGCGAGGGTACCGCAGACCTACCACGCTTCGAGGTATAAACGCTC	–
down-cg1226-as	AGTGAATTCCAAGGAAGGCGGTTGCTACTGC	*Eco*RI
del-cg1226-s	TAAATGGTGGAGATACCAAACTGTGAAGC	–
del-cg1226-as	CGAGTTCTTCTTCGTGTTCGCGATC	–
Deletion of cg2625-40		
up-cg2625-40-s	ACATCTAGAGGTCGGCGAATCAAGCTCCATG	*Xba*I
up-cg2625-40-as	CGTCTCGAGTTCACATATGCAACGCGTGCTCAAGATGACAATATCTTGAGGGTTCATTTTTTGATCCTTAATTTAG	–
down-cg2625-40-s	TTGAGCACGCGTTGCATATGTGAACTCGAGACGGTCGGTGGAGGCGACCAGGGATAAC	–
down-cg2625-40-as	TCTGAATTCATCAAGGCCAATCATGATGAGTGCGAAAC	*Eco*RI
del-cg2625-40-s	AAGAGGAGTTGATGGGATGGTCGAACAATC	–
del-cg2625-40-as	GTTGGCATGCCAGCTTTGTGGGATG	–
Deletion of cg0502		
up-cg0502-s	ACGAAGCTTTGTCCGGCATGCTGGCTGAC	*Hind*III
up-cg0502-as	TGCGCATATGTGGCCGTCTAGATACGCGTACGTCAAACAAACAGTGGCAATGGATGTACGCATG	–
down-cg0502-s	ACGTACGCGTATCTAGACGGCCACATATGCGCAATCGAGCGGGGAATCCCAAACTAGCATC	–
down-cg0502-as	TATGGATCCTACGCCTGTACACCGTCGCACGTC	*Bam*HI
del-cg0502-s	GTGAACATTGTGTTTACTGTGTGGGCACTGTC	–
del-cg0502-as	TGATGTTCAGGCCGTTGAAGCCAAGGTAGAG	–
Cloning primers		
stsAh-s	ATACCATGGTAAGGAGGACAGCTATGGTGTCCGTGTCCGGCATC	*Nco*I
stsAh-as	CTCGGTACCTTTAGATTGCCATAGAGCGCAGCACCAC	*Kpn*I
4clPc-s	AGCGGTACCTAAGGAGGTGGACAATGGGCGATTGCGTGGCAC	*Kpn*I
4clPc-as	CTGGGATCCAGGACTAGTTTCCAGAGTACTATTACTTTGGCAGATCACCGGATGCGATC	*Bam*HI
chsPh-s	GTATCTAGAAAGGAGGTCGAAGATGGTGACCGTGGAAGAATACCGCAAG	*Xba*I
chsPh-as	CTCCCATGGTTAGGTTGCCACGGAGTGCAGCAC	*Nco*I
chiPh-s	CTCCCATGGTGCTAAAGGAGGTCGAAGATGTCCCCACCAGTGTCCGTGACCAAG	*Nco*I
chiPh-as	CTGGGATCCTTACACGCCGATCACTGGGATGGTG	*Bam*HI
aroHEc-s	CTCGGATCCAAGGAGGTCATATCATGAACAGAACTGACGAACTCCGTACTGCGCGTATTG	*Bam*HI
aroHEc-as	TACGCTCTTCTGATTTAGAAGCGGGTATCTACCGCAGAGGCGAG	*Sap*I
talFj-s	TTCGCTCTTCAATCTGGCAAGGAGGGATCCGTATGAACACCATCAACGAATACCTGTCCCTGGAAG	*Sap*I
talFj-as	ATCGAATTCTTAGTTGTTGATCAGGTGATCCTTCACCTTCTGCAC	*Eco*RI

restriction sites (Table 2). PCR products were used for cloning of genes into plasmid vectors using the introduced restrictions site. For plasmids containing more than one insert, genes were cloned sequentially. In-frame deletions or integration of genes into the genome of *C. glutamicum* was performed using the pK19mobsacB system (Schäfer et al., 1994) by a two-step homologous recombination method described previously (Niebisch and Bott, 2001). All constructed plasmids were finally verified by DNA sequencing at Eurofins MWG Operon (Ebersberg, Germany).

2.3. Metabolite extraction using ethyl acetate

Metabolite extracts from cultivation broth were prepared for GC-TOF-MS and LC-MS analysis by mixing 1 mL of the culture broth with 1 mL ethyl acetate and vigorous shaking (1400 rpm; 10 min, 20 °C) in an Eppendorf thermomixer (Hamburg, Germany). The suspension was centrifuged for five minutes at 16,000*g* and the ethyl acetate layer (800 μL) was transferred to an organic solvent resistant deep-well plate (Eppendorf, Hamburg, Germany). After evaporation of the ethyl acetate overnight, dried extracts were resuspended in the same volume of acetonitrile and directly used for GC-TOF-MS analysis or LC-MS analysis.

2.4. GC-TOF-MS analysis

Prior to analysis 130 μL aliquots of extracted samples were shock frozen in liquid nitrogen, then lyophilized overnight in a LT-105 freeze drier (Martin Christ Gefriertrocknungsanlagen, Osterode am Harz, Germany) and then stored at −20 °C. The dried samples were consecutively derivatized with 50 μL MeOX (20 mg/mL *O*-methylhydroxylamine in pyridine) for 90 min at 30 °C and 600 rpm in an Eppendorf Thermomixer followed by an incubation with additional 80 μL of MSTFA (N-acetyl-N-(trimethylsilyl)-trifluoroacetamide) for 90 min at 40 °C and 600 rpm. For the determination of the derivatized metabolites an Agilent 6890N gas chromatograph (Agilent, Waldbronn, Germany) was used coupled to a Waters Micromass GCT Premier high resolution time-of-flight mass spectrometer (Eschborn, Germany). The system was controlled by Waters MassLynx 4.1 software. Injections were performed by a Gerstel MPS 2 (Mülheim an der Ruhr, Germany) controlled by Maestro software. 1 μL sample was injected into a split/splitless injector at 280 °C at varying split modes. The GC was equipped with a 30 m Agilent EZ-Guard VF-5ms+10 m guard column (Agilent, Waldbronn, Germany). Constant helium flow was set to 1 mL/min. The GC temperature program starts at 60 °C with a hold time of 2 min, followed by a temperature ramp of +12 °C/min up to the final temperature of 300 °C and hold time of 8 min. This leads to a total run time of 30 min. The transfer line temperature was set to 300 °C. The TOF-MS was operated in positive electron impact $[EI]^+$ mode at an electron energy of 70 eV. Ion source temperature was set to 180 °C. The MS was tuned and calibrated with the mass fragmentation pattern of Heptacosa

(heptacosafluorotributylamine). During analysis, the accurate masses were corrected to a single point lock mass of CPFB (chloropentafluoro-benzene) as an external reference at 201.9609 *m/z*. Data acquisition was done in centroid mode with a scan rate of 0.09 s and an interscan delay of 0.01 s, that means 10 scans/s. For the identification of known metabolites we used a baseline noise substracted fragment pattern in comparison to our in-house database JuPoD and the commercial database NIST11 (National Institute of Standards and Technology, Gaithersburg, USA). Unknown peaks were identified by structural combination of elemental compositions and verified by virtual derivatization and fragmentation of the predicted structure.

2.5. LC-MS analysis for quantification of stilbenes and flavanones

Stilbenes and (2*S*)-flavanones in extracted samples were quantified by LC-MS using an ultra-high-performance LC (uHPLC) 1290 Infinity System coupled to a 6130 Quadrupole LC-MS System (Agilent, Waldbronn, Germany). LC separation was carried out with a Kinetex 1.7u C_{18} 100 Å pore size column (50 mm by 2.1 mm [internal diameter]; Phenomenex, Torrance, CA, USA) at 50 °C. For elution, 0.1% acetic acid (solvent A) and acetonitrile supplemented with 0.1% acetic acid (solvent B) were applied as the mobile phases at a flow rate of 0.5 mL/min. A gradient was used, where the amount of solvent B was increased stepwise: minute 0–6: 10–30%, minute 6–7: 30–50%, minute 7–8: 50–100% and minute 8–8.5: 100–10%. The mass spectrometer was operated in the negative electrospray ionization (ESI) mode, and data acquisition was performed in selected-ion-monitoring (SIM) mode. Authentic metabolite standards were purchased from Sigma-Aldrich (Schnelldorf, Germany). Area values for $[M\text{-}H]^-$ mass signals were linear up to metabolite concentrations of at least 250 mg/L. Benzoic acid (final concentration 100 mg/L) was used as internal standard. Calibration curves were calculated based on analyte/internal standard ratios for the obtained area values.

3. Results and discussion

3.1. Chromosomal deletion of genes involved in the catabolism of aromatic compounds in C. glutamicum

Microbial synthesis of stilbenes and (2*S*)-flavanones from supplemented phenylpropanoids with an engineered *C. glutamicum* strain harboring a synthetic plant polyphenol pathway would interfere with this organism's capability to degrade the phenylpropanoid precursors. In this case, the implemented synthetic polyphenol anabolism would compete with the endogenous phenylpropanoid catabolism for phenylpropanoid CoA-thioesters as common pathway intermediates (Fig. 1). In order to abolish degradation of phenylpropanoids, the *phdBCDE* operon (cg0344-47) essential for phenylpropanoid utilization via the Phd-pathway was deleted in the genome of *C. glutamicum* MB001(DE3). In this context, the genes for the phenylpropanoid transporter PhdT (Cg0340) and the phenylpropanoid: CoA ligase PhdA (Cg0341) responsible for phenylpropanoid uptake and formation of phenylpropanoyl-CoA thioesters, respectively, were not deleted as both proteins can be also exploited for desired plant polyphenol production with *C. glutamicum*.

An unspecific conversion of the phenylpropanoid substrates and pathway intermediates may also occur by enzyme-catalyzed ring hydroxylation or ring cleavage reactions as the natural substrates of the 4-hydroxybenzoate-3-hydroxylase PobA and protocatechuate dioxygenase PcaGH are structurally very similar to phenylpropanoid intermediates (Chang and Zylstra, 2008; Hammer et al., 1996). Therefore, the genes *pobA* (cg1226) and a gene

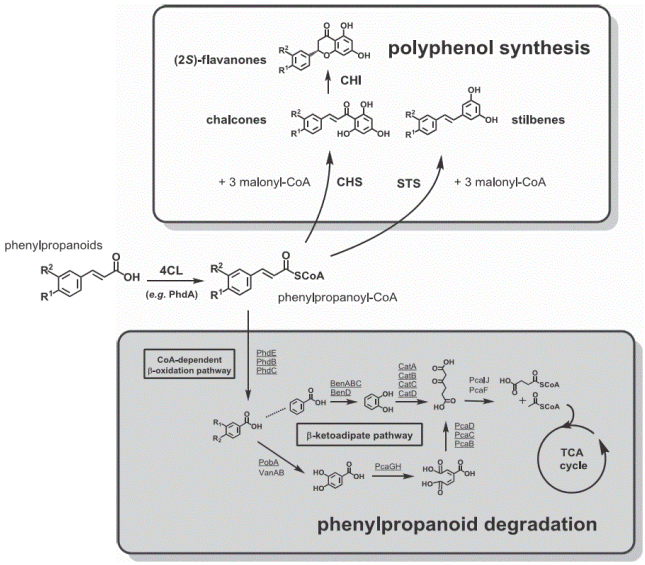

Fig. 1. Pathway overview of polyphenol synthesis and phenylpropanoid degradation. Phenylpropanoids can either be converted into stilbenes or (2*S*)-flavanones (polyphenol synthesis) or are degraded to succinyl-CoA and acetyl-CoA by a CoA-dependent, β-oxidative phenylpropanoid catabolic pathway and the β-ketoadipate pathway (phenylpropanoid degradation). Genes coding for underlined enzymes are deleted in the *C. glutamicum* DelAro^3 strain. Phenylpropanoids supplemented for stilbene or (2*S*)-flavanone production include cinnamic acid (R^1=H, R^2=H), *p*-coumaric acid (R^1=OH, R^2=H), caffeic acid (R^1=OH, R^2=OH) and ferulic acid (R^1=OH, R^2=OCH_3). 4CL: 4-coumarate: CoA ligase; CHS: chalcone synthase; CHI: chalcone isomerase, STS: stilbene synthase.

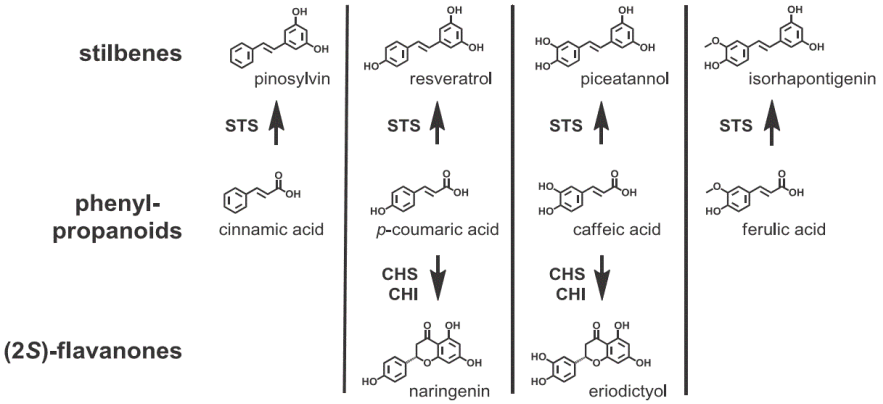

Fig. 2. Phenylpropanoids tested as substrates for stilbene or (2*S*)-flavanone production with *C. glutamicum*. Supplemented phenylpropanoids are either converted to their corresponding stilbenes by activity of stilbene synthase (STS) or to (2*S*)-flavanones by coupled action of chalcone synthase (CHS) and chalcone isomerase (CHI). For simplicity, the 4-coumarate:CoA ligase reaction being essential for the conversion of phenylpropanoids to their corresponding CoA-thioesters prior to polyphenol formation is not depicted.

cluster harboring *cat*, *ben* and *pca* genes (cg2625-40) essential for the degradation of 4-hydroxybenzoate, catechol, benzoate and protocatechuate were also deleted (Table S1). The gene clusters did not contain any genes coding for regulator proteins and transporter proteins. We designated the resulting strain with deletion of three gene clusters containing altogether 20 genes *C. glutamicum* DelAro^3 (Table S1). Cultivation experiments confirmed that the strain is unable to utilize phenylpropanoids as sole carbon and energy source. The strain also failed to degrade 4-hydroxybenzoate and protocatechuate and no catabolic intermediates stemming from supplemented phenylpropanoids could be detected during cultivation in cell crude extracts using GC-TOF

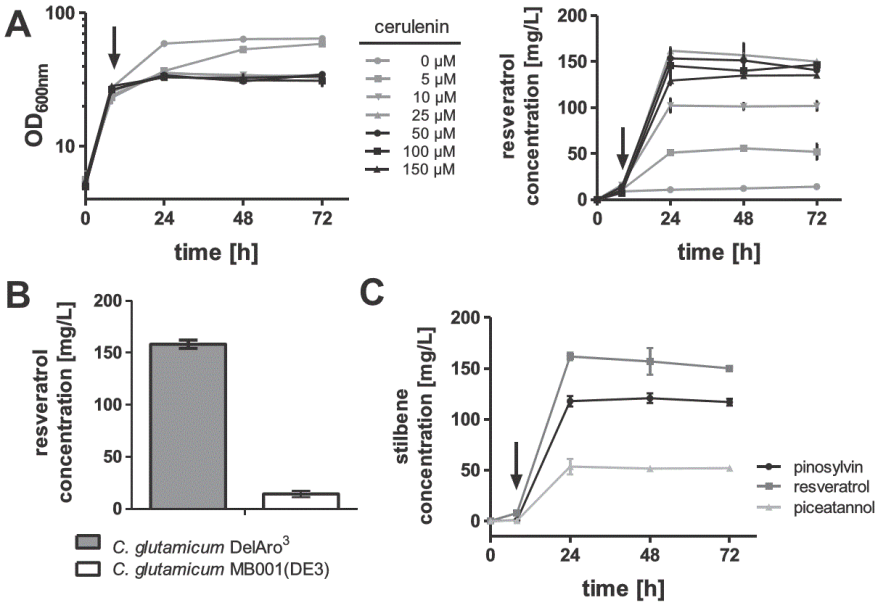

Fig. 3. Cell growth and stilbene production from supplemented phenylpropanoids with *C. glutamicum*. (A) *C. glutamicum* DelAro^3 pMKEx2_sts_{Ah}_$4cl_{Pc}$ was cultivated in presence of 5 mM of *p*-coumaric acid and of different cerulenin concentrations ranging from 0 to 150 µM. The time point of addition of cerulenin after seven hours is indicated by an arrow. (B) Maximal resveratrol titers with either strain *C. glutamicum* MB001(DE3) or *C. glutamicum* DelAro^3 each harboring pMKEx2_sts_{Ah}_$4cl_{Pc}$ in presence of 5 mM *p*-coumaric acid and 25 µM cerulenin. (C) *C. glutamicum* DelAro^3 pMKEx2_sts_{Ah}_$4cl_{Pc}$ was cultivated in presence of 5 mM of the three phenylpropanoids cinnamic acid, *p*-coumaric acid and caffeic acid leading to production of pinosylvin, resveratrol and piceatannol, respectively. Data of each graph represent average values and standard deviations from three biological replicates.

analysis (data not shown).

3.2. Microbial production of plant stilbenes with C. glutamicum DelAro^3

Starting from phenylpropanoids as precursors, expression of a heterologous two-step pathway comprising a 4-coumarate: CoA ligase (4CL) and a stilbene synthase (STS) enabled the synthesis of the stilbenes resveratrol, pinosylvin and piceatannol (Fig. 2). With the aim for a strong expression of the heterologous genes, the plasmid pMKEx2 was used, which allows for IPTG-inducible gene expression from the strong T7 promoter. The recombinant plasmid pMKEx2_sts_{Ah}_$4cl_{Pc}$ harbored two codon-optimized genes coding for STS from peanut (*Arachis hypogaea*) and 4CL from parsley (*Petroselinum crispum*) (Lozoya et al., 1988; Watts et al., 2006). Plasmid-based gene expression in the *C. glutamicum* DelAro^3 strain in defined CGXII medium with 4% glucose and supplemented with 1 mM IPTG and 5 mM *p*-coumaric acid led to production of 12 ± 2 mg/L resveratrol, which is to the best of our knowledge the first report of polyphenol production in *C. glutamicum* (Fig. 3A). Interestingly, we found that codon-optimization of heterologous genes was a key step for polyphenol production in *C. glutamicum*, as the initial attempt to produce stilbenes with strains expressing the same, but non-codon-optimized gene versions, was not successful (data not shown).

Malonyl-CoA is often recognized as major bottleneck for microbial production of plant polyphenols (Kim and Ahn, 2014; Leonard et al., 2007; Lim et al., 2011; Wu et al., 2013; Yang et al., 2015; Zha et al., 2009). A common strategy to increase the availability of malonyl-CoA is the supplementation of the antibiotic cerulenin, which binds to the β-ketoacyl-acyl carrier protein (ACP) synthase of the fatty acid synthesis machinery, thereby inhibiting its enzymatic activity (Santos et al., 2011; van Summeren-Wesenhagen and Marienhagen, 2015). This in turn results in an increased intracellular malonyl-CoA pool as the fatty acid synthesis is blocked. Indeed, also in *C. glutamicum* resveratrol concentrations could be increased in presence of cerulenin. Addition of 5 μM, 10 μM and 25 μM cerulenin enhanced maximal resveratrol concentration 5-fold, 8-fold and 13-fold, respectively, whereas even higher cerulenin concentrations ranging from 50 to 150 μM did not further increase resveratrol titers (Fig. 3A). Supplementation of 25 μM cerulenin proved to be optimal for *C. glutamicum* under the experimental conditions tested. The highest titer corresponded to 158 ± 4 mg/L resveratrol (Fig. 3A). Addition of 25 μM cerulenin arrested growth of *C. glutamicum* completely one hour after addition to the culture medium.

In order to confirm that the capability for degrading aromatic compounds, in particular of phenylpropanoids, impedes stilbene production with *C. glutamicum*, the reference strain *C. glutamicum* MB001(DE3) harboring pMK2_stsAh_4clPc was cultivated under optimized cultivation conditions described above. When supplemented with 5 mM *p*-coumaric acid and in presence of 25 μM cerulenin (added after 7 h of cultivation), a resveratrol titer of only 14 ± 3 mg/L was reached, which is less than 10% of the resveratrol concentration obtained with the production strain constructed on the basis of *C. glutamicum* DelAro3 (Fig. 3B). This shows that the abolishment of competing degradation pathways for aromatic compounds represents the key step for production of high titers of polyphenols in *C. glutamicum*.

The stilbene synthase from peanut was also shown to convert CoA-thioesters of cinnamic acid and caffeic acid to their corresponding stilbenes pinosylvin and piceatannol, respectively (Fig. 2) (Watts et al., 2006). Thus, the two phenylpropanoids were also tested as alternative phenylpropanoid starter units in *C. glutamicum*. In the presence of 25 μM cerulenin, 121 ± 2 mg/L pinosylvin (from 5 mM cinnamic acid) and 56 ± 3 mg/L piceatannol (from 5 mM caffeic acid) could be produced with *C. glutamicum* DelAro^3 pMK2_sts_{Ah}_$4cl_{Pc}$ (Fig. 3C). In addition to LC-MS analysis, the identity of produced resveratrol, pinosylvin and piceatannol was confirmed by GC-TOF-MS based on the individual molecule fragmentation patterns (Figs. S2-S7). A possible conversion of the precursor phenylpropanoid ferulic acid was also tested, but the expected stilbene isorhapontigenin was not formed (Fig. 2). This is in line with published results for the employed STS from peanut, as only tri- and tetraketide lactones accumulate when supplementing ferulic acid (Watts et al., 2006). This suggests that the STS from peanut cannot properly accommodate and fold the tetraketide to the corresponding stilbene structure. However, formation of such tri- and tetraketide lactones could also not be observed during the experiments with *C. glutamicum* DelAro^3 pMK2_sts_{Ah}_$4cl_{Pc}$. Instead, a yet unidentified compound was synthesized (data not shown).

3.3. Production of (2S)-flavanones as precursors of flavonoids with C. glutamicum DelAro^3

(2*S*)-Flavanones are synthesized from the same phenylpropanoid precursors as stilbenes but their formation involves a different enzyme-catalyzed reaction mechanism. After synthesis of a chalcone, conversion into the (2*S*)-flavanone requires an isomerization step leading to the formation of the non-aromatic C-ring (Fig. 1) (van Summeren-Wesenhagen and Marienhagen, 2013). These two reactions are catalyzed by chalcone synthases (CHS) and chalcone isomerases (CHI). CHS and CHI originating from petunia (*Petunia x hybrida*) were evaluated for (2*S*)-flavanone production with *C. glutamicum* (Fig. 2) as both enzymes were already successfully used for microbial production of natural compounds (Leonard et al., 2006; Malla et al., 2012; Wu et al., 2013). The strain *C. glutamicum* DelAro^3-$4cl_{Pc}$ was constructed, which carries the *4cl* gene of *P. crispum* under control of the T7 promoter in the chromosome. *C. glutamicum* DelAro^3-$4cl_{Pc}$ pMKEx2_chs_{Ph}_chi_{Ph} accumulated up to 35 ± 2 mg/L naringenin from supplemented 5 mM *p*-coumaric acid and 37 ± 4 mg/L eriodictyol from 5 mM caffeic acid in the presence of 25 μM cerulenin and 1 mM IPTG (Fig. 4).

At this stage, we also tested if expression of the endogenous

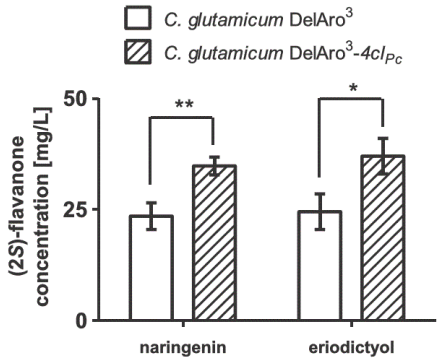

Fig. 4. (2*S*)-Flavanone production in *C. glutamicum* DelAro^3 and *C. glutamicum* DelAro^3-$4cl_{Pc}$ both harboring pMKEx2_chs_{Ph}_chi_{Ph}. *C. glutamicum* DelAro^3 and *C. glutamicum* DelAro^3-$4cl_{Pc}$ both harboring pMKEx2_chs_{Ph}_chi_{Ph} were cultivated in presence of 5 mM *p*-coumaric acid or 5 mM caffeic acid for producing naringenin or eriodictyol, respectively. Data represent average values and standard deviations of (2*S*)-flavanone concentrations from three biological replicates. 25 μM cerulenin was added to all cultures seven hours after inoculation. Asterisks indicate *P*-values with * $P \leq 0.05$, ** $P \leq 0.01$.

phdA gene coding for the 4CL involved in phenylpropanoid catabolism of *C. glutamicum* from its native (regulated) promoter in the genome of *C. glutamicum* is sufficient for (2*S*)-flavanone production. This would reduce the burden of heterologous gene expression as two instead of three heterologous genes need to be expressed. Indeed, 24 ± 3 mg/L naringenin and 25 ± 4 mg/L eriodictyol were produced in *C. glutamicum* DelAro^3 pMKEx2_chs_{Ph}_chi_{Ph} (Fig. 4). In consequence, expression of a heterologous *4cl* gene can be omitted in the future, when constructing *C. glutamicum* strains for the synthesis of naringenin- or eriodictyol-derived flavonoids, which require the expression of additional heterologous genes.

3.4. Production of resveratrol and naringenin from glucose

Until now, efforts for producing stilbenes and (2*S*)-flavanones with microorganisms focused mainly on *E. coli* and *S. cerevisiae* (Trantas et al., 2009; van Summeren-Wesenhagen and Marienhagen, 2015; Wu et al., 2014). For both organisms, production of stilbenes and (2*S*)-flavanones from glucose could already be achieved (Li et al., 2015; Santos et al., 2011; Wang et al., 2011). Hence, it was also highly desirable to enable polyphenol production directly from glucose with *C. glutamicum* DelAro^3 as this would eliminate the need for supplementation phenylpropanoids as expensive precursor metabolites. In case of resveratrol and naringenin synthesis, deregulation of the shikimate pathway for overproducing L-tyrosine and implementation of a tyrosine ammonia lyase (TAL) for the conversion of L-tyrosine to *p*-coumaric acid are key steps for connecting the endogenous amino acid anabolism from glucose to the synthetic polyphenol pathway (Fig. 5A).

The 3-deoxy-D-arabinoheptulosonate-7-phosphate (DAHP) synthase catalyzes the highly regulated committed first step of the shikimate pathway towards aromatic amino acid synthesis in *C. glutamicum* consuming the precursor molecules erythrose-4-phosphate and phosphoenolpyruvate (Ikeda, 2006) (Fig. S1). While the two DAHP synthase isoenzymes of *C. glutamicum* are feedback-inhibited by the shikimate pathway intermediates prephenate and chorismate (Li et al., 2009), is the DAHP synthase AroH of *E. coli* only feedback-regulated by L-tryptophan (Ray et al., 1988). We tested if heterologous expression of the $aroH_{Ec}$ gene in *C. glutamicum* allows for synthesis of sufficient L-tyrosine levels for polyphenol synthesis. In addition, a TAL catalyzing the subsequent non-oxidative deamination of L-tyrosine is needed for the synthesis of the phenylpropanoid *p*-coumaric acid. Recently, several TALs were tested for activity in *E. coli*, *Lactococcus lactis* and *S. cerevisiae* (Jendresen et al., 2015). Based on these findings, we evaluated the TAL from *Flavobacterium johnsoniae* (TAL_{Fj}) for an application in *C. glutamicum*. The corresponding gene tal_{Fj}, optimized to the codon usage of *C. glutamicum*, was cloned in combination with $aroH_{Ec}$, which was PCR-amplified from genomic DNA of *E. coli* into the *C. glutamicum* expression plasmid pEKEx3 yielding pEKEx3_$aroH_{Ec}$_tal_{Fj}. When $aroH_{Ec}$ and tal_{Fj} were expressed in *C. glutamicum* DelAro^3 harboring the plasmid pEKEx3_$aroH_{Ec}$_tal_{Fj}, the strain produced 0.9 g/L protocatechuate but no production of L-tyrosine or *p*-coumaric acid could be observed (data not shown). We assumed that the degradation pathway for shikimate and quinate present in *C. glutamicum*

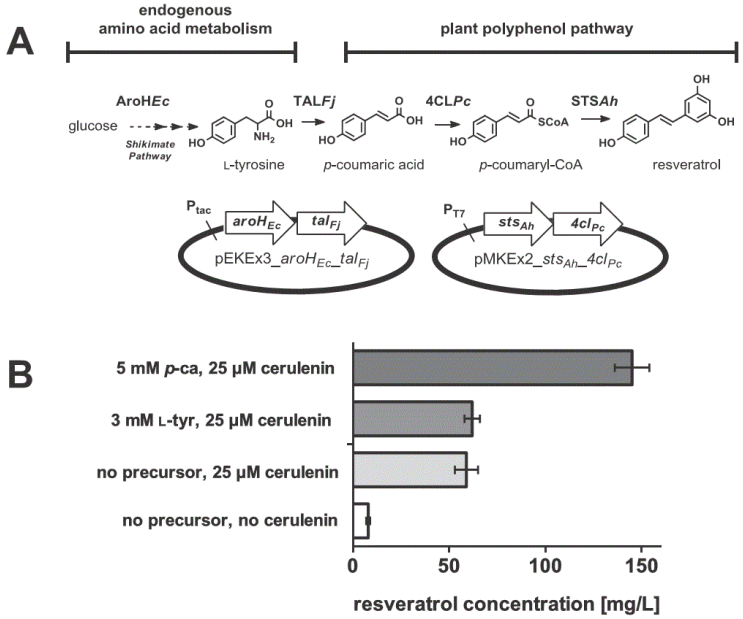

Fig. 5. Resveratrol production with *C. glutamicum* DelAro^4 pMKEx2_sts_{Ah}_$4cl_{Pc}$ pEKEx3_$aroH_{Ec}$_tal_{Fj} in presence of different precursor metabolites. Simplified schematic representation of the overall pathway for resveratrol production from glucose and two plasmids harboring relevant genes for resveratrol production are shown. The genes $aroH_{Ec}$ and tal_{Fj} were expressed as synthetic operon under control of the P_{tac} promoter in pEKEx3, *4clPc* and *stsAh* were cloned as synthetic operon into pMKEx2 under control of the T7 promoter. (B) Resveratrol titers obtained during the cultivation of *C. glutamicum* DelAro^4 pMKEx2_sts_{Ah}_$4cl_{Pc}$ pEKEx3_$aroH_{Ec}$_tal_{Fj} with the indicated culture supplementations. Mean values and standard deviations of three biological replicates are depicted. Abbreviations: $AroH_{Ec}$=3-Deoxy-D-arabino-heptulosonate-7-phosphate synthase from *Escherichia coli*, TAL_{Fj}=tyrosine ammonia lyase from *Flavobacterium johnsoniae*, $4CL_{Pc}$=4-coumarate: CoA-ligase from *Petroselinum crispum*, STS_{Ah}=stilbene synthase from *Arachis hypogaea; p*-ca: *p*-coumaric acid, L-tyr: L-tyrosine.

prohibited L-tyrosine production since the shikimate pathway intermediate 3-dehydroshikimate (3-DS) was converted to protocatechuate (Teramoto et al., 2009) (Fig. S1). The catabolic pathway for quinate or shikimate degradation and the anabolic shikimate pathway for synthesis of aromatic amino acids in *C. glutamicum* partly overlap. In both pathways, 3-DS represents the common intermediate (Fig. S1). In the catabolic pathway the non-aromatic 3-DS is dehydrated to protocatechuate (3,4-dihydroxybenzoate), which cannot be further catabolized by the constructed strain *C. glutamicum* DelAro^3. Due to the gain of aromaticity when forming protocatechuate, the reaction catalyzed by the 3-dehydroshikimate dehydratase QsuB is thermodynamically irreversible. Therefore, the gene *qsuB* (cg0502) was deleted. The gene *qsuB* is part of an operon comprised of essential genes of the anabolic shikimate pathway in *C. glutamicum*, which is expressed in the presence of shikimate and quinate (Kubota et al., 2014). Precise in-frame deletion of *qsuB* in *C. glutamicum* DelAro^3 yielded *C. glutamicum* DelAro^4 (Table S1). As a result of this modification, protocatechuate accumulation of *C. glutamicum* DelAro^4 pEKEx3_$aroH_{Ec}$_tal_{Fj} was drastically reduced to 50 mg/L when expression of $aroH_{Ec}$ and tal_{Fj} (data not shown).

C. glutamicum DelAro^4 pMK2_sts_{Ah}_$4cl_{Pc}$ pEKEx3_$aroH_{Ec}$_tal_{Fj} was cultivated under conditions optimized for polyphenol production to produce resveratrol without addition of *p*-coumaric acid or L-tyrosine (Fig. 5A). The recombinant strain produced 59 ± 6 mg/L resveratrol directly from glucose simultaneous to formation of biomass in defined medium (Fig. 5B). Interestingly, when adding 3 mM L-tyrosine to the culture medium, obtained resveratrol titers were nearly identical in comparison to cultivations without L-tyrosine (Fig. 5B). This indicates that the intracellularly available L-tyrosine concentration of the engineered strains appears not to be limiting for resveratrol production with *C. glutamicum* at this stage. It can be assumed that this effect is due to the kinetic parameters of the employed TAL from *Flavobacterium johnsoniae* exhibiting a very low K_M value of 7 μM for L-tyrosine compared to other described TALs (Jendresen et al., 2015). In the same manner, naringenin was also produced directly from glucose in the constructed strain *C. glutamicum* DelAro^4-$4cl_{Pc}$ pMKEx2_chs_{Ph}-chi_{Ph} pEKEx3_$aroH_{Ec}$_tal_{Fj}. A maximal product titer of 32 ± 1 mg/L naringenin could be obtained after 36 h of cultivation, which is similar to the final naringenin concentrations obtained when supplementing 5 mM *p*-coumaric acid.

In particular resveratrol titers were significantly reduced without cerulenin supplementation since only 12 mg/L resveratrol could be detected compared to 158 mg/L resveratrol in the presence of 25 μM cerulenin (Fig. 5B). Therefore, future optimization efforts could focus on reactions or pathways increasing the intracellular malonyl-CoA pool, *e.g.* by overexpression of genes coding for the dimeric acetyl-CoA carboxylase AccBC-AccD1 in *C. glutamicum*. This strategy already proved to be successful for optimizing stilbene and (2*S*)-flavanone production in *E. coli* and *S. cerevisiae* (Fowler and Koffas, 2009; Katsuyama et al., 2007a, 2007b). Alternative approaches aimed at the expression of heterologous genes coding for a malonyl-CoA synthetase and a malonate importer protein, which allow for generating malonyl-CoA from supplemented malonic acid (Wu et al., 2014). This approach however, requires the addition of malonic acid as precursor metabolite.

Titers of resveratrol and naringenin produced by the constructed *C. glutamicum* strains are lower in direct comparison to other already published microbial production strains. However, highest reported product titers of 2.3 g/L resveratrol and 0.5 g/L naringenin were achieved when starting from supplemented p-coumaric acid using engineered *E. coli* strains (Lim et al., 2011; Xu et al., 2011). *De novo* production of stilbenes and (2*S*)-flavanones starting from glucose or ethanol focused on using *S. cerevisiae* as production host. Titers of either 0.5 g/L resveratrol or 0.1 g/L naringenin could achieved (Koopman et al., 2012; Li et al., 2015). However, the constructed plant polyphenol-producing *C. glutamicum* strains represent ideal candidates for additional strain engineering towards increased polyphenol production. Particularly advantageous, *C. glutamicum* has previously been shown to exhibit high natural tolerance against a broad range of aromatic compounds as they represent common sources of carbon and energy for this organism (Liu et al., 2013). The observed product formation in our experiments occurs simultaneous to biomass formation in defined cultivation medium, which eliminates the need for preceding cultivation steps in complex medium for achieving sufficient biomass concentrations. In addition, the one-step cultivation also allows for an easy and more flexible scale-up of the production process.

Taken together, the constructed platform strain *C. glutamicum* DelAro^4 is highly attractive, not only for production of plant-derived stilbenes and (2*S*)-flavanones, but also for a much broader spectrum of aromatic compounds of commercial interest.

Acknowledgments

We would like to thank the European Union Framework Program 7 "BacHBerry" (www.bachberry.eu), Project No. FP7- 613793 for financial support.

Appendix A. Supplementary material

Supplementary data associated with this article can be found in the online version at http://dx.doi.org/10.1016/j.ymben.2016.06.003.

References

Baumgart, M., Unthan, S., Rückert, C., Sivalingam, J., Grünberger, A., Kalinowski, J., Bott, M., Noack, S., Frunzke, J., 2013. Construction of a prophage-free variant of *Corynebacterium glutamicum* ATCC 13032 for use as a platform strain for basic research and industrial biotechnology. Appl. Environ. Microbiol. 79 (19), 6006–6015.

Becker, J., Zelder, O., Häfner, S., Schröder, H., Wittmann, C., 2011. From zero to hero – design-based systems metabolic engineering of *Corynebacterium glutamicum* for L-lysine production. Metab. Eng. 13 (2), 159–168.

Bertani, G., 1951. Studies on lysogenesis I: the mode of phage liberation by lysogenic *Escherichia coli*. J. Bacteriol. 62 (3), 293–300.

Chang, H.-K., Zylstra, G.J., 2008. Examination and expansion of the substrate range of *m*-hydroxybenzoate hydroxylase. Biochem. Biophys. Res. Commun. 371 (1), 149–153.

Eggeling, L., Bott, M., 2005. Handbook of *Corynebacterium glutamicum*. CRC Press, Taylor & Francis Group, Boca Raton, FL, USA.

Erlund, I., 2004. Review of the flavonoids quercetin, hesperetin, and naringenin. Dietary sources, bioactivities, bioavailability, and epidemiology. Nutr. Res. 24 (10), 851–874.

Fowler, Z.L., Koffas, M.A., 2009. Biosynthesis and biotechnological production of flavanones: current state and perspectives. Appl. Microbiol. Biotechnol. 83 (5), 799–808.

Gande, R., Dover, L.G., Krumbach, K., Besra, G.S., Sahm, H., Oikawa, T., Eggeling, L., 2007. The two carboxylases of *Corynebacterium glutamicum* essential for fatty acid and mycolic acid synthesis. J. Bacteriol. 189 (14), 5257–5264.

Hammer, A., Stolz, A., Knackmuss, H.-J., 1996. Purification and characterization of a novel type of protocatechuate 3,4-dioxygenase with the ability to oxidize 4-sulfocatechol. Arch. Microbiol. 166 (2), 92–100.

Harborne, J.B., 2013. The Flavonoids: Advances in Research Since 1980. Springer Science And Business Media Dordrecht Originally Published By Chapman And Hall, 1988.

Heider, S.A., Wendisch, V.F., 2015. Engineering microbial cell factories: metabolic engineering of *Corynebacterium glutamicum* with a focus on non-natural products. Biotechnol. J. 10 (8), 1170–1184.

Ikeda, M., 2003. Microbial production of L-amino acids. Adv. Biochem. Eng./Biotechnol. 79, 1–35.

Ikeda, M., 2006. Towards bacterial strains overproducing L-tryptophan and other aromatics by metabolic engineering. Appl. Microbiol. Biotechnol. 69 (6), 615–626.

Jendresen, C.B., Stahlhut, S.G., Li, M., Gaspar, P., Siedler, S., Förster, J., Maury, J.,

Borodina, H., Nielsen, A.T., 2015. Novel highly active and specific tyrosine ammonia-lyases from diverse origins enable enhanced production of aromatic compounds in bacteria and yeast. Appl. Environ. Microbiol. 81, 4458–4476.
Kallscheuer, N., Vogt, M., Kappelmann, J., Krumbach, K., Noack, S., Bott, M., Marienhagen, J., 2016. Identification of the *phd* gene cluster responsible for phenylpropanoid utilization in *Corynebacterium glutamicum*. Appl. Microbiol. Biotechnol. 100 (4), 1871–1881.
Katsuyama, Y., Funa, N., Miyahisa, I., Horinouchi, S., 2007a. Synthesis of unnatural flavonoids and stilbenes by exploiting the plant biosynthetic pathway in *Escherichia coli*. Chem. Biol. 14 (6), 613–621.
Katsuyama, Y., Miyahisa, I., Funa, N., Horinouchi, S., 2007b. One-pot synthesis of genistein from tyrosine by coincubation of genetically engineered *Escherichia coli* and *Saccharomyces cerevisiae* cells. Appl. Microbiol. Biotechnol. 73 (5), 1143–1149.
Keilhauer, C., Eggeling, L., Sahm, H., 1993. Isoleucine synthesis in *Corynebacterium glutamicum*: molecular analysis of the *ilvB-ilvN-ilvC* operon. J. Bacteriol. 175 (17), 5595–5603.
Kim, B.G., Ahn, J.H., 2014. Biosynthesis of pinocembrin from glucose using engineered *Escherichia coli*. J. Microbiol. Biotechnol. 24 (11), 1536–1541.
Koffas, M.A., Jung, G.Y., Stephanopoulos, G., 2003. Engineering metabolism and product formation in *Corynebacterium glutamicum* by coordinated gene overexpression. Metab. Eng. 5 (1), 32–41.
Koopman, F., Beekwilder, J., Crimi, B., van Houwelingen, A., Hall, R.D., Bosch, D., van Maris, A.J., Pronk, J.T., Daran, J.-M., 2012. *De novo* production of the flavonoid naringenin in engineered *Saccharomyces cerevisiae*. Microb. Cell Fact. 11, 155.
Kortmann, M., Kuhl, V., Klaffl, S., Bott, M., 2015. A chromosomally encoded T7 RNA polymerase-dependent gene expression system for *Corynebacterium glutamicum*: construction and comparative evaluation at the single-cell level. Microb. Biotechnol. 8 (2), 253–265.
Kubota, T., Tanaka, Y., Takemoto, N., Watanabe, A., Hiraga, K., Inui, M., Yukawa, H., 2014. Chorismate-dependent transcriptional regulation of quinate/shikimate utilization genes by LysR-type transcriptional regulator QsuR in *Corynebacterium glutamicum*: carbon flow control at metabolic branch point. Mol. Microbiol. 92 (2), 356–368.
Leonard, E., Chemler, J., Lim, K.H., Koffas, M.A., 2006. Expression of a soluble flavone synthase allows the biosynthesis of phytoestrogen derivatives in *Escherichia coli*. Appl. Microbiol. Biotechnol. 70 (1), 85–91.
Leonard, E., Lim, K.-H., Saw, P.-N., Koffas, M.A., 2007. Engineering central metabolic pathways for high-level flavonoid production in *Escherichia coli*. Appl. Environ. Microbiol. 73 (12), 3877–3886.
Li, M., Kildegaard, K.R., Chen, Y., Rodriguez, A., Borodina, I., Nielsen, J., 2015. *De novo* production of resveratrol from glucose or ethanol by engineered *Saccharomyces cerevisiae*. Metab. Eng. 32, 1–11.
Li, P.-P., Liu, Y.-J., Liu, S.-J., 2009. Genetic and biochemical identification of the chorismate mutase from *Corynebacterium glutamicum*. Microbiology 155 (10), 3382–3391.
Lim, C.G., Fowler, Z.L., Hueller, T., Schaffer, S., Koffas, M.A., 2011. High-yield resveratrol production in engineered *Escherichia coli*. Appl. Environ. Microbiol. 77 (10), 3451–3460.
Liu, Y.-B., Long, M.-X., Yin, Y.-J., Si, M.-R., Zhang, L., Lu, Z.-Q., Wang, Y., Shen, X.-H., 2013. Physiological roles of mycothiol in detoxification and tolerance to multiple poisonous chemicals in *Corynebacterium glutamicum*. Arch. Microbiol. 195 (6), 419–429.
Lozoya, E., Hoffmann, H., Douglas, C., Schulz, W., Scheel, D., Hahlbrock, K., 1988. Primary structures and catalytic properties of isoenzymes encoded by the two 4-coumarate: CoA ligase genes in parsley. Eur. J. Biochem. 176, 661–667.
Malla, S., Koffas, M.A., Kazlauskas, R.J., Kim, B.-G., 2012. Production of 7-*O*-methyl aromadendrin, a medicinally valuable flavonoid *Escherichia coli*. *Appl. Environ. Microbiol.* 78 (3), 684–694.
Marienhagen, J., Bott, M., 2013. Metabolic engineering of microorganisms for the synthesis of plant natural products. J. Biotechnol. 163 (2), 166–178.
Niebisch, A., Bott, M., 2001. Molecular analysis of the cytochrome bc1-aa3 branch of the *Corynebacterium glutamicum* respiratory chain containing an unusual diheme cytochrome c1. Arch. Microbiol. 175 (4), 282–294.
Pandey, R.P., Parajuli, P., Koffas, M.A., Sohng, J.K., 2016. Microbial production of natural and non-natural flavonoids: Pathway engineering, directed evolution and systems/synthetic biology. Biotechnol. Adv. (epub Ahead of print, available online 3 march 2016)
Pangeni, R., Sahni, J.K., Ali, J., Sharma, S., Baboota, S., 2014. Resveratrol: review on therapeutic potential and recent advances in drug delivery. Expert Opin. Drug Deliv. 11 (8), 1285–1298.
Ray, J.M., Yanofsky, C., Bauerle, R., 1988. Mutational analysis of the catalytic and feedback sites of the tryptophan-sensitive 3-deoxy-D-arabino-heptulosonate-7-phosphate synthase of *Escherichia coli*. J. Bacteriol. 170 (12), 5500–5506.
Sambrook, J., Russell, D., 2001. Molecular Cloning. vol. 1–3. Cold Spring Harbor Laboratory Press, Cold Spring Harbor, NY.
Santos, C.N.S., Koffas, M., Stephanopoulos, G., 2011. Optimization of a heterologous pathway for the production of flavonoids from glucose. Metab. Eng. 13 (4), 392–400.
Schäfer, A., Tauch, A., Jäger, W., Kalinowski, J., Thierbach, G., Pühler, A., 1994. Small mobilizable multi-purpose cloning vectors derived from the *Escherichia coli* plasmids pK18 and pK19: selection of defined deletions in the chromosome of *Corynebacterium glutamicum*. Gene 145 (1), 69–73.
Shen, X., Liu, S., 2005. Key enzymes of the protocatechuate branch of the β-ketoadipate pathway for aromatic degradation in *Corynebacterium glutamicum*. Sci. China Ser. C: Life Sci. 48 (3), 241–249.
Shen, X.-H., Zhou, N.-Y., Liu, S.-J., 2012. Degradation and assimilation of aromatic compounds by *Corynebacterium glutamicum*: another potential for applications for this bacterium? Appl. Microbiol. Biotechnol. 95 (1), 77–89.
Shen, X.-H., Jiang, C.-Y., Huang, Y., Liu, Z.-P., Liu, S.-J., 2005. Functional identification of novel genes involved in the glutathione-independent gentisate pathway in *Coryn ebacterium glutamicum*. Appl. Environ. Microbiol. 71 (7), 3442–3452.
Teramoto, H., Inui, M., Yukawa, H., 2009. Regulation of expression of genes involved in quinate and shikimate utilization in *Corynebacterium glutamicum*. Appl. Environ. Microbiol. 75 (11), 3461–3468.
Trantas, E., Panopoulos, N., Ververidis, F., 2009. Metabolic engineering of the complete pathway leading to heterologous biosynthesis of various flavonoids and stilbenoids in *Saccharomyces cerevisiae*. Metab. Eng. 11 (6), 355–366.
van Summeren-Wesenhagen, P.V., Marienhagen, J., 2013. Putting bugs to the blush: metabolic engineering for phenylpropanoid-derived products in microorganisms. Bioengineered 4 (6), 355–362.
van Summeren-Wesenhagen, P.V., Marienhagen, J., 2015. Metabolic engineering of *Escherichia coli* for the synthesis of the plant polyphenol pinosylvin. Appl. Environ. Microbiol. 81 (3), 840–849.
Wang, Y., Halls, C., Zhang, J., Matsuno, M., Zhang, Y., Yu, O., 2011. Stepwise increase of resveratrol biosynthesis in yeast *Saccharomyces cerevisiae* by metabolic engineering. Metab. Eng. 13 (5), 455–463.
Watts, K.T., Lee, P.C., Schmidt-Dannert, C., 2006. Biosynthesis of plant-specific stilbene polyketides in metabolically engineered *Escherichia coli*. BMC Biotechnol. 6 (1), 22.
Wu, J., Du, G., Zhou, J., Chen, J., 2013. Metabolic engineering of *Escherichia coli* for (2*S*)-pinocembrin production from glucose by a modular metabolic strategy. Metab. Eng. 16, 48–55.
Wu, J., Zhou, T., Du, G., Zhou, J., Chen, J., 2014. Modular optimization of heterologous pathways for *de novo* synthesis of (2*S*)-naringenin in *Escherichia coli*. PLoS One 9 (7), e101492.
Xu, P., Ranganathan, S., Fowler, Z.L., Maranas, C.D., Koffas, M.A., 2011. Genome-scale metabolic network modeling results in minimal interventions that cooperatively force carbon flux towards malonyl-CoA. Metab. Eng. 13 (5), 578–587.
Yang, Y., Lin, Y., Li, L., Linhardt, R.J., Yan, Y., 2015. Regulating malonyl-CoA metabolism via synthetic antisense RNAs for enhanced biosynthesis of natural products. Metab. Eng. 29, 217–226.
Zha, W., Rubin-Pitel, S.B., Shao, Z., Zhao, H., 2009. Improving cellular malonyl-CoA level in *Escherichia coli* via metabolic engineering. Metab. Eng. 11 (3), 192–198.

2.3 Production of more complex polyphenols in *C. glutamicum*

Journal of Biotechnology 258 (2017) 190–196

Contents lists available at ScienceDirect

Journal of Biotechnology

journal homepage: www.elsevier.com/locate/jbiotec

Functional expression of plant-derived *O*-methyltransferase, flavanone 3-hydroxylase, and flavonol synthase in *Corynebacterium glutamicum* for production of pterostilbene, kaempferol, and quercetin

Nicolai Kallscheuer, Michael Vogt, Michael Bott, Jan Marienhagen*

Institute of Bio- and Geosciences, IBG-1: Biotechnology, Forschungszentrum Jülich, D-52425 Jülich, Germany

ARTICLE INFO

Article history:
Received 8 December 2016
Received in revised form 16 January 2017
Accepted 24 January 2017
Available online 28 January 2017

Keywords:
Resveratrol
Pterostilbene
Flavonols
Quercetin
Kaempferol
Corynebacterium glutamicum

ABSTRACT

Plant polyphenols receive significant attention due to their anti-oxidative and health-promoting properties, and several microorganisms are currently engineered towards producing these valuable compounds. Previously, *Corynebacterium glutamicum* has been engineered for synthesizing polyphenol core structures such as the stilbene resveratrol and the (2*S*)-flavanone naringenin. Decoration of these compounds by *O*-methylation or hydroxylation would provide access to polyphenols of even higher commercial interest. In this study, introduction of a heterologous *O*-methyltransferase into a resveratrol-producing *C. glutamicum* strain allowed synthesis of 42 mg/L (0.16 mM) of the di-*O*-methylated pterostilbene from *p*-coumaric acid. A prerequisite for reaching this product titer was a fusion of *O*-methyltransferase with the maltose-binding protein of *Escherichia coli* lacking its signal peptide, thereby increasing the solubility of the *O*-methyltransferase. Furthermore, expression of heterologous dioxygenase genes in (2*S*)-flavanone-producing *C. glutamicum* strains enabled the production of flavanonols and flavonols starting from the phenylpropanoids *p*-coumaric acid and caffeic acid. For the flavonols kaempferol and quercetin, maximum product titers of 23 mg/L (0.08 mM) and 10 mg/L (0.03 mM) could be achieved, respectively. The obtained results demonstrate that *C. glutamicum* is a suitable host organism for the production of more complex plant polyphenols.

1. Introduction

Plant polyphenols constitute a large family of aromatic compounds of the secondary plant metabolism (Scalbert et al., 2005). The health-promoting effects of many polyphenols exhibiting anti-microbial, anti-cancer, anti-inflammatory, or anti-diabetic activities were extensively studied in recent years (Zhang and Tsao, 2016). Polyphenols can be further subdivided into stilbenes, chalcones, curcumins, benzophenones, biphenyls, and some smaller groupes (Schröder, 1997). Stilbenes and chalcones are synthesized from phenylpropanoid CoA-thioesters and malonyl-CoA by stilbene synthases (STS) and chalcone synthases (CHS), respectively. Both of these type III polyketide synthases convert the same substrates, but due to different reaction mechanisms, different products are eventually formed (Tropf et al., 1994; van Summeren-Wesenhagen and Marienhagen, 2013). Stilbenes can be further modified by the activity of decorating enzymes such as *O*-methyltransferases (OMT) and glycosyltransferases (Hüsken et al., 2005; Schmidlin et al., 2008). These modifications increase the bioactivity of polyphenols by increasing solubility, stability, or uptake into human cells (McCormack and McFadden, 2013). Chalcones are isomerized by chalcone isomerases (CHI) yielding (2*S*)-flavanones, which serve as precursors of anthocyanidins, flavonols, and other flavonoids (Wong, 1968). The (2*S*)-flavanone core structure is a three-ring molecule with an aromatic A and B ring and an aliphatic heterocyclic C ring. This core structure can be further modified by hydroxylases and reductases. Furthermore, chalcones and derived flavonoids are often decorated by acyltransferases and glycosyltransferases (Ross et al., 2001; D'Auria, 2006). When considering this broad range of possible chemical modifications, it is not surprising that more than 4,000 different compounds, which belong to the plant flavonoid metabolism, are known today (de Souza and De Giovani, 2013).

In the last years, microbial strains were constructed for the production of several value-added plant polyphenols (Yan et al., 2005b; Wang et al., 2016). These efforts nearly exclusively focused on establishing *Escherichia coli* and *Saccharomyces cerevisiae* as production hosts, but more recently also the actinomycetes *Corynebacterium glutamicum* and *Streptomyces venezuelae* proved to be promising microbial platform organisms for the synthesis of

* Corresponding author.
E-mail address: j.marienhagen@fz-juelich.de (J. Marienhagen).

http://dx.doi.org/10.1016/j.jbiotec.2017.01.006
0168-1656/

these aromatic compounds (Park et al., 2009; Kallscheuer et al., 2016a). In many studies, the central carbon metabolism of the host strains was extensively engineered for significantly increasing overall product titers. For example, to achieve overproduction of the polyphenol precursor L-tyrosine, several feedback-regulated enzymes of the shikimate pathway were replaced by feedback-resistant variants and other pathway genes were overexpressed by using strong promoters. (Santos et al., 2011; Wu et al., 2013). Furthermore, low intracellular availability of malonyl-CoA was identified as a major bottleneck for microbial polyphenol production (Fowler et al., 2009). This challenge was addressed in *E. coli* by overexpression of endogenous genes for enabling increased acetate assimilation to yield more acetyl-CoA and improved carboxylation of acetyl-CoA to malonyl-CoA (Fowler et al., 2009). Other studies showed that polyphenol synthesis in engineered microbial strains could be improved by elimination of endogenous pathways converting substrates, intermediates, or products of the heterologous polyphenol pathways (Leonard et al., 2008; Fowler et al., 2009). In case of *C. glutamicum*, it was initially found that this bacterium is able to grow with phenylpropanoids as sole carbon and energy source following a hitherto unknown catabolic pathway (Kallscheuer et al., 2016b). Abolishment of the identified CoA-dependent, β-oxidative chain shortening pathway for phenylpropanoid degradation by deletion of the gene cluster *phdBCDE* turned out to be the key step towards enabling polyphenol production in *C. glutamicum* (Kallscheuer et al., 2016a). Heterologous expression of plant-derived genes in microbes for the functional integration of the pathways can be very challenging. Codon-optimization prior to gene synthesis can help to increase the synthesis rate of functional enzymes, but improper folding of proteins of eukaryotic origin often requires laborious and time consuming screening for suitable expression conditions (Sullivan et al., 2004; Kirubakaran and Sakthivel, 2007). In such cases, fine-tuning of gene expression or fusion of the target enzyme with highly soluble tags or proteins (such as poly-His tag, SUMO solubility tag or the maltose-binding protein from *E. coli*) are useful strategies to avoid undesired protein aggregation (Zhang et al., 2006; van Summeren-Wesenhagen et al., 2015).

In this study, we aimed at producing more complex plant polyphenols derived from the stilbene resveratrol and (2*S*)-flavanone core structures, which are provided by previously engineered *C. glutamicum* strains (Kallscheuer et al., 2016a). Mono-*O*-methylated pinostilbene and the di-*O*-methylated pterostilbene could be synthesized from resveratrol by introduction of a suitable OMT, whereas conversion of (2*S*)-flavanones to flavanonols and flavonols required the activity of plant-derived dioxygenases.

2. Material and methods

2.1. Bacterial strains, plasmids, media, and growth conditions

All bacterial strains and plasmids used in this study as well as their relevant characteristics are listed in Table 1. *C. glutamicum* strains were routinely cultivated aerobically at 30 °C in brain heart infusion (BHI) medium (Difco Laboratories, Detroit, USA) or defined CGXII medium with glucose as sole carbon and energy source (Keilhauer et al., 1993). *E. coli* DH5α was used for plasmid constructions and was cultivated in LB medium (Bertani, 1951) at 37 °C. Where appropriate, kanamycin (50 μg/mL for *E. coli* or 25 μg/mL for *C. glutamicum*) or spectinomycin (100 μg/mL for *E. coli* and *C. glutamicum*) was added to the medium. Bacterial growth was followed by measuring the optical density at 600 nm (OD_{600}).

For the production of polyphenols, *C. glutamicum* precultures were grown for 6–8 h in test tubes with 5 mL BHI medium on a rotary shaker at 170 rpm (first preculture) and were subsequently inoculated into 50 mL CGXII medium with 4% (w/v) glucose in 500 mL baffled Erlenmeyer flasks (second preculture). The cultures were incubated overnight on a rotary shaker at 130 rpm. The main culture was inoculated to an OD_{600} of 7 in defined CGXII medium with 4% (w/v) glucose. If indicated, 5 mM of *p*-coumaric acid or caffeic acid was added. Heterologous gene expression was induced one hour after inoculation using 1 mM IPTG. When indicated, 25 μM of the fatty acid synthesis inhibitor cerulenin was added to the culture medium after seven hours of cultivation (at an OD_{600} of 20–25). For flavanonol and flavonol production, 2.5 mM ascorbic acid was added as cofactor for 2-oxoglutarate-dependent dioxygenases (Vissers et al., 2014). 1 mL of the culture broth was collected for polyphenol quantification at the indicated time points and stored at −20 °C until extraction.

2.2. Plasmid and strain construction

Standard protocols for molecular cloning, such as PCR, DNA restriction, and ligation were carried out for recombinant DNA work (Sambrook and Russell, 2001). Techniques specific for *C. glutamicum*, *e.g.* electroporation for transformation of strains, were performed as described previously (Eggeling and Bott, 2005). All enzymes were obtained from Thermo Fisher Scientific (Schwerte, Germany). Codon-optimized synthetic genes for *C. glutamicum* ATCC 13032 were obtained from LifeTechnologies (Darmstadt, Germany). Genes were amplified by PCR using oligonucleotides containing unique restriction sites (Table 2). PCR products were used for cloning of genes into plasmid vectors using the introduced restriction sites. For the one-step assembly of two genes and simultaneous cloning into pEKEx3 using the indicated restriction sites, the Electra Cloning strategy was applied (Whitman et al., 2013). *Sap*I restriction sites leading to compatible overhangs after *Sap*I cleavage were added to the primer sequences used for the amplification of the respective genes. All constructed plasmids were finally verified by DNA sequencing at Eurofins MWG Operon (Ebersberg, Germany).

2.3. Metabolite extraction using ethyl acetate

Metabolite extracts from cultivation broth were prepared for LC–MS analysis by mixing 1 mL of the culture broth with 1 mL ethyl acetate and vigorous shaking (1400 rpm; 10 min, 20 °C) in a thermomixer (Eppendorf, Hamburg, Germany). The suspension was centrifuged for 5 min at 16,000g and the ethyl acetate layer (800 μL) was transferred to an organic solvent-resistant deep-well plate (Eppendorf, Hamburg, Germany). After evaporation of ethyl acetate at room temperature overnight, dried extracts were resuspended in 800 μL of acetonitrile and directly used for the LC–MS analysis.

2.4. LC–MS analysis for quantification of polyphenols

Polyphenols extracted from the culture samples were quantified by LC–MS using an ultra-high-performance LC (uHPLC) 1290 Infinity System coupled to a 6130 Quadrupole LC–MS System (Agilent, Waldbronn, Germany). LC separation was carried out with a Kinetex 1.7u C_{18} 100 Å pore size column (50 mm by 2.1 mm [internal diameter]; Phenomenex, Torrance, CA, USA) at 50 °C. For elution, 0.1% (v/v) acetic acid (solvent A) and acetonitrile supplemented with 0.1% (v/v) acetic acid (solvent B) were used as mobile phases at a flow rate of 0.5 mL/min. A gradient was used, where the amount of solvent B was increased stepwise: minute 0–6: 10% to 30%, minute 6–7: 30% to 50%, minute 7–8: 50% to 100%. From minute 8 to 8.5 solvent B was decreased from 100% to 10%. The mass spectrometer was operated in the positive electrospray ionization (ESI) mode for the quantification of pinostilbene and pterostilbene while the

Table 1
Strains and plasmids used in this study.

Strain or plasmid	Relevant characteristics	Source or reference
C. glutamicum strains		
MB001(DE3)	prophage-free derivate of wild type ATCC 13032 with chromosomally encoded T7 *gene 1* (cg1122-P_{lacI}-*lacI*-P_{lacUV5}-*lacZα*-T7 *gene 1*-cg1121)	(Kortmann et al., 2015)
DelAro^4	MB001(DE3) derivative with in-frame deletions of cg0344-47, cg2625-40, cg1226 and cg0502	(Kallscheuer et al., 2016a)
DelAro^4-*4cl*$_{Pc}$	derivative of *C. glutamicum* DelAro^4 with a codon-optimized 4-coumarate: CoA-ligase gene from *Petroselinum crispum* under control of the T7 promoter integrated into the Δcg0344-47 locus	(Kallscheuer et al., 2016a)
E. coli strains		
DH5α	F− Φ80*lacZ*ΔM15 Δ(*lacZYA-argF*)U169 *recA1 endA1 hsdR17* (rK−, mK+) *phoA supE44* λ− *thi-1 gyrA96 relA1*	Invitrogen (Karlsruhe, Germany)
Plasmids		
pMKEx2	*kan*^{r}; *E. coli-C. glutamicum* shuttle vector (*lacI*, P_{T7}, lacO1, pHM1519 ori_{Cg}; pACYC177 ori_{Ec})	(Kortmann et al., 2015)
pMKEx2-*sts*$_{Ah}$-*4cl*$_{Pc}$	*kan*^{r}; pMKEx2 derivative containing codon-optimized genes coding for stilbene synthase from *Arachis hypogaea* and for 4-coumarate: CoA ligase from *Petroselinum crispum*	(Kallscheuer et al., 2016a)
pMKEx2-*chs*$_{Ph}$-*chi*$_{Ph}$	*kan*^{r}; pMKEx2 derivative containing codon-optimized genes coding for chalcone synthase and for chalcone isomerase from *Petunia hybrida*	(Kallscheuer et al., 2016a)
pEKEx3	*spec*^{r}; *E. coli-C. glutamicum* shuttle vector (*lacI*, P_{tac}, lacO1, pBL1ori_{Cg}; pUCori_{Ec})	(Gande et al., 2007)
pEKEx3-*omt*$_{Vv}$	*spec*^{r}; pEKEx3 derivative containing codon-optimized gene coding for resveratrol-di-*O*-methyltransferase from *Vitis vinifera*	this study
pEKEx3-*metK*$_{Ec}$-*omt*$_{Vv}$	*spec*^{r}; pEKEx3 derivative containing genes coding for *S*-adenosylmethionine synthase MetK from *Escherichia coli* and for resveratrol-di-*O*-methyltransferase from *Vitis vinifera*	this study
pEKEx3-*malE*$_{Ec}$-*omt*$_{Vv}$	*spec*^{r}; pEKEx3 derivative containing *malE* gene from *E. coli* fused to the codon-optimized gene coding for resveratrol-di-*O*-methyltransferase from *Vitis vinifera*	this study
pEKEx3-*f3h*$_{Ph}$-*fls*$_{Pd}$	*spec*^{r}; pEKEx3 derivative containing codon-optimized genes coding for flavanone 3-hydroxylase from *Petunia hybrida* and for flavonol synthase from *Populus deltoides*	this study

Table 2
Oligonucleotides used in this study. Relevant restriction sites used for cloning are underlined. *Sap*I cleaves outside of its recognition site. The resulting overhangs after cleavage with *Sap*I used for sticky end ligation are shown in bold.

oligo-nucleotide	sequence (5′-3′)	restriction site
stsAh-s	ATA<u>CCATGG</u>TAAGGAGGACAGCTATGGTGTCCGTGTCCGGCATC	*Nco*I
stsAh-as	CTC<u>GGTACC</u>TTTAGATTGCCATAGAGCGCAGCACCAC	*Kpn*I
4clPc-s	AGC<u>GGTACC</u>TAAGGAGGTGGACAATGGGCGATTGCGTGGCAC	*Kpn*I
4clPc-as	CTG<u>GGATCC</u>AGGACTAGTTTCCAGAGTACTATTACTTTGGCAGATCACCGGATGCGATC	*Bam*HI
chsPh-s	GTA<u>TCTAGA</u>AAGGAGGTCGAAGATGGTGACCGTGGAAGAATACCGCAAG	*Xba*I
chsPh-as	CTC<u>CCATGG</u>TTAGGTTGCCACGGAGTGCAGCAC	*Nco*I
chiPh-s	CTC<u>CCATGG</u>TGCTAAAGGAGGTCGAAGATGTCCCCACCAGTGTCCGTGACCAAG	*Nco*I
chiPh-as	CTG<u>GGATCC</u>TTACACGCCGATCACTGGGATGGTG	*Bam*HI
omtVv-s	TCT<u>GGATCC</u>AAAGGAGGTCTGGAATGGACCTGGCAAACGGCGTGATCTC	*Bam*HI
omtVv-as	ATT<u>GAATTC</u>GATTATGGGTACACTTCGATCAGGGAGCGCAG	*Eco*RI
malEEc-s	TTC<u>GGATCC</u>TAAGGAGGATCGGCATGAAAACTGAAGAAGGTAAACTGGTAATCTGGATTAACGGCGATAAAGGCTATAAC	*BamHI*
Fus_malEEc-as	TAC<u>GCTCTTC</u>T**GCC**GGAACCGGAAGAGGAAGTCTGCGCGTCTTTCAGGGCTTCATCGAC	*Sap*I
Fus_omtVv-s	CTC<u>GCTCTTC</u>A**GGC**GACCTGGCAAACGGCGTGATCTCC	*Sap*I
metKEc-s	TCT<u>CTGCAG</u>AAGGAGGATATCTATGGCTCAGCCAACCGCCGTCC	*Xho*I
metKEc-as	TCT<u>GGATCC</u>TGCGATCTTAGGCCAACTTGAGGGCTGCGCGAAG	*Bam*HI
f3hPh-s	TTC<u>GGATCC</u>TAAGGAGGATCGGCATGGCACCATCCACCCTGACCGCAC	*Bam*HI
f3hPh-as	ATA<u>GCTCTTC</u>T**ACC**TTATGCCAGGATTTCTTCGATTGGCTTGGATTC	*Sap*I
flsPd-s	ACC<u>GCTCTTC</u>A**GGT**CTGCTTAAGGAGGATATCTATGGAATTTGATCGCGTGCAGGCAATC	*Sap*I
flsPd-as	ATT<u>GAATTC</u>GATTACTGTGGCAGCTTGTTCAGCTTGCAGTACAC	*Eco*RI

concentration of all other compounds was measured in the negative ESI mode. The injection volume was 10 μL (positive mode) or 1 μL (negative mode) and data acquisition was performed in selected-ion-monitoring (SIM) mode. Area values for $[M-H]^-$ (negative mode) and for $[M+H]^+$ mass signals (positive mode) were linear up to metabolite concentrations of at least 250 mg/L. Benzoic acid (final concentration 100 mg/L, 0.82 mM) was used as internal standard. Authentic metabolite standards were purchased from Sigma-Aldrich (Schnelldorf, Germany) and dissolved in acetonitrile. Six different metabolite concentrations ranging from 10 to 250 mg/L were measured for each calibration curve. Calibration curves were calculated based on analyte/internal standard ratios for the obtained area values. All target compounds (stilbenoids, (2S)-flavanones, flavanonols, and flavonols) were unambigously identified by selective ion monitoring of the respective masses for $[M-H]^-$ or $[M+H]^+$ using LC–MS (Figs. S2–S8). The observed retention times correlated with the retention times of commercially available metabolite standards.

3. Results

3.1. Production of O-methylated resveratrol derivatives in C. glutamicum

In a previous study, *C. glutamicum* DelAro^4 was constructed as platform strain for the production of aromatic compounds

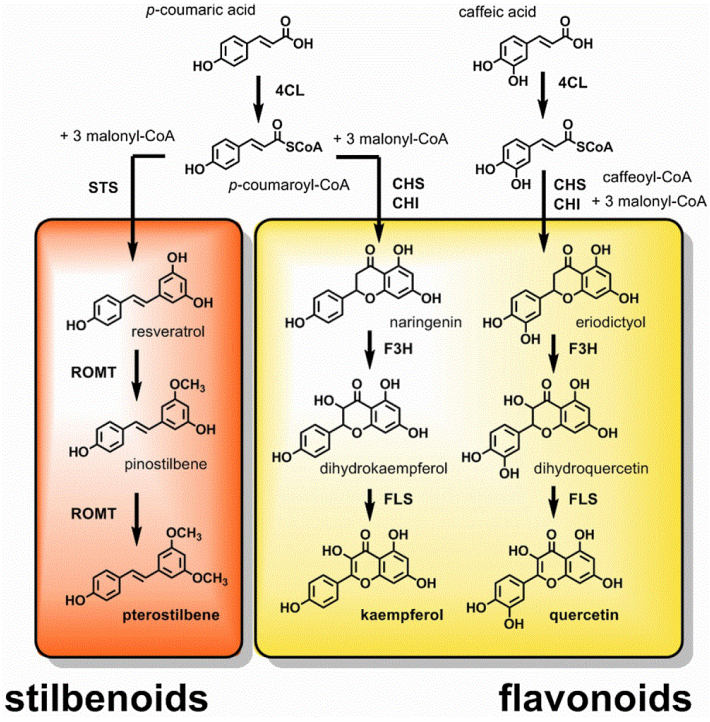

Fig. 1. Schematic overview of the pathways leading to production of *O*-methylated stilbenes and of flavonols in *C. glutamicum*. Biosynthetic pathways for the microbial production of pterostilbene and for the flavonols kaempferol and quercetin starting from phenylpropanoids are depicted. After conversion of the phenylpropanoids to the corresponding CoA-thioesters by a 4-coumarate: CoA ligase (4CL), stilbene synthase (STS) or chalcone synthase (CHS) and chalcone isomerase (CHI) catalyze the synthesis of either stilbenes (in this case resveratrol) or (2S)-flavanones (naringenin or eriodictyol), respectively. Resveratrol is *O*-methylated by resveratrol-di-*O*-methyltransferase (ROMT) leading to pinostilbene or ultimately pterostilbene. (2S)-flavanones are converted to flavonols by the activity of the 2-oxoglutarate-dependent dioxygenases flavanone 3-hydroxylase (F3H) and flavonol synthase (FLS).

(Kallscheuer et al., 2016a). This strain background already proved to be suitable to produce the stilbene resveratrol, either from the phenylpropanoid *p*-coumaric acid or directly from glucose. By the activity of plant-derived OMTs, resveratrol should be converted to the mono-*O*-methylated pinostilbene and the di-*O*-methylated pterostilbene (Fig. 1). For the production of pterostilbene, the strain *C. glutamicum* DelAro^4 pMKEx2-sts_{Ah}-$4cl_{Pc}$ pEKEx3-omt_{Vv} was constructed, which expresses codon-optimized genes for a 4-coumarate: CoA ligase (4CL) from *Petroselinum crispum* (Uniprot entry P14913), a stilbene synthase (STS) from *Arachis hypogaea* (Uniprot entry Q9SLV5), and a resveratrol-di-*O*-methyltransferase (OMT) from *Vitis vinifera* (Uniprot entry B6VJS4). The constructed strain was cultivated in defined CGXII medium with 4% (w/v) glucose as sole carbon and energy source and supplemented with 5 mM *p*-coumaric acid. Cultivations were performed either without IPTG or with 10 μM or 1 mM IPTG, which induces plasmid-based heterologous gene expression. After 7 h of cultivation, (OD_{600} = 20–25), supplementation of 25 μM of the fatty acid synthase inhibitor cerulenin, which is known to increase the intracellular availability of malonyl-CoA for polyphenol production, caused a growth stop in the exponential phase at an OD_{600} of 25. No accumulation of resveratrol could be detected without IPTG, whereas induction of gene expression with 1 mM IPTG resulted in the accumulation of 140 mg/L (0.61 mM) resveratrol after 50 h of cultivation. Unfortunately, under all tested conditions, neither pinostilbene nor pterostilbene could be detected in the culture extracts. First, it was assumed that the production of *O*-methylated resveratrol derivatives in *C. glutamicum* might be hindered by low intracellular availability of the methyl donor *S*-adenosyl methionine (SAM), which is essential for the *O*-methylation of the hydroxy groups of resveratrol. To this end, the plasmid pEKEx3-$metK_{Ec}$-omt_{Vv} was constructed, which additionally harbors the *metK* gene of *Escherichia coli* coding for a SAM synthetase. However, the resulting strain *C. glutamicum* DelAro^4 pMKEx2-sts_{Ah}-$4cl_{Pc}$ pEKEx3-$metK_{Ec}$-omt_{Vv} also failed to synthesize *O*-methylated resveratrol derivatives while resveratrol production was unaffected by the expression of this additional gene (data not shown).

At this stage it was speculated that there was no functional translation of OMT_{Vv}, e.g. because OMT_{Vv} simply folds improperly during translation in in . Soluble and insoluble protein fractions in cell lysates of *C. glutamicum* either harboring pEKEx3-omt_{Vv} or the empty plasmid pEKEx3 were used for SDS-PAGE analysis. Unfortunately, no band corresponding to OMT_{Vv} (40.1 kDa) was visible in any fraction and no difference in the overall protein abundance was found in comparison to the control strain har-

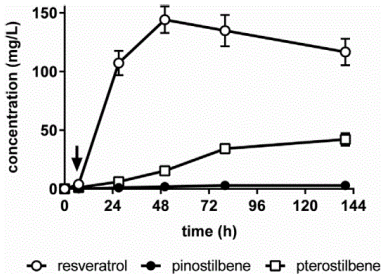

Fig. 2. Production of the stilbenoids resveratrol, pinostilbene, and pterostilbene in *C. glutamicum*. *C. glutamicum* DelAro^4 pMKEx2_sts_{Ah}_$4cl_{Pc}$ pEKEx3_$malE_{Ec}$-omt_{Vv} was cultivated in defined CGXII medium in the presence of 4% (w/v) glucose and 820 mg/L (5 mM) *p*-coumaric acid. When reaching an OD_{600} of 20 (seven hours after inoculation), cerulenin was added to a final concentration of 25 μM (time point indicated by the black arrow). Concentrations of resveratrol and its mono- and di-*O*-methylated derivatives pinostilbene and pterostilbene were determined at the indicated time points. The data represent average values and standard deviation from three biological replicates.

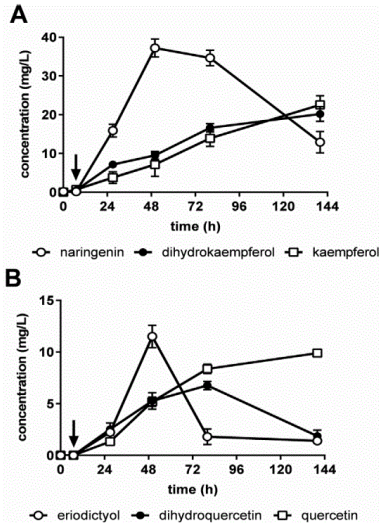

Fig. 3. Production of flavanonols and flavonols in *C. glutamicum*. *C. glutamicum* DelAro^4-$4cl_{Pc}$ pMKEx2_chs_{Ph}_chi_{Pc} pEKEx3_$f3h_{Ph}$-fls_{Pd} was cultivated in defined CGXII medium with 4% (w/v) glucose and 820 mg/L (5 mM) *p*-coumaric acid (A) or 900 mg/L (5 mM) caffeic acid (B). When reaching an OD_{600} of 20 (seven hours after inoculation) cerulenin was added to a final concentration of 25 μM (time point indicated by the black arrow). Concentrations of the respective (2*S*)-flavanones, flavanonols, and flavonols obtained from *p*-coumaric acid or caffeic acid were determined at the indicated time points. The data represent average values and standard deviations from biological triplicates.

boring the empty plasmid (Fig. S1). With the aim to increase the solubility of OMT_{Vv}, the plasmid pEKEx3_$malE_{Ec}$-omt_{Vv} was constructed, which allows for the synthesis of a $MalE_{Ec}$-OMT_{Vv} fusion protein. In this protein, the N-terminus of OMT_{Vv} is fused to a variant of the maltose-binding protein MalE of *E. coli* lacking its native signal peptide (Duplay et al., 1984). An additional DNA sequence coding for a serine- and glycine-rich flexible linker (H_2N-$MalE_{Ec}$-SSSGSG-OMT_{Vv}-COOH) was inserted between the two open reading frames. SDS-PAGE analysis of cell-free extracts of *C. glutamicum* DelAro^4 pEKEx3_$malE_{Ec}$-omt_{Vv} showed that no protein band representing $MalE_{Ec}$-OMT_{Vv} (80.7 kDa) could be identified, neither in the soluble nor in the insoluble protein fraction (Fig. S1). Nevertheless, during cultivation of the production strain *C. glutamicum* DelAro^4 pMKEx2_sts_{Ah}_$4cl_{Pc}$ pEKEx3_$malE_{Ec}$-omt_{Vv} also expressing the genes coding for the $MalE_{Ec}$-OMT_{Vv} fusion protein, accumulation of pinostilbene and pterostilbene could be observed. This indicates that the increased solubility of the fusion protein was a suitable strategy for establishing OMT activity and *O*-methylation of resveratrol in *C. glutamicum* (Fig. 2). Addition of cerulenin seven hours after inoculation led to a strong increase in resveratrol production from 1 mg/L (0.004 mM) at this time point to a maximum of 144 mg/L (0.63 mM) after 50 h. The pterostilbene titer increased steadily during the whole cultivation to a maximum of 42 mg/L (0.16 mM) after 140 h. The concentration of the mono-*O*-methylated pinostilbene never exceeded 3 mg/L (0.01 mM) (Fig. 2).

3.2. Production of flavanonols and flavonols in engineered C. glutamicum strains

(2*S*)-flavanones are synthesized from phenylpropanoids by consecutive activities of a 4CL, a CHS and a CHI (Fig. 1). In plants, flavanone 3-hydroxylases (F3H) can hydroxylate these (2*S*)-flavanones yielding flavanonols, which can be subsequently oxidized to flavonols by flavonol synthases (FLS). The strain *C. glutamicum* DelAro^4-$4cl_{Pc}$ pMKEx2_chs_{Ph}_chi_{Ph}, expressing codon-optimized genes for 4CL from *P. crispum* as well as CHS and CHI from Petunia x hybrida, produces the (2*S*)-flavanones naringenin and eriodictyol from *p*-coumaric acid and caffeic acid, respectively (Kallscheuer et al., 2016a). With the aim to produce flavanonols and flavonols from these (2*S*)-flavanones, different plant-derived F3H and FLS enzymes were evaluated for an application in *C. glutamicum*. First, F3H (Uniprot entry O22530) and FLS (Uniprot entry Q07512) from petunia were tested. Codon-optimized genes coding for both enzymes were used for the construction of the plasmid pEKEx3_$f3h_{Ph}$_fls_{Ph}, but to our surprise, no clone with a correctly assembled plasmid could be isolated although several different cloning strategies were pursued. Since a plasmid harboring $f3h_{Ph}$ alone could be easily obtained, a codon-optimized gene for an alternative FLS from *Populus deltoides* was selected for heterologous expression in *C. glutamicum* as this particular gene could already be functionally expressed in *E. coli* (Kim et al., 2010). In this case, the desired plasmid pEKEx3_$f3h_{Ph}$_fls_{Pd} could be successfully constructed. The resulting strain *C. glutamicum* DelAro^4-$4cl_{Pc}$ pMKEx2_chs_{Ph}_chi_{Ph} pEKEx3_$f3h_{Ph}$_fls_{Pd} was cultivated in CGXII medium with 4% (w/v) glucose in analogy to the pterostilbene production experiments. As precursors 5 mM of either *p*-coumaric acid or caffeic acid were supplemented and heterologous gene expression was induced with 1 mM IPTG. In presence of 820 mg/L (5 mM) *p*-coumaric acid, up to 37 mg/L (0.14 mM) of the intermediate naringenin could be detected after 50 h of cultivation (Fig. 3A). Product concentrations of dihydrokaempferol and kaempferol linearly increased over the whole cultivation time, resulting in maximum product titers of 20 mg/L (0.07 mM) and 23 mg/L (0.08 mM) after 140 h, respectively (Fig. 3A). Most likely due to limited malonyl-CoA availability when reaching the stationary phase, naringenin production did not continue after 50 h of cultivation. However, after this time point, conversion of naringenin to dihydrokaempferol, and ultimately to kaempferol continued whereas the naringenin concentration steadily decreased. At the end of the cultivation, a residual concentration of only 13 mg/L (0.05 mM) naringenin could be detected in the culture extracts (Fig. 3A). A similar trend could be observed when feeding 900 mg/L (5 mM) caffeic acid as precursor for the (2*S*)-flavanone intermediate eriodictyol and the products dihydroquercetin and quercetin (Fig. 3B).

However, the overall concentrations were lower in comparison to dihydrokaempferol and kaempferol production from *p*-coumaric acid (Fig. 3A). Maximum polyphenol titers of 12 mg/L (0.04 mM) eriodictyol and 7 mg/L (0.02 mM) dihydroquercetin could be determined after 50 and 80 h, respectively (Fig. 3B). The concentration of both polyphenols dropped below 2 mg/L towards the end of the cultivation but at the same time quercetin accumulated to a final concentration of 10 mg/L (0.03 mM) (Fig. 3B). 80% (4 mM) of both supplemented phenylpropanoid precursors *p*-coumaric acid and caffeic acid could be still detected in the culture medium after 140 h (data not shown). This could hint to a limited malonyl-CoA supply during polyphenol synthesis as glucose was already depleted after 50 h.

4. Discussion

Up to now, polyphenol production in microbes mainly focused on *E. coli* and *S. cerevisiae* as production hosts and both organisms have been engineered to synthesize several different polyphenols (Yan et al., 2005a; van Summeren-Wesenhagen and Marienhagen, 2015; Liang et al., 2016). *E. coli* was already engineered to produce the resveratrol derivatives pinostilbene and pterostilbene starting from *p*-coumaric acid. The best strains allow for the production of 34 mg/L (0.14 mM) pinostilbene and 50 mg/L (0.20 mM) pterostilbene (Jeong et al., 2014; Wang et al., 2015). From our experimental data we concluded that the insolubility of the heterologous OMT from *V. vinifera* in *C. glutamicum* initially hindered the production of *O*-methylated resveratrol derivatives. In our experiments, fusion of the codon-optimized omt_{Vv} gene with a linker sequence to the $malE_{Ec}$ gene turned out to be the key for establishing OMT activity in *C. glutamicum*. Fusion to MalE is a common strategy to enhance the solubility of target proteins (Kaspar et al., 1999; Riggs, 2000; Chen et al., 2005; Carter and Hausinger, 2010). In this context, the translational fusion to MalE was previously found to increase the activity of a fungal *cis*-aconitate decarboxylase leading to increased itaconic acid production in *C. glutamicum* (Otten et al., 2015). In our experiments, the synthesis of the $MalE_{Ec}$-OMT_{Vv} fusion protein enabled the production of 42 mg/L (0.16 mM) pterostilbene in the constructed *C. glutamicum* strain after six days of cultivation. The product titer is comparable to the highest reported titer of 50 mg/L (0.20 mM) pterostilbene produced from the precursor *p*-coumaric acid in *E. coli*, also employing the OMT from *V. vinifera* (Wang et al., 2015). In *E. coli*, the enzyme enabled predominantly the accumulation of pterostilbene accompanied by only low amounts of pinostilbene, which is in line with the results obtained with *C. glutamicum* in this study. Application of an OMT from *Sorghum bicolor* in *E. coli* almost exclusively allowed for the formation of pinostilbene (Jeong et al., 2014). Hence, it appears as if depending on the desired product, different enzymes can be used to specifically produce either pinostilbene or pterostilbene. Furthermore, also in *E. coli*, fusion of the OMT to a tag increasing the overall protein solubility was crucial for establishing OMT activity and similar to the results obtained with *C. glutamicum*, resveratrol was not completely converted to pterostilbene. This indicates that the activity of OMT is rate-limiting during product synthesis (Wang et al., 2015). Probably the overall folding of the fusion proteins is still non-optimal, which could negatively affect the resulting OMT activity. In addition, low intracellular levels of the methyl-donor SAM or the SAM precursor L-methionine could limit *O*-methylation of resveratrol. This is also in good agreement with the observation that glucose in the cultivation medium was already completely depleted after 30 h of cultivation.

In addition, *C. glutamicum* could be engineered for the production of flavanonols and flavonols starting from two different phenylpropanoids. In the course of experiments it was decided to implement the CHS from petunia as it participates in naringenin and eriodictyol biosynthesis, starting from *p*-coumaric acid and caffeic acid, respectively (Yan et al., 2005a). The F3H is able to hydroxylate both (2*S*)-flavanones to yield the corresponding flavanonols dihydrokaempferol and dihydroquercetin, respectively (Britsch and Grisebach, 1986). The FLS from *P. deltoides* in turn accepted both flavanonols as substrate yielding the respective flavonols kaempferol and quercetin after heterologous protein production in *E. coli* (Kim et al., 2010). The highest titer reported for microbial kaempferol production was 15 mg/L (0.05 mM) using *E. coli* (Miyahisa et al., 2006). For quercetin, maximum product titers of only 1.1 mg/L (0.004 mM) and 0.4 mg/L (0.001 mM) could be determined in *E. coli* and *S. cerevisiae*, respectively (Leonard et al., 2006; Trantas et al., 2009). The obtained flavonol titers of 23 mg/L (0.08 mM) kaempferol and 10 mg/L (0.03 mM) quercetin produced with *C. glutamicum* are, to the best of our knowledge, the highest flavonol titers obtained in microbes to date. Production of 57 mg/L kaempferol 3-*O*-rhamnoside (0.13 mM) could be already achieved in *E. coli* but no accumulation of kaempferol as direct precursor molecule was mentioned in this study (Yang et al., 2014). For the production of quercetin in *C. glutamicum* we found that eriodictyol and dihydroquercetin were nearly completely depleted at the end of the cultivation. Hence, for increasing quercetin production in *C. glutamicum*, alternative CHS enzymes exhibiting higher activities with the substrate caffeoyl-CoA could be tested. A suitable candidate is CHS2 (eriodictyol/homoeriodictyol synthase) from barley (*Hordeum vulgare*), as this enzyme can convert caffeoyl-CoA and feruloyl-CoA to the respective chalcone at two-fold higher rates compared to *p*-coumaroyl-CoA (Christensen et al., 1998).

In summary, we demonstrated that *C. glutamicum* is a suitable host for the microbial production of pterostilbene and the flavonols kaempferol and quercetin. The (2*S*)-flavanones and flavanonols as intermediates in the pathways leading to kaempferol and quercetin represent precursor molecules for various plant polyphenols such as flavones, anthocyanidins, and isoflavones. These compounds are of commercial interest as colorants or nutraceuticals and could be possibly also produced by engineered *C. glutamicum* strains. Future efforts towards increasing polyphenol production in *C. glutamicum* should include fine-tuning of heterologous gene expression and additional engineering of the endogenous microbial metabolism towards increased availability of relevant precursor metabolites, which were found to be rate-limiting during polyphenol synthesis.

Acknowledgment

We would like to thank the European Union Framework Program 7 "BacHBerry" (www.bachberry.eu), Project No. FP7-613793 for financial support.

Appendix A. Supplementary data

Supplementary data associated with this article can be found, in the online version, at http://dx.doi.org/10.1016/j.jbiotec.2017.01.006.

References

Bertani, G., 1951. Studies on lysogenesis I: the mode of phage liberation by lysogenic *Escherichia coli*. J. Bacteriol. 62, 293.

Britsch, L., Grisebach, H., 1986. Purification and characterization of (2*S*)-flavanone 3-hydroxylase from *Petunia hybrida*. Eur. J. Biochem. 156, 569–577.

Carter, E.L., Hausinger, R.P., 2010. Characterization of the *Klebsiella aerogenes* urease accessory protein UreD in fusion with the maltose binding protein. J. Bacteriol. 192, 2294–2304.

Chen, Y., Xing, X.-H., Lou, K., 2005. Construction of recombinant *Escherichia coli* for over-production of soluble heparinase I by fusion to maltose-binding protein. Biochem. Eng. J. 23, 155–159.

Christensen, A.B., Gregersen, P.L., Schröder, J., Collinge, D.B., 1998. A chalcone synthase with an unusual substrate preference is expressed in barley leaves in response to UV light and pathogen attack. Plant Mol. Biol. 37, 849–857.

D'Auria, J.C., 2006. Acyltransferases in plants: a good time to be BAHD. Curr. Opin. Plant Biol. 9, 331–340.

de Souza, R.F., De Giovani, W.F., 2013. Antioxidant properties of complexes of flavonoids with metal ions. Redox Rep. 9, 97–104.

Duplay, P., Bedouelle, H., Fowler, A., Zabin, I., Saurin, W., Hofnung, M., 1984. Sequences of the *malE* gene and of its product, the maltose-binding protein of *Escherichia coli* K12. J. Biol. Chem. 259, 10606–10613.

Eggeling, L., Bott, M., 2005. Handbook of *Corynebacterium glutamicum*. CRC press, Taylor and Francis Group, Boca Raton, FL, USA.

Fowler, Z.L., Gikandi, W.W., Koffas, M.A., 2009. Increased malonyl coenzyme A biosynthesis by tuning the *Escherichia coli* metabolic network and its application to flavanone production. Appl. Environ. Microbiol. 75, 5831–5839.

Gande, R., Dover, L.G., Krumbach, K., Besra, G.S., Sahm, H., Oikawa, T., Eggeling, L., 2007. The two carboxylases of *Corynebacterium glutamicum* essential for fatty acid and mycolic acid synthesis. J. Bacteriol. 189, 5257–5264.

Hüsken, A., Baumert, A., Milkowski, C., Becker, H.C., Strack, D., Möllers, C., 2005. Resveratrol glucoside (Piceid) synthesis in seeds of transgenic oilseed rape (Brassica napus L.). Theor. Appl. Genet. 111, 1553–1562.

Jeong, Y.J., An, C.H., Woo, S.G., Jeong, H.J., Kim, Y.-M., Park, S.-J., et al., 2014. Production of pinostilbene compounds by the expression of resveratrol *O*-methyltransferase genes in *Escherichia coli*. Enzyme Microb. Technol. 54, 8–14.

Kallscheuer, N., Vogt, M., Stenzel, A., Gätgens, J., Bott, M., Marienhagen, J., 2016a. Construction of a *Corynebacterium glutamicum* platform strain for the production of stilbenes and (2*S*)-flavanones. Metab. Eng. 38, 47–55.

Kallscheuer, N., Vogt, M., Kappelmann, J., Krumbach, K., Noack, S., Bott, M., Marienhagen, J., 2016b. Identification of the *phd* gene cluster responsible for phenylpropanoid utilization in *Corynebacterium glutamicum*. Appl. Microbiol. Biotechnol. 100, 1871–1881.

Kaspar, S., Perozzo, R., Reinelt, S., Meyer, M., Pfister, K., Scapozza, L., Bott, M., 1999. The periplasmic domain of the histidine autokinase CitA functions as a highly specific citrate receptor. Mol. Microbiol. 33, 858–872.

Keilhauer, C., Eggeling, L., Sahm, H., 1993. Isoleucine synthesis in *Corynebacterium glutamicum*: molecular analysis of the *ilvB-ilvN-ilvC* operon. J. Bacteriol. 175, 5595–5603.

Kim, B.-G., Joe, E.J., Ahn, J.-H., 2010. Molecular characterization of flavonol synthase from poplar and its application to the synthesis of 3-*O*-methylkaempferol. Biotechnol. Lett. 32, 579–584.

Kirubakaran, S.I., Sakthivel, N., 2007. Cloning and overexpression of antifungal barley chitinase gene in *Escherichia coli*. Protein Expr. Purif. 52, 159–166.

Kortmann, M., Kuhl, V., Klaffl, S., Bott, M., 2015. A chromosomally encoded T7 RNA polymerase-dependent gene expression system for *Corynebacterium glutamicum*: construction and comparative evaluation at the single-cell level. Microb. Biotechnol. 8, 253–265.

Leonard, E., Yan, Y., Koffas, M.A., 2006. Functional expression of a P450 flavonoid hydroxylase for the biosynthesis of plant-specific hydroxylated flavonols in *Escherichia coli*. Metab. Eng. 8, 172–181.

Leonard, E., Yan, Y., Fowler, Z.L., Li, Z., Lim, C.-G., Lim, K.-H., Koffas, M.A., 2008. Strain improvement of recombinant *Escherichia coli* for efficient production of plant flavonoids. Mol. Pharm. 5, 257–265.

Liang, J., Guo, L., Lin, J., He, Z., Cai, F., Chen, J., 2016. A novel process for obtaining pinosylvin using combinatorial bioengineering in *Escherichia coli*. World J. Microbiol. Biotechnol. 32, 1–10.

McCormack, D., McFadden, D., 2013. A review of pterostilbene antioxidant activity and disease modification. Oxid. Med. Cell. Longev. 2013, Article ID 575482.

Miyahisa, I., Funa, N., Ohnishi, Y., Martens, S., Moriguchi, T., Horinouchi, S., 2006. Combinatorial biosynthesis of flavones and flavonols in *Escherichia coli*. Appl. Microbiol. Biotechnol. 71, 53–58.

Otten, A., Brocker, M., Bott, M., 2015. Metabolic engineering of *Corynebacterium glutamicum* for the production of itaconate. Metab. Eng. 30, 156–165.

Park, S.R., Yoon, J.A., Paik, J.H., Park, J.W., Jung, W.S., Ban, Y.-H., et al., 2009. Engineering of plant-specific phenylpropanoids biosynthesis in *Streptomyces venezuelae*. J. Biotechnol. 141, 181–188.

Riggs, P., 2000. Expression and purification of recombinant proteins by fusion to maltose-binding protein. Mol. Biotechnol. 15, 51–63.

Ross, J., Li, Y., Lim, E.-K., Bowles, D.J., 2001. Higher plant glycosyltransferases. Genome Biol. 2 (2), reviews3004.1-3004.6.

Sambrook, J., Russell, D., 2001. Molecular Cloning, vol. 1–3. Cold Spring Harbor Laboratory Press, Cold Spring Harbor, NY.

Santos, C.N.S., Koffas, M., Stephanopoulos, G., 2011. Optimization of a heterologous pathway for the production of flavonoids from glucose. Metab. Eng. 13, 392–400.

Scalbert, A., Johnson, I.T., Saltmarsh, M., 2005. Polyphenols: antioxidants and beyond. Am. J. Clin. Nutr. 81, 215S–217S.

Schmidlin, L., Poutaraud, A., Claudel, P., Mestre, P., Prado, E., Santos-Rosa, M., et al., 2008. A stress-inducible resveratrol *O*-methyltransferase involved in the biosynthesis of pterostilbene in grapevine. Plant Physiol. 148, 1630–1639.

Schröder, J., 1997. A family of plant-specific polyketide synthases: facts and predictions. Trends Plant Sci. 2, 373–378.

Sullivan, M.L., Hatfield, R.D., Thoma, S.L., Samac, D.A., 2004. Cloning and characterization of red clover polyphenol oxidase cDNAs and expression of active protein in *Escherichia coli* and transgenic alfalfa. Plant Physiol. 136, 3234–3244.

Trantas, E., Panopoulos, N., Ververidis, F., 2009. Metabolic engineering of the complete pathway leading to heterologous biosynthesis of various flavonoids and stilbenoids in *Saccharomyces cerevisiae*. Metab. Eng. 11, 355–366.

Tropf, S., Lanz, T., Rensing, S., Schröder, J., Schröder, G., 1994. Evidence that stilbene synthases have developed from chalcone synthases several times in the course of evolution. J. Mol. Evol. 38, 610–618.

van Summeren-Wesenhagen, P.V., Marienhagen, J., 2013. Putting bugs to the blush: metabolic engineering for phenylpropanoid-derived products in microorganisms. Bioengineered 4, 355–362.

van Summeren-Wesenhagen, P.V., Marienhagen, J., 2015. Metabolic engineering of *Escherichia coli* for the synthesis of the plant polyphenol pinosylvin. Appl. Environ. Microbiol. 81, 840–849.

van Summeren-Wesenhagen, P.V., Voges, R., Dennig, A., Sokolowsky, S., Noack, S., Schwaneberg, U., Marienhagen, J., 2015. Combinatorial optimization of synthetic operons for the microbial production of *p*-coumaryl alcohol with *Escherichia coli*. Microb. Cell Fact. 14, 1.

Vissers, M.C., Kuiper, C., Dachs, G.U., 2014. Regulation of the 2-oxoglutarate-dependent dioxygenases and implications for cancer. Biochem. Soc. Trans. 42, 945–951.

Wang, Y., Bhuiya, M.W., Zhou, R., Yu, O., 2015. Pterostilbene production by microorganisms expressing resveratrol *O*-methyltransferase. Ann. Microbiol. 65, 817–826.

Wang, J., Guleria, S., Koffas, M.A., Yan, Y., 2016. Microbial production of value-added nutraceuticals. Curr. Opin. Biotechnol. 37, 97–104.

Whitman, L., Gore, M., Ness, J., Theodorou, E., Gustafsson, C., Minshull, J., 2013. Rapid, scarless cloning of gene fragments using the electra vector system. Genet. Eng. Biotechnol. 33 (42).

Wong, E., 1968. The role of chalcones and flavanones in flavonoid biosynthesis. Phytochemistry 7, 1751–1758.

Wu, J., Du, G., Zhou, J., Chen, J., 2013. Metabolic engineering of *Escherichia coli* for (2*S*)-pinocembrin production from glucose by a modular metabolic strategy. Metab. Eng. 16, 48–55.

Yan, Y., Kohli, A., Koffas, M.A., 2005a. Biosynthesis of natural flavanones in *Saccharomyces cerevisiae*. Appl. Environ. Microbiol. 71, 5610–5613.

Yan, Y., Chemler, J., Huang, L., Martens, S., Koffas, M.A., 2005b. Metabolic engineering of anthocyanin biosynthesis in *Escherichia coli*. Appl. Environ. Microbiol. 71, 3617–3623.

Yang, S.-M., Han, S.H., Kim, B.-G., Ahn, J.-H., 2014. Production of kaempferol 3-*O*-rhamnoside from glucose using engineered *Escherichia coli*. J. Ind. Microbiol. Biotechnol. 41, 1311–1318.

Zhang, H., Tsao, R., 2016. Dietary polyphenols, oxidative stress and antioxidant and anti-inflammatory effects. Curr. Opin. Food Sci. 8, 33–42.

Zhang, Y., Li, S.-Z., Li, J., Pan, X., Cahoon, R.E., Jaworski, J.G., et al., 2006. Using unnatural protein fusions to engineer resveratrol biosynthesis in yeast and mammalian cells. J. Am. Chem. Soc. 128, 13030–13031.

ACS SyntheticBiology

Letter

pubs.acs.org/synthbio

A Novel Synthetic Pathway Enables Microbial Production of Polyphenols Independent from the Endogenous Aromatic Amino Acid Metabolism

Nicolai Kallscheuer, Michael Vogt, and Jan Marienhagen*

Institute of Bio- and Geosciences, IBG-1: Biotechnology, Forschungszentrum Jülich, D-52425 Jülich, Germany

ABSTRACT: Numerous plant polyphenols have potential applications as pharmaceuticals or nutraceuticals. Stilbenes and flavonoids as most abundant polyphenols are synthesized from phenylpropanoids, which are exclusively derived from aromatic amino acids in nature. Several microorganisms were engineered for the synthesis of biotechnologically interesting plant polyphenols; however, low activity of heterologous ammonia lyases, linking endogenous microbial aromatic amino acid biosynthesis to phenylpropanoid synthesis, turned out to be the limiting step during microbial synthesis. We here developed an alternative strategy for polyphenol production from cheap benzoic acids by reversal of a β-oxidative phenylpropanoid degradation pathway avoiding any ammonia lyase activity. The synthetic pathway running in the non-natural direction is feasible with respect to thermodynamics and involved reaction mechanisms. Instantly, product titers of 5 mg/L resveratrol could be achieved in recombinant *Corynebacterium glutamicum* strains indicating that phenylpropanoid synthesis from 4-hydroxybenzoic acid can in principle be implemented independently from aromatic amino acids and ammonia lyase activity.

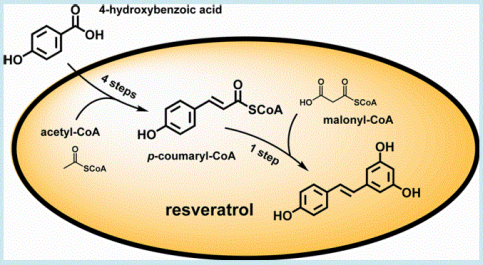

KEYWORDS: *phenylpropanoids, reverse β-oxidation, plant secondary metabolites, resveratrol, Corynebacterium glutamicum*

Plant polyphenols constitute a large group of secondary metabolites enabling plants to interact with their biotic and abiotic environment. Among many others, major functions of these compounds include defense against pathogens, UV filtration and pigmentation.[1,2] Many polyphenols exhibit health-promoting activities in humans including anticancer, antimicrobial, antidiabetic, and anti-inflammatory effects.[3,4]

Naturally occurring plant polyphenols are derived from phenylpropanoids, which are structurally characterized by a benzene residue attached to a propene tail. Phenylpropanoids in turn are exclusively synthesized from the aromatic amino acids L-phenylalanine (L-phe) and L-tyrosine (L-tyr) and thus can be regarded as the metabolic link between the primary carbon metabolism and pathways for the synthesis of polyphenolic compounds of the plant secondary metabolism. The first committed step toward phenylpropanoid synthesis is the nonoxidative deamination of L-phe and L-tyr catalyzed by L-phenylalanine ammonia lyases (PAL) and L-tyrosine ammonia lyases (TAL) yielding cinnamic acid and *p*-coumaric acid, respectively.[5] Subsequently, the phenylpropanoids are converted to their corresponding CoA-thioesters by the activity of 4-coumarate: CoA ligases (4CL) (Figure 1A). The most abundant groups of polyphenolic compounds, stilbenes and flavonoids, are produced from phenylpropanoid CoA-thioesters by the enzymatic activity of either stilbene synthases (STS) or chalcone synthases (CHS).[6]

Due to the health-promoting activities of many plant polyphenols, metabolic engineering of microorganisms for the biotechnological production of these compounds received a lot of attention in the past few years.[7] These efforts mainly focused on engineering *Escherichia coli* and *Saccharomyces cerevisiae* for the microbial synthesis of monolignols, stilbenes, and (2*S*)-flavanones.[8−10] Very recently, we were able to establish stilbene and (2*S*)-flavanone production in an engineered *Corynebacterium glutamicum* strain devoid of catabolic pathways involved in the metabolization of phenylpropanoids and other aromatic compounds.[11,12] *C. glutamicum* is a well-known platform organism for industrial biotechnology and used for the million ton scale production of amino acids for food and feed applications.[13] In general, synthesis of phenylpropanoid-derived polyphenols in microbes from glucose requires overproduction of aromatic amino acids as precursors, and highly active PAL and TAL enzymes. However, the shikimate pathway, essential for production of aromatic amino acids, is costly for the cell in terms of carbon- and energy consumption. Moreover, the limited activity of the employed heterologous PAL or TAL enzymes in microbial host systems often proved to be the rate-limiting step during microbial polyphenol production.[11,14−16]

With the aim to overcome these limitations during microbial plant polyphenol synthesis we designed and constructed a

Received: October 12, 2016
Published: December 11, 2016

DOI: 10.1021/acssynbio.6b00291
ACS Synth. Biol. XXXX, XXX, XXX−XXX

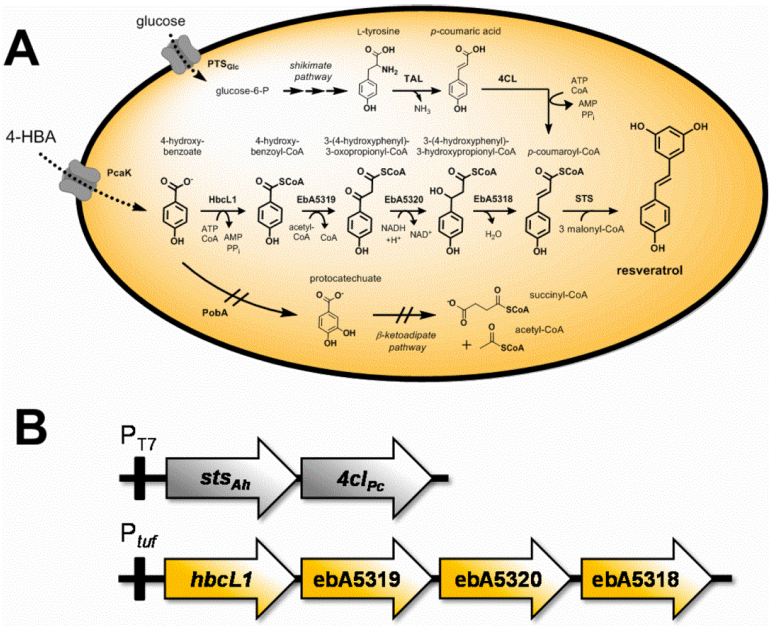

Figure 1. Synthetic reverse β-oxidation pathway for the synthesis of resveratrol from 4-hydroxybenzoate. (A) The novel synthetic pathway for resveratrol production from 4-hydroxybenzoic acid by reversal of β-oxidation and the natural synthesis route from L-tyrosine in plants are shown. The genes coding for enzymes involved in the degradation of 4-hydroxybenzoate were deleted in the course of the construction of the platform strain *C. glutamicum* DelAro[4] (crossed-out arrows). (B) Organization of genes coding for enzymes of the reverse β-oxidation pathway as well as for 4CL and STS in the constructed plasmids. Abbreviations: TAL: tyrosine ammonia lyase, 4CL: 4-coumarate: CoA ligase, STS: stilbene synthase, HbcL1:4-hydroxybenzoate: CoA ligase, EbA5319: β-ketothiolase, EbA5320:3-hydroxyacyl-CoA dehydrogenase, EbA5318: enoyl-CoA hydratase, PTS$_{Glc}$: glucose phosphotransferase system, PcaK: 4-hydroxybenzoate importer, PobA: 4-hydroxybenzoate 3-hydroxylase, 4-HBA: 4-hydroxybenzoate.

synthetic pathway based on a β-oxidative phenylpropanoid degradation pathway identified in the facultative denitrifying betaproteobacterium *Azoarcus* sp. EbN1 (inofficial designation "*Aromatoleum aromaticum*" EbN1).[17] On the basis of the finding that β-oxidation is generally recognized as reversible[18] we here engineered the degradation pathway to run in the anabolic direction for the synthesis of phenylpropanoid CoA-thioesters starting from cheap benzoic acids.

The novel synthetic pathway for phenylpropanoids represents an engineered reversal of a CoA-dependent, β-oxidative degradation pathway for phenylpropanoids from "*Aromatoleum aromaticum*" EbN1.[17] In the catabolic direction, CoA-activated *p*-coumaric acid undergoes a classical β-oxidation including hydration, oxidation and thiolytic cleavage yielding 4-hydroxybenzoyl-CoA and acetyl-CoA as products. In "*A. aromaticum*" EbN1 the reactions are catalyzed by an enoyl-CoA hydratase (EbA5318), a 3-hydroxyacyl-CoA dehydrogenase (EbA5320) and a β-ketothiolase (EbA5319), respectively.[17] To enable the pathway to run in the desired opposite, anabolic direction starting from 4-hydroxybenzoic acid (4-HBA), an additional step for the conversion of 4-HBA to 4-hydroxybenzoyl-CoA is required (Figure 1A).

Interestingly, a gene coding for an enzyme with the corresponding 4-hydroxybenzoate: CoA-ligase activity (HbcL1, EbA5368) is also present in "*A. aromaticum*" EbN1.[19] In the synthetic pathway, a subsequent acetyl-CoA dependent chain elongation step of 4-hydroxybenzoyl-CoA, catalyzed by the β-ketothiolase EbA5319, would lead to the formation of 3-(4-hydroxyphenyl)-3-oxopropionyl-CoA (Figure 1A). The enzymatic mechanism of β-ketothiolases (acyl-CoA: C-acetyltransferases) permits reversal of the catalyzed reaction.[20] From the stage of 3-(4-hydroxyphenyl)-3-oxopropionyl-CoA the subsequent reaction steps catalyzed by 3-hydroxyacyl-CoA dehydrogenase and enoyl-CoA dehydratase are also reversible with respect to the underlying reaction mechanisms.[21]

The complete synthetic pathway from 4-hydroxybenzoic acid and acetyl-CoA to *p*-coumaroyl-CoA was also analyzed with regard to thermodynamic feasibility by calculating the change of Gibbs free energy for each reaction step individually. The Gibbs free energy values for the involved metabolites were obtained from the BioCYC database[22] (Table 1A). If the calculated $\Delta G^{0\prime}$ for a reaction is negative (exergonic reaction) the reaction is assumed to be favored in the shown direction, whereas for positive $\Delta G^{0\prime}$ values the reaction is endergonic and therefore thermodynamically unfavorable. The ATP-driven CoA-ligation of 4-hydroxybenzoate was calculated to be feasible with $\Delta G^{0\prime}$ of −53.2 kJ/mol (Table 1B). For the β-ketothiolase-catalyzed chain elongation reaction on 4-hydroxybenzoyl-CoA the calculated $\Delta G^{0\prime}$ value of +29.6 kJ/mol is positive. This value is in accordance with the elongation reaction for butyrate production using an analogous reverse β-oxidation pathway.[18]

DOI: 10.1021/acssynbio.6b00291
ACS Synth. Biol. XXXX, XXX, XXX−XXX

Table 1. Gibbs Free Energies for Involved Compounds and Calculated $\Delta G^{0\prime}$ Values for the Reactions of the Reverse β-Oxidation Pathway for the Production of *p*-Coumaroyl-CoA Starting from 4-Hydroxybenzoate[a]

(A)

compound	Gibbs free energy (kJ/mol)
3-(4-hydroxyphenyl)-3-oxopropionyl-CoA	−2086.5
3-(4-hydroxyphenyl)-3-hydroxypropionyl-CoA	−2027.6
4-hydroxybenzoate	−173.7
4-hydroxybenzoyl-CoA	−2060.4
acetyl-CoA	−2122.2
AMP	−569.0
ATP	−2318.3
CoA	−2066.6
diphosphate	−1982.4
H^+	+1.8
H_2O	−151.3
NAD^+	−1416.8
NADH	−1361.6
p-coumaroyl-CoA	−1887.4

(B)

enzyme	reaction (substrates → products)	$\Delta G^{0\prime}$ (kJ/mol)
4-hydroxybezoate: CoA-ligase	4-hydroxybenzoate + CoA + ATP → 4-hydroxybenzoyl-CoA + AMP + diphosphate	−53.2
3-oxoacyl-CoA thiolase	4-hydroxybenzoyl-CoA + acetyl-CoA → 3-(4-hydroxyphenyl)-3-oxopropionyl-CoA + CoA	+29.6
3-hydroxyacyl-CoA dehydrogenase	3-(4-hydroxyphenyl)-3-oxopropionyl-CoA + NADH + H^+ → 3-(4-hydroxyphenyl)-3-hydroxypropionyl-CoA + NAD^+	+2.0
enoyl-CoA hydratase	3-(4-hydroxyphenyl)-3-hydroxypropionyl-CoA → *p*-coumaroyl-CoA + H_2O	−11.1
overall reaction	4-hydroxybenzoate + acetyl-CoA + ATP + NADH + H^+ → *p*-coumaroyl-CoA + AMP + diphosphate + NAD^+ + H_2O	−32.8

[a](A) The Gibbs free energies for the compounds involved in the reverse β-oxidation pathway were obtained from the BioCYC database (pathway: 4-hydroxybenzoate biosynthesis V) and are shown in alphabetical order. The original values given in kcal/mol were converted to kJ/mol (1 kcal/mol = 4.187 kJ/mol). (B) The $\Delta G^{0\prime}$ values for each reaction were calculated using the Gibbs free energy values for the corresponding compound participating in each reaction. The change of Gibbs free energy $\Delta G^{0\prime}$ corresponds to the sum of Gibbs free energies of each reaction substrate subtracted from the sum of Gibbs free energies of each product of the reaction: $\Delta G^{0\prime} = \Sigma(G^{0\prime}_{\text{products}}) - \Sigma(G^{0\prime}_{\text{substrates}})$.

As the biosynthetic (anabolic) reaction catalyzed by β-ketothiolases is generally recognized to be thermodynamically unfavorable, it was proposed that the formation of 3-oxoacyl-CoA is driven by the intracellular excess of substrates and removal of the product by further enzymatic conversion.[23] The NADH-dependent reduction of the keto group in 3-(4-hydroxyphenyl)-3-oxopropionyl-CoA appears to be negligible with respect to the overall thermodynamics ($\Delta G^{0\prime}$ = +2.0 kJ/mol). Formation of *p*-coumaroyl-CoA by dehydration of 3-(4-hydroxyphenyl)-3-hydroxypropionyl-CoA is expected to be feasible based on the calculated $\Delta G^{0\prime}$ of −11.1 kJ/mol. Taken together, the overall synthetic route from 4-hydroxybenzoate to *p*-coumaroyl-CoA with NADH as electron donor is estimated to be feasible with a total $\Delta G^{0\prime}$ of −32.8 kJ/mol (Table 1B). For the subsequent stilbene synthase reaction yielding resveratrol a $\Delta G^{0\prime}$ of −69.2 kJ/mol was calculated.

The plasmid pMKEx2_sts_{Ah}_$4cl_{Pc}$ was constructed earlier by us for engineering *C. glutamicum* to produce the pharmacologically interesting plant stilbene resveratrol.[11] This plasmid harbors codon-optimized genes coding for an STS and a 4CL originally found in peanut (*Arachis hypogaea*) and parsley (*Petroselinum crispum*), respectively. Both genes constitute a bicistronic operon under control of the IPTG-inducible T7 promoter (Figure 1B). The constructed platform strain *C. glutamicum* DelAro[4] was used as chassis strain as it is unable to degrade phenylpropanoids and benzoic acids.[11] However, it cannot be excluded that produced *p*-coumaroyl-CoA is hydrolyzed to *p*-coumaric acid either spontaneously or by thioesterase activity in *C. glutamicum*. With the aim to compensate for this undesired side reaction we also introduced a heterologous 4CL activity to enable CoA-activation of *p*-coumaric acid to *p*-coumaroyl-CoA.

With the aim to establish a reversal of β-oxidation as alternative production route for resveratrol, the genes ebA5368, ebA5319, ebA5320 and ebA5318 coding for the enzymes of the phenylpropanoid degradation pathway of "*A. aromaticum*" EbN1 were assembled as synthetic operon under control of the strong constitutive *tuf* promoter[24] (Figure 1B). The complete operon was subsequently cloned into the *C. glutamicum* expression plasmid pEKEx3 yielding pEKEx3_RevBeta.

The strain *C. glutamicum* DelAro[4] pMKEx2_sts_{Ah}_$4cl_{Pc}$ pEKEx3_RevBeta was tested for resveratrol production starting from 4-HBA, which can be imported by *C. glutamicum* by the endogenous transporter PcaK[25] (Figure 1A). In addition to *p*-coumaroyl-CoA formed from 4-HBA, three molecules of malonyl-CoA are consumed by the STS for the synthesis of resveratrol. As the low intracellular level of malonyl-CoA represents a known bottleneck for polyphenol production in microbes, the cultivation of *C. glutamicum* was performed in the presence of the fatty acid synthesis inhibitor cerulenin, which was already shown to improve production of resveratrol by increasing the availability of malonyl-CoA in *C. glutamicum*.[11]

To this end, *C. glutamicum* DelAro[4] pMKEx2_sts_{Ah}_$4cl_{Pc}$ pEKEx3_RevBeta was cultivated in defined CGXII medium with 4% glucose, 5 mM 4-HBA, and 25 μM cerulenin (Figure 2A). Heterologous expression of the *sts* and *4cl* genes was induced with 1 mM IPTG. The addition of 5 mM 4-HBA did not have a negative effect on growth of the constructed *C. glutamicum* strain (data not shown) and after 24 h of cultivation, a maximal titer of 4.8 ± 0.3 mg/L (0.02 ± 0.001

DOI: 10.1021/acssynbio.6b00291
ACS Synth. Biol. XXXX, XXX, XXX−XXX

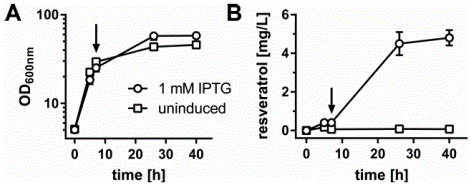

Figure 2. Synthesis of *trans*-resveratrol in *C. glutamicum* from 4-hydroxybenzoate. Strain *C. glutamicum* DelAro[4] pMKEx2_sts_{Ah}_$4cl_{Pc}$ pEKEx3_RevBeta was cultivated in defined CGXII medium with 4% glucose and 5 mM 4-hydroxybenzoic acid in presence or absence of 1 mM IPTG for induction of the gene expression of *sts* and *4cl*. Twenty-five μM cerulenin was added in the exponential growth phase at OD_{600} 20–25 (time point of addition is indicated by an arrow). The resveratrol concentrations were determined after ethyl acetate extraction of the culture broth by LC–MS analysis. The highest concentration of 4.8 mg/L resveratrol after 40 h of cultivation corresponds to 0.02 mM. Data represent average values and standard deviation from three biological replicates.

mM) resveratrol could be detected (Figure 2B). This indicates that the engineered reverse β-oxidative pathway works, although the overall yield is quite low at this stage of development (0.4 %). This could be simply due to an imbalanced expression of the six heterologous genes. Interestingly, doubling the precursor concentration from 5 mM to 10 mM had no positive effect on the final product titer (data not shown). In cultivations of the same strain under identical conditions but without induction of gene expression, no resveratrol production was found (Figure 2B). The same was also true for cultivations without any supplemented 4-HBA and for a strain harboring the empty plasmids pMKEx2 and pEKEx3. No resveratrol was found when 4-HBA was added to a strain harboring only pMKEx2_sts_{Ah}_$4cl_{Pc}$ but not pEKEx3_RevBeta (data not shown).

Interestingly, during LC–MS analysis, two distinct peaks (peaks b and c) for commercially available resveratrol could be detected (Figure 3A), whereas for resveratrol produced by the established synthetic reverse β-oxidation pathway only one peak corresponding to peak c of the metabolite standard was found (Figure 3B). From the molecular geometry of the *cis*- and *trans*-isomers of resveratrol, we assume that peak b represents *cis*-resveratrol as it is bulkier and has a weaker interaction with the stationary phase leading to an earlier elution from the chromatography column compared to the *trans*-isomer (peak c). In consequence, the synthetic reverse β-oxidation pathway appears to be specific for the production of *trans*-resveratrol. This finding is in line with the underlying reaction mechanisms of the involved enzymes. The *trans*-enoyl-CoA intermediate (in this case *p*-coumaryl-CoA) is produced from (*S*)-3-hydroxyacyl-CoA, which in turn is the product of the 3-hydroxyacyl-CoA dehydrogenase in β-oxidation pathways.[26,27] It can be argued that catalysis of the enzymes in the non-native direction produces exclusively *trans*-*p*-coumaroyl-CoA assuming the same reaction mechanisms also for the employed enzymes.[17] If the stilbene synthase does not alter the stereochemistry of the CoA-thioester, the observed exclusive synthesis of the *trans*-isomer of resveratrol is the consequence and in line with the finding in our study.

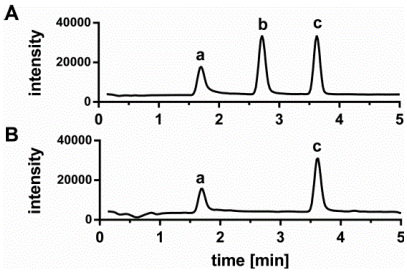

Figure 3. LC–MS chromatograms of commercially available resveratrol and of resveratrol produced using the reverse β-oxidation pathway. LC–MS chromatograms of commercially available resveratrol (A) or resveratrol produced from 4-hydroxybenzoic acid *via* the synthetic β-oxidative pathway (B). Peak a: benzoic acid (internal standard, retention time 1.70 min.), peak b: *cis*-resveratrol (retention time 2.72 min), peak c: *trans*-resveratrol (retention time 3.62 min). The LC–MS analysis was performed in the selected ion monitoring (SIM) mode for *m*/*z* 121 and *m*/*z* 227 corresponding to the $[M - H]^-$ masses of benzoic acid and of resveratrol, respectively.

We here demonstrate that microbial production of resveratrol can be achieved by following a reverse β-oxidation pathway starting from 4-HBA. Previously, reverse β-oxidative pathways were employed to produce fatty acids, dicarboxylic acids, and alcohols of different chain length, but no aromatic compounds of biotechnological significance have been synthesized following this synthetic strategy.[18,21,28–30] The orthogonal β-oxidative pathway now successfully implemented into the metabolism of *C. glutamicum* allows for resveratrol synthesis only demanding for acetyl-CoA and malonyl-CoA supply by the host metabolism. In addition, the pathway requires NADH and ATP as coenzymes, but otherwise operates independently from the shikimate pathway. At this stage, further optimization of the reverse β-oxidation pathway, *e.g.*, by improving and balancing the heterologous gene expression, is required.

Taken together, the novel pathway provides a promising alternative to the classical microbial phenylpropanoid production pathway and has the potential to be employed for the production of phenylpropanoids, stilbenes and flavonoids from benzoic acids in engineered microbial production strains in the future.

METHODS

Bacterial Strains, Plasmids, Media, and Growth Conditions. All bacterial strains, plasmids, and oligonucleotides used in this study as well as their relevant characteristics are listed in Table 2. *E. coli* DH5α was used for plasmid constructions and was cultivated in LB medium[31] at 37 °C. *C. glutamicum* strains were routinely cultivated aerobically at 30 °C in brain heart infusion (BHI) medium (Difco Laboratories, Detroit, USA) or defined CGXII medium with glucose as sole carbon and energy source.[32] Where appropriate, kanamycin (50 μg/mL for *E. coli* or 25 μg/mL for *C. glutamicum*) or spectinomycin (100 μg/mL for *E. coli* and *C. glutamicum*) was added to the medium. Bacterial growth was followed by measuring the optical density at 600 nm (OD_{600}).

C. glutamicum was grown for 6–8 h in test tubes with 5 mL BHI medium on a rotary shaker at 170 rpm (first preculture) and subsequently inoculated into 50 mL CGXII medium with 4% glucose in 500 mL baffled Erlenmeyer flasks (second preculture). The cell suspensions were cultivated overnight on

DOI: 10.1021/acssynbio.6b00291
ACS Synth. Biol. XXXX, XXX, XXX–XXX

Table 2. Strains, Plasmids, and Oligonucleotides Used in This Study

	relevant characteristics	source or reference
Strains		
C. glutamicum strains		
MB001(DE3)	prophage-free derivate of wild type ATCC 13032 with chromosomally encoded T7 *gene 1* (cg1122-P_{lacI}-*lacI*-P_{lacUV5} − *lacZα*-T7 *gene 1*-cg1121)	36
DelAro[4]	MB001(DE3) derivative with in-frame deletions of cg0344−47, cg2625−40, cg1226 and cg0502	11
E. coli strains		
DH5α	F− Φ80*lacZ*ΔM15 Δ(*lacZYA-argF*)U169 *recA1 endA1 hsdR*17 (rK−, mK+) *phoA supE44 λ− thi-1 gyrA96 relA1*	Invitrogen (Karlsruhe, Germany)
Plasmids[a]		
pMKEx2	kan^R; *E. coli-C. glutamicum* shuttle vector (*lacI*, P_{T7}, lacO1, $pHM1519ori_{Cg}$; $pACYC177ori_{Ec}$)	36
pMKEx2_sts_{Ah}_$4cl_{Pc}$	kan^R; pMKEx2 derivative containing codon-optimized genes coding for stilbene synthase and 4-coumarate: CoA ligase	this study
pEKEx3	$spec^R$; *E. coli-C. glutamicum* shuttle vector (*lacI*, lacO1, $pBL1ori_{Cg}$; $pUCori_{Ec}$)	37
pEKEx3_RevBeta	$spec^R$; pEKEx3 derivative containing *hbcL1*, ebA5319, ebA5320, ebA5318 from "*Aromatoleum aromaticum*" EbN1 under control of P_{tuf}	this study
Oligonucleotides[b]		
P_{tuf}-hbcL1-s	ATCGGATCCAGTTAGCTGGCCGTTACCCTGCGAATG	*Bam*HI
hbcL1-as	CACGGTCTC**AATT**CTCAGGACACGGCGACGGCGCTC	*Bsa*I
ebA5319-s	TATGGTCTC**AGAAT**AAGGAGGTACGAAATGAACACGACCAATTCCTACGCCGCGTC	*Bsa*I
ebA5319-as	GGAGGTCTC**TCGCC**TCAGCCGACGTTCTCGACGACG	*Bsa*I
ebA5320-s	AGCGGTCTC**AGGCG**AGGAGGAACATCATGAAACTCGAAAGCAGCACTTTTATCGTCACC	*Bsa*I
ebA5320-as	AATGGTCTC**TACAA**TTAGCGGGGCGCGAGGCGGATC	*Bsa*I
ebA5318-s	GCTGGTCTC**ATTGT**CAGGAGGTGCAACATGAATCACGAAAGGATCATCCTGATGAC	*Bsa*I
ebA5318-as	ATCGAATTCATTCTCTAGATCATCGCTGCGCTCCCTGAC	*Eco*RI
stsAh-s	ATACCATGGTAAGGAGGACAGCTATGGTGTCCGTGTCCGGCATC	*Nco*I
stsAh-as	CTCGGTACCTTTAGATTGCCATAGAGCGCAGCACCAC	*Kpn*I
4clPc-s	AGCGGTACCTAAGGAGGTGGACAATGGGCGATTGCGTGGCAC	*Kpn*I
4clPc-as	CTGGGATCCAGGACTAGTTTCCAGAGTACTATTACTTTGGCAGATCACCGGATGCGATC	*Bam*HI

[a] kan^R: kanamycin resistance; $spec^R$: spectinomycin resistance. [b] Primer sequences are given in 5′−3′ orientation. Restriction sites used for cloning are underlined. The obtained complementary overhangs after *Bsa*I cleavage used for gene assembly are depicted in bold.

a rotary shaker at 130 rpm. The main culture was inoculated to an OD_{600} of 7 in CGXII medium with 4% glucose. Heterologous gene expression was induced one hour after inoculation using 1 mM IPTG. If indicated 25 μM cerulenin was added to the culture medium 7 h after inoculation. One mL of the culture broth was collected at defined time points and stored at −20 °C until extraction.

Construction of Plasmids and Strains. Standard protocols of molecular cloning, such as PCR, DNA restriction, and ligation[33] were carried out for recombinant DNA work. Techniques specific for *C. glutamicum*, *e.g.*, electroporation for transformation of strains, were done as described previously.[34] The constructed strains and plasmids are listed in Table 2. All restriction enzymes were obtained from ThermoScientific (Schwerte, Germany). Synthetic genes were obtained from LifeTechnologies (Darmstadt, Germany). The RevBeta operon was assembled from PCR products using the Golden Gate Cloning method[35] and subsequently cloned into pEKEx3 using restriction sites *Bam*HI/*Eco*RI (Table 2). The cloned genes were verified by DNA sequencing performed at Eurofins MWG Operon (Ebersberg, Germany).

Metabolite Extraction. Metabolite extracts from cultivation broth were prepared for LC−MS analysis by mixing 1 mL of the culture broth with 1 mL ethyl acetate and vigorous shaking (1400 rpm; 10 min, 20 °C) in an Eppendorf thermomixer (Hamburg, Germany). The suspension was centrifuged for 5 min at 16 000*g* and the ethyl acetate layer (800 μL) was transferred to an organic solvent resistant deep-well plate (Eppendorf, Hamburg, Germany). After evaporation of the ethyl acetate overnight, dried extracts were resuspended in the same volume of acetonitrile and directly used for LC−MS analysis.

LC−MS Analysis. Resveratrol was quantified in extracted samples by LC−MS using an ultrahigh-performance LC (uHPLC) 1290 Infinity System coupled to a 6130 Quadrupole LC−MS System (Agilent, Waldbronn, Germany). LC separation was carried out with a Kinetex 1.7u C_{18} 100 Å pore size column (50 mm by 2.1 mm [internal diameter]; Phenomenex, Torrance, CA, USA) at 50 °C. For elution, 0.1% acetic acid (solvent A) and acetonitrile supplemented with 0.1% acetic acid (solvent B) were applied as the mobile phases at a flow rate of 0.5 mL/min. A gradient was used, where the amount of solvent B was increased stepwise: minute 0 to 6:10% to 30%, minute 6 to 7:30% to 50%, minute 7 to 8:50% to 100%, and minute 8 to 8.5:100% to 10%. The mass spectrometer was operated in the negative electrospray ionization (ESI) mode, and data acquisition was performed in selected-ion-monitoring (SIM) mode. Authentic metabolite standards were purchased from Sigma-Aldrich (Schnelldorf, Germany). Area values for $[M - H]^-$ mass signals were linear up to metabolite concentrations of at least 250 mg/L. Benzoic acid (final concentration 100 mg/L) was used as internal standard. Calibration curves were calculated on the basis of analyte/internal standard ratios for the obtained area values.

AUTHOR INFORMATION

Corresponding Author

*Phone: +49 2461 61 2843. E-mail j.marienhagen@fz-juelich.de.

ORCID

Jan Marienhagen: 0000-0001-5513-3730

Notes

The authors declare no competing financial interest.

DOI: 10.1021/acssynbio.6b00291
ACS Synth. Biol. XXXX, XXX, XXX−XXX

■ ACKNOWLEDGMENTS

We would like to thank the European Union Framework Program 7 "BacHBerry" (www.bachberry.eu), Project No. FP7-613793 for financial support.

■ REFERENCES

(1) Seigler, D. S. (2012) *Plant Secondary Metabolism*; Springer Science & Business Media.
(2) Tissier, A., Ziegler, J., and Vogt, T. (2014) Specialized Plant Metabolites: Diversity and Biosynthesis, In *Ecological Biochemistry*, pp 14−37, Wiley-VCH Verlag GmbH & Co. KGaA.
(3) Manach, C., Scalbert, A., Morand, C., Rémésy, C., and Jiménez, L. (2004) Polyphenols: food sources and bioavailability. *Am. J. Clin. Nutr. 79*, 727−747.
(4) Spatafora, C., and Tringali, C. (2012) Natural-derived polyphenols as potential anticancer agents. *Anti-Cancer Agents Med. Chem. 12*, 902−918.
(5) Jangaard, N. O. (1974) The characterization of phenylalanine ammonia-lyase from several plant species. *Phytochemistry 13*, 1765−1768.
(6) Tropf, S., Kärcher, B., Schröder, G., and Schröder, J. (1995) Reaction Mechanisms of Homodimeric Plant Polyketide Synthases (Stilbene and Chalcone Synthase): A single active site for the condensing reactions is sufficient for the synthesis of stilbenes, chalcones and 6′-deoxychalcones. *J. Biol. Chem. 270*, 7922−7928.
(7) Marienhagen, J., and Bott, M. (2013) Metabolic engineering of microorganisms for the synthesis of plant natural products. *J. Biotechnol. 163*, 166−178.
(8) Lim, C. G., Fowler, Z. L., Hueller, T., Schaffer, S., and Koffas, M. A. (2011) High-yield resveratrol production in engineered *Escherichia coli*. *Appl. Environ. Microbiol. 77*, 3451−3460.
(9) Koopman, F., Beekwilder, J., Crimi, B., van Houwelingen, A., Hall, R. D., Bosch, D., van Maris, A. J., Pronk, J. T., and Daran, J.-M. (2012) De novo production of the flavonoid naringenin in engineered *Saccharomyces cerevisiae*. *Microb. Cell Fact. 11*, 155.
(10) van Summeren-Wesenhagen, P. V., and Marienhagen, J. (2015) Metabolic engineering of *Escherichia coli* for the synthesis of the plant polyphenol pinosylvin. *Appl. Environ. Microbiol. 81*, 840−849.
(11) Kallscheuer, N., Vogt, M., Stenzel, A., Gätgens, J., Bott, M., and Marienhagen, J. (2016) Construction of a *Corynebacterium glutamicum* platform strain for the production of stilbenes and (2*S*)-flavanones. *Metab. Eng. 38*, 47−55.
(12) Kallscheuer, N., Vogt, M., Kappelmann, J., Krumbach, K., Noack, S., Bott, M., and Marienhagen, J. (2016) Identification of the *phd* gene cluster responsible for phenylpropanoid utilization in *Corynebacterium glutamicum*. *Appl. Microbiol. Biotechnol. 100*, 1871−1881.
(13) Becker, J., and Wittmann, C. (2012) Bio-based production of chemicals, materials and fuels − *Corynebacterium glutamicum* as versatile cell factory. *Curr. Opin. Biotechnol. 23*, 631−640.
(14) Eudes, A., Juminaga, D., Baidoo, E. E., Collins, F. W., Keasling, J. D., and Loqué, D. (2013) Production of hydroxycinnamoyl anthranilates from glucose in *Escherichia coli*. *Microb. Cell Fact. 12*, 62.
(15) Lin, Y., and Yan, Y. (2012) Biosynthesis of caffeic acid in *Escherichia coli* using its endogenous hydroxylase complex. *Microb. Cell Fact. 11*, 42.
(16) Zhou, S., Liu, P., Chen, J., Du, G., Li, H., and Zhou, J. (2016) Characterization of mutants of a tyrosine ammonia-lyase from *Rhodotorula glutinis*. *Appl. Microbiol. Biotechnol. 100*, 10443.
(17) Trautwein, K., Wilkes, H., and Rabus, R. (2012) Proteogenomic evidence for β-oxidation of plant-derived 3-phenylpropanoids in "*Aromatoleum aromaticum*" EbN1. *Proteomics 12*, 1402−1413.
(18) Dellomonaco, C., Clomburg, J. M., Miller, E. N., and Gonzalez, R. (2011) Engineered reversal of the β-oxidation cycle for the synthesis of fuels and chemicals. *Nature 476*, 355−359.
(19) Wöhlbrand, L., Kallerhoff, B., Lange, D., Hufnagel, P., Thiermann, J., Reinhardt, R., and Rabus, R. (2007) Functional proteomic view of metabolic regulation in "*Aromatoleum aromaticum*" strain EbN1. *Proteomics 7*, 2222−2239.
(20) Haapalainen, A. M., Meriläinen, G., and Wierenga, R. K. (2006) The thiolase superfamily: condensing enzymes with diverse reaction specificities. *Trends Biochem. Sci. 31*, 64−71.
(21) Clomburg, J. M., Vick, J. E., Blankschien, M. D., Rodríguez-Moyá, M., and Gonzalez, R. (2012) A synthetic biology approach to engineer a functional reversal of the β-oxidation cycle. *ACS Synth. Biol. 1*, 541−554.
(22) Caspi, R., Billington, R., Ferrer, L., Foerster, H., Fulcher, C. A., Keseler, I. M., Kothari, A., Krummenacker, M., Latendresse, M., and Mueller, L. A. (2016) The MetaCyc database of metabolic pathways and enzymes and the BioCyc collection of pathway/genome databases. *Nucleic Acids Res. 44*, D471−D480.
(23) Modis, Y., and Wierenga, R. K. (1999) A biosynthetic thiolase in complex with a reaction intermediate: the crystal structure provides new insights into the catalytic mechanism. *Structure 7*, 1279−1290.
(24) Pátek, M., Holátko, J., Busche, T., Kalinowski, J., and Nešvera, J. (2013) *Corynebacterium glutamicum* promoters: a practical approach. *Microb. Biotechnol. 6*, 103−117.
(25) Chaudhry, M. T., Huang, Y., Shen, X.-H., Poetsch, A., Jiang, C.-Y., and Liu, S.-J. (2007) Genome-wide investigation of aromatic acid transporters in *Corynebacterium glutamicum*. *Microbiology 153*, 857−865.
(26) Agnihotri, G., and Liu, H.-w. (2003) Enoyl-CoA hydratase: Reaction, mechanism, and inhibition. *Bioorg. Med. Chem. 11*, 9−20.
(27) Noyes, B. E., Glatthaar, B. E., Garavelli, J. S., and Bradshaw, R. A. (1974) Structural and Functional Similarities Between Mitochondrial Malate Dehydrogenase and L-3-Hydroxyacyl CoA Dehydrogenase. *Proc. Natl. Acad. Sci. U. S. A. 71*, 1334−1338.
(28) Clomburg, J. M., Blankschien, M. D., Vick, J. E., Chou, A., Kim, S., and Gonzalez, R. (2015) Integrated engineering of β-oxidation reversal and ω-oxidation pathways for the synthesis of medium chain ω-functionalized carboxylic acids. *Metab. Eng. 28*, 202−212.
(29) Babu, T., Yun, E. J., Kim, S., Kim, D. H., Liu, K. H., Kim, S. R., and Kim, K. H. (2015) Engineering *Escherichia coli* for the production of adipic acid through the reversed β-oxidation pathway. *Process Biochem. 50*, 2066−2071.
(30) Gulevich, A. Y., Skorokhodova, A. Y., Sukhozhenko, A. V., Shakulov, R. S., and Debabov, V. G. (2012) Metabolic engineering of *Escherichia coli* for 1-butanol biosynthesis through the inverted aerobic fatty acid β-oxidation pathway. *Biotechnol. Lett. 34*, 463−469.
(31) Bertani, G. (1951) Studies on Lysogenesis I: The Mode of Phage Liberation by Lysogenic *Escherichia coli*. *J. Bacteriol. 62*, 293.
(32) Keilhauer, C., Eggeling, L., and Sahm, H. (1993) Isoleucine synthesis in *Corynebacterium glutamicum*: molecular analysis of the *ilvB-ilvN-ilvC* operon. *J. Bacteriol. 175*, 5595−5603.
(33) Sambrook, J., and Russell, D. (2001) *Molecular Cloning*, Vol. *1*−*3*, Cold Spring Harbor Laboratory Press, Cold Spring Harbor, NY.
(34) Eggeling, L., and Bott, M. (2005) *Handbook of Corynebacterium glutamicum*; CRC Press.
(35) Engler, C., Gruetzner, R., Kandzia, R., and Marillonnet, S. (2009) Golden gate shuffling: a one-pot DNA shuffling method based on type IIs restriction enzymes. *PLoS One 4*, e5553.
(36) Kortmann, M., Kuhl, V., Klaffl, S., and Bott, M. (2015) A chromosomally encoded T7 RNA polymerase-dependent gene expression system for *Corynebacterium glutamicum*: construction and comparative evaluation at the single-cell level. *Microb. Biotechnol. 8*, 253−265.
(37) Gande, R., Dover, L. G., Krumbach, K., Besra, G. S., Sahm, H., Oikawa, T., and Eggeling, L. (2007) The two carboxylases of *Corynebacterium glutamicum* essential for fatty acid and mycolic acid synthesis. *J. Bacteriol. 189*, 5257−5264.

DOI: 10.1021/acssynbio.6b00291
ACS Synth. Biol. XXXX, XXX, XXX−XXX

2.5 Production of chemicals and polymer building blocks by reversal of β-oxidation

Metabolic Engineering 42 (2017) 33–42

Contents lists available at ScienceDirect

Metabolic Engineering

journal homepage: www.elsevier.com/locate/meteng

Reversal of β-oxidative pathways for the microbial production of chemicals and polymer building blocks

Nicolai Kallscheuer, Tino Polen, Michael Bott, Jan Marienhagen*

Institute of Bio- and Geosciences, IBG-1: Biotechnology, Forschungszentrum Jülich, D-52425 Jülich, Germany

ARTICLE INFO

Keywords:
Reverse β-oxidation
Carboxylic acid
Polymer building blocks
Metabolic engineering
Biopolymers

ABSTRACT

β-Oxidation is the ubiquitous metabolic strategy to break down fatty acids. In the course of this four-step process, two carbon atoms are liberated per cycle from the fatty acid chain in the form of acetyl-CoA. However, typical β-oxidative strategies are not restricted to monocarboxylic (fatty) acid degradation only, but can also be involved in the utilization of aromatic compounds, amino acids and dicarboxylic acids. Each enzymatic step of a typical β-oxidation cycle is reversible, offering the possibility to also take advantage of reversed metabolic pathways for applied purposes. In such cases, 3-oxoacyl-CoA thiolases, which catalyze the final chain-shortening step in the catabolic direction, mediate the condensation of an acyl-CoA starter molecule with acetyl-CoA in the anabolic direction. Subsequently, the carbonyl-group at C3 is stepwise reduced and dehydrated yielding a chain-elongated product. In the last years, several β-oxidation pathways have been studied in detail and reversal of these pathways already proved to be a promising strategy for the production of chemicals and polymer building blocks in several industrially relevant microorganisms. This review covers recent advancements in this field and discusses constraints and bottlenecks of this metabolic strategy in comparison to alternative production pathways.

1. Introduction

1.1. Fatty acid synthesis and β-oxidation

Fatty acid synthesis and β-oxidation are well-studied metabolic strategies for synthesis and degradation of fatty acids, respectively (Schulz, 1991; Wakil, 1961) (Fig. 1). The intermediates of both pathways are chemically identical, but different enzymes and cofactors are employed to prevent metabolic cross-talk. In eukaryotes, separation of both modules of fatty acid metabolism is also supported by localization in different compartments as β-oxidation is exclusively located in the mitochondria whereas fatty acid synthesis is located in the cytosol (Bartlett and Eaton, 2004).

Fatty acid synthesis is catalyzed by the fatty acid synthase complex (FAS), which keeps the growing fatty acid chain bound to an acyl carrier protein (ACP) during all steps of catalysis. The FAS exclusively uses malonyl-CoA, which is obtained from the carboxylation of acetyl-CoA, for chain elongation yielding 3-oxoacyl-ACP as first intermediate. For the subsequent reductions of 3-oxoacyl-ACP and enoyl-ACP, FAS employs NADPH as cofactor (Wakil, 1989) (Fig. 1). Multiple rounds of chain elongation and reduction of the carbonyl group at C3 in the growing carbon chain can be catalyzed by the FAS. Finally, the thioesterase domain of FAS cleaves the long-chain acyl-ACP releasing free fatty acids with a typical chain length of 16 or 18 carbon atoms.

In principal, β-oxidation is the reversal of fatty acid synthesis but involved enzymes are solely active on CoA-activated thioesters and do not convert the acyl-ACP thioesters of fatty acid synthesis. In the first step, an acyl-CoA synthetase is responsible for CoA-activation of fatty acids yielding the respective acyl-CoA thioesters (Groot et al., 1976) (Fig. 1). An acyl-CoA dehydrogenase uses FAD for the oxidation of acyl-CoA to *trans*-enoyl-CoA (Thorpe and Kim, 1995), which is then hydrated to 3-hydroxyacyl-CoA by an enoyl-CoA hydratase (Schomburg and Salzmann, 1990). Subsequently, a 3-hydroxyacyl-CoA dehydrogenase catalyzes the NAD^+-dependent oxidation of 3-hydroxyacyl-CoA to 3-oxoacyl-CoA (Schomburg and Stephan, 1995). The final chain shortening reaction is catalyzed by a 3-oxoacyl-CoA thiolase cleaving 3-oxoacyl-CoA to yield acetyl-CoA and a shortened $acyl_{n-2}$-CoA (Fig. 1), which can be further processed in subsequent β-oxidation cycles (Schomburg and Stephan, 1996). Released acetyl-CoA is metabolized in the citric acid cycle.

1.2. β-Oxidation-like strategies enable degradation of aliphatic and aromatic compounds

The mechanism of β-oxidation for the purpose of carbon chain-shortening is quite common in nature, not only in the context of fatty

* Correspondence to: Institut für Bio- und Geowissenschaften IBG-1: Biotechnologie, Forschungszentrum Jülich GmbH, 52425 Jülich, Germany.
E-mail address: j.marienhagen@fz-juelich.de (J. Marienhagen).

http://dx.doi.org/10.1016/j.ymben.2017.05.004
Received 19 February 2017; Received in revised form 28 April 2017; Accepted 22 May 2017
Available online 23 May 2017

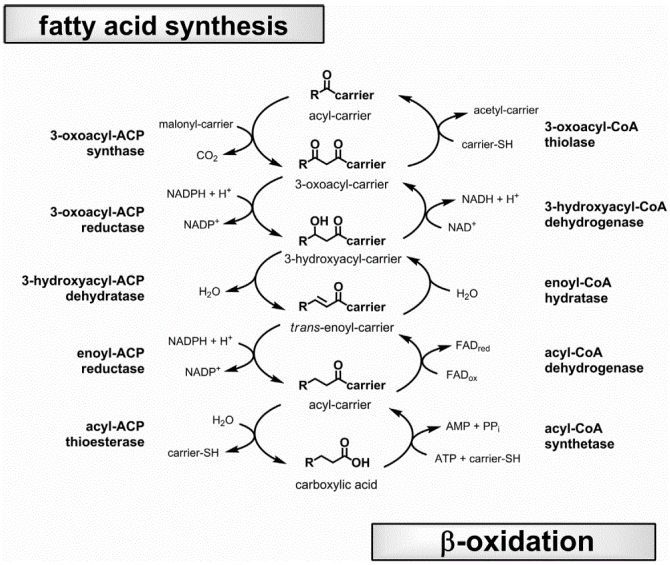

Fig. 1. Fatty acid synthesis and β-oxidation. One cycle of acyl chain elongation during the fatty acid synthesis pathway or acyl chain shortening by β-oxidation is shown. The acyl-carrier protein (ACP) and coenzyme A (CoA) are the respective carriers during fatty acid synthesis and β-oxidation, respectively. R represents a non-branched aliphatic carbon chain (= $(CH_2)_n$-CH_3).

acid catabolism (Fig. 2A), but also for the degradation of aliphatic and aromatic compounds. Phenylacetic acid is an aromatic compound derived from L-phenylalanine (Schneider et al., 1997). The aerobic degradation pathway for phenylacetic acid found in *Escherichia coli* leads to the formation of acetyl-CoA and 2,3-dehydroadipyl-CoA (a *trans*-enoyl-CoA) as intermediate, which undergoes β-oxidation including hydration, oxidation and thiolytic cleavage leading to succinyl-CoA and acetyl-CoA (Teufel et al., 2010) (Fig. 2B). Subsequently, both CoA-activated compounds are channeled into the citric acid cycle for further metabolization. In a similar manner, the dicarboxylic acid adipic acid is degraded in *Acinetobacter baylyi* (formerly *Acinetobacter sp.* ADP1) (Parke et al., 2001) (Fig. 2B). However, two preceding steps for CoA-activation of adipic acid and introduction of the double bond yielding 2,3-dehydroadipyl-CoA are required. Subsequent reaction steps for conversion of 2,3-dehydroadipyl-CoA to succinyl-CoA and acetyl-CoA are identical in *E. coli* and *A. baylyi*.

β-Oxidative chain-shortening reactions are also responsible for the aerobic microbial degradation of phenylpropanoids such as *p*-coumaric acid, which represent prominent plant-derived aromatic compounds (de Sousa, 2014) (Fig. 2C). A common CoA-dependent, β-oxidative degradation pathway for conversion of phenylpropanoids into benzoic acids was characterized in the soil-inhabiting bacteria *Rhodococcus jostii* RHA1, *Azoarcus sp.* EbN1 (inofficial designation "*Aromatoleum aromaticum*") and more recently also in *Corynebacterium glutamicum* (Kallscheuer et al., 2016b; Otani et al., 2014; Trautwein et al., 2012). In *Azoarcus* sp. EbN1 the final 3-oxoacyl-CoA thiolase-catalyzed chain-shortening step in the phenylpropanoid degradation pathway yields 4-hydroxybenzoyl-CoA and acetyl-CoA from *p*-coumaric acid (Trautwein et al., 2012). In contrast, in *R. jostii* and *C. glutamicum*, a ketohydrolase was found to catalyze the ultimate step yielding 4-hydroxybenzoic acid and acetyl-CoA (Kallscheuer et al., 2016b; Otani et al., 2014). 4-Hydroxybenzoic acid is hydroxylated to protocatechuic acid, which is then aerobically degraded by the β-ketoadipate pathway. The ultimate step in the β-ketoadipate pathway of *R. jostii* and *C. glutamicum* is the thiolytic cleavage of 3-oxoadipyl-CoA yielding succinyl-CoA and acetyl-CoA (Fig. 2) (Patrauchan et al., 2005; Shen and Liu, 2005).

The anaerobic degradation of toluene in *Thauera aromatica* proceeds *via* (*R*)-2-benzylsuccinyl-CoA, which is converted to benzoyl-CoA and succinyl-CoA, also employing a β-oxidative route with the corresponding enoyl-CoA, 3-hydroxyacyl-CoA and 3-oxoacyl-CoA thioesters as intermediates (Leutwein and Heider, 2001) (Fig. 2D). By using one of two different branches of the central anaerobic benzoic acid degradation pathway benzoyl-CoA is further metabolized to pimeloyl-CoA, the CoA-thioester of the C_7 dicarboxylic acid pimelic acid (Harwood et al., 1998). Pimeloyl-CoA in turn is converted to glutaryl-CoA and acetyl-CoA *via* β-oxidation (Fig. 2E). This pathway was investigated in detail *e.g.* in *Rhodopseudomonas palustris* (Harrison and Harwood, 2005). Oxidation of glutaryl-CoA and decarboxylation of the pathway intermediate glutaconyl-CoA lead to the formation of crotonyl-CoA, which undergoes another round of β-oxidation yielding two additional molecules of acetyl-CoA (Harrison and Harwood, 2005) (Fig. 2F). Several strictly anaerobic bacteria such as *Acidaminococcus fermentans* follow the same β-oxidative pathway starting from crotonyl-CoA during the fermentation of L-glutamate using the hydroxyglutarate pathway (Buckel, 2001) (Fig. 2F).

1.3. β-Oxidative pathways are mechanistically and thermodynamically reversible metabolic routes

3-Oxoacyl-CoA thiolases do not only catalyze the final thiolytic cleavage reaction during a typical β-oxidation, but also the reverse reaction: C-C bond formation following a Claisen condensation reaction mechanism (Haapalainen et al., 2006) (Fig. 3A). The simplest reaction is the condensation of two molecules of acetyl-CoA yielding acetoacetyl-CoA (a 3-oxoacyl-CoA). According to a thermodynamic analysis based on literature data, the reaction is endergonic as the change of Gibbs free energy $\Delta G'^{\circ}$ for acetoacetyl-CoA formation is positive ($\Delta G'^{0}$ = + 29.6 kJ/mol) (Dellomonaco et al., 2011) (Fig. 3B). This calculation is in line with the finding that the anabolic (3-oxoacyl-CoA-forming) reaction is thermodynamically unfavorable (Thompson et al.,

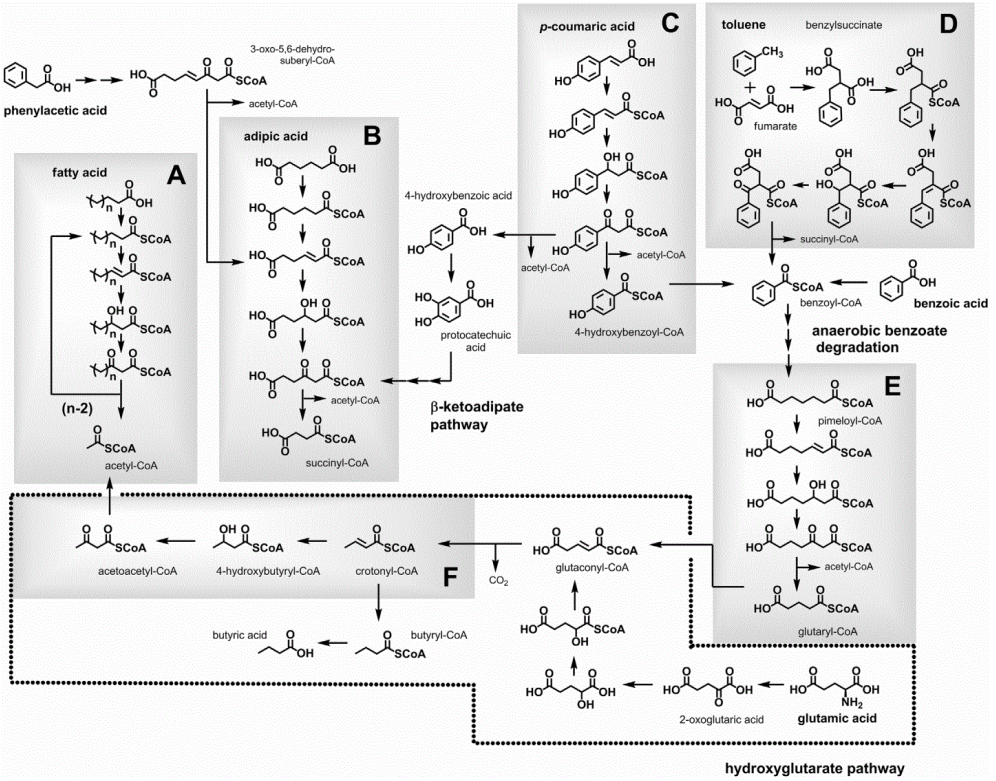

Fig. 2. β-Oxidative degradation pathways for aliphatic and aromatic compounds. β-Oxidation-like pathways are involved in the aerobic and anaerobic catabolism of diverse aliphatic and aromatic compounds including monocarboxylic acids, dicarboxylic acids and amino acids. The β-oxidative routes as part of the depicted degradation pathways are shown in grey. If no compound name is given, the name follows the typical nomenclature of β-oxidation intermediates: acyl-CoA, 2,3-dehydroacyl-CoA, 3-hydroxyacyl-CoA and 3-oxoacyl-CoA, where the affix "acyl-" is replaced by the respective substrate (A: acyl- B: adipyl-, C: *p*-coumaroyl-, D: benzylsuccinyl-, E: pimeloyl-).

1989). It was proposed that the condensation reaction is mainly driven by the excess of substrates and rapid product removal through subsequent conversion of the reaction product (including recycling of released CoA) (Modis and Wierenga, 1999). The following stereospecific NADH-dependent reduction of 3-oxoacyl-CoA to (*S*)-3-hydroxyacyl-CoA and its dehydration to *trans*-enoyl-CoA are reversible reactions (Jiang et al., 1997; Yang et al., 1991) (Fig. 3A). The reduction of the double bond of the *trans*-enoyl-CoA intermediate is catalyzed by FAD-dependent acyl-CoA dehydrogenases (Thorpe and Kim, 1995). Unexpectedly, the *trans*-enoyl-CoA substrate needs to be pulled thermodynamically uphill in the catabolic direction of oxidation (Ghisla and Thorpe, 2004) (Fig. 3B). In consequence, the formation of acyl-CoA in the anabolic direction is expected to be thermodynamically preferred over formation of the *trans*-enoyl-CoA, a notion, which is further supported by thermodynamic *in silico* analyses (Dellomonaco et al., 2011) (Fig. 3B).

The carbon atom C3 in the first intermediate 3-oxoacyl-CoA is in the oxidation state +II. Altogether four electrons supplied by NADH and reduced FAD are required to reduce C3 to the oxidation state -II in acyl-CoA in the anabolic direction (Fig. 3A). The CoA-dependence of such reverse β-oxidative pathways requires an additional step in which the synthesized carboxylic acid is released from CoA. In the natural catabolic direction, AMP-forming acyl-CoA synthetases convert carboxylic acids to their corresponding CoA-thioesters in an enzymatic two-step reaction for initiating β-oxidation (Fig. 1) (Black et al., 1997). Unfortunately, rapid hydrolysis of the side product pyrophosphate to inorganic phosphate renders the CoA-ligation irreversible. Thus, AMP-forming acyl-CoA synthetases cannot be exploited for the release of the carboxylic acid from its CoA-thioester.

Instead, acyl-CoA thioesterases can be used for hydrolysis, thereby releasing the product from CoA (Fig. 1). Alternatively, CoA-transferases or ADP-forming acyl-CoA synthetases can be exploited for catalysis of this reaction step (Selmer and Buckel, 1999). Citric acid cycle enzyme succinyl-CoA synthetases (SCS) from Archaea such as *Thermococcus kodakaraensis* are characterized by a broader substrate spectrum, which can be employed for the production of compounds with medium-chain length (Shikata et al., 2007). Additionally, organisms naturally harboring reverse β-oxidation pathways can serve as source for enzymes catalyzing the acid release from acyl-CoA. Typically, CoA transferases accepting different substrates are found in these organisms, *e.g.* in clostridia (Barker et al., 1978). *E. coli* harbors two acyl-CoA thioesterases, both known to hydrolyze a broad range of acyl-CoA molecules of different chain length (Nie et al., 2008).

Mechanistic and thermodynamical reversibility of β-oxidations enables the exploitation of this metabolic strategy for the microbial

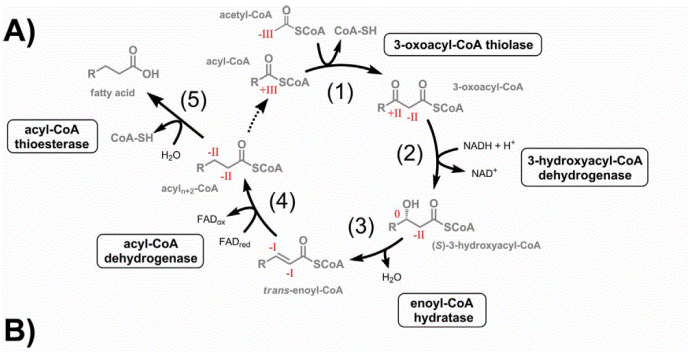

B)

(1)	2 acetyl-CoA → acetoacetyl-CoA + CoA	($\Delta G'^0$ = + 29.6 kJ/mol)
(2)	acetoacetyl-CoA + NADH + H^+ → (S)-3-hydroxybutyryl-CoA + NAD^+	($\Delta G'^0$ = - 4.5 kJ/mol)
(3)	(S)-3-hydroxybutyryl-CoA → crotonyl-CoA + H_2O	($\Delta G'^0$ = + 9.1 kJ/mol)
(4a)	crotonyl-CoA + FAD_{red} → butyryl-CoA + FAD_{ox}	($\Delta G'^0$ = - 88.9 kJ/mol)
(4b)	*crotonyl-CoA + NADH + H^+ → butyryl-CoA + NAD^+*	*($\Delta G'^0$ = - 58.1 kJ/mol)*
(5)	butyryl-CoA + H_2O → *n*-butyrate + CoA	($\Delta G'^0$ = - 31.7 kJ/mol)

Overall reaction:

2 acetyl-CoA + NADH + H^+ + FAD_{red} → *n*-butyrate + 2 CoA + NAD^+ + FAD_{ox}	($\Delta G'^0$ = - 86.5 kJ/mol)
2 acetyl-CoA + 2 NADH + 2 H^+ → *n*-butyrate + 2 CoA + 2 NAD^+	($\Delta G'^0$ = - 55.7 kJ/mol)

Fig. 3. The reverse β-oxidation cycle. A) The five depicted reaction steps and the enzymes responsible for catalysis represent a functional reverse β-oxidation cycle for chain elongation of acyl-CoA with n carbon atoms to a fatty acid with n + 2 carbon atoms. The dashed arrow indicates the possibility of multiple consecutive cycles of reverse β-oxidation-like reactions starting from $acyl_{n+2}$-CoA. Red numbers indicate the oxidation numbers of relevant carbon atoms C2 and C3. B) Reactions and exemplary thermodynamic analysis of the reverse β-oxidation cycle yielding *n*-butyrate from acetyl-CoA (R = CH_3 in figure part A). The Gibbs free energies ($\Delta G'^0$) for the involved reactions were obtained from the BioCyc database. In the β-oxidation cycle, the acyl-CoA dehydrogenase step (4) is typically catalyzed by FAD-dependent enzymes (reaction shown as 4a). In engineered pathways also NAD-dependent enzymes are used for catalysis of this step (shown as 4b). The overall reaction is depicted for both scenarios (with step 4 dependent on reduced FAD or NADH). (For interpretation of the references to color in this figure legend, the reader is referred to the web version of this article.)

production of valuable chemicals. Noteworthy, as a result of the broad range of accepted starter and elongation units, the product spectrum is not restricted to naturally occurring compounds. In addition, novel and non-natural fermentative products can be synthesized (Cheong et al., 2016) rendering reversal of β-oxidative pathways a promising alternative strategy over existing metabolic engineering approaches. Accessible products include monocarboxylic acids and alcohols (Section 2.1), dicarboxlic acids (Section 2.2), aromatic compounds (Section 2.3) and polyhydroxyalkanoates (Section 2.4).

2. Reversal of β-oxidative routes enables the production of valuable compounds

2.1. Monocarboxylic acids and alcohols

β-oxidation is typically recognized as a catabolic strategy during metabolization of fatty acids and aromatic compounds. Interestingly, naturally-occurring reverse β-oxidative pathways are also known for a long time. Already in 1886, caproic acid (hexanoic acid) was identified as a major fermentation product obtained from ethanol in natural open cultures (Béchamp, 1868; Barker and Taha, 1942), although the underlying pathways were not known at that time. Strictly anaerobic bacteria such as *Clostridium acetobutylicum* produce *n*-butanol from butyryl-CoA, which is obtained from acetyl-CoA by one round of reverse β-oxidation (Hartmanis and Gatenbeck, 1984). Current knowledge of naturally occurring reversed β-oxidation pathways has been reviewed recently (Angenent et al., 2016).

Inspired by nature, several microbial production strains for a broad range of interesting small molecules were developed in the last years, which take advantage of this metabolic strategy (Table 1). An incomplete reversal of β-oxidation with CoA-release from intermediates enables the production of 3-oxo-, 3-hydroxy- or α,β-unsaturated carboxylic acids (Fig. 4). In addition, the acyl-CoA intermediate can be also reduced to yield *n*-alcohols, or the (final) carboxylic acid can be further oxidized to ω-hydroxyacids or dicarboxylic acids (Fig. 4).

In the first study, *E. coli* was engineered for the production of *n*-butanol from glucose *via* acetyl-CoA by following one round of reverse β-oxidation initially yielding butyryl-CoA and subsequent reduction of this compound to *n*-butanol (Dellomonaco et al., 2011). To this end, the host genome was modified to obtain an *E. coli* strain in which the expression of genes involved in β-oxidation is no longer regulated by the catabolite repressor Crp, the global regulator ArcA, the acetoacetate metabolism regulatory protein AtoC and the fatty acid metabolism regulator protein FadR. This extensive deregulation of gene expression resulted in the constitutive expression of genes coding for the native β-oxidation enzymes in *E. coli*. In addition, competing pathways consuming acetyl-CoA and ultimately leading to the production of acetate, ethanol and succinate were abolished. No production of *n*-butanol was detected due to a missing enzymatic activity for the alcohol-forming reaction, while the native 3-oxoacyl-CoA thiolase activity was also assumed to be rate-limiting during production. Thus, the strain was further engineered for the overexpression of native *yqeF* and *fucO* genes coding for acetoacetyl-CoA thiolase (pathway initiation) and L−1,2-propanediol oxidoreductase (for conversion of butyraldehyde to *n*-butanol), respectively. This allowed for the production of 14 g/L *n*-butanol in bioreactor cultivations with a yield of 0.33 g *n*-butanol per g glucose. Gene knockout and gene complementation experiments showed that YqeF (acetoacetyl-CoA thiolase), FadB (3-hydroxyacyl-CoA dehydrogenase / enoyl-CoA hydratase) and YdiO (putative acyl-CoA dehydrogenase) mainly catalyze reactions of the reverse β-oxidation cycle up to the level of butyryl-CoA in this strain. Very recently, an engineered *E. coli* strain expressing heterologous genes from *Ralstonia eutropha* (also known as *Cupriavidus necator or Alcaligenes eutrophus*), *Treponema denticola* and *Aeromonas caviae* produced up to 12.3 g/L butyrate under optimized conditions in a bioreactor (Kataoka et al., 2017).

In principle, multiple cycles of reverse β-oxidation would give access to acyl-CoA molecules of different chain length. For such a

Table 1
Production of chemicals and biopolymers by reversed β-oxidative pathways in engineered microorganisms. In all published studies acetyl-CoA served as elongation unit.

Carbon source	Priming CoA ester	Final product	host organism	Cultivation strategy	Titer (g/L)	Reference
monocarboxylic acids						
glycerol	acetyl-CoA	butyric acid	*E. coli*	shaking flask	3.4	Clomburg et al. (2012)
glucose	acetyl-CoA	butyric acid	*E. coli*	fermenter	12.3	Kataoka et al. (2017)
glycerol	butyryl-CoA	hexanoic acid	*E. coli*	shaking flask	0.5	Clomburg et al. (2015)
glycerol	hexanoyl-CoA	octanoic acid	*E. coli*	shaking flask	0.16	Clomburg et al. (2015)
glycerol	octanoyl-CoA	decanoic acid	*E. coli*	shaking flask	0.34	Clomburg et al. (2015)
n-alcohols						
CO_2	acetyl-CoA	*n*-butanol	*S. elongatus*	shaking flask	0.01	Lan and Liao (2011)
glucose	acetyl-CoA	*n*-butanol	*S. cerevisiae*	shaking flask	0.02	Krivoruchko et al. (2013)
glucose	acetyl-CoA	*n*-butanol	*S. cerevisiae*	shaking flask	0.02	Lian and Zhao (2014)
glycerol	actetyl-CoA	*n*-butanol	*E. coli*	shaking flask	0.8	Kim et al. (2015)
glucose	acetyl-CoA	*n*-butanol	*E. coli*	shaking flask	2.2	Dellomonaco et al. (2011)
glucose	acetyl-CoA	*n*-butanol	*E. coli*	shaking flask	6.5	Dekishima et al. (2011)
glucose	acetyl-CoA	*n*-butanol	*E. coli*	fermenter	14.0	Dellomonaco et al. (2011)
glucose	butyryl-CoA	*n*-hexanol	*E. coli*	shaking flask	0.05	Dekishima et al. (2011)
glycerol	butyryl-CoA	*n*-hexanol	*E. coli*	shaking flask	0.2	Kim et al. (2015)
glycerol	hexanoyl-CoA	*n*-octanol	*E. coli*	shaking flask	0.06	Kim et al. (2015)
glycerol	octanoyl-CoA	*n*-decanol	*E. coli*	shaking flask	0.04	Kim et al. (2015)
dicarboxylic acids						
glucose	succinyl-CoA	adipic acid	*E. coli*	shaking flask	1×10^{-5}	Babu et al. (2015)
glucose	succinyl-CoA	adipic acid	*E. coli*	shaking flask	6×10^{-4}	Yu et al. (2014)
glucose	succinyl-CoA	adipic acid	*E. coli*	shaking flask	0.04	Kallscheuer et al. (2016a)
glycerol	butyryl-CoA	adipic acid	*E. coli*	shaking flask	0.2	Clomburg et al. (2015)
glycerol	succinyl-CoA	adipic acid	*E. coli*	shaking flask	0.4	Cheong et al. (2016)
glucose	succinyl-CoA	adipic acid	*T. fusca*	shaking flask	2.2	Deng and Mao (2015)
glycerol	succinyl-CoA	adipic acid	*E. coli*	fermenter	2.5	Cheong et al. (2016)
glycerol	hexanoyl-CoA	suberic acid	*E. coli*	shaking flask	0.3	Clomburg et al. (2015)
glycerol	octanoyl-CoA	sebacic acid	*E. coli*	shaking flask	0.06	Clomburg et al. (2015)
ω-hydroxy acids						
glycerol	butyryl-CoA	6-hydroxyhexanoic acid	*E. coli*	shaking flask	0.3	Cheong et al. (2016)
glycerol	glutaryl-CoA	7-hydroxyhepatanoic acid	*E. coli*	shaking flask	0.09	Cheong et al. (2016)
glycerol	hexanoyl-CoA	8-hydroxyoctanoic acid	*E. coli*	shaking flask	0.1	Clomburg et al. (2015)
glycerol	octanoyl-CoA	10-hydroxydecanoic acid	*E. coli*	shaking flask	0.08	Clomburg et al. (2015)
aromatic compounds						
glycerol	phenylacetyl-CoA	4-phenylbutyric acid	*E. coli*	shaking flask	0.2	Cheong et al. (2016)
glucose	4-hydroxybenzoyl-CoA	resveratrol	*C. glutamicum*	shaking flask	0.005	Kallscheuer et al. (2016c)
polyhydroxyalkanoates						
xylose	acetyl-CoA	polyhydroxybutyrate	*S. cerevisiae*	shaking flask	0.1	Sandström et al. (2015)
glucose	acetyl-CoA	polyhydroxybutyrate	*E. coli*	shaking flask	6.8	Lin et al. (2015)
glucose	acetyl-CoA	polyhydroxybutyrate	*E. coli*	fermenter	35.9	Lin et al. (2015)

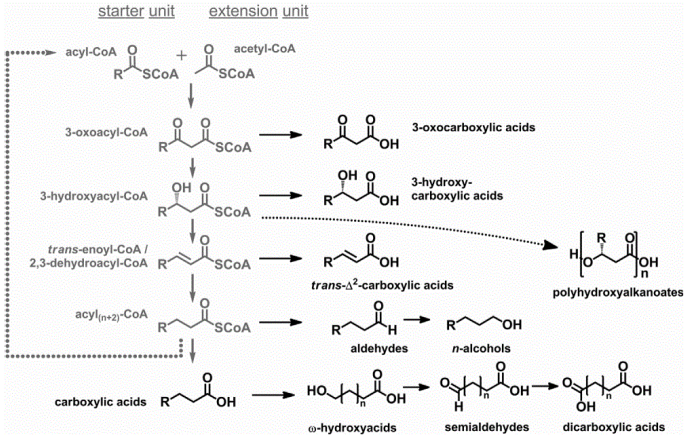

Fig. 4. Product classes accessible through reverse β-oxidative pathways. Several different functionalized molecules can be derived from reverse β-oxidation pathways converting different CoA-activated starter units and acetyl-CoA as extension unit(s). The products are formed *via* hydrolysis of pathway intermediates or by further conversion of the resulting fatty acids. 3-hydroxyacyl-CoA can also serve as building block for the production of polyhydroxyalkanoates.

purpose, other acyl-CoA thioesterases with different substrate specificities were evaluated. Indeed, accumulation of long-chain fatty acids (C_{12}, C_{14}, C_{16}, C_{18}) and medium-chain alcohols (C_6, C_8, C_{10}), all characterized by an even numbers of carbon atoms, could be detected in the engineered *E. coli* strains (Dellomonaco et al., 2011). In contrast, supplementation of propionic acid as alternative starting molecule resulted in the accumulation of medium-chain *n*-alcohols, all with an odd numbers of carbon atoms (C_5, C_7, C_9, each between 100 and 200 mg/L). However, when supplementing propionic acid also *n*-alcohols with an even numbers of carbon atoms could be also detected (C_6, C_8, C_{10}, each below 15 mg/L) due to the presence of acetyl-CoA. An increase in the production of medium-chain fatty acids could be achieved by additional modification of already existing *E. coli* producer strains (Kim et al., 2015).

Based on the functional pathway for *n*-butanol production, additional enzymes were evaluated in *E. coli* with the aim to produce *n*-hexanol using two consecutive reverse β-oxidation cycles starting from acetyl-CoA (Dekishima et al., 2011). Expression of heterologous genes coding for the 3-oxoacyl-CoA thiolase BktB from *R. eutropha*, the 3-hydroxybutyrate dehydrogenase Hbd, the crotonase Crt (both from *C. acetobutylicum*) and the enoyl-CoA reductase Ter from *Euglena gracilis* enabled the synthesis of hexanoyl-CoA from altogether three molecules of acetyl-CoA. The aldehyde/alcohol dehydrogenase AdhE2 from *C. acetobutylicum* turned out to be suitable for converting the obtained hexanoyl-CoA to *n*-hexanol (Dekishima et al., 2011). However, whereas the maximal obtained titers of *n*-butanol of 6.5 g/L were quite high, only trace amounts of up to 0.05 g/L *n*-hexanol could be obtained (Dekishima et al., 2011). Although AdhE2 was shown to have a considerable activity with hexanoyl-CoA, butyryl-CoA was identified as the most suitable substrate for this particular enzyme (Dekishima et al., 2011). This explains the increased production of *n*-butanol (obtained from butyryl-CoA, the product of the first elongation cycle) over *n*-hexanol (produced from hexanoyl-CoA obtained from the second elongation cycle).

In principle, multiple rounds of chain elongation and reverse β-oxidation allow for the production of functionalized compounds with the desired chain length. This often requires coupling of the chain elongation pathway to downstream pathways for further conversion of the resulting acyl-CoA molecules. In any downstream pathway, highly specific enzymes should be employed to avoid by-product formation as a result of a conversion of short-chain acyl-CoA molecules from the early elongation cycles.

Saccharomyces cerevisiae was also engineered for the production of *n*-butanol and fatty acids by reversal of β-oxidative pathways (Krivoruchko et al., 2013; Lian and Zhao, 2014). Although the assembled pathway was functional, the obtained maximal *n*-butanol titer of 20 mg/L was much lower in comparison to the product titer achieved with engineered *E. coli* strains (Dellomonaco et al., 2011). Lower production in *S. cerevisiae* might be related to the compartmentalization as the required heterologous enzymes of the reversed β-oxidation pathway for *n*-butanol production from acetyl-CoA are located in the cytosol. In contrast, acetyl-CoA is mainly synthesized in the mitochondria in *S. cerevisiae* and this organism simply lacks a machinery for the export of acetyl-CoA from the mitochondria to the cytosol (Strijbis and Distel, 2010). Therefore the major source of acetyl-CoA in the cytosol is CoA-activation of acetate by an acetyl-CoA synthetase consuming two ATP equivalents for each acetyl-CoA molecule formed (Lian and Zhao, 2014).

n-Butanol production could be also achieved from CO_2 in engineered photoautotrophic bacteria using the established β-oxidative core pathway starting from acetyl-CoA (Lan and Liao, 2011). To this end, the heterologous genes *hbd*, *crt* and *adhE2* required for *n*-butanol production in *C. acetobutylicum* in combination with *atoB* (coding for 3-oxoacyl-CoA thiolase) from *E. coli* were integrated into the genome of the cyanobacterium *Synechococcus elongatus*. The genes were organized as a tetracistronic operon under control of the inducible *lac* promoter. In clostridia, the butyryl-CoA dehydrogenase Bcd catalyzes the required reduction of crotonyl-CoA to butyryl-CoA. This reaction is coupled to ferredoxins involving the electron-transfer flavoprotein EtfAB (Li et al., 2008). With the aim to by-pass the need for EtfAB and ferredoxins in recombinant *S. elongatus*, the gene *ter* coding for an NADH-dependent *trans*-enoyl-CoA reductase from *T. denticola* was expressed. Increased stability of Ter was achieved by fusion with an N-terminal His-tag. The best-performing strain was capable of accumulating up to 13 mg/L *n*-butanol from CO_2 (Lan and Liao, 2011).

In order to determine the characteristics and constraints for the production of different carboxylic acids, *n*-alcohols (and alkanes) by reverse β-oxidation in *E. coli* an *in silico* analysis was conducted (Cintolesi et al., 2014). It turned out that abolishment of native fermentative pathways in *E. coli* enables coupling of production to cell growth, which maximizes the production with regard to production rate, titer and yield. Based on the *in silico* analysis reversal of β-oxidation was recognized to be superior over alternative metabolic routes (fatty acid synthesis, 2-oxo acid pathways), which are limited by energetic or redox constraints. By simulating the combination of different priming units and termination pathways during the performed analysis, a broad range of potential products of reverse β-oxidative pathways was identified (Cintolesi et al., 2014).

2.2. Dicarboxylic acids

The established reverse β-oxidation core pathway can be combined with ω-oxidation pathways for the production of dicarboxylic acids. During ω-oxidation, the carbon atom most distant from the carboxyl group of the fatty acid is hydroxylated. The resulting alcohol is further oxidized to the corresponding aldehyde or to the carboxylic acid giving rise to either semialdehydes or dicarboyxlic acids (Fig. 4). In *E. coli*, coupling the activity of the ω-hydroxylase AlkBGT of the alkane monooxygenase system of *Pseudomonas putida* with an aldehyde dehydrogenase and an alcohol dehydrogenase from *Acinetobacter* sp. enabled the production of medium-chain ω-hydroxy acids and dicarboxylic acids in the scale of 0.5 – 0.8 g/L from glycerol (Clomburg et al., 2015). One of the products, the C_6 dicarboxylic acid adipic acid, is an important chemical building block for the synthesis of the polymer nylon-6,6 and several strategies for the sustainable production of adipic acid exist (Bart and Cavallaro, 2015; Deng et al., 2016; Polen et al., 2013).

Interestingly, a second metabolic design for the microbial production of adipic acid, different from the ω-oxidation pathway just described, turned out to be successful too. This strategy, also including a β-oxidative pathway, is based on the last steps of the phenylacetic acid degradation pathway of *E. coli*, which ultimately yields succinyl-CoA and acetyl-CoA (Teufel et al., 2010) (Fig. 2). Here, three enzymes of the phenylacetate catabolic pathway, namely PaaZ (3-oxoadipyl-CoA thiolase), PaaH (3-hydroxyadipyl-CoA dehydrogenase) and PaaF (2,3-dehydroadipyl-CoA hydratase) were combined with the broad-spectrum enoyl-CoA reductases Ter from *E. gracilis* or Bcd from *C. acetobutylicum* (Yu et al., 2014). For product release, adipyl-CoA was first converted to adipyl-phosphate by the phosphate butyryltransferase Ptb from *C. acetobutylicum* and subsequently dephosphorylated by the butyrate kinase Buk1 originating from the same organism. However, only low adipic acid titers of 0.6 mg/L could be obtained when following this metabolic strategy (Yu et al., 2014). The observed low product titer can most likely be attributed to the employed enzymes showing only limited activity with the pathway intermediates. This is in particular true for Ter from *E. gracilis*, which was shown to mainly convert *trans*-enoyl-CoA molecules derived from monocarboxylic acids (Hoffmeister et al., 2005). Probably, this enzyme was assumed to be suitable for adipic acid production based on the similarity of 2,3-dehydroadipyl-CoA to the accepted substrate *trans*−2-hexenoyl-CoA but an enzymatic activity with 2,3-dehydroadipyl-CoA could never be experimentally confirmed. Recently, other enzymes for adipate production by reverse β-oxidation were tested, which increased the obtained product titer of an

engineered *E. coli* strain to 36 mg/L (Kallscheuer et al., 2016a). The reversed β-oxidative pathway yielding adipate from succinyl-CoA was also identified in a retro-synthetic approach aiming at producing the nylon precursor caprolactam (Turk et al., 2015). *E. coli* strains with increased production of succinate and abolished pathways for acetate and lactate formation enabled the production of 2.5 g/L adipate from glycerol in a bioreactor (Cheong et al., 2016).

A β-oxidative degradation pathway for adipic acid is present in the thermophilic *Thermobifida fusca* B6 (Deng and Mao, 2015). Hence, overexpression of the adipyl-CoA dehydrogenase gene Tfu_1647 in the genetic background of a wild-type strain was already sufficient to enable the production of 2.2 g/L adipic acid from 50 g/L glucose. The final conversion step of adipyl-CoA to adipic acid in *T. fusca* is catalyzed by an ADP-dependent succinyl-CoA synthetase with broad substrate spectrum (Deng and Mao, 2015). Typically, acyl-CoA thioesterases were used for cleaving adipyl-CoA to yield adipic acid. However, when hydrolyzed, the energy of the energy-rich thioester bond of adipyl-CoA cannot be conserved. In contrast, if catalyzed by an ADP-dependent CoA-synthetase, product release could be coupled to ATP-generation, thereby conserving the energy of the thioester. Feasibility of this approach could be successfully demonstrated *in vitro* for the succinyl-CoA synthetase from the hyperthermophilic Archaea *T. kodakarensis* (Shikata et al., 2007). In *in vitro* enzyme assays, this heterodimeric enzyme was found to catalyze the reversible interconversion of adipyl-CoA and adipic acid and concomitant ATP formation could be detected.

2.3. Aromatic compounds

When aromatic CoA-thioesters serve as priming units for reverse β-oxidation pathways, chain elongation reactions also enable the synthesis of functionalized aromatic compounds. In *E. coli*, phenylacetyl-CoA as first intermediate of the phenylacetate degradation pathway served as substrate for one and two rounds of chain-elongation leading to the production of 4-phenylbutyric acid and 6-phenylhexanoic acid, respectively (Cheong et al., 2016). Titers of 180 mg/L 4-phenylbutyric acid and 50 mg/L 6-phenylhexanoic acid could be achieved. Release of the products from their corresponding CoA thioesters was catalyzed by unknown, endogenous enzymes, most likely CoA-transferases or acyl-CoA thioesterases of *E. coli*. In *C. glutamicum*, 4-hydroxybenzoic acid was used as a precursor to demonstrate production of CoA-activated phenylpropanoids (Kallscheuer et al., 2016c). This was achieved by the functional integration of a β-oxidative degradation pathway for phenylpropanoids originating from *Azoarcus* sp. EbN1 (Fig. 2C). In *Azoarcus* sp. EbN1 this pathway degrades the phenylpropanoid *p*-coumaric acid yielding 4-hydroxybenzoyl-CoA and acetyl-CoA (Trautwein et al., 2012). The corresponding genes from *Azoarcus* sp. EbN1 were expressed in an engineered *C. glutamicum* strain, which is devoid of catabolic pathways involved in the degradation of aromatic compounds (Kallscheuer et al., 2016d). *p*-Coumaroyl-CoA, produced from supplemented 4-hydroxybenzoic acid by this strategy, served as direct precursor for the synthesis of the plant stilbene resveratrol. This synthetic pathway represents a novel approach towards synthesis of valuable plant polyphenols since plants exclusively synthesize such compounds starting from aromatic amino acids (Marienhagen and Bott, 2013).

2.4. Polyhydroxyalkanoates

In carbon-rich environments with simultaneous limitation of nitrogen or phosphate, some bacteria store carbon and energy in form of polyhydroxyalkanoates (Pötter and Steinbüchel, 2005; Quelas et al., 2016). These compounds aggregate in the cytosol and form insoluble granules, which can make up to 96% of the cell dry weight (Fukui and Doi, 1997). The production of polyhydroxybutyrate (PHB) has been extensively studied in the facultative autotrophic hydrogen-oxidizing ("Knallgas") bacterium *R. eutropha* (Kuchta et al., 2007; Pötter et al., 2004). PHB is polymerized from 3-hydroxybutyryl-CoA units as monomeric building blocks, which in turn are produced *via* an incomplete and reversed β-oxidative pathway starting from acetyl-CoA. Here, chain elongation and subsequent reduction of the 3-oxo group of acetoacetyl-CoA yields 3-hydroxybutyryl-CoA (Budde et al., 2010; Peoples and Sinskey, 1989) (Fig. 4). In *R. eutropha*, the chain elongation reaction catalyzed by the acetoacetyl-CoA thiolase was found to be rate-limiting (Budde et al., 2010). This result is in line with thermodynamic equilibrium proposed for the 3-oxoacyl-CoA thiolase reaction (Modis and Wierenga, 1999). It is likely that the condensation reaction is mainly driven by the excess of acetyl-CoA and constant removal of acetoacetyl-CoA upon reduction yielding 3-hydroxybutyryl-CoA and its further polymerization to PHB.

To enable production of PHB in microbes, various strategies were followed focusing mainly on using waste materials as carbon and energy sources (da Cruz Pradella et al., 2012; Koutinas et al., 2007; Verlinden et al., 2011). In the course of these studies *E. coli* and *S. cerevisiae* were engineered for production of PHB by functional integration of heterologous production pathways. In engineered *E. coli*, accumulation of up to 36 g/L PHB could be detected during bioreactor cultivations whereas the production in *S. cerevisiae* reached the scale of 100 mg/L (Lin et al., 2015; Sandström et al., 2015). Due to the broad substrate specificity of the tested polyhydroxyalkanoate synthases, incorporation of different 3-hydroxyacyl-CoA thioesters, either obtained during the degradation of fatty acids or from chain elongation of propionyl-CoA, was possible (Antonio et al., 2000; Luo et al., 2006). In this context, already established reversed β-oxidative pathways providing different CoA-activated thioesters allowed for the synthesis of polyhydroxyalkanoates with new properties (Aldor and Keasling, 2003; Chen et al., 2015; Wang et al., 2014).

3. Are reversed β-oxidative pathways competitive to alternative metabolic strategies?

For the production of mono- and dicarboxylic acids and derived compounds thereof, three different metabolic strategies can be pursued: α-reduction, reversal of β-oxidation (coupled to ω-oxidation for dicarboxylic acid production), or "classical" fatty acid synthesis.

Adipic acid is a suitable example for comparing the tested metabolic strategies for chain elongation as biosynthesis of this dicarboxylic acid is accessible *via* α-reduction and reverse β-oxidation. Adipate production starting from succinyl-CoA by reverse β-oxidation was already described earlier (Section 2.2). A proposed α-reductive pathway for adipate production is based on the α-aminoadipate pathway, the metabolic route to L-lysine in fungi (Xu et al., 2006). The pathway intermediate 2-oxoadipate can be obtained from 2-oxoglutarate and acetyl-CoA *via* homocitrate and homoisocitrate as intermediates. For subsequent conversion of 2-oxoadipate to adipate, a CoA-dependent, α-reductive pathway needs to be established. Suitable enzymes for almost all required reaction steps could be already identified (Parthasarathy et al., 2011). The most critical reaction with regard to the reaction mechanism is the dehydration of 2-hydroxyadipyl-CoA to 2,3-dehydroadipyl-CoA as this step requires the elimination of the non-acidic proton at the C3 position. Despite the mechanistic challenge, the enzyme 2-hydroxyglutaryl-CoA dehydratase from *Clostridium symbiosum* was found to be able to catalyze this reaction (Parthasarathy et al., 2011). Whereas microbial production of adipic acid from 2-oxoadipate has not been reported yet, glutaconate (2,3-dehydroglutarate) could be already produced from 2-oxoglutarate by a heterologous α-reductive pathway in *E. coli* (Djurdjevic et al., 2011). Typically, 2-oxo acids are obtained from transamination of amino acids. Before a corresponding α-reductive pathway can be used for production purposes suitable enzymes required for reduction of the 2-oxo group (α-reduction) need to be identified. A recent example for cinnamic acid production from phenylpyruvate (the transamination product of L-phenylalanine) shows that in principle such a pathway can be functionally implemented (Masuo et al., 2016). Still, the expected product spectrum is restricted

to compounds containing the identical residues as present in natural amino acids. Moreover, natural biosynthesis pathways for amino acids branch off from distinct metabolites of the central carbon metabolism. In contrast, reversed β-oxidation pathways start from different acyl-CoA starter units plus acetyl-CoA. This highly facilitates engineering of the microbial host metabolism towards precursor supply. Due to an easy standardization and modularization of a reverse β-oxidation pathway it can be regarded as the more flexible metabolic strategy.

In the recent years, huge effort was put into metabolic engineering of microorganisms towards the production of free fatty acids by manipulation of the endogenous fatty acid synthesis and degradation machinery with simultaneous expression of heterologous genes coding for acyl-ACP thioesterases (Li et al., 2012; Liu et al., 2010; Steen et al., 2010). As fatty acid synthesis follows an iterative cycle catalyzed by the FAS complex, the directed synthesis of one specific product is highly challenging. In most cases, microbial production yields a complex mixture of saturated and unsaturated fatty acids with a chain length of 14–18 carbon atoms (Lu et al., 2008; Zhang et al., 2011). For chain elongation of acyl-ACP, malonyl-CoA is used as extension unit. Malonyl-CoA is produced by ATP-dependent carboxylation of acetyl-CoA and was shown to be the major rate-controlling enzyme of the fatty acid synthesis pathway both in *E. coli* and *S. cerevisiae* (Davis et al., 2000; Schneiter et al., 2000). In contrast, the non-decarboxylative Claisen condensation reaction for chain elongation catalyzed by 3-oxoacyl-CoA thiolases directly consumes acetyl-CoA as extension unit. Thus, application of reverse β-oxidation pathways circumvents the energy-consuming carboxylation step of acetyl-CoA. In consequence, reverse β-oxidation enables production at maximum carbon and energy efficiency.

Thermodynamic analyses revealed that the rate-limiting reaction in reverse β-oxidation pathways is likely to be the 3-oxoacyl-CoA thiolase-catalyzed chain elongation of the starter acyl-CoA molecule. However, it was proposed that this thermodynamically unfavorable condensation reaction can be efficiently driven by a large substrate excess (“push”) and fast product removal (“pull”) (Modis and Wierenga, 1999). Indeed, the established pathway for the production of polyhydroxyalkanoates in *R. eutropha* demonstrates that this potential bottleneck can be overcome (Khanna and Srivastava, 2005).

4. Conclusions

The enzymes of the β-oxidation pathway for degradation of fatty acids accept substrates with a chain length of up to 18 carbon atoms. This “flexibility” is prerequisite for the iterative degradation of long-chain fatty acids to acetyl-CoA units and also enables the production of a broad range of different industrially interesting compounds when employing this pathway in the anabolic direction. However, as a direct consequence, production of individual compounds is a major challenge when employing such pathways. Often, the chain elongation pathway is coupled to downstream pathways for production of functionalized compounds such as *n*-alcohols or dicarboxylic acids. In such cases, highly specific enzymes in the downstream pathways should be used to avoid formation of undesired by-products.

Very recently, it could be demonstrated that propionyl-CoA and glycolyl-CoA can also serve as elongation units in reverse β-oxidation pathways in addition to acetyl-CoA. Combination of these diverse elongation units with different priming units allowed the production of 18 different compounds from ten different product classes (Cheong et al., 2016). Some of these products are non-natural, meaning that they cannot be produced by any endogenous pathways in microorganisms. This interesting aspect renders reversal of β-oxidation a unique production strategy for such compounds.

Although reversed β-oxidative pathways are superior to other known pathways in terms of energy and reduction equivalent consumption, obtained product titers are much lower. Possible strategies for improving overall product titers include additional engineering of the microbial host strains, *e.g.* by selecting and combining more suitable (codon-optimized) heterologous genes or fine-tuning of gene expression (van Summeren-Wesenhagen et al., 2015). Acetyl-CoA, which serves as elongation unit during reversed β-oxidative pathways is a key metabolite in the cellular carbon metabolism. Therefore, endogenous pathways subtracting this metabolite have to controlled for increasing flux towards the desired product(*s*). Non-decarboxylative chain elongation of the acyl-CoA catalyzed by 3-oxoacyl-CoA thiolases was identified to be thermodynamically unfavorable in the anabolic direction. Hence, future engineering of the host strain could focus on the overproduction of acyl-CoA and acetyl-CoA as substrates of this enzyme. In combination with measures for a fast removal of the product 3-oxoacyl-CoA by subsequent reaction steps and efficient recycling of released CoA, this would drastically increase the flux in the anabolic direction.

Acknowledgments

We would like to thank the European Union Framework Program 7 "BacHBerry" (www.bachberry.eu), Project No. FP7-613793 for financial support.

References

Aldor, I.S., Keasling, J.D., 2003. Process design for microbial plastic factories: metabolic engineering of polyhydroxyalkanoates. Curr. Opin. Biotechnol. 14, 475–483.
Angenent, L.T., Richter, H., Buckel, W., Spirito, C.M., Steinbusch, K.J., Plugge, C.M., Strik, T.B., Grootscholten, T.I.M., Buisman, C.J.N., Hamelers, H.V., 2016. Chain elongation with reactor microbiomes: open-culture biotechnology to produce biochemicals. Environ. Sci. Technol. 50 (6), 2796–2810.
Antonio, R.V., Steinbüchel, A., Rehm, B.H., 2000. Analysis of in vivo substrate specificity of the PHA synthase from *Ralstonia eutropha*: formation of novel copolyesters in recombinant *Escherichia coli*. FEMS Microbiol. Lett. 182, 111–117.
Babu, T., Yun, E.J., Kim, S., Kim, D.H., Liu, K.H., Kim, S.R., Kim, K.H., 2015. Engineering *Escherichia coli* for the production of adipic acid through the reversed β-oxidation pathway. Process Biochem. 50, 2066–2071.
Barker, H.A., Jeng, I.M., Neff, N., Robertson, J.M., Tam, F.K., Hosaka, S., 1978. Butyryl-CoA: acetoacetate CoA-transferase from a lysine-fermenting *Clostridium*. J. Biol. Chem. 253 (4), 1219–1225.
Barker, H.A., Taha, S.M., 1942. *Clostridium kluyverii*, an organism concerned in the formation of caproic acid from ethyl alcohol. J. Bacteriol. 43 (3), 347–363.
Bart, J.C., Cavallaro, S., 2015. Transiting from adipic acid to bioadipic acid. Part II. Biosynthetic pathways. Ind. Eng. Chem. Res. 54, 567–576.
Bartlett, K., Eaton, S., 2004. Mitochondrial β-oxidation. Eur. J. Biochem. 271, 462–469.
Béchamp, M.A., 1868. Lettre de M. A. Béchamp a M. Dumas. Ann. Chim. Phys. 4 (13), 103–111.
Black, P.N., Zhang, Q., Weimar, J.D., DiRusso, C.C., 1997. Mutational analysis of a fatty acyl-coenzyme A synthetase signature motif identifies seven amino acid residues that modulate fatty acid substrate specificity. J. Biol. Chem. 272, 4896–4903.
Buckel, W., 2001. Unusual enzymes involved in five pathways of glutamate fermentation. Appl. Microbiol. Biotechnol. 57, 263–273.
Budde, C.F., Mahan, A.E., Lu, J., Rha, C., Sinskey, A.J., 2010. Roles of multiple acetoacetyl coenzyme A reductases in polyhydroxybutyrate biosynthesis in *Ralstonia eutropha* H16. J. Bacteriol. 192, 5319–5328.
Chen, G.-Q., Hajnal, I., Wu, H., Lv, L., Ye, J., 2015. Engineering biosynthesis mechanisms for diversifying polyhydroxyalkanoates. Trends Biotechnol. 33, 565–574.
Cheong, S., Clomburg, J.M., Gonzalez, R., 2016. Energy-and carbon-efficient synthesis of functionalized small molecules in bacteria using non-decarboxylative Claisen condensation reactions. Nat. Biotechnol. 34, 556–561.
Cintolesi, A., Clomburg, J.M., Gonzalez, R., 2014. In silico assessment of the metabolic capabilities of an engineered functional reversal of the β-oxidation cycle for the synthesis of longer-chain (C≥ 4) products. Metab. Eng. 23, 100–115.
Clomburg, J.M., Blankschien, M.D., Vick, J.E., Chou, A., Kim, S., Gonzalez, R., 2015. Integrated engineering of β-oxidation reversal and ω-oxidation pathways for the synthesis of medium chain ω-functionalized carboxylic acids. Metab. Eng. 28, 202–212.
Clomburg, J.M., Vick, J.E., Blankschien, M.D., Rodríguez-Moya, M., Gonzalez, R., 2012. A synthetic biology approach to engineer a functional reversal of the β-oxidation cycle. ACS Synth. Biol. 1, 541–554.
da Cruz Pradella, J.G., Ienczak, J.L., Delgado, C.R., Taciro, M.K., 2012. Carbon source pulsed feeding to attain high yield and high productivity in poly (3-hydroxybutyrate) (PHB) production from soybean oil using *Cupriavidus necator*. Biotechnol. Lett. 34, 1003–1007.
Davis, M.S., Solbiati, J., Cronan, J.E., 2000. Overproduction of acetyl-CoA carboxylase activity increases the rate of fatty acid biosynthesis in *Escherichia coli*. J. Biol. Chem. 275, 28593–28598.
de Sousa, D.P., 2014. A review on anti-inflammatory activity of phenylpropanoids found in essential oils. Molecules 19, 1459–1480.
Dekishima, Y., Lan, E.I., Shen, C.R., Cho, K.M., Liao, J.C., 2011. Extending carbon chain length of 1-butanol pathway for 1-hexanol synthesis from glucose by engineered

Escherichia coli. J. Am. Chem. Soc. 133, 11399–11401.
Dellomonaco, C., Clomburg, J.M., Miller, E.N., Gonzalez, R., 2011. Engineered reversal of the β-oxidation cycle for the synthesis of fuels and chemicals. Nature 476, 355–359.
Deng, Y., Ma, L., Mao, Y., 2016. Biological production of adipic acid from renewable substrates: current and future methods. Biochem. Eng. J. 105, 16–26.
Deng, Y., Mao, Y., 2015. Production of adipic acid by the native-occurring pathway in *Thermobifida fusca* B6. J. Appl. Microbiol. 119, 1057–1063.
Djurdjevic, I., Zelder, O., Buckel, W., 2011. Production of glutaconic acid in a recombinant *Escherichia coli* strain. Appl. Environ. Microbiol. 77, 320–322.
Fukui, T., Doi, Y., 1997. Cloning and analysis of the poly (3-hydroxybutyrate-co-3-hydroxyhexanoate) biosynthesis genes of *Aeromonas caviae*. J. Bacteriol. 179, 4821–4830.
Ghisla, S., Thorpe, C., 2004. Acyl-CoA dehydrogenases. Eur. J. Biochem. 271, 494–508.
Groot, P., Scholte, H., Hulsmann, W., 1976. Fatty acid activation: specificity, localization, and function. Adv. Lipid Res. 14, 75–126.
Haapalainen, A.M., Meriläinen, G., Wierenga, R.K., 2006. The thiolase superfamily: condensing enzymes with diverse reaction specificities. Trends Biochem. Sci. 31, 64–71.
Harrison, F.H., Harwood, C.S., 2005. The *pimFABCDE* operon from *Rhodopseudomonas palustris* mediates dicarboxylic acid degradation and participates in anaerobic benzoate degradation. Microbiology 151, 727–736.
Hartmanis, M.G., Gatenbeck, S., 1984. Intermediary metabolism in *Clostridium acetobutylicum*: levels of enzymes involved in the formation of acetate and butyrate. Appl. Environ. Microbiol. 47 (6), 1277–1283.
Harwood, C.S., Burchhardt, G., Herrmann, H., Fuchs, G., 1998. Anaerobic metabolism of aromatic compounds via the benzoyl-CoA pathway. FEMS Microbiol. Rev. 22 (5), 439–458.
Hoffmeister, M., Piotrowski, M., Nowitzki, U., Martin, W., 2005. Mitochondrial *trans*-2-enoyl-CoA reductase of wax ester fermentation from *Euglena gracilis* defines a new family of enzymes involved in lipid synthesis. J. Biol. Chem. 280, 4329–4338.
Jiang, L.L., Kurosawa, T., Sato, M., Suzuki, Y., Hashimoto, T., 1997. Physiological role of d-3-hydroxyacyl-CoA dehydratase/d-3-hydroxyacyl-CoA dehydrogenase bifunctional protein. J. Biochem. 121, 506–513.
Kallscheuer, N., Gätgens, J., Lübcke, M., Pietruszka, J., Bott, M., Polen, T., 2016a. Improved production of adipate with *Escherichia coli* by reversal of β-oxidation. Appl. Microbiol. Biotechnol. 1–12.
Kallscheuer, N., Vogt, M., Kappelmann, J., Krumbach, K., Noack, S., Bott, M., Marienhagen, J., 2016b. Identification of the *phd* gene cluster responsible for phenylpropanoid utilization in *Corynebacterium glutamicum*. Appl. Microbiol. Biotechnol. 100, 1871–1881.
Kallscheuer, N., Vogt, M., Marienhagen, J., 2016c. A novel synthetic pathway enables microbial production of polyphenols independent from the endogenous aromatic amino acid metabolism. ACS Synth. Biol. 6 (3), 410–415. http://dx.doi.org/10.1021/acssynbio.6b00291.
Kallscheuer, N., Vogt, M., Stenzel, A., Gätgens, J., Bott, M., Marienhagen, J., 2016d. Construction of a *Corynebacterium glutamicum* platform strain for the production of stilbenes and (2*S*)-flavanones. Metab. Eng. 38, 47–55.
Kataoka, N., Vangnai, A.S., Pongtharangkul, T., Yakushi, T., Matsushita, K., 2017. Butyrate production under aerobic growth conditions by engineered *Escherichia coli*. J. Biosci. Bioeng. http://dx.doi.org/10.1016/j.jbiosc.2016.12.008.
Khanna, S., Srivastava, A.K., 2005. Statistical media optimization studies for growth and PHB production by *Ralstonia eutropha*. Process Biochem. 40, 2173–2182.
Kim, S., Clomburg, J.M., Gonzalez, R., 2015. Synthesis of medium-chain length (C6–C10) fuels and chemicals via β-oxidation reversal in *Escherichia coli*. J. Ind. Microbiol. Biotechnol. 42, 465–475.
Koutinas, A.A., Xu, Y., Wang, R., Webb, C., 2007. Polyhydroxybutyrate production from a novel feedstock derived from a wheat-based biorefinery. Enzym. Microb. Technol. 40, 1035–1044.
Krivoruchko, A., Serrano-Amatriain, C., Chen, Y., Siewers, V., Nielsen, J., 2013. Improving biobutanol production in engineered *Saccharomyces cerevisiae* by manipulation of acetyl-CoA metabolism. J. Ind. Microbiol. Biotechnol. 40, 1051–1056.
Kuchta, K., Chi, L., Fuchs, H., Pötter, M., Steinbüchel, A., 2007. Studies on the influence of phasins on accumulation and degradation of PHB and nanostructure of PHB granules in *Ralstonia eutropha* H16. Biomacromolecules 8, 657–662.
Lan, E.I., Liao, J.C., 2011. Metabolic engineering of cyanobacteria for 1-butanol production from carbon dioxide. Metab. Eng. 13, 353–363.
Leutwein, C., Heider, J., 2001. Succinyl-CoA:(*R*)-benzylsuccinate CoA-transferase: an enzyme of the anaerobic toluene catabolic pathway in denitrifying bacteria. J. Bacteriol. 183, 4288–4295.
Li, F., Hinderberger, J., Seedorf, H., Zhang, J., Buckel, W., Thauer, R.K., 2008. Coupled ferredoxin and crotonyl coenzyme A (CoA) reduction with NADH catalyzed by the butyryl-CoA dehydrogenase/Etf complex from *Clostridium kluyveri*. J. Bacteriol. 190, 843–850.
Li, M., Zhang, X., Agrawal, A., San, K.-Y., 2012. Effect of acetate formation pathway and long chain fatty acid CoA-ligase on the free fatty acid production in *E. coli* expressing acy-ACP thioesterase from *Ricinus communis*. Metab. Eng. 14, 380–387.
Lian, J., Zhao, H., 2014. Reversal of the β-oxidation cycle in *Saccharomyces cerevisiae* for production of fuels and chemicals. ACS Synth. Biol. 4, 332–341.
Lin, Z., Zhang, Y., Yuan, Q., Liu, Q., Li, Y., Wang, Z., Ma, H., Chen, T., Zhao, X., 2015. Metabolic engineering of *Escherichia coli* for poly (3-hydroxybutyrate) production via threonine bypass. Microb. Cell Fact. 14, 1.
Liu, T., Vora, H., Khosla, C., 2010. Quantitative analysis and engineering of fatty acid biosynthesis in *E coli*.. Metab. Eng. 12, 378–386.
Lu, X., Vora, H., Khosla, C., 2008. Overproduction of free fatty acids in *E. coli*: implications for biodiesel production. Metab. Eng. 10, 333–339.
Luo, R., Chen, J., Zhang, L., Chen, G., 2006. Polyhydroxyalkanoate copolyesters produced by *Ralstonia eutropha* PHB^{-4} harboring a low-substrate-specificity PHA synthase PhaC2$_{Ps}$ from *Pseudomonas stutzeri* 1317. Biochem. Eng. J. 32, 218–225.
Marienhagen, J., Bott, M., 2013. Metabolic engineering of microorganisms for the synthesis of plant natural products. J. Biotechnol. 163, 166–178.
Masuo, S., Kobayashi, Y., Oinuma, K.I., Takaya, N., 2016. Alternative fermentation pathway of cinnamic acid production via phenyllactic acid. Appl. Microbiol. Biotechnol. 100 (20), 8701–8709.
Modis, Y., Wierenga, R.K., 1999. A biosynthetic thiolase in complex with a reaction intermediate: the crystal structure provides new insights into the catalytic mechanism. Structure 7, 1279–1290.
Nie, L., Ren, Y., Janakiraman, A., Smith, S., Schulz, H., 2008. A novel paradigm of fatty acid β-oxidation exemplified by the thioesterase-dependent partial degradation of conjugated linoleic acid that fully supports growth of *Escherichia coli*. Biochemistry 47 (36), 9618–9626.
Otani, H., Lee, Y.-E., Casabon, I., Eltis, L.D., 2014. Characterization of *p*-hydroxycinnamate catabolism in a soil Actinobacterium. J. Bacteriol. 196, 4293–4303.
Parke, D., Garcia, M., Ornston, L., 2001. Cloning and genetic characterization of *dca* genes required for β-oxidation of straight-chain dicarboxylic acids in *Acinetobacter* sp. strain ADP1. Appl. Environ. Microbiol. 67, 4817–4827.
Parthasarathy, A., Pierik, A.J., Kahnt, J., Zelder, O., Buckel, W., 2011. Substrate specificity of 2-hydroxyglutaryl-CoA dehydratase from *Clostridium symbiosum*: toward a bio-based production of adipic acid. Biochemistry 50, 3540–3550.
Patrauchan, M.A., Florizone, C., Dosanjh, M., Mohn, W.W., Davies, J., Eltis, L.D., 2005. Catabolism of benzoate and phthalate in *Rhodococcus* sp. strain RHA1: redundancies and convergence. J. Bacteriol. 187, 4050–4063.
Peoples, O.P., Sinskey, A.J., 1989. Poly-beta-hydroxybutyrate biosynthesis in *Alcaligenes eutrophus* H16. Characterization of the genes encoding beta-ketothiolase and acetoacetyl-CoA reductase. J. Biol. Chem. 264, 15293–15297.
Polen, T., Spelberg, M., Bott, M., 2013. Toward biotechnological production of adipic acid and precursors from biorenewables. J. Biotechnol. 167, 75–84.
Pötter, M., Müller, H., Reinecke, F., Wieczorek, R., Fricke, F., Bowien, B., Friedrich, B., Steinbüchel, A., 2004. The complex structure of polyhydroxybutyrate (PHB) granules: four orthologous and paralogous phasins occur in *Ralstonia eutropha*. Microbiology 150, 2301–2311.
Pötter, M., Steinbüchel, A., 2005. Poly (3-hydroxybutyrate) granule-associated proteins: impacts on poly (3-hydroxybutyrate) synthesis and degradation. Biomacromolecules 6, 552–560.
Quelas, J., Mesa, S., Mongiardini, E., Jendrossek, D., Lodeiro, A., 2016. Regulation of polyhydroxybutyrate synthesis in the soil bacterium *Bradyrhizobium diazoefficiens*. Appl. Environ. Microbiol. AEM (00757-16).
Sandström, A.G., Heras, De. Las, Portugal-Nunes, A.M., Gorwa-Grauslund, M. F, D., 2015. Engineering of *Saccharomyces cerevisiae* for the production of poly-3-d-hydroxybutyrate from xylose. AMB Express 5, 1.
Schneider, S., Mohamed, M.-S., Fuchs, G., 1997. Anaerobic metabolism of L-phenylalanine via benzoyl-CoA in the denitrifying bacterium *Thauera aromatica*. Arch. Microbiol. 168, 310–320.
Schneiter, R., Guerra, C.E., Lampl, M., Tatzer, V., Zellnig, G., Klein, H.L., Kohlwein, S.D., 2000. A novel cold-sensitive allele of the rate-limiting enzyme of fatty acid synthesis, acetyl coenzyme A carboxylase, affects the morphology of the yeast vacuole through acylation of Vac8p. Mol. Cell. Biol. 20, 2984–2995.
Schomburg, D., Salzmann, M., 1990. Enoyl-CoA hydratase. Enzyme Handbook 1. Springerpp. 651–656.
Schomburg, D., Stephan, D., 1995. 3-Hydroxyacyl-CoA dehydrogenase. Enzyme Handbook 9. Springerpp. 197–201.
Schomburg, D., Stephan, D., 1996. Acetyl-CoA C-acetyltransferase. Enzyme Handbook 11. Springerpp. 639–644.
Schulz, H., 1991. Beta oxidation of fatty acids. Biochi. Biophys. Acta - Lipids Lipid Metab. 1081, 109–120.
Selmer, T., Buckel, W., 1999. Oxygen exchange between acetate and the catalytic glutamate residue in glutaconate CoA-transferase from *Acidaminococcus fermentans*: implications for the mechanism of CoA-ester hydrolysis. J. Biol. Chem. 274, 20772–20778.
Shen, X., Liu, S., 2005. Key enzymes of the protocatechuate branch of the β-ketoadipate pathway for aromatic degradation in *Corynebacterium glutamicum*. Sci. China Ser. C: Life Sci. 48, 241–249.
Shikata, K., Fukui, T., Atomi, H., Imanaka, T., 2007. A novel ADP-forming succinyl-CoA synthetase in *Thermococcus kodakaraensis* structurally related to the archaeal nucleoside diphosphate-forming acetyl-CoA synthetases. J. Biol. Chem. 282, 26963–26970.
Steen, E.J., Kang, Y., Bokinsky, G., Hu, Z., Schirmer, A., McClure, A., Del Cardayre, S.B., Keasling, J.D., 2010. Microbial production of fatty-acid-derived fuels and chemicals from plant biomass. Nature 463, 559–562.
Strijbis, K., Distel, B., 2010. Intracellular acetyl unit transport in fungal carbon metabolism. Eukaryot. Cell. 9 (12), 1809–1815.
Teufel, R., Mascaraque, V., Ismail, W., Voss, M., Perera, J., Eisenreich, W., Haehnel, W., Fuchs, G., 2010. Bacterial phenylalanine and phenylacetate catabolic pathway revealed. Proc. Natl. Acad. Sci. 107, 14390–14395.
Thompson, S., Mayerl, F., Peoples, O.P., Masamune, S., Sinskey, A.J., Walsh, C.T., 1989. Mechanistic studies on beta-ketoacyl thiolase from *Zoogloea ramigera*: identification of the active-site nucleophile as Cys89, its mutation to Ser89, and kinetic and thermodynamic characterization of wild-type and mutant enzymes. Biochemistry 28, 5735–5742.
Thorpe, C., Kim, J., 1995. Structure and mechanism of action of the acyl-CoA dehydrogenases. FASEB J. 9, 718–725.
Trautwein, K., Wilkes, H., Rabus, R., 2012. Proteogenomic evidence for β-oxidation of plant-derived 3-phenylpropanoids in "*Aromatoleum aromaticum*" EbN1. Proteomics

12, 1402–1413.
Turk, S.C., Kloosterman, W.P., Ninaber, D.K., Kolen, K.P., Knutova, J., Suir, E., Schürmann, M., Raemakers-Franken, P.C., Müller, M., de Wildeman, S.M., 2015. Metabolic engineering toward sustainable production of nylon-6. ACS Synth. Biol. 5, 65–73.
van Summeren-Wesenhagen, P.V., Voges, R., Dennig, A., Sokolowsky, S., Noack, S., Schwaneberg, U., Marienhagen, J., 2015. Combinatorial optimization of synthetic operons for the microbial production of *p*-coumaryl alcohol with *Escherichia coli*. Microb. Cell Fact. 14 (1), 79.
Verlinden, R.A., Hill, D.J., Kenward, M.A., Williams, C.D., Piotrowska-Seget, Z., Radecka, I.K., 2011. Production of polyhydroxyalkanoates from waste frying oil by *Cupriavidus necator*. AMB Express 1, 11.
Wakil, S.J., 1961. Mechanism of fatty acid synthesis. J. Lipid Res. 2, 1–24.
Wakil, S.J., 1989. Fatty acid synthase, a proficient multifunctional enzyme. Biochemistry 28, 4523–4530.
Wang, Y., Yin, J., Chen, G.-Q., 2014. Polyhydroxyalkanoates, challenges and opportunities. Curr. Opin. Biotechnol. 30, 59–65.
Xu, H., Andi, B., Qian, J., West, A.H., Cook, P.F., 2006. The α-aminoadipate pathway for lysine biosynthesis in fungi. Cell Biochem. Biophys. 46, 43–64.
Yang, X.Y.H., Schulz, H., Elzinga, M., Yang, S.Y., 1991. Nucleotide sequence of the promoter and *fadB* gene of the *fadBA* operon and primary structure of the multifunctional fatty acid oxidation protein from *Escherichia coli*. Biochemistry 30, 6788–6795.
Yu, J.L., Xia, X.X., Zhong, J.J., Qian, Z.G., 2014. Direct biosynthesis of adipic acid from a synthetic pathway in recombinant *Escherichia coli*. Biotechnol. Bioeng. 111, 2580–2586.
Zhang, X., Li, M., Agrawal, A., San, K.-Y., 2011. Efficient free fatty acid production in Escheri*chia coli* using plant acyl-ACP thioesterases. Metab. Eng. 13, 713–722.

2.6 Improved production of adipate in *E. coli*

Appl Microbiol Biotechnol
DOI 10.1007/s00253-016-8033-3

BIOTECHNOLOGICALLY RELEVANT ENZYMES AND PROTEINS

Improved production of adipate with *Escherichia coli* by reversal of β-oxidation

Nicolai Kallscheuer[1] · **Jochem Gätgens**[1] · **Marvin Lübcke**[2] · **Jörg Pietruszka**[2] · **Michael Bott**[1] · **Tino Polen**[1]

Received: 9 August 2016 / Revised: 23 November 2016 / Accepted: 26 November 2016

Abstract The linear C_6 dicarboxylic acid adipic acid is an important bulk chemical in the petrochemical industry as precursor of the polymer nylon-6,6-polyamide. In recent years, efforts were made towards the biotechnological production of adipate from renewable carbon sources using microbial cells. One strategy is to produce adipate via a reversed β-oxidation pathway. Hitherto, the adipate titers were very low due to limiting enzyme activities for this pathway. In most cases, the CoA intermediates are non-natural substrates for the tested enzymes and were therefore barely converted. We here tested heterologous enzymes in *Escherichia coli* to overcome these limitations and to improve the production of adipate via a reverse β-oxidation pathway. We tested in vitro selected enzymes for the efficient reduction of the enoyl-CoA and in the final reaction for the thioester cleavage. The genes encoding the enzymes which showed in vitro the highest activity were then used to construct an expression plasmid for a synthetic adipate pathway. Expression of *paaJ*, *paaH*, *paaF*, *dcaA*, and *tesB* in *E. coli* BL21(DE3) resulted in the production of up to 36 mg/L of adipate after 30 h of cultivation. Beside the activities of the pathway enzymes, the availability of metabolic precursors may limit the synthesis of adipate, providing another key target for further strain engineering towards high-yield production of adipate with *E. coli*.

Keywords Adipic acid, adipate · Reverse β-oxidation · Carbon chain elongation · *Escherichia coli* · Metabolic engineering

Electronic supplementary material The online version of this article (doi:10.1007/s00253-016-8033-3) contains supplementary material, which is available to authorized users.

✉ Nicolai Kallscheuer
n.kallscheuer@fz-juelich.de

✉ Tino Polen
t.polen@fz-juelich.de

[1] IBG-1: Biotechnology, Institute of Bio- and Geosciences, Forschungszentrum Jülich GmbH, 52425 Jülich, Germany

[2] Institute of Bioorganic Chemistry, Heinrich-Heine-Universität, Düsseldorf, 52425 Jülich, Germany

Introduction

Adipic acid is the most important commercial aliphatic dicarboxylic acid in the industry with primary application in the chemical production of nylon-6,6 polyamide. The global production of adipic acid has been estimated to be at 2.6 million tons/year in 2012 and is expected to reach 3.7 million tons/year in 2020 (Grand View Research 2014). To date, adipic acid is produced by established large-scale chemical processes using non-renewable petroleum-based benzene as precursor (Grand View Research 2014; Musser 2005). In the past years, efforts were made to find alternative routes for the production of adipate from renewable carbon sources by biotechnological processes with suitable microbes. It appeared promising to combine a biotechnological process for fermentative production of the chemical precursor *cis*, *cis*-muconate, and an environmentally conscious chemo-catalytic process for the conversion of this precursor to adipate (Thomas et al. 2003). Biocatalytic production of *cis*, *cis*-muconate from glucose or glycerol, was achieved with *Escherichia coli* (Niu et al. 2002; Zhang et al. 2015) and from benzoate with *Pseudomonas putida* (van Duuren et al. 2011). In addition, the ability of *Saccharomyces cerevisiae* to produce *cis*, *cis*-muconate from glucose, was demonstrated (Suastegui et al. 2016). Also, to yield adipate directly with engineered microbes, a new α-reductive biocatalytic pathway was proposed (Fig. 1), in which the precursor 2-oxoadipate is converted to adipate

Published online: 08 December 2016

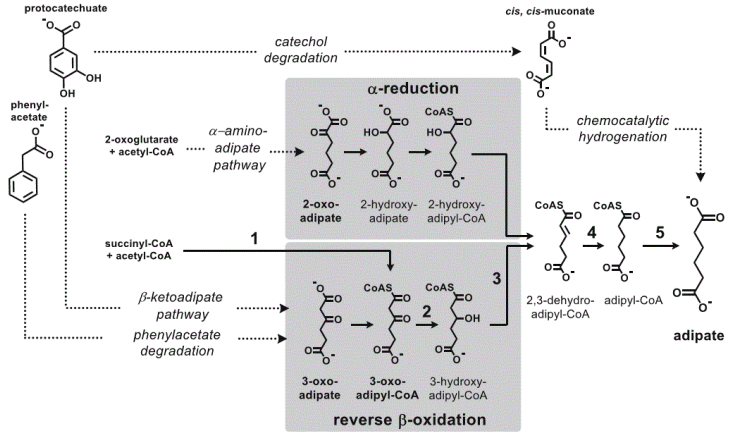

Fig. 1 Metabolic pathways that can be exploited for the biological production of adipate. Adipate is in principle accessible by biosynthesis from 2-oxoadipate via α-reduction (Parthasarathy et al. 2011) and from 3-oxoadipyl-CoA via reverse β-oxidation. Both precursors can be obtained by condensation of the citric acid cycle intermediates 2-oxoglutarate and succinyl-CoA with acetyl-CoA, respectively. The degradation of the aromatic compounds protocatechuate and phenylacetate leads to 3-oxoadipate as a common intermediate. Protocatechuate can also be degraded to *cis*, *cis*-muconate that can be chemically converted to yield adipate. The production of adipate from glucose via reverse β-oxidation requires enzyme activities of 3-oxoadipyl-CoA thiolase (*1*), 3-hydroxyadipyl-CoA dehydrogenase (*2*), 2,3-dehydroadipyl-CoA hydratase (*3*), adipyl-CoA dehydrogenase (*4*), and adipyl-CoA thioesterase (*5*)

(Parthasarathy et al. 2011). As discussed by Buckel and co-workers, several obstacles remain to be solved before this proposed pathway for adipate production might work. These and other options towards a bio-based production of adipate have been reviewed recently (Bart and Cavallaro 2015a; Bart and Cavallaro 2015b; Bugg and Rahmanpour 2015; Polen et al. 2013).

A promising alternative to the α-reduction of 2-oxoadipate is the formation of adipate from 3-oxoadipate or 3-oxoadipyl-CoA by reverse β-oxidation (Fig. 1). 3-Oxoadipate is an intermediate in the catabolic pathway for phenylacetate as well as in the well-studied β-ketoadipate pathway for aerobic degradation of benzoate and protocatechuate (Teufel et al. 2010; Wells and Ragauskas 2012). Both catabolic pathways for aromatics terminate with a 3-oxoacyl-CoA thiolase-catalyzed cleavage of 3-oxoadipyl-CoA to succinyl-CoA and acetyl-CoA, thereby supplying intermediates for the central carbon metabolism (Kaschabek et al. 2002). By mechanism, reactions catalyzed by 3-oxoacyl-CoA thiolases are generally recognized as reversible and suitable enzymes can be used for purpose of carbon chain elongation (Haapalainen et al. 2006). Since the first publication on engineered reversal of β-oxidation (Dellomonaco et al. 2011), several approaches for the synthesis of carboxylic acids, aldehydes, and alcohols using acetyl-CoA-dependent carbon chain elongation have been demonstrated. The corresponding reaction cascades have been used exemplarily for the microbial production of butyrate and 1-butanol in the g/L scale using *E. coli* (Clomburg et al. 2015; Dellomonaco et al. 2011). Hexanoate and 1-hexanol were synthesized in analogy using two elongation cycles starting from acetyl-CoA and subsequent reduction of the carboxylic acid to the alcohol (Dekishima et al. 2011). Moreover, with β-reduction reactions which can accept a variety of functionalized primers and functionalized extender units, 18 functionalized small molecules from 10 classes were obtained including adipic acid (Cheong et al. 2016).

The metabolic route for biosynthesis of adipate by reversal of β-oxidation, which we have tested, initiates with the formation of 3-oxoadipyl-CoA from succinyl-CoA and acetyl-CoA catalyzed by a 3-oxoadipyl-CoA thiolase operating in the (non-native) condensation direction (Fig. 1). Four subsequent reaction steps lead to adipate via the intermediates 3-hydroxyadipyl-CoA, 2,3-dehydroadipyl-CoA, and adipyl-CoA (Fig. 1). The first three reactions in this pathway can be catalyzed by 3-oxoadipyl-CoA thiolase (PaaJ), 3-hydroxyadipyl-CoA dehydrogenase (PaaH), and 2,3-dehydroadipyl-CoA hydratase (PaaF) of the phenylacetate catabolic pathway of *E. coli* (Teufel et al. 2010). With these enzymes assembled to a reverse β-oxidation pathway for dicarboxylic acids, up to 0.6 mg/L of adipate was obtained (Babu et al. 2015; Yu et al. 2014). The last two reactions, the reduction of 2,3-dehydroadipyl-CoA and the cleavage of adipyl-CoA, were found to be rate limiting for production of adipic acid with *E. coli*. In our study, we aimed at the identification of suitable enzymes that can be exploited for the last two reactions of the reverse β-oxidation pathway to increase

the production of adipate from glucose with *E. coli*. With the candidates identified, a significantly improved production of adipate from glucose was achieved.

Materials and methods

Bacterial strains, plasmids, media, and growth conditions

Strains and plasmids constructed or used in this study are listed in Table 1. *E. coli* DH5α was used for cloning purposes, while *E. coli* Rosetta-gami 2(DE3) and *E. coli* BL21(DE3) were used as hosts for heterologous gene expression and adipic acid production, respectively. Growth was monitored by measuring the optical density at 600 nm (OD_{600}). For cultivation of *E. coli*, the following media were used at 37 °C. For routine cultivations, lysogeny broth (LB) contained 10 g/L NaCl, 10 g/L tryptone (Becton Dickinson), and 5 g/L yeast extract (BD). For agar plates, 1.5% (*w/v*) agar (Becton Dickinson) was added. If necessary, the media contained kanamycin (50 μg/mL), carbenicillin (100 μg/mL), chloramphenicol (34 μg/mL), or tetracycline (12.5 μg/mL). For (heterologous) gene expression, cells were grown in terrific broth (TB) containing 12 g/L tryptone, 24 g/L yeast extract, 4 mL glycerol, and phosphate buffer prepared as 10× stock solution (final concentration in medium 6.3 g/L K_2HPO_4 and 1.3 g/L KH_2PO_4). For the production of adipic acid, a modified mineral medium was used based on the medium from Clomburg et al. (Clomburg et al. 2012) and designated as adipic acid production medium (APM). APM (pH 7.2) contained 125 mM MOPS (3-(*N*-morpholino)propanesulfonic acid), 1.5 mM Na_2HPO_4, 5 mM $(NH_4)_2SO_4$, 30 mM NH_4Cl, 1 mM $MgSO_4 \times 7\ H_2O$, 0.5 mM $CaCl_2 \times 2\ H_2O$, 5 mM calcium pantothenate, 111 mM glucose, and 1 mL trace element stock solution per L medium (Clomburg et al. 2012). The trace element stock solution (pH 7.5) contained 13.4 mM EDTA, 31 mM $FeCl_3$, 6 mM $ZnCl_2$, 1.6 mM H_3BO_3, 0.8 mM $CuCl_2 \times 2\ H_2O$, 0.4 mM $CoCl_2 \times 6\ H_2O$, and 0.08 mM $MnCl_2 \times 4\ H_2O$.

Recombinant DNA work

The oligonucleotides used for cloning were obtained from Eurofins Genomics. The enzymes for recombinant DNA work were obtained from Thermo Scientific or New England BioLabs. Routine methods such as PCR, restriction, and ligation were carried out according to standard protocols (Sambrook et al. 1989). Genes were amplified by PCR from genomic DNA of the respective donor organism using oligonucleotides (Table 2).

For expression of genes coding for His-tagged adipyl-CoA dehydrogenase candidates, $dcaA_{Ab}$ (Uniprot entry Q937T2) and Reut_B3882 (designated acd_{Cn}, Uniprot entry Q46UE5) were amplified by PCR from genomic DNA of *Acinetobacter baylyi* ADP1 and *Cupriavidus necator* JMP228 using

Table 1 Strains and plasmids used or constructed in this study

Strain/plasmid	Relevant characteristics	Reference
E. coli MG1655	F^-, lambda$^-$, rph-1	Blattner et al. (1997)
E. coli DH5α	F^- Φ80*lacZ*Δ*M15* Δ(*lacZYA-argF*) U169 *recA1 endA1 hsdR17* (rK^-, mK^+) *phoA supE44* λ$^-$ *thi*-1 *gyrA96 relA1*	Invitrogen
E. coli BL21(DE3)	F^- *ompT gal dcm lon hsdSB*(rB^- mB^-) λ(DE3 [*lacI lacUV5*-T7 gene 1 ind1 sam7 nin5])	Invitrogen
E. coli Rosetta-gami 2 (DE3)	Δ(*ara-leu*)*7697* Δ*lacX74* Δ*phoA Pvu*II *phoR araD139 ahpC galE galK rpsL* (DE3) F'[lac^+ $lacI^q$ *pro*] *gor522*::Tn*10 trxB* pRARE2 (cam^R, str^R, tet^R)	EMD Millipore
C. necator H16	Former *Ralstonia eutropha* H16	DSM 428
C. necator JMP228	JMP134 derivate cured from plasmid pJP4	DSM 5450
A. baylyi ADP1	Former *Acinetobacter* sp. ADP1	DSM 24193
T. gammatolerans	Type strain BD-4	DSM 15229
Plasmid		
pET22b(+)	T7 polymerase-based expression vector (amp^R, pBR322 ori, *lacIq*, His_6)	Novagen
pET22b_$dcaA_{Ab}$	Contains *dcaA* from *A. baylyi* ADP1	this study
pET22b_acd_{Cn}	Contains *acd* (Reut_B3882) from *C. necator* JMP228	this study
pET22b_$tesB_{Ec}$	Contains *tesB* from *E. coli* MG1655	this study
pET22b_$yciA_{Cn}$	Contains *yciA* (H16_A0465) from *C. necator* H16	this study
pET22b_scs_{Tg}	Contains *acdA-1* (TGAM_0218) and *acdB-1* (TGAM_0742) from *T. gammatolerans*	this study
pET22b_Adip1	Contains gene cluster $paaJ_{Ec}$-$paaH_{Ec}$-$paaF_{Ec}$-$dcaA_{Ab}$-$tesB_{Ab}$ as a synthetic operon under control of promoter P_{syn}	this study

amp^R ampicillin/carbenicillin resistance, cam^R chloramphenicol resistance, str^R streptomycin resistance, tet^R tetracycline resistance

Table 2 DNA oligonucleotides used in this study

Name	Sequence (5′-3′)	Enzyme
Cloning		
P_dcaA$_{Ab}$-s	AGAGGTCTCACGTAAAGGAGAACACATATGATTCGCGATGAAGGGATGTTGC	*Bsa*I, *Nde*I
P_dcaA$_{Ab}$-as	CACGGTCTCC**CGAG**AAGCTTGGACGTCACTTCCTTAATCATATTTTTGGCAATAATAATTTGC	*Bsa*I, *Hin*dIII
P_acd$_{Cn}$-s	AGACATATGATGATCCGTGACACCGCTCG	*Nde*I
P_acd$_{Cn}$-as	CACAAGCTTGTCCCCCACAGGCTCCGC	*Hin*dIII
P_tesB$_{Ec}$-s	CTCCATATGAGTCAGGCGCTAAAAAATTTACTGACATTG	*Nde*I
P_tesB$_{Ec}$-as	GAGAAGCTTATTGTGATTACGCATCACCCCTTCCTGAAC	*Hin*dIII
P_yciA$_{Cn}$-s	AGACATATGATGCCCGCCGACGCC	*Nde*I
P_yciA$_{Cn}$-as	CACCTCGAGAGCCGACGGCAGCATCCG	*Xho*I
P_acdB1$_{Tg}$-s	ACACATATGAAGGAGGAAGCCCTCAAAGTTATCGAG	*Nde*I
P_acdB1$_{Tg}$-as	AGAGGTCTC**TGAAT**TCAGGCACACCTCTCCTTGTACTCGG	*Bsa*I
P_acdA1$_{Tg}$-s	CACGGTCTCA**ATTC**AAAGGAGAACAGGATGGAGAGCCTCGACTTCCTGTTTTACC	*Bsa*I
P_acdA1$_{Tg}$-as	AGAGGATCCTCAGAGTTTCCCGTTTTCCCTGAGC	*Bam*HI
P_check-T7-s	CGAAATTAATACGACTCACTATAGG	–
P_check-T7-as	TATGCTAGTTATTGCTCAGCGGTG	–
Operon assembly		
P_P$_{syn}$-s	GGATCCAGTATAAAAATAATTCTTGACATATTTGCTAAAATTTGGTATAATATGCGCC ATCGATCAGGCAAGGAGA	*Bam*HI
P_P$_{syn}$-as	GAATTCTCCTTGCCTGATCGATGGCGCATATTATACCAAATTTTAGCAAATATGTCA AGAATTATTTTTATACTG	–
P_paaJ$_{Ec}$-s	GGTCTCA**ATTC**ATGCGTGAAGCCTTTATTTGTGAC	*Bsa*I
P_paaJ$_{Ec}$-as	GGTCTCT**CGCC**TCAAACACGCTCCAGAATCATG	*Bsa*I
P_paaH$_{Ec}$-s	GGTCTCA**GGCG**AAGGAGAATCAAATGATGATAAATGTGCAAACTGTGG	*Bsa*I
P_paaH$_{Ec}$-as	GGTCTCT**TTGT**TTATGACTCATAACCGCTCTCC	*Bsa*I
P_paaF$_{Ec}$-s	GGTCTCA**ACAA**AAGGAGATGATCATGAGCGAACTGATCGTCAG	*Bsa*I
P_paaF$_{Ec}$-as	GGTCTCA**GGAA**TTAGCGTCCTTTAAAGTCGGG	*Bsa*I
P_dcaA$_{Ab}$-s	AGAGGTCTCT**TTCC**AAGGAGAACTCTGATGATTCGCGATGAAGGGATGTTG	*Bsa*I
P_dcaA$_{Ab}$-as	CACGGTCTCA**TACG**TTAGGACGTCACTTCCTTAATCATATTTTTGGCAATAATAATTTG	*Bsa*I
P_tesB$_{Ab}$-s	AGAGGTCTCA**CGTA**AAGGAGAACAGGATGAATACACTAACCCAAGAACTGGTTGAA CTTTTATCTCTAG	*Bsa*I
P_tesB$_{Ab}$-as	TGCAAGCTTAGATTACTGTGTTTCAATTTCACGAAGGCGCATTAAAC	*Hin*dIII

Recognition sites of restriction enzymes are underlined. Resulting 5′ overhangs after *Bsa*I cleavage are shown in bold. Promoter fragment P$_{syn}$ containing suitable overhangs was generated using the two oligonucleotides P$_{syn}$-s and P$_{syn}$-as

oligonucleotide pairs P_dcaA$_{Ab}$-s/P_dcaA$_{Ab}$-as and P_acd$_{Cn}$-s/P_acd$_{Cn}$-as, respectively, and cloned individually into the *E. coli* expression vector pET22b(+) using *Nde*I and *Hin*dIII restriction sites to obtain plasmids pET22b_*dcaA$_{Ab}$* and pET22b_*acd$_{Cn}$*. For expression of genes coding for His-tagged acyl-CoA thioesterase candidates, *tesB* from *E. coli* MG1655 (Uniprot entry P0AGG2) and *yciA* from *C. necator* H16 (Uniprot entry Q0KEF6) were amplified from genomic host DNA by PCR using the oligonucleotide pairs P_tesB$_{Ec}$-s/P_tesB$_{Ec}$-as and P_yciA$_{Cn}$-s/P_yciA$_{Cn}$-as, respectively, and cloned individually into pET22b(+) using *Nde*I/*Hin*dIII and *Xho*I/*Hin*dIII restriction sites to obtain pET22b_*tesB$_{Ec}$* and pET22b_*yciA$_{Cn}$*. For the expression of genes coding for an annotated heterodimeric succinyl-CoA synthetase from *Thermococcus gammatolerans*, the encoding genes TGAM_0218 (*acdA-1$_{Tg}$*, Uniprot entry C5A3A8) and TGAM_0742 (*acdB-1$_{Tg}$*, Uniprot entry C5A4T2) were amplified by PCR from genomic host DNA using the oligonucleotide pairs P_acdB1$_{Tg}$-s/P_acdB1$_{Tg}$-as and P_acdA1$_{Tg}$-s/P_acdA1$_{Tg}$-as. *Bsa*I restriction sites creating compatible overhangs were introduced after the stop codon of *acdB-1$_{Tg}$* and in front of the ribosomal binding site of *acdA-1$_{Tg}$*, which were subsequently used for the assembly of the artificial operon *acdB-1$_{Tg}$-acdA-1$_{Tg}$*. The assembled fragment was cloned into pET22b(+) using *Nde*I and *Bam*HI to obtain pET22b_*scs$_{Tg}$*. For assembly of the synthetic adipate pathway operon consisting of *paaJ$_{Ec}$*, *paaH$_{Ec}$*, *paaF$_{Ec}$*, *dcaA$_{Ab}$*, and *tesB$_{Ab}$*, the genes were individually amplified by PCR from genomic host DNA with the respective oligonucleotides for operon assembly (Table 2). Each PCR product is flanked by *Bsa*I sites creating pairwise unique overhangs after cleavage with *Bsa*I allowing to assemble a pentacistronic operon in the designed

order of genes using the GoldenGate cloning strategy (Engler et al. 2009). The PCR products of the five genes were digested with *Bsa*I and mixed with the annealed oligonucleotides P_P_{syn}-s/P_P_{syn}-as generating the constitutive strong synthetic promoter P_{syn} (Giacomini et al. 1994). This mixture was used for ligation and cloning of the operon fragment into pET22b(+) using *Bam*HI and *Hin*dIII to obtain plasmid pET22b_Adip1. *E. coli* was transformed by electroporation using the Biorad GenePulserXCell (Bio-Rad) with operation parameters of 25 μF, 1500 V, and 800 Ω for 5 ms. Plasmids were isolated using the GeneJET Plasmid Miniprep Kit (Thermo Scientific). The correctness of the genes inserted in the recombinant plasmids was verified by DNA sequencing (Eurofins Genomics) using plasmid-specific primers P_check-T7-s and P_check-T7-as (Table 2) binding upstream and downstream of the multiple cloning site of pET22b(+).

Gene expression, protein purification, and protein identification

For plasmid-based gene expression, cultivations were performed in 500 mL TB broth using recombinant *E. coli* Rosetta-gami 2(DE3) in a 2-L Erlenmeyer flask shaken at 120 rpm and 37 °C. Plasmid-borne gene expression was induced at an OD_{600} of 2 by addition of 0.5 mM IPTG. Subsequently, cells were cultivated for another 4 h and then centrifuged (10 min; 4 °C; 4000×*g*). Cells were resuspended in NNI20 buffer (50 mM sodium phosphate, 300 mM NaCl, 20 mM imidazole, pH 8.0) (1 g wet weight/mL buffer). Cell-free extracts were obtained by ultra-sonification for 6 min at 4 °C with Sonifier 250 (Branson) and subsequent centrifugation (10 min; 4 °C; 16,000×*g*). His-tagged proteins were purified by affinity chromatography using Ni-NTA Superflow (Qiagen) using NNI buffer (50 mM sodium phosphate, 300 mM NaCl, pH 8.0, and stepwise increased imidazole concentrations ranging from 20 to 400 mM). Heat-stable heterodimeric succinyl-CoA synthetase from *T. gammatolerans* heterologously produced in *E. coli* was purified by heat precipitation of host proteins via incubation of the cell-free extract for 10 min at 90 °C. Cell-free crude protein extracts, fractions of Ni-NTA purifications, and the purified proteins were subjected to SDS-PAGE and Coomassie staining to check the purity of the enriched enzymes. Peptide mass fingerprinting using MALDI-TOF-MS analysis for protein identification was carried out as described (Küberl et al. 2014).

Preparation and purification of adipic acid anhydride and adipyl-CoA

Adipic acid anhydride was synthesized in analogy to a described procedure utilizing adipic acid, isopropenyl acetate, and Montmorillonite (Villemin et al. 1993). The microwave-assisted transformation was worked up after 5 min; the crude solid product was used directly for the next step. Adipyl-CoA was prepared from adipic acid anhydride as described elsewhere (Parthasarathy et al. 2011). Adipyl-CoA was purified using Sep.-Pak C18 Vac reverse phase columns (Waters). A column was prepared with methanol and equilibrated with 0.1% (*v*/*v*) trifluoroacetic acid (TFA) in distilled water. After application of the sample, the column was washed three times with one column volume of 0.1% TFA. Adipyl-CoA bound to the column was eluted with 0.1% TFA in 50% (*v*/*v*) acetonitrile. The concentration of adipyl-CoA was determined photometrically at 259 nm using an extinction coefficient of 15.4 mM^{-1} cm^{-1} (Karl et al. 1995).

Enzymatic activity assays

If not stated otherwise, substrates were obtained from Sigma-Aldrich. The adipyl-CoA dehydrogenase activity was measured using ferrocenium hexafluorophosphate as artificial electron acceptor (Lehman et al. 1990). The acyl-CoA synthetase assay was performed as described (Shikata et al. 2007) using a coupled enzyme assay with pyruvate kinase and lactate dehydrogenase with the following modifications; concentrations of NADH and CoA were reduced to 0.3 and 0.5 mM, respectively. The assay temperature was reduced to 42 °C. Adipyl-CoA thioesterase activity was measured using 5,5′-dithiobis-(2-nitrobenzoic acid) (DTNB). The assay mix contained 175 mM potassium phosphate (pH 8.0) with 0.2 mM DTNB and 0.1 mM adipyl-CoA. Formation of 2-nitro-5-thiobenzoate (NTB) upon release of CoA-SH from adipyl-CoA was followed at 412 nm and 37 °C using an extinction coefficient of 13.6 mM^{-1} cm^{-1} (Nie et al. 2008).

Identification of metabolites by GC-TOF-MS analysis

Adipate and intermediates of the proposed pathway were qualitatively identified by GC-TOF-MS analysis. For determination of intracellular metabolites, *E. coli* cells from 50-mL culture (OD_{600} = 15–20) were sedimented (3 min; 4 °C; 4000×*g*) and the cells were washed with 5 mL of 2.7% NaCl solution (4 °C). After another centrifugation step (3 min; 4 °C; 4000×*g*), cell pellets were resuspended in 2 mL methanol and disrupted by incubation for 30 min at 65 °C in an ultrasonic cleaner USC 500D (VWR) to obtain cell-free intracellular extracts which were shock-frozen in liquid nitrogen. For determination of extracellular metabolites, 130 μL samples of cell-free culture supernatants were shock-frozen in liquid nitrogen. Frozen samples were processed for GC-TOF-MS analysis and measured as described (Paczia et al. 2012). The identification of known metabolites was conducted by comparison of baseline-noise-substracted fragment patterns to our in-house database JuPoD, the commercial database NIST08 (National Institute of Standards and Technology, USA), and the freely available database GMD

(MPI of Molecular Plant Physiology, Germany). Unknown peaks were identified by structural combination of elemental compositions and verified by virtual derivatization and fragmentation of the predicted structure.

Quantification of adipate using LC-MS analysis

Adipate in culture supernatants was quantified by LC-MS using an Agilent ultra-High-Performance LC (uHPLC) 1290 Infinity system coupled to a 6130 Quadrupole LC-MS system (Agilent Technologies). LC separation was carried out with a Kinetex 1.7u C_{18} 100-Å pore-size column (50 by 2.1 mm, Phenomenex) at 50 °C. For elution, 0.1% (v/v) acetic acid (solvent A) and acetonitrile supplemented with 0.1% (*v/v*) acetic acid (solvent B) were applied as the mobile phases at a flow rate of 0.5 mL/min. A gradient was used, where the amount of solvent B was increased stepwise, minute 0 to 6 10 to 30%, minute 6 to 7 30 to 50%, minute 7 to 8 50 to 100%, and minute 8 to 8.5 100 to 10%. The mass spectrometer was operated in the negative electrospray ionization mode (ESI). Data acquisition was performed in selected ion-monitoring mode (SIM). Mass signals were linear up to adipate concentrations from 1 to at least 150 mg/L. Benzoic acid (final concentration 100 mg/L) was used as internal standard. Calibration curves were calculated based on analyte/internal standard ratios calculated from the obtained area values.

Results

In silico analysis of the adipic acid production pathway thermodynamics

To estimate the equilibrium for each reaction of the reverse β-oxidation pathway for adipic acid and possible limiting reactions, we calculated the change of the Gibbs free energy ($\Delta G^{0\prime}$) based on the Gibbs free energy values for all involved metabolites (Table S1). Starting from succinyl-CoA and acetyl-CoA, the metabolic route to adipate by reverse β-oxidation using a thioesterase as terminal step is thermodynamically feasible with a calculated overall $\Delta G^{0\prime}$ of −78.4 kJ/mol (Table S2). For the 3-oxoadipyl-CoA thiolase initiation reaction $\Delta G^{0\prime}$ of +26.8 kJ/mol is positive for operation of the enzyme in the condensation reaction (Table S2). In line with this finding and as also proposed earlier, the biosynthetic (anabolic) thiolase reaction is thermodynamically unfavorable, but the formation of 3-oxoadipyl-CoA could be driven by the intracellular excess of substrates and removal of the product shifting the reaction to the condensation direction (Modis and Wierenga 1999). The hydratase and the thioesterase reaction appear to be negligible with respect to the overall thermodynamics (Table S2). At least for the thioesterase reaction, this is surprising as the loss of the intrinsic energy of the thioester is expected to result in a negative $\Delta G^{0\prime}$. The changes of the Gibbs free energy show that the adipate formation is mainly driven by the adipyl-CoA dehydrogenase reaction ($\Delta G^{0\prime}$ of −71.2 kJ/mol) and also by the reduction of 3-oxoadipyl-CoA favoring the formation of 3-hydroxyadipyl-CoA ($\Delta G^{0\prime}$ of −40.2 kJ/mol). Taken together, the calculated values for the adipate production pathway are in good agreement with the values reported for the reverse β-oxidation pathway for butyrate production (Dellomonaco et al. 2011).

The identification of suitable enzymes for the adipyl-CoA dehydrogenase reaction and for the cleavage of adipyl-CoA should enhance the production of adipate, while the first three reactions in the adipate pathway can be catalyzed by the enzymes 3-oxoadipyl-CoA thiolase (PaaJ), 3-hydroxyadipyl-CoA dehydrogenase (PaaH), and 2,3-dehydroadipyl-CoA hydratase (PaaF) (Babu et al. 2015; Teufel et al. 2010; Yu et al. 2014). Therefore, we here tested enzymes that could be exploited for the last two reactions to improve the production of adipate by reverse β-oxidation.

Purification and in vitro enzymatic activity of putative adipyl-CoA dehydrogenases

In our literature search for candidate adipyl-CoA dehydrogenase enzymes to reduce 2,3-dehydroadipyl-CoA to adipyl-CoA, we found the putative adipyl-CoA dehydrogenase DcaA, which was already proposed to play a role in the catabolic adipate pathway in *A. baylyi* ADP1 (Parke et al. 2001). On the other hand, in a preliminary test, *C. necator* was able to consume adipic acid in the presence of a carbon and energy source (not shown), suggesting that a similar degradation pathway as in *A. baylyi* may be present also in *C. necator*. Therefore, $DcaA_{Ab}$ and the orthologous enzyme Acd_{Cn} encoded by Reut_B3882 in *C. necator* JMP228 sharing 53% identity (85% similarity) in their amino acid sequences were chosen as promising candidates and the purified enzymes were tested in vitro. To this end, expression was carried out in *E. coli* Rosetta-gami 2(DE3) using plasmids pET22b_$dcaA_{Ab}$ and pET22b_acd_{Cn} and the C-terminally His-tagged versions of $DcaA_{Ab}$ and of Acd_{Cn} were purified by Ni-NTA affinity chromatography. Both proteins were enriched to very high purity as judged by SDS-PAGE analysis of the Ni-NTA elution fractions (Fig. 2a, b). Both enzymes are annotated as flavoproteins which usually contain FAD as bound redox cofactor (Thorpe and Kim 1995). The samples containing the enriched proteins showed a yellow color suggesting that both also contain FAD as a cofactor. However, since the native terminal electron acceptor of both enzymes is not known, ferrocenium hexafluorophosphate was used as artificial electron acceptor (Lehman et al. 1990).

The oxidation of adipyl-CoA leads to the reduction of the ferrocenium ion to oxygen-stable ferrocene, thereby reoxidizing the FAD cofactor. Thus, the reaction tested in

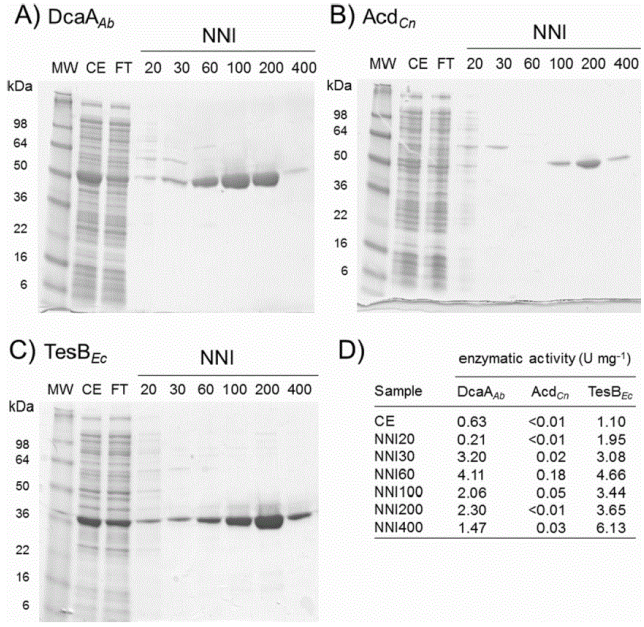

D)

	enzymatic activity (U mg^{-1})		
Sample	DcaA$_{Ab}$	Acd$_{Cn}$	TesB$_{Ec}$
CE	0.63	<0.01	1.10
NNI20	0.21	<0.01	1.95
NNI30	3.20	0.02	3.08
NNI60	4.11	0.18	4.66
NNI100	2.06	0.05	3.44
NNI200	2.30	<0.01	3.65
NNI400	1.47	0.03	6.13

Fig. 2 SDS-PAGE analysis and activities of DcaA$_{Ab}$ and Acd$_{Cn}$ in the adipyl-CoA dehydrogenase assay and of TesB$_{Ec}$ in the adipyl-CoA thioesterase assay. **a**–**c** Coomassie-stained SDS-PAGE analysis of protein samples from purification of His$_6$-tagged adipyl-CoA dehydrogenase DcaA$_{Ab}$ **a** from *A. baylyi* ADP1 (43.5 kDa) and Acd$_{Cn}$ **b** from *C. necator* JMP228 (43.9 kDa) as well as acyl-CoA/adipyl-CoA thioesterase TesB$_{Ec}$ **c** from *E. coli* (33.5 kDa) heterologously produced in *E. coli* Rosetta-gami 2(DE3). **d** The specific enzymatic activities in protein samples were assayed with adipyl-CoA as substrate for DcaA$_{Ab}$ and Acd$_{Cn}$ using the ferrocenium hexafluorophosphate enzymatic assay. Adipyl-CoA thiosterase activity of TesB$_{Ec}$ was measured by following CoA formation with DTNB. The values are given as average of triplicate measurements. *MW* molecular mass in kDa, *CE* cell-free crude protein extract, *FT* Ni-NTA flow-through, *NNI20 to NNI400* elution fractions using buffers with the indicated imidazole concentrations in mM for stepwise elution of protein during Ni-NTA affinity chromatography

the enzyme assay in vitro is the reverse of the desired reaction in the synthetic pathway in vivo. The enzyme activities with adipyl-CoA as substrate were measured in cell-free crude extracts and in the elution fractions. Purified DcaA$_{Ab}$ showed a maximal activity of 4.1 μmol min^{-1} mg^{-1} under the tested reaction conditions (Fig. 2d). This finding confirms the proposed role of DcaA$_{Ab}$ in the adipate catabolic pathway of *A. baylyi* ADP1 (Parke et al. 2001). In contrast, Acd$_{Cn}$ from *C. necator* JMP228 annotated as butyryl-CoA dehydrogenase showed no or only very low activity with adipyl-CoA as substrate (Fig. 2d). Therefore, we selected DcaA$_{Ab}$ as adipyl-CoA dehydrogenase and included *dcaA$_{Ab}$* in the operon assembly to express and test the adipate production pathway in *E. coli*.

Catalytic activity of candidate enzymes for release of adipic acid from adipyl-CoA

For the last step of the pathway, the release of adipic acid from its CoA-thioester, we selected three candidate enzymes for in vitro enzyme assays to test their activity. TesB from *E. coli* MG1655 and YciA from *C. necator* H16 are putative broad-spectrum acyl-CoA thioesterases that could be used to hydrolyse adipyl-CoA to release adipic acid. Also, the putative broad-spectrum activity may hydrolyze other similar CoA esters, which could simultaneously allow monitoring the intermediates of the pathway. However, the hydrolysis is not preserving the energy of the thioester bond, yet preserving the energy in ATP would be advantageous. The heterodimeric TCA cycle enzyme succinyl-CoA synthetase (SCS) of the thermophilic archaeon *Thermococcus kodakarensis*, which comprises a different domain architecture compared to SCS enzymes characterized so far, was shown to catalyze the CoA activation of adipate (Shikata et al. 2007). As the enzyme is an ADP-forming CoA synthetase, the catalyzed reaction is fully reversible (Shikata et al. 2007). Thus, such an enzyme could also be suitable for catalysis of adipyl-CoA cleavage. We chose to test the archaeal succinyl-CoA synthetase from the closely related organism *T. gammatolerans* consisting of a α- and β- subunit (SCS$_{Tg}$).

Overexpression of the selected candidate genes was carried out in *E. coli* Rosetta-gami 2(DE3) using the plasmids pET22b_*tesB*$_{Ec}$, pET22b_*yciA*$_{Cn}$, and pET22b_*scs*$_{Tg}$. With plasmid pET22b_*yciA*$_{Cn}$, no production of recombinant protein could be detected at cultivation temperatures of 30 or 37 °C and YciA$_{Cn}$ could not be purified by Ni-NTA affinity chromatography. TesB$_{Ec}$ could be enriched to high purity as judged by SDS-PAGE analysis of the Ni-NTA elution fractions (Fig. 2c). In the adipyl-CoA hydrolysis assay, TesB$_{Ec}$ accepted adipyl-CoA as substrate and led to its rapid hydrolysis. Under the conditions tested, the maximal specific activity of the purified enzyme was 6.1 μmol min^{-1} mg^{-1} with adipyl-CoA as substrate (Fig. 2d). SCS$_{Tg}$ is heat stable and both subunits could be enriched in the supernatant after heat treatment and centrifugation of the cell-free extract prepared from the *E. coli* expression culture. However, the β-subunit appeared to be in high excess over the α-subunit as judged by the band intensities in the SDS-PAGE analysis (Fig. S1). Peptide mass fingerprinting using MALDI-TOF-MS analysis confirmed the presence of the α- (11 peptides, 30% coverage) and the β-subunit (11 peptides, 46% coverage) in bands corresponding to the masses of the monomeric subunits. Furthermore, both the α- and β-subunit were also detected in a band corresponding to about 100 kDa (Fig. S1). The enzymatic activity of SCS$_{Tg}$ was measured in the direction of adipyl-CoA formation. A coupled assay using pyruvate kinase and lactate dehydrogenase for the detection of ADP formed upon production of adipyl-CoA from adipate led to the demonstration of a maximal activity of 0.12 μmol min^{-1} mg^{-1} (Fig. S1). In contrast, no activity (<0.01 μmol min^{-1} mg^{-1}) was measured in the supernatant after heat precipitation of the control strain harboring the empty plasmid pET22b(+) (data not shown). Thus, SCS$_{Tg}$ could be exploited for adipate production. However, due to the relatively low activity of SCS$_{Tg}$ in vitro and possible difficulties to obtain balanced levels of the α- and β-subunit in an artificially assembled pathway operon, we chose to use a TesB homolog for the test of the adipate production pathway in *E. coli*. Restriction sites present in the gene sequence of TesB$_{Ec}$ interfered with our selected strategy for the assembly of the synthetic five-gene operon, while the restriction sites were absent in the gene of the TesB homolog from *A. baylyi* ADP1 (TesB$_{Ab}$) that exhibits a high amino acid sequence similarity (78%) to TesB$_{Ec}$. Furthermore, both proteins exhibit the same domain architecture with a HotDog domain (HotDog_dom, Interpro IPR029069) and an acyl-CoA thioesterase domain (Acyl_CoA_thio, Interpro IPR003703). Therefore, we assumed the broad substrate specificity including medium-chain length acyl-CoA thioesters also for TesB$_{Ab}$ (Nie et al. 2008) and used *tesB*$_{Ab}$ for the operon assembly and test of adipate production with *E. coli*.

Adipic acid production is improved in *E. coli* with DcaA$_{Ab}$ and TesB$_{Ab}$

To test the production of adipate from glucose with *E. coli* via reverse β-oxidation using the five selected enzymes PaaJ$_{Ec}$, PaaH$_{Ec}$, PaaF$_{Ec}$, DcaA$_{Ab}$, and TesB$_{Ab}$, we constructed the plasmid pET22b_Adip1 (Fig. 3). This plasmid contains the encoding genes each with ribosomal binding site AAGGAGG in a distance of five nucleotides to the start codon (Chen et al. 1994) as a synthetic operon under control of the strong constitutive synthetic promoter P$_{syn}$ constructed for gene expression in Gram-negative bacteria (Giacomini et al. 1994). *E. coli* BL21(DE3)/pET22b_Adip1 was inoculated to an OD$_{600}$ of 0.3 in adipate production medium (APM) with 2% glucose as sole carbon and energy source. The strain reached a final OD$_{600}$ of 4.5 and accumulated up to 6 ± 1 mg/L of adipate in the culture supernatant (Fig. 4). We then tested if the presence of selected supplements in the APM positively influences the accumulation of adipate. The addition of LB or BHI medium (10% *v*/*v*) led to a 3- or 5-fold increased final OD$_{600}$, while the titers of adipate increased 2.7-fold to 16 ± 1 mg/L or 3.2-fold to 19 ± 2 mg/L, respectively (Fig. 4). Without supplement, the growth rate was 0.36 h^{-1} in the exponential phase, while in the presence of complex medium, it was 0.52 to 0.54 h^{-1}. When 50 mM of the precursor succinate was added to the APM with glucose, both final biomass and adipate titer (8 ± 2 mg/L) were increased approximately 1.3-fold (Fig. 4). Since the addition of complex media and of succinate individually improved production of adipate, we combined the supplements to check for a synergistic effect. With 10% (*v*/*v*) BHI medium and 50 mM succinate in the APM with glucose, *E. coli* BL21(DE3)/pET22b_Adip1 accumulated 36 ± 3 mg/L in the culture supernatant after 30 h, which is 6-fold higher compared to the adipate titer in APM without supplement (Fig. 4) and is also the highest specific adipate titer per biomass (2.5 mg/L/OD$_{600}$).

Since we assumed that putative broad-spectrum acyl-CoA thioesterases may cleave also the other CoA intermediates of the production pathway, we checked for the presence of the corresponding acids 3-oxo-, 3-hydroxy-, and 2,3-dehydroadipic acid by GC-TOF-MS analysis. Indeed, we found all three acids (Figs. 5 and S2–S5). While the use of a broad-spectrum thioesterase is non-optimal for production of adipate due to the cleavage of the CoA intermediates, it may help to analyze and monitor the reactions of the pathway in further work to improve the adipate production.

Discussion

Attempts for the biological production of the dicarboxylic bulk chemical adipate directly in microbial cells focused on the use of a reverse β-oxidative pathway starting with

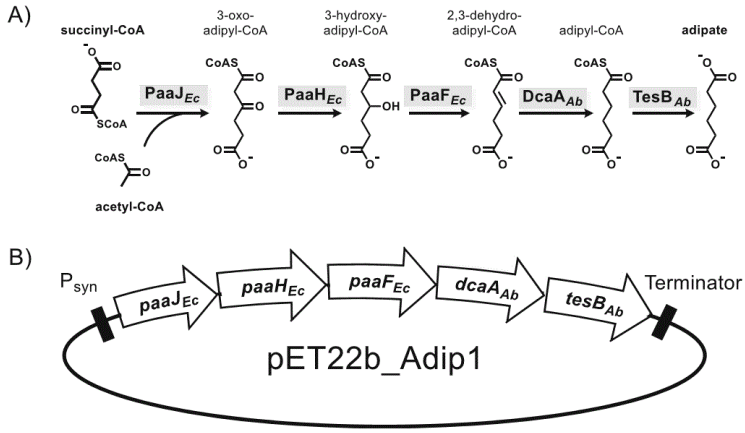

Fig. 3 Scheme of the adipic acid production pathway (**a**) and the constructed plasmid pET22b_Adip1 harboring the genes encoding the selected enzymes (**b**). Based on published data for PaaJ, PaaH, and PaaF from *E. coli* (Teufel et al. 2010) and our results for DcaA and TesB, we chose these five enzymes to test for the production of adipic acid by reversal of β-oxidation of 3-oxoadipyl-CoA formed from succinyl-CoA and acetyl-CoA. The genes were assembled in a synthetic operon under control of the constitutive strong synthetic promoter P_{syn} and cloned into the expression plasmid pET22b(+) yielding plasmid pET22b_Adip1. PaaJ 3-oxoadipyl-CoA thiolase, PaaH 3-hydroxyadipyl-CoA dehydrogenase, PaaF 2,3-dehydroadipyl-CoA hydratase, DcaA adipyl-CoA dehydrogenase, TesB acyl-CoA thioesterase

succinyl-CoA and acetyl-CoA, both of which are provided by the central carbon metabolism (Babu et al. 2015; Yu et al. 2014). The obtained low adipate titers of 12 μg/L and 0.6 mg/L produced with *E. coli* from glucose were proposed to be caused by the incapability of some tested enzymes to convert the CoA intermediates of the pathway which are non-natural substrates for these enzymes. The rate-limiting step for adipate production was proposed to be the reduction of 2,3-dehydroadipyl-CoA (Babu et al. 2015; Yu et al. 2014) due to limited enzymatic activity of the tested acyl-CoA dehydrogenases rather than due to thermodynamics of the catalyzed reaction. With respect to the thermodynamic in silico analysis, reactions catalyzed by acyl-CoA dehydrogenases are suggested to prefer the formation of the saturated acyl-CoA as it was also reported earlier when the reaction was coupled to ferredoxin (Dellomonaco et al. 2011). Interestingly, these enzymes (i.e., for the degradation of fatty acids) naturally operate in the opposite direction for the synthesis of α,β-unsaturated enoyl-CoA, and it was indeed shown that the substrate is pulled thermodynamically uphill upon formation of enoyl-CoA (Becker et al. 1994; Cummings et al. 1992).

An enzymatic activity for the reduction of 2,3-dehydroadipyl-CoA has not been experimentally confirmed until now. Instead, putative broad-spectrum reductases were tested (Babu et al. 2015; Yu et al. 2014). The common enzyme used was the enoyl-CoA reductase Ter from *Euglena gracilis*,

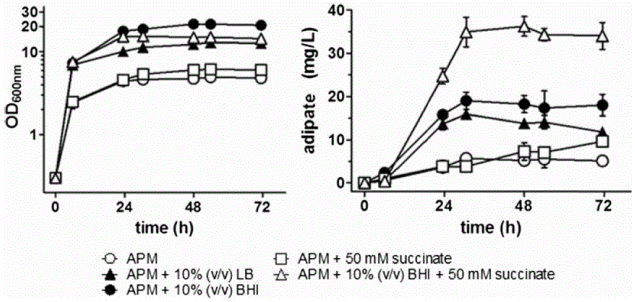

Fig. 4 Growth of *E. coli* BL21(DE3)/pET22b_Adip1 and adipate titers in culture supernatants. **a** *E. coli* BL21(DE3)/pET22b_Adip1 was cultivated in adipate production medium (APM) containing 2% (*w/v*) glucose. Supplements were added as indicated. **b** Adipate titers were determined by LC-MS in cell-free culture supernatants. Data represent mean values and standard deviations of three biological replicates

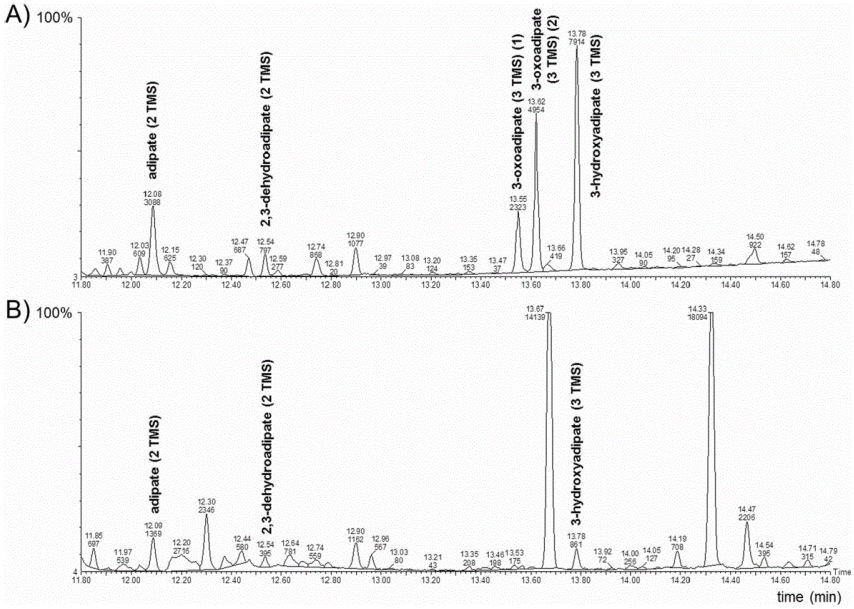

Fig. 5 GC-TOF-MS analysis for identification of adipate pathway intermediates. GC-TOF-MS analysis revealed the presence of 3-oxoadipate, 3-hydroxyadipate, and 2,3-dehydroadipate during production of adipate via a reverse β-oxidation pathway in APM with 2% (*w*/*v*) glucose, 10% (*v*/*v*) BHI medium, and 50 mM succinate. After 48 h of cultivation (OD_{600} of 13.9), samples were collected for GC-TOF-MS analysis of cell-free culture supernatant (**a**) and intracellular extracts after hot methanol lysis (**b**)

which mainly converts enoyl-CoA molecules derived from monocarboxylic acids (Hoffmeister et al. 2005). This enzyme was assumed to be feasible for adipate production based on the similarity of 2,3-dehydroadipyl-CoA to the accepted substrate *trans*-2-hexenoyl-CoA. We here confirmed in vitro that the adipyl-CoA dehydrogenase DcaA of *A. baylyi* ADP1 is a suitable biocatalyst for the reduction of 2,3-dehydroadipyl-CoA, since this compound is the natural substrate of DcaA in the catabolic pathway for adipate (Parke et al. 2001). In contrast, the putative acyl-CoA dehydrogenase Acd_{Cn} of *C. necator* JMP228, annotated as butyryl-CoA dehydrogenase, did not convert adipyl-CoA with significant activity in our in vitro assay. The natural substrate of Acd_{Cn} remains to be elucidated.

For the release of adipate from adipyl-CoA, we chose the thioesterase $TesB_{Ab}$ to test the feasibility of the presented production route for adipic acid (Fig. 3). Most likely due to the broad substrate spectrum of $TesB_{Ab}$, all CoA intermediates of the pathway were cleaved and we could detect the released acids of the pathway intermediates by GC-TOF-MS analyses. Since $TesB_{Ec}$ showed only low activity towards C_2 to C_4 acyl-CoA thioesters (Nie et al. 2008), we assumed that acetyl-CoA and succinyl-CoA are not significantly cleaved by the thioesterase $TesB_{Ab}$. However, the cleavage of the intermediate CoA esters releasing 3-oxo-, 3-hydroxy-, and 2,3-dehydroadipate besides adipate limits the accumulation of adipate and makes such a broad-spectrum thioesterase not suitable for high-yield production of adipate. Alternative enzymes should be identified and tested, including optimized expression of the genes coding for the SCS_{Tg} subunits, for further improvement of the pathway also with respect to the question of energy conservation. In this view, CoA-transferases and ADP-forming acyl-CoA synthetases represent promising enzymes for the conversion of CoA-thioesters, here for adipyl-CoA, to release the (di)carboxylic acid. In view of the overall energy balance of the pathway (Table S2), the intrinsic energy of the thioester bond could be preserved in ATP by a synthetase or in a new thioester bond when the CoA is transferred by a CoA-transferase to an acceptor. For the release of adipate from adipyl-CoA and formation of ATP from ADP and P_i, we calculated a $\Delta G^{0\prime}$ of −5.5 kJ/mol based on the values in Table S1. As this value is close to zero, it can be suggested that this reaction is thermodynamically feasible in both directions. The succinyl-CoA synthetase from *T. gammatolerans* (SCS_{Tg}) exhibited activity with adipate according to our in vitro result. The relatively low activity of SCS_{Tg} we found may be attributed to the apparent imbalance of the α- and β-subunit that can be improved by

suitable cloning and expression strategies in further studies. Further candidate enzymes for the release of adipate from adipyl-CoA have been published (Binieda et al. 1999; Nolte et al. 2014).

In the thermophilic microbe *Thermobifida fusca* B6, reversal of the native β-oxidative adipate degradation pathway was tested for adipate production. The overexpression of one single gene, Tfu_1647, encoding an adipyl-CoA dehydrogenase exhibiting 70% similarity to $DcaA_{Ab}$, was sufficient to reach a final adipate titer of 2.2 g/L from 50 g/L glucose (Deng and Mao 2015). Therefore, Tfu_1647 is a promising candidate to also improve adipate production in *E. coli*. The results obtained with *T. fusca* thereby also nicely demonstrate that production of adipate in the g/L scale can be achieved using the presented pathway. In this organism, an ADP-forming succinyl-CoA synthetase encoded by Tfu_2576 and Tfu_2577 catalyzes the release of adipate from adipyl-CoA. Therefore, eventually, adipate production could be coupled to formation of ATP in the last enzymatic step (Deng and Mao 2015).

In our study, we found that the maximal adipate titers with *E. coli* in APM were higher in the presence of complex media and highest for complex BHI medium plus succinate. From that, we assume that mainly the precursor availability for the adipate pathway is limiting the production under the tested conditions, yet the positive effect could also be attributed to improved expression and increased enzyme activities. However, the adipate titer obtained with *E. coli* could be increased considerably using strategies to increase the supply of the precursors succinyl-CoA and acetyl-CoA (Lin et al. 2006; Thakker et al. 2012) and sophisticated expression strategies for multiple and optimized genes of a synthetic pathway.

Compliance with ethical standards

Ethical approval This article does not contain any studies with human participants or animals performed by any of the authors.

Conflict of interest The authors declare that they have no conflict of interest.

References

Babu T, Yun EJ, Kim S, Kim DH, Liu KH, Kim SR, Kim KH (2015) Engineering *Escherichia coli* for the production of adipic acid through the reversed β-oxidation pathway. Process Biochem 50(12):2066–2071

Bart JCJ, Cavallaro S (2015a) Transiting from adipic acid to bioadipic acid. 1, petroleum-based processes. Ind Eng Chem Res 54(1):1–46. doi:10.1021/ie5020734

Bart JCJ, Cavallaro S (2015b) Transiting from adipic acid to bioadipic acid. Part II Biosynthetic pathways Ind Eng Chem Res 54(2):567–576. doi:10.1021/ie502074d

Becker DF, Fuchs JA, Stankovich MT (1994) Product binding modulates the thermodynamic properties of a *Megasphaera elsdenii* short-chain acyl-CoA dehydrogenase active-site mutant. Biochemistry 33(23):7082–7087. doi:10.1021/bi00189a010

Binieda A, Fuhrmann M, Lehner B, Rey-Berthod C, Frutiger-Hughes S, Hughes G (1999) Purification, characterization, DNA sequence and cloning of a pimeloyl-CoA synthetase from *Pseudomonas mendocina* 35. Biochem J 340(3):793–801

Blattner FR, Plunkett G 3rd, Bloch CA, Perna NT, Burland V, Riley M, Collado-Vides J, Glasner JD, Rode CK, Mayhew GF, Gregor J, Davis NW, Kirkpatrick HA, Goeden MA, Rose DJ, Mau B, Shao Y (1997) The complete genome sequence of *Escherichia coli* K-12. Science (New York, NY) 277(5331):1453–1462

Bugg TD, Rahmanpour R (2015) Enzymatic conversion of lignin into renewable chemicals. Curr Opin Chem Biol 29:10–17. doi:10.1016/j.cbpa.2015.06.009

Chen H, Bjerknes M, Kumar R, Jay E (1994) Determination of the optimal aligned spacing between the Shine–Dalgarno sequence and the translation initiation codon of *Escherichia coli* mRNAs. Nucleic Acids Res 22(23):4953–4957. doi:10.1093/nar/22.23.4953

Cheong S, Clomburg JM, Gonzalez R (2016) Energy- and carbon-efficient synthesis of functionalized small molecules in bacteria using non-decarboxylative Claisen condensation reactions. Nature Biotechnol 34(5):556–561. doi:10.1038/nbt.3505

Clomburg JM, Vick JE, Blankschien MD, Rodriguez-Moya M, Gonzalez R (2012) A synthetic biology approach to engineer a functional reversal of the beta-oxidation cycle. ACS Synth Biol 1(11):541–554. doi:10.1021/sb3000782

Clomburg JM, Blankschien MD, Vick JE, Chou A, Kim S, Gonzalez R (2015) Integrated engineering of β-oxidation reversal and ω-oxidation pathways for the synthesis of medium chain ω-functionalized carboxylic acids. Metab Eng 28:202–212

Cummings JG, Lau SM, Powell PJ, Thorpe C (1992) Reductive half-reaction in medium-chain acyl-CoA dehydrogenase: modulation of internal equilibrium by carboxymethylation of a specific methionine residue. Biochemistry 31(36):8523–8529

Dekishima Y, Lan EI, Shen CR, Cho KM, Liao JC (2011) Extending carbon chain length of 1-butanol pathway for 1-hexanol synthesis from glucose by engineered *Escherichia coli*. J Am Chem Soc 133(30):11399–11401

Dellomonaco C, Clomburg JM, Miller EN, Gonzalez R (2011) Engineered reversal of the β-oxidation cycle for the synthesis of fuels and chemicals. Nature 476(7360):355–359

Deng Y, Mao Y (2015) Production of adipic acid by the native-occurring pathway in *Thermobifida fusca* B6. J Appl Microbiol 119(4):1057–1063

Engler C, Gruetzner R, Kandzia R, Marillonnet S (2009) Golden gate shuffling: a one-pot DNA shuffling method based on type IIs restriction enzymes. PLoS One 4(5):e5553

Giacomini A, Ollero FJ, Squartini A, Nuti MP (1994) Construction of multipurpose gene cartridges based on a novel synthetic promoter for high-level gene expression in Gram-negative bacteria. Gene 144(1):17–24

Haapalainen AM, Merilainen G, Wierenga RK (2006) The thiolase superfamily: condensing enzymes with diverse reaction specificities. Trends Biochem Sci 31(1):64–71. doi:10.1016/j.tibs.2005.11.011

Hoffmeister M, Piotrowski M, Nowitzki U, Martin W (2005) Mitochondrial trans-2-enoyl-CoA reductase of wax ester fermentation from *Euglena gracilis* defines a new family of enzymes involved in lipid synthesis. J Biol Chem 280(6):4329–4338

Karl RM, Hupperich M, Thomer A, Eggerer H (1995) Inhibition of 3-hydroxy-3-methylglutaryl-CoA reductase and citrate synthase by sulfoxides and sulfones of substrate-analogue CoA-thioether derivatives. Eur J Biochem 227(1–2):292–295

Kaschabek SR, Kuhn B, Müller D, Schmidt E, Reineke W (2002) Degradation of aromatics and chloroaromatics by *Pseudomonas* sp. strain B13: purification and characterization of 3-oxoadipate:

succinyl-coenzyme A (CoA) transferase and 3-oxoadipyl-CoA thiolase. J Bacteriol 184(1):207–215

Küberl A, Fränzel B, Eggeling L, Polen T, Wolters DA, Bott M (2014) Pupylated proteins in *Corynebacterium glutamicum* revealed by MudPIT analysis. Proteomics 14(12):1531–1542. doi:10.1002/pmic.201300531

Lehman TC, Hale DE, Bhala A, Thorpe C (1990) An acyl-CoA dehydrogenase assay utilizing the ferrocenium ion. Anal Biochem 186:280–284

Lin H, Castro NM, Bennett GN, San K-Y (2006) Acetyl-CoA synthetase overexpression in *Escherichia coli* demonstrates more efficient acetate assimilation and lower acetate accumulation: a potential tool in metabolic engineering. Appl Microbiol Biotechnol 71(6):870–874

Modis Y, Wierenga RK (1999) A biosynthetic thiolase in complex with a reaction intermediate: the crystal structure provides new insights into the catalytic mechanism. Structure 7(10):1279–1290

Musser MT (2005) Adipic acid. *ULLMANN'S Encyclopedia of Industrial Chemistry* (Volume 1). Wiley-VCH Verlag GmbH & Co. KGaA, Weinheim, pp 537–48

Nie L, Ren Y, Janakiraman A, Smith S, Schulz H (2008) A novel paradigm of fatty acid β-oxidation exemplified by the thioesterase-dependent partial degradation of conjugated linoleic acid that fully supports growth of *Escherichia coli*. Biochemistry 47(36):9618–9626

Niu W, Draths KM, Frost JW (2002) Benzene-free synthesis of adipic acid. Biotechnol Prog 18(2):201–211

Nolte JC, Schürmann M, Schepers C-L, Vogel E, Wübbeler JH, Steinbüchel A (2014) Novel characteristics of succinate coenzyme A (succinate-CoA) ligases: conversion of malate to malyl-CoA and CoA-thioester formation of succinate analogues in vitro. Appl Environ Microb 80(1):166–176

Paczia N, Nilgen A, Lehmann T, Gatgens J, Wiechert W, Noack S (2012) Extensive exometabolome analysis reveals extended overflow metabolism in various microorganisms. Microb Cell Factories 11:122. doi:10.1186/1475-2859-11-122

Parke D, Garcia MA, Ornston LN (2001) Cloning and genetic characterization of *dca* genes required for beta-oxidation of straight-chain dicarboxylic acids in *Acinetobacter* sp. strain ADP1. Appl Environ Microb 67(10):4817–4827

Parthasarathy A, Pierik AJ, Kahnt J, Zelder O, Buckel W (2011) Substrate specificity of 2-hydroxyglutaryl-CoA dehydratase from *Clostridium symbiosum*: toward a bio-based production of adipic acid. Biochemistry 50(17):3540–3550

Polen T, Spelberg M, Bott M (2013) Toward biotechnological production of adipic acid and precursors from biorenewables. J Biotechnol 167(2):75–84

Grand View Research (2014) Adipic acid market analysis and segment forecasts to 2020.

Sambrook J, Fritsch EF, Maniatis T (1989) Molecular cloning: a laboratory manual, 2nd ed Cold Spring Harbor Laboratory Press, Cold Spring Harbor, NY

Shikata K, Fukui T, Atomi H, Imanaka T (2007) A novel ADP-forming succinyl-CoA synthetase in *Thermococcus kodakaraensis* structurally related to the archaeal nucleoside diphosphate-forming acetyl-CoA synthetases. J Biol Chem 282(37):26963–26970. doi:10.1074/jbc.M702694200

Suastegui M, Matthiesen JE, Carraher JM, Hernandez N, Rodriguez Quiroz N, Okerlund A, Cochran EW, Shao Z, Tessonnier JP (2016) Combining metabolic engineering and electrocatalysis: application to the production of polyamides from sugar. Angew Chem 55(7):2368–2373. doi:10.1002/anie.201509653

Teufel R, Mascaraque V, Ismail W, Voss M, Perera J, Eisenreich W, Haehnel W, Fuchs G (2010) Bacterial phenylalanine and phenylacetate catabolic pathway revealed. Proc Natl Acad Sci 107(32):14390–14395. doi:10.1073/pnas.1005399107

Thakker C, Martínez I, San KY, Bennett GN (2012) Succinate production in *Escherichia coli*. Biotechnol J 7(2):213–224

Thomas JM, Raja R, Johnson BF, O'Connell TJ, Sankar G, Khimyak T (2003) Bimetallic nanocatalysts for the conversion of muconic acid to adipic acid. Chem Commun (Camb) 21(10):1126–1127

Thorpe C, Kim J (1995) Structure and mechanism of action of the acyl-CoA dehydrogenases. FASEB J 9(9):718–725

van Duuren JB, Wijte D, Leprince A, Karge B, Puchalka J, Wery J, Dos Santos VA, Eggink G, Mars AE (2011) Generation of a *catR* deficient mutant of *P. putida* KT2440 that produces *cis*, *cis*-muconate from benzoate at high rate and yield. J Biotechnol 156(3):163–172

Villemin D, Labiad B, Loupy A (1993) Clay catalysis: a convenient and rapid formation of anhydride from carboxylic acid and isopropenyl acetate under microwave irradiation. Synth Commun 23(4):419–424. doi:10.1080/00397919308009796

Wells T, Ragauskas AJ (2012) Biotechnological opportunities with the β-ketoadipate pathway. Trends Biotechnol 30(12):627–637

Yu JL, Xia XX, Zhong JJ, Qian ZG (2014) Direct biosynthesis of adipic acid from a synthetic pathway in recombinant *Escherichia coli*. Biotechnol Bioeng 111(12):2580–2586

Zhang H, Li Z, Pereira B, Stephanopoulos G (2015) Engineering *E. coli–E. coli* cocultures for production of muconic acid from glycerol. Microb Cell Factories 14(1):1

3. References

Ahuja, I., Kissen, R., and Bones, A.M. (2012) Phytoalexins in defense against pathogens. *Trends in Plant Science* 17: 73-90.

Austin, M.B., Bowman, M.E., Ferrer, J.-L., Schröder, J., and Noel, J.P. (2004) An aldol switch discovered in stilbene synthases mediates cyclization specificity of type III polyketide synthases. *Chemistry & Biology* 11: 1179-1194.

Becker, J., and Wittmann, C. (2012) Bio-based production of chemicals, materials and fuels – *Corynebacterium glutamicum* as versatile cell factory. *Current Opinion in Biotechnology* 23: 631-640.

Becker, J., Zelder, O., Häfner, S., Schröder, H., and Wittmann, C. (2011) From zero to hero — design-based systems metabolic engineering of *Corynebacterium glutamicum* for L-lysine production. *Metabolic Engineering* 13: 159-168.

Biegert, T., Fuchs, G., and Heider, J. (1996) Evidence that anaerobic oxidation of toluene in the denitrifying bacterium *Thauera aromatica* is initiated by formation of benzylsuccinate from toluene and fumarate. *European Journal of Biochemistry* 238: 661-668.

Boots, A.W., Haenen, G.R., and Bast, A. (2008) Health effects of quercetin: from antioxidant to nutraceutical. *European Journal of Pharmacology* 585: 325-337.

Braus, G.H. (1991) Aromatic amino acid biosynthesis in the yeast *Saccharomyces cerevisiae*: a model system for the regulation of a eukaryotic biosynthetic pathway. *Microbiological Reviews* 55: 349-370.

Britsch, L., and Grisebach, H. (1986) Purification and characterization of (2*S*)-flavanone 3-hydroxylase from *Petunia hybrida*. *European Journal of Biochemistry* 156: 569-577.

Brune, I., Jochmann, N., Brinkrolf, K., Hüser, A.T., Gerstmeir, R., Eikmanns, B.J. et al. (2007) The IclR-type transcriptional repressor LtbR regulates the expression of leucine and tryptophan biosynthesis genes in the amino acid producer *Corynebacterium glutamicum*. *Journal of Bacteriology* 189: 2720-2733.

Chaudhry, M.T., Huang, Y., Shen, X.-H., Poetsch, A., Jiang, C.-Y., and Liu, S.-J. (2007) Genome-wide investigation of aromatic acid transporters in *Corynebacterium glutamicum*. *Microbiology* 153: 857-865.

Chemler, J.A., Fowler, Z.L., McHugh, K.P., and Koffas, M.A. (2010) Improving NADPH availability for natural product biosynthesis in *Escherichia coli* by metabolic engineering. *Metabolic Engineering* 12: 96-104.

Clomburg, J.M., Vick, J.E., Blankschien, M.D., Rodríguez-Moyá, M., and Gonzalez, R. (2012) A synthetic biology approach to engineer a functional reversal of the β-oxidation cycle. *ACS Synthetic Biology* 1: 541-554.

Cress, B.F., Leitz, Q.D., Kim, D.C., Amore, T.D., Suzuki, J.Y., Linhardt, R.J., and Koffas, M.A. (2017) CRISPRi-mediated metabolic engineering of *E. coli* for *O*-methylated anthocyanin production. *Microbial Cell Factories* 16: 10.

D'Auria, J.C. (2006) Acyltransferases in plants: a good time to be BAHD. *Current Opinion in Plant Biology* 9: 331-340.

Davis, M.S., Solbiati, J., and Cronan, J.E. (2000) Overproduction of acetyl-CoA carboxylase activity increases the rate of fatty acid biosynthesis in *Escherichia coli*. *Journal of Biological Chemistry* 275: 28593-28598.

Dellomonaco, C., Clomburg, J.M., Miller, E.N., and Gonzalez, R. (2011) Engineered reversal of the β-oxidation cycle for the synthesis of fuels and chemicals. *Nature* 476: 355-359.

Du, L., Ma, L., Qi, F., Zheng, X., Jiang, C., Li, A. et al. (2016) Characterization of a unique pathway for 4-cresol catabolism initiated by phosphorylation in *Corynebacterium glutamicum*. *Journal of Biological Chemistry* 291: 6583-6594.

Duplay, P., Bedouelle, H., Fowler, A., Zabin, I., Saurin, W., and Hofnung, M. (1984) Sequences of the *malE* gene and of its product, the maltose-binding protein of *Escherichia coli* K12. *Journal of Biological Chemistry* 259: 10606-10613.

Eggeling, L., and Bott, M. (2005) Handbook of *Corynebacterium glutamicum*: CRC Press, Boca Raton, Florida, USA.

Erlund, I. (2004) Review of the flavonoids quercetin, hesperetin, and naringenin. Dietary sources, bioactivities, bioavailability, and epidemiology. *Nutrition Research* 24: 851-874.

Eudes, A., Juminaga, D., Baidoo, E.E., Collins, F.W., Keasling, J.D., and Loqué, D. (2013) Production of hydroxycinnamoyl anthranilates from glucose in *Escherichia coli*. *Microbial Cell Factories* 12: 62.

Fazel, A., and Jensen, R. (1979) Obligatory biosynthesis of L-tyrosine via the pretyrosine branchlet in coryneform bacteria. *Journal of Bacteriology* 138: 805-815.

Fowler, Z.L., Gikandi, W.W., and Koffas, M.A. (2009) Increased malonyl coenzyme A biosynthesis by tuning the *Escherichia coli* metabolic network and its application to flavanone production. *Applied and Environmental Microbiology* 75: 5831-5839.

Fuchs, G., Boll, M., and Heider, J. (2011) Microbial degradation of aromatic compounds — from one strategy to four. *Nature Reviews Microbiology* 9: 803-816.

Hagino, H., and Nakayama, K. (1975) L-Tryptophan production by analog-resistant mutants derived from a phenylalanine and tyrosine double auxotroph of *Corynebacterium glutamicum*. *Agricultural and Biological Chemistry* 39: 343-349.

Harborne, J.B., and Mabry, T.J. (2013) The flavonoids: advances in research, Springer Science+Business Media LLC, New York, Philadelphia, USA

Harrison, F.H., and Harwood, C.S. (2005) The *pimFABCDE* operon from *Rhodopseudomonas palustris* mediates dicarboxylic acid degradation and participates in anaerobic benzoate degradation. *Microbiology* 151: 727-736.

Harwood, C.S., and Parales, R.E. (1996) The β-ketoadipate pathway and the biology of self-identity. *Annual Reviews in Microbiology* 50: 553-590.

Hasslacher, M., Ivessa, A., Paltauf, F., and Kohlwein, S. (1993) Acetyl-CoA carboxylase from yeast is an essential enzyme and is regulated by factors that control phospholipid metabolism. *Journal of Biological Chemistry* 268: 10946-10952.

Heider, S.A., and Wendisch, V.F. (2015) Engineering microbial cell factories: Metabolic engineering of *Corynebacterium glutamicum* with a focus on non-natural products. *Biotechnology Journal* 10: 1170-1184.

Humphreys, J.M., and Chapple, C. (2002) Rewriting the lignin roadmap. *Current Opinion in Plant Biology* 5: 224-229.

Ikeda, M. (2006) Towards bacterial strains overproducing L-tryptophan and other aromatics by metabolic engineering. *Applied Microbiology and Biotechnology* 69: 615.

Ikeda, M., and Katsumata, R. (1992) Metabolic engineering to produce tyrosine or phenylalanine in a tryptophan-producing *Corynebacterium glutamicum* strain. *Applied and Environmental Microbiology* 58: 781-785.

Ikeda, M., Ozaki, A., and Katsumata, R. (1993) Phenylalanine production by metabolically engineered *Corynebacterium glutamicum* with the *pheA* gene of *Escherichia coli*. *Applied Microbiology and Biotechnology* 39: 318-323.

Inoue, K., Sewalt, V.J., Ballance, G.M., Ni, W., Stürzer, C., and Dixon, R.A. (1998) Developmental expression and substrate specificities of alfalfa caffeic acid 3-*O*-methyltransferase and caffeoyl coenzyme A 3-*O*-methyltransferase in relation to lignification. *Plant Physiology* 117: 761-770.

Inui, M., Kawaguchi, H., Murakami, S., Vertès, A.A., and Yukawa, H. (2005) Metabolic engineering of *Corynebacterium glutamicum* for fuel ethanol production under oxygen-deprivation conditions. *Journal of Molecular Microbiology and Biotechnology* 8: 243-254.

Jendresen, C.B., Stahlhut, S.G., Li, M., Gaspar, P., Siedler, S., Förster, J. et al. (2015) Novel highly active and specific tyrosine ammonia-lyases from diverse origins enable enhanced production of aromatic compounds in bacteria and yeast. *Applied and Environmental Microbiology* 81(13): 4458-4476

Kalinowski, J., Bathe, B., Bartels, D., Bischoff, N., Bott, M., Burkovski, A. et al. (2003) The complete *Corynebacterium glutamicum* ATCC 13032 genome sequence and its impact on the production of L-aspartate-derived amino acids and vitamins. **Journal of Biotechnology** 104: 5-25.

Kaneko, M., Hwang, E.I., Ohnishi, Y., and Horinouchi, S. (2003) Heterologous production of flavanones in *Escherichia coli*: potential for combinatorial biosynthesis of flavonoids in bacteria. *Journal of Industrial Microbiology and Biotechnology* 30: 456-461.

Kang, S.-Y., Lee, J.K., Choi, O., Kim, C.Y., Jang, J.-H., Hwang, B.Y., and Hong, Y.-S. (2014) Biosynthesis of methylated resveratrol analogs through the construction of an artificial biosynthetic pathway in *E. coli*. *BMC Biotechnology* 14: 67.

Katsumata, R., and Ikeda, M. (1993) Hyperproduction of tryptophan in *Corynebacterium glutamicum* by pathway engineering. *Nature Biotechnology* 11: 921-925.

Katsuyama, Y., Funa, N., Miyahisa, I., and Horinouchi, S. (2007) Synthesis of unnatural flavonoids and stilbenes by exploiting the plant biosynthetic pathway in *Escherichia coli*. *Chemistry & Biology* 14: 613-621.

Kikuchi, Y., Tsujimoto, K., and Kurahashi, O. (1997) Mutational analysis of the feedback sites of phenylalanine-sensitive 3-deoxy-D-arabino-heptulosonate-7-phosphate synthase of *Escherichia coli*. *Applied and Environmental Microbiology* 63: 761-762.

Kim, B.-G., Joe, E.J., and Ahn, J.-H. (2010) Molecular characterization of flavonol synthase from poplar and its application to the synthesis of 3-*O*-methylkaempferol. *Biotechnology Letters* 32: 579-584.

Kim, B.G., Yang, S.M., Kim, S.Y., Cha, M.N., and Ahn, J.-H. (2015) Biosynthesis and production of glycosylated flavonoids in *Escherichia coli*: current state and perspectives. *Applied Microbiology and Biotechnology* 99: 2979-2988.

Kinoshita, S., Udaka, S., and Shimono, M. (1957) Studies on the amino acid fermentation. *The Journal of General and Applied Microbiology* 3: 193-205.

Knoot, C.J., Purpero, V.M., and Lipscomb, J.D. (2015) Crystal structures of alkylperoxo and anhydride intermediates in an intradiol ring-cleaving dioxygenase. *Proceedings of the National Academy of Sciences* 112: 388-393.

Kogure, T., Kubota, T., Suda, M., Hiraga, K., and Inui, M. (2016) Metabolic engineering of *Corynebacterium glutamicum* for shikimate overproduction by growth-arrested cell reaction. *Metabolic Engineering* 38: 204-216.

Kortmann, M., Kuhl, V., Klaffl, S., and Bott, M. (2015) A chromosomally encoded T7 RNA polymerase-dependent gene expression system for *Corynebacterium glutamicum*: construction and comparative evaluation at the single-cell level. *Microbial biotechnology* 8: 253-265.

Krause, F.S., Blombach, B., and Eikmanns, B.J. (2010) Metabolic engineering of *Corynebacterium glutamicum* for 2-ketoisovalerate production. *Applied and Environmental Microbiology* 76: 8053-8061.

Kubota, T., Watanabe, A., Suda, M., Kogure, T., Hiraga, K., and Inui, M. (2016) Production of *para*-aminobenzoate by genetically engineered *Corynebacterium glutamicum* and non-biological formation of an N-glucosyl byproduct. *Metabolic Engineering* 38: 322-330.

Kubota, T., Tanaka, Y., Takemoto, N., Watanabe, A., Hiraga, K., Inui, M., and Yukawa, H. (2014) Chorismate-dependent transcriptional regulation of quinate/shikimate utilization genes by LysR-type transcriptional regulator QsuR in *Corynebacterium glutamicum*: carbon flow control at metabolic branch point. *Molecular Microbiology* 92: 356-368.

Lee, J.-H., and Wendisch, V.F. (2016) Biotechnological production of aromatic compounds of the extended shikimate pathway from renewable biomass. *Journal of Biotechnology*, *in press*, doi: 10.1016/j.jbiotec.2016.11.016

Leonard, E., Lim, K.-H., Saw, P.-N., and Koffas, M.A. (2007) Engineering central metabolic pathways for high-level flavonoid production in *Escherichia coli*. *Applied and Environmental Microbiology* 73: 3877-3886.

Leonard, E., Yan, Y., Fowler, Z.L., Li, Z., Lim, C.-G., Lim, K.-H., and Koffas, M.A. (2008) Strain improvement of recombinant *Escherichia coli* for efficient production of plant flavonoids. *Molecular Pharmaceutics* 5: 257-265.

Li, M., Kildegaard, K.R., Chen, Y., Rodriguez, A., Borodina, I., and Nielsen, J. (2015) *De novo* production of resveratrol from glucose or ethanol by engineered *Saccharomyces cerevisiae*. *Metabolic Engineering* 32: 1-11.

Li, P.-P., Liu, Y.-J., and Liu, S.-J. (2009) Genetic and biochemical identification of the chorismate mutase from *Corynebacterium glutamicum*. *Microbiology* 155: 3382-3391.

Li, P.-P., Li, D.-F., Liu, D., Liu, Y.-M., Liu, C., and Liu, S.-J. (2013) Interaction between DAHP synthase and chorismate mutase endows new regulation on DAHP synthase activity in *Corynebacterium glutamicum*. *Applied Microbiology and Biotechnology* 97: 10373-10380.

Lim, C.G., Fowler, Z.L., Hueller, T., Schaffer, S., and Koffas, M.A. (2011) High-yield resveratrol production in engineered *Escherichia coli*. *Applied and Environmental Microbiology* 77: 3451-3460.

Lin, Y., and Yan, Y. (2012) Biosynthesis of caffeic acid in *Escherichia coli* using its endogenous hydroxylase complex. *Microbial Cell Factories* 11: 42.

Liu, Y.-B., Long, M.-X., Yin, Y.-J., Si, M.-R., Zhang, L., Lu, Z.-Q. et al. (2013) Physiological roles of mycothiol in detoxification and tolerance to multiple poisonous chemicals in *Corynebacterium glutamicum*. *Archives of Microbiology* 195: 419-429.

Liu, Y.-J., Li, P.-P., Zhao, K.-X., Wang, B.-J., Jiang, C.-Y., Drake, H.L., and Liu, S.-J. (2008) *Corynebacterium glutamicum* contains 3-deoxy-D-arabino-heptulosonate 7-phosphate synthases that display novel biochemical features. *Applied and Environmental Microbiology* 74: 5497-5503.

MacDonald, M.J., and D'Cunha, G.B. (2007) A modern view of phenylalanine ammonia lyase. *Biochemistry and Cell Biology* 85: 273-282.

Manach, C., Scalbert, A., Morand, C., Rémésy, C., and Jiménez, L. (2004) Polyphenols: food sources and bioavailability. *The American Journal of Clinical Nutrition* 79: 727-747.

Marienhagen, J., and Bott, M. (2013) Metabolic engineering of microorganisms for the synthesis of plant natural products. *Journal of Biotechnology* 163: 166-178.

McCormack, D., and McFadden, D. (2012) Pterostilbene and cancer: current review. *Journal of Surgical Research* 173: e53-e61.

Merkens, H., Beckers, G., Wirtz, A., and Burkovski, A. (2005) Vanillate metabolism in *Corynebacterium glutamicum*. *Current Microbiology* 51: 59-65.

Mierziak, J., Kostyn, K., and Kulma, A. (2014) Flavonoids as important molecules of plant interactions with the environment. *Molecules* 19: 16240-16265.

Miyahisa, I., Kaneko, M., Funa, N., Kawasaki, H., Kojima, H., Ohnishi, Y., and Horinouchi, S. (2005) Efficient production of (2*S*)-flavanones by *Escherichia coli* containing an artificial biosynthetic gene cluster. *Applied Microbiology and Biotechnology* 68: 498-504.

Nijveldt, R.J., Van Nood, E., Van Hoorn, D.E., Boelens, P.G., Van Norren, K., and Van Leeuwen, P.A. (2001) Flavonoids: a review of probable mechanisms of action and potential applications. *The American Journal of Clinical Nutrition* 74: 418-425.

Okai, N., Miyoshi, T., Takeshima, Y., Kuwahara, H., Ogino, C., and Kondo, A. (2016) Production of protocatechuic acid by *Corynebacterium glutamicum* expressing chorismate-pyruvate lyase from *Escherichia coli*. *Applied Microbiology and Biotechnology* 100: 135-145.

Otten, A., Brocker, M., and Bott, M. (2015) Metabolic engineering of *Corynebacterium glutamicum* for the production of itaconate. *Metabolic Engineering* 30: 156-165.

Pangeni, R., Sahni, J.K., Ali, J., Sharma, S., and Baboota, S. (2014) Resveratrol: review on therapeutic potential and recent advances in drug delivery. *Expert Opinion on Drug Delivery* 11: 1285-1298.

Pátek, M., and Nešvera, J. (2013) Promoters and plasmid vectors of *Corynebacterium glutamicum*. In *Corynebacterium glutamicum* Biology and Biotechnology, Volume 23 of the series *Microbiology Monographs*, Springer, pp. 51-88.

Plaza, M., Pozzo, T., Liu, J., Gulshan Ara, K.Z., Turner, C., and Nordberg Karlsson, E. (2014) Substituent effects on in vitro antioxidizing properties, stability, and solubility in flavonoids. *Journal of Agricultural and Food Chemistry* 62: 3321-3333.

Price, A.C., Choi, K.-H., Heath, R.J., Li, Z., White, S.W., and Rock, C.O. (2001) Inhibition of β-ketoacyl-acyl carrier protein synthases by thiolactomycin and cerulenin structure and mechanism. *Journal of Biological Chemistry* 276: 6551-6559.

Quideau, S., Deffieux, D., Douat-Casassus, C., and Pouysegu, L. (2011) Plant polyphenols: chemical properties, biological activities, and synthesis. *Angewandte Chemie* International Edition 50: 586-621.

Radmacher, E., Alderwick, L.J., Besra, G.S., Brown, A.K., Gibson, K.J., Sahm, H., and Eggeling, L. (2005) Two functional FAS-I type fatty acid synthases in *Corynebacterium glutamicum*. *Microbiology* 151: 2421-2427.

Ross, J., Li, Y., Lim, E.-K., and Bowles, D.J. (2001) Higher plant glycosyltransferases. *Genome Biology* 2: reviews 3004.1.

Santos, C.N.S., Koffas, M., and Stephanopoulos, G. (2011) Optimization of a heterologous pathway for the production of flavonoids from glucose. *Metabolic Engineering* 13: 392-400.

Schulz, H. (1991) Beta oxidation of fatty acids. *Biochimica et Biophysica Acta - Lipids and Lipid Metabolism* 1081: 109-120.

Shen, X.-H., Zhou, N.-Y., and Liu, S.-J. (2012) Degradation and assimilation of aromatic compounds by *Corynebacterium glutamicum*: another potential for applications for this bacterium? *Applied Microbiology and Biotechnology* 95: 77-89.

Shen, X.-H., Jiang, C.-Y., Huang, Y., Liu, Z.-P., and Liu, S.-J. (2005) Functional identification of novel genes involved in the glutathione-independent gentisate pathway in *Corynebacterium glutamicum*. *Applied and Environmental Microbiology* 71: 3442-3452.

Shen, X., and Liu, S. (2005) Key enzymes of the protocatechuate branch of the β-ketoadipate pathway for aromatic degradation in *Corynebacterium glutamicum*. *Science in China Series C: Life Sciences* 48: 241-249.

Shin, S.-Y., Han, N.S., Park, Y.-C., Kim, M.-D., and Seo, J.-H. (2011) Production of resveratrol from *p*-coumaric acid in recombinant *Saccharomyces cerevisiae* expressing 4-coumarate: coenzyme A ligase and stilbene synthase genes. *Enzyme and Microbial Technology* 48: 48-53.

Shin, S.-Y., Jung, S.-M., Kim, M.-D., Han, N.S., and Seo, J.-H. (2012) Production of resveratrol from tyrosine in metabolically engineered *Saccharomyces cerevisiae*. *Enzyme and Microbial Technology* 51: 211-216.

Siebert, D., and Wendisch, V.F. (2015) Metabolic pathway engineering for production of 1,2-propanediol and 1-propanol by *Corynebacterium glutamicum*. *Biotechnology for Biofuels* 8: 91.

Siemann, E., and Creasy, L. (1992) Concentration of the phytoalexin resveratrol in wine. *American Journal of Enology and Viticulture* 43: 49-52.

Takeno, S., Takasaki, M., Urabayashi, A., Mimura, A., Muramatsu, T., Mitsuhashi, S., and Ikeda, M. (2013) Development of fatty acid-producing *Corynebacterium glutamicum* strains. *Applied and Environmental Microbiology* 79: 6776-6783.

Teramoto, H., Inui, M., and Yukawa, H. (2009) Regulation of expression of genes involved in quinate and shikimate utilization in *Corynebacterium glutamicum*. *Applied and Environmental Microbiology* 75: 3461-3468.

Trautwein, K., Wilkes, H., and Rabus, R. (2012) Proteogenomic evidence for β-oxidation of plant-derived 3-phenylpropanoids in "*Aromatoleum aromaticum*" EbN1. *Proteomics* 12: 1402-1413.

Tropf, S., Lanz, T., Rensing, S., Schröder, J., and Schröder, G. (1994) Evidence that stilbene synthases have developed from chalcone synthases several times in the course of evolution. *Journal of Molecular Evolution* 38: 610-618.

Tsuge, Y., Hasunuma, T., and Kondo, A. (2015) Recent advances in the metabolic engineering of *Corynebacterium glutamicum* for the production of lactate and succinate from renewable resources. *Journal of Industrial Microbiology & Biotechnology* 42: 375-389.

van Summeren-Wesenhagen, P.V., and Marienhagen, J. (2015) Metabolic engineering of *Escherichia coli* for the synthesis of the plant polyphenol pinosylvin. *Applied and Environmental Microbiology* 81: 840-849.

Vogt, M., Brüsseler, C., van Ooyen, J., Bott, M., and Marienhagen, J. (2016) Production of 2-methyl-1-butanol and 3-methyl-1-butanol in engineered *Corynebacterium glutamicum*. *Metabolic Engineering* 38: 436-445.

Wallace, B., and Pittard, J. (1967) Genetic and biochemical analysis of the isoenzymes concerned in the first reaction of aromatic biosynthesis in *Escherichia coli*. *Journal of Bacteriology* 93: 237-244.

Wang, S., Zhang, S., Xiao, A., Rasmussen, M., Skidmore, C., and Zhan, J. (2015) Metabolic engineering of *Escherichia coli* for the biosynthesis of various phenylpropanoid derivatives. *Metabolic Engineering* 29: 153-159.

Watts, K.T., Lee, P.C., and Schmidt-Dannert, C. (2006) Biosynthesis of plant-specific stilbene polyketides in metabolically engineered *Escherichia coli*. *BMC Biotechnology* 6: 22.

Wendisch, V., Eberhardt, D., Herbst, M., and Jensen, J. (2014) Biotechnological Production of Amino acids and nucleotides, In: Biotechnological production of natural ingredients for food industry, Bentham Science eBooks, pp. 60-163.

Wöhlbrand, L., Kallerhoff, B., Lange, D., Hufnagel, P., Thiermann, J., Reinhardt, R., and Rabus, R. (2007) Functional proteomic view of metabolic regulation in "*Aromatoleum aromaticum*" strain EbN1. *Proteomics* 7: 2222-2239.

Wu, J., Du, G., Zhou, J., and Chen, J. (2013a) Metabolic engineering of *Escherichia coli* for (2*S*)-pinocembrin production from glucose by a modular metabolic strategy. *Metabolic Engineering* 16: 48-55.

Wu, J., Zhou, T., Du, G., Zhou, J., and Chen, J. (2014) Modular optimization of heterologous pathways for *de novo* synthesis of (2*S*)-naringenin in *Escherichia coli*. *PloS One* 9: e101492.

Wu, J., Liu, P., Fan, Y., Bao, H., Du, G., Zhou, J., and Chen, J. (2013b) Multivariate modular metabolic engineering of *Escherichia coli* to produce resveratrol from L-tyrosine. *Journal of Biotechnology* 167: 404-411.

Yamamoto, S., Suda, M., Niimi, S., Inui, M., and Yukawa, H. (2013) Strain optimization for efficient isobutanol production using *Corynebacterium glutamicum* under oxygen deprivation. *Biotechnology and Bioengineering* 110: 2938-2948.

Yan, Y., Kohli, A., and Koffas, M.A. (2005) Biosynthesis of natural flavanones in *Saccharomyces cerevisiae*. *Applied and Environmental Microbiology* 71: 5610-5613.

Yang, X., Li, X., and Ren, J. (2014) From French Paradox to cancer treatment: anti-cancer activities and mechanisms of resveratrol. *Anti-Cancer Agents in Medicinal Chemistry* (formerly *Current Medicinal Chemistry-Anti-Cancer Agents*) 14: 806-825.

Yonekura-Sakakibara, K., and Saito, K. (2009) Functional genomics for plant natural product biosynthesis. *Natural Product Reports* 26: 1466-1487.

Zha, W., Rubin-Pitel, S.B., Shao, Z., and Zhao, H. (2009) Improving cellular malonyl-CoA level in *Escherichia coli* via metabolic engineering. *Metabolic Engineering* 11: 192-198.

Zhang, C., Zhang, J., Kang, Z., Du, G., Yu, X., Wang, T., and Chen, J. (2013) Enhanced production of L-phenylalanine in *Corynebacterium glutamicum* due to the introduction of *Escherichia coli* wild-type gene *aroH*. *Journal of Industrial Microbiology & Biotechnology* 40: 643-651.

Zhu, S., Wu, J., Du, G., Zhou, J., and Chen, J. (2014) Efficient synthesis of eriodictyol from L-tyrosine in *Escherichia coli*. *Applied and Environmental Microbiology* 80: 3072-3080.

4. Appendix

4.1 Authors‘ Contributions

1.) Kallscheuer, N., Vogt, M., Kappelmann, J., Krumbach, K., Noack, S., Bott, M., & Marienhagen, J. (2016). Identification of the *phd* gene cluster responsible for phenylpropanoid utilization in *Corynebacterium glutamicum*. *Applied Microbiology and Biotechnology*, 100(4): 1871-1881.

NK analyzed the DNA microarray data, constructed and cultivated the generated strain variants and wrote 50 % of the manuscript. MV (shared first author) performed RNA extractions and DNA microarray experiments, growth experiments with phenylpropanoids and wrote 50 % of the manuscript. JK performed the LC-MS/MS measurements for identification of pathway intermediates. KK constructed the plasmids for complementation of deletion mutants. SN and JM contributed to the data analysis. JM and MB revised the manuscript.

Overall contribution NK: 40%

2.) Kallscheuer, N., Vogt, M., Stenzel, A., Gätgens, J., Bott, M., & Marienhagen, J. (2016). Construction of a *Corynebacterium glutamicum* platform strain for the production of stilbenes and (2*S*)-flavanones. *Metabolic Engineering* 38: 47-55

NK constructed the plasmids and strains, conducted the cultivation experiments, metabolite extraction and LC-MS analyses and wrote the manuscript. MV contributed to strain construction, optimization of cultivation conditions and preparation of the manuscript. AS constructed the plasmid for polyphenol production starting from glucose. JG performed the GC-TOF-MS analysis. MB and JM revised the manuscript.

Overall contribution NK: 70%

3.) Kallscheuer, N., Vogt, M., Bott, M., & Marienhagen, J. (2017). Functional expression of plant-derived *O*-methyltransferase, flavanone 3-hydroxylase, and flavonol synthase in *Corynebacterium glutamicum* for production of pterostilbene, kaempferol, and quercetin. *Journal of Biotechnology* 258: 190-196

NK constructed the plasmids and strains, performed the cultivation experiments, metabolite extraction, LC-MS analysis and wrote the manuscript. MV contributed to optimization of the cultivation conditions and manuscript preparation. MB and JM revised the manuscript.

Overall contribution NK: 80%

4.) Kallscheuer, N., Vogt, M., & Marienhagen, J. (2017). A novel synthetic pathway enables microbial production of polyphenols independent from the endogenous aromatic amino acid metabolism. *ACS Synthetic Biology* 6 (3): 410–415

NK searched for suitable enzyme candidates, designed the synthetic pathway, performed the *in silico* thermodynamic analysis, constructed the plasmids and strains, performed the cultivation experiments, LC-MS analysis and wrote the manuscript. MV analyzed the data and contributed to manuscript preparation. JM contributed to the pathway design, manuscript preparation and revised the manuscript.

Overall contribution NK: 90%

5.) Kallscheuer, N., Gätgens, J., Lübcke, M., Pietruszka, J., Bott, M., & Polen, T. (2016). Improved production of adipate with *Escherichia coli* by reversal of β-oxidation. *Applied Microbiology and Biotechnology* 101: 2371-2382

NK performed cloning work, protein purification, preparation of substrates and enzymatic activity assays, constructed the adipate production strain, conducted the cultivation experiments and the LC-MS analysis. JG identified the pathway intermediates using GC-TOF-MS analysis. ML synthesized adipic anhydride. TP contributed to data analysis and manuscript preparation. TP, JP and MB revised the manuscript.

Overall contribution NK: 80%

6.**) Kallscheuer, N., Polen, T., Bott, M. & Marienhagen, J.** (2017). Reversal of β-oxidation pathways for the microbial production of chemicals and polymer building blocks (review article), Metabolic Engineering 42: 33-42

NK performed the literature and database search, collected and compiled the material. NK, TP and JM discussed the structure of the manuscript. JM, TP and MB revised the manuscript.

Overall contribution NK: 70%

4.2 Other activities

Kallscheuer N., & Marienhagen, J. (2017) Produktion pflanzlicher Polyphenole mit *Corynebacterium glutamicum*, Bio*Spektrum* 03/2017 (Erscheinungstermin: 08. Mai 2017)

Danksagung

Bei **Herrn Prof. Dr. Michael Bott** bedanke ich mich für die Übernahme des Erstgutachtens und für das Interesse am Fortgang dieser Arbeit.

Frau Prof. Dr. Martina Pohl danke ich für die Übernahme des Korreferats und die Bereitschaft, die Zeit als Doktorand als Mentorin zu begleiten.

Bei **Dr. Jan Marienhagen** bedanke ich mich sehr herzlich für die Überlassung des sehr interessanten Themas und die äußerst engagierte Betreuung des Projektes. Dies beinhaltet insbesondere die vielen Stunden zur Diskussion des experimentellen Vorgehens und zur Publikation der Ergebnisse.

Dr. Michael Vogt gilt mein uneingeschränkter Dank für die hervorragende Zusammenarbeit im Rahmen dieses Projektes. Vielen Dank für die tollen Aktionen auch außerhalb des Labors.

Anton Stenzel und **Lars Milke** danke ich für die exzellente Mitarbeit im Projekt, aus der nicht nur sehr gute Abschlussarbeiten hervorgingen, sondern die auch für diese Doktorarbeit einen wertvollen Beitrag geleistet haben.

Der Arbeitsgruppe „Synthetische Zellfabriken“ danke ich für die sehr gute Arbeitsatmosphäre und die wertvollen Tipps zur Durchführung so manch kniffliger Experimente. Vielen Dank an **Jenny H.** („Primer-Jenny“), **Jenny A.** („Möhrchen“) (auch für die Spaziergänge), **Chris** („Triple B“), **Lion** („Leon“, „Mr. Flachabart“), **Christiane** (für die Schwäbisch-Kurse), **Bastian** („What did you do?“), **Hugo, Sascha J.** und natürlich **Sascha S.** und **Karin** (Wieso habt ihr eigentlich noch keine Spitznamen?). Ich danke auch den ehemaligen Mitgliedern der Gruppe **Philana** und **Sabrina**.

Jochem Gätgens, **Jannick Kappelmann** und **Dr. Stefan Noack** danke ich für die Durchführung und Auswertung der GC-TOF-MS- bzw. LC-MS/MS-Analytik.

Der „Nachsitzungs“-Truppe (**Jenny P.**, **Meike**, **Sabrina**, **Andi**, **Micha**) danke ich für die Erkundung der Jülicher Pizza- und Pasta-Kultur.

Mein Dank geht auch an alle Mitarbeiter des Instituts (inkl. Infrastruktur) für die Hilfe bei den „Kleinigkeiten“ im Laboralltag.

Beim gesamten BacHBerry-Konsortium (insbesondere WP6) bedanke ich mich für die sehr gute Zusammenarbeit und Unterstützung in den letzten drei Jahren.

Danksagung

Ein ganz besonderer Dank geht an meine Familie für die großartige Unterstützung während der gesamten Studienzeit.

Band / Volume 149
Kinetic and thermodynamic considerations on the formation of heteromolecular layers on metal surfaces
C. Henneke (2017), vii, 157, XIV pp
ISBN: 978-3-95806-245-0

Band / Volume 150
Spectroscopic characterization of local valence change processes in resistively switching complex oxides
C. Bäumer (2017), x, 206 pp
ISBN: 978-3-95806-246-7

Band / Volume 151
Magnetic structure in relation to the magnetic field induced ferroelectricity in Y-type hexaferrite $Ba_{2-x}Sr_xZn_2Fe_{12}O_{22}$
P. Thakuria (2017), 17, 180 pp
ISBN: 978-3-95806-250-4

Band / Volume 152
Statistical analysis tools for assessing the functional relevance of higher-order correlations in massively parallel spike trains
V. Rostami (2017), x, 176 pp
ISBN: 978-3-95806-251-1

Band / Volume 153
The influence of the substrate on the structure and electronic properties of carbon-based 2D materials
J. Sforzini (2017), XIII, 145 pp
ISBN: 978-3-95806-255-9

Band / Volume 154
Gate-All-Around Silicon Nanowire Tunnel FETs for Low Power Applications
G. V. Luong (2017), ii, 136 pp
ISBN: 978-3-95806-259-7

Band / Volume 155
Graphene Devices for Extracellular Measurements
D. Kireev (2017), ix, 169 pp
ISBN: 978-3-95806-265-8

Band / Volume 156
Nanoscale 3D structures towards improved cell-chip coupling on microelectrode arrays
S. D. Weidlich (2017), II, 154 pp
ISBN: 978-3-95806-278-8

Band / Volume 157
Interface phenomena in $La_{1/3}Sr_{2/3}FeO_3$ / $La_{2/3}Sr_{1/3}MnO_3$ heterostructures and a quest for p-electron magnetism
M. Waschk (2017), ix, 205 pp
ISBN: 978-3-95806-281-8

Band / Volume 158
Physics of Life
Lecture Notes of the 49th IFF Spring School 2018
26 February – 09 March 2018, Jülich, Germany
ed. by G. Gompper, J. Dhont, J. Elgeti, C. Fahlke, D. Fedosov, S. Förster, P. Lettinga, A. Offenhäusser (2018), ca 1000 pp
ISBN: 978-3-95806-286-3

Band / Volume 159
Identifizierung von Bindungsdeterminanten von Tat-Vorläuferproteinen an den TatBCRezeptorkomplex während der Tat-abhängigen Proteintranslokation in *Escherichia coli*
A. Ulfig (2018), 186 pp
ISBN: 978-3-95806-290-0

Band / Volume 160
***Corynebacterium glutamicum* – a novel platform for the production of plant polyphenols**
N. Kallscheuer (2018), X, 98 pp
ISBN: 978-3-95806-291-7

Schlüsseltechnologien / Key Technologies
Band / Volume 160
ISBN 978-3-95806-291-7

Mitglied der Helmholtz-Gemeinschaft

JÜLICH
Forschungszentrum